NPS ARCHIVE
1997.04
NULL, G.

DUDLEY KNOX LIBRARY
NAVAL POSTGRADUATE SCHOOL
MONTEREY CA 93943-5101

NAVAL POSTGRADUATE SCHOOL
Monterey, California

THESIS

COMPUTER SIMULATION OF THE THERMAL EFFECTS ON A CONCENTRIC CANISTER MISSILE LAUNCHER WITH A FIRE IN AN ADJACENT COMPARTMENT

by

Gary L. Null

September, 1997

Thesis Advisor: M. D. Kelleher

Approved for public release; distribution is unlimited.

REPORT DOCUMENTATION PAGE

Form Approved OMB No. 0704-0188

Public reporting burden for this collection of information is estimated to average 1 hour per response, including the time for reviewing instruction, searching existing data sources, gathering and maintaining the data needed, and completing and reviewing the collection of information. Send comments regarding this burden estimate or any other aspect of this collection of information, including suggestions for reducing this burden, to Washington Headquarters Services, Directorate for Information Operations and Reports, 1215 Jefferson Davis Highway, Suite 1204, Arlington, VA 22202-4302, and to the Office of Management and Budget, Paperwork Reduction Project (0704-0188) Washington DC 20503.

1. AGENCY USE ONLY *(Leave blank)*	2. REPORT DATE	3. REPORT TYPE AND DATES COVERED
	September 1997	Engineer's Thesis

4. TITLE AND SUBTITLE **COMPUTER SIMULATION OF THE THERMAL EFFECTS ON A CONCENTRIC CANISTER MISSILE LAUNCHER WITH A FIRE IN AN ADJACENT COMPARTMENT**	5. FUNDING NUMBERS
6. AUTHOR(S) Null, Gary L.	
7. PERFORMING ORGANIZATION NAME(S) AND ADDRESS(ES) Naval Postgraduate School Monterey CA 93943-5000	8. PERFORMING ORGANIZATION REPORT NUMBER
9. SPONSORING/MONITORING AGENCY NAME(S) AND ADDRESS(ES) Naval Air Warfare Center - Weapons Division, China Lake CA	10. SPONSORING/MONITORING AGENCY REPORT NUMBER

11. SUPPLEMENTARY NOTES The views expressed in this thesis are those of the author and do not reflect the official policy or position of the Department of Defense or the U.S. Government.

12a. DISTRIBUTION/AVAILABILITY STATEMENT	12b. DISTRIBUTION CODE
Approved for public release; distribution is unlimited.	

13. ABSTRACT *(maximum 200 words)*

The thermal effects in the Concentric Canister "missile" Launcher (CCL) due to a fire in an adjacent compartment are simulated using computational fluid dynamics (CFD). A commercial code developed by CFD Research Corporation (CFDRC) was used to implement the process. This study developed a model for the center section of the A-module, placed in the forward missile launcher of the Arleigh Burke (DDG-51) class destroyer. Two fire scenerios are applied to the aft bulkhead of the launcher. The first fire scenerio is indicative of the high temperature fire caused by unburned Exocet missile propellant experienced by the USS STARK (FFG-31) in the Arabian Gulf. The second fire scenerio applied to the model simulates the conditions caused by a ruptured shipboard F-76 diesel fuel tank, due to a collision at sea. The fire scenerios are used to predict the time and location of the critical cook-off temperatures of the missile's solid and liquid fuel propellants in the CCL.

14. SUBJECT TERMS: Concentric Canister Launcher, Fire Modeling, Cook-Off	15. NUMBER OF PAGES 215
	16. PRICE CODE

17. SECURITY CLASSIFICATION OF REPORT	18. SECURITY CLASSIFICATION OF THIS PAGE	19. SECURITY CLASSIFICATION OF ABSTRACT	20. LIMITATION OF ABSTRACT
Unclassified	Unclassified	Unclassified	UL

NSN 7540-01-280-5500

Standard Form 298 (Rev. 2-89)
Prescribed by ANSI Std. 239-18 298-102

Approved for public release; distribution is unlimited

COMPUTER SIMULATION OF THE THERMAL EFFECTS ON A CONCENTRIC CANISTER MISSILE LAUNCHER WITH A FIRE IN AN ADJACENT COMPARTMENT

Gary L. Null
Lieutenant, United States Navy
B.S., United States Naval Academy, 1991

Submitted in partial fulfillment of the
requirements for the degree of

MECHANICAL ENGINEER

from the

NAVAL POSTGRADUATE SCHOOL
September, 1997

NPS ARCHIVE
1997.09
NULL, G.

DUDLEY KNOX LIBRARY
NAVAL POSTGRADUATE SCHOOL
MONTEREY CA 93943-5101

ABSTRACT

The thermal effects in the Concentric Canister "missile" Launcher (CCL) due to a fire in an adjacent compartment are simulated using computational fluid dynamics (CFD). A commercial code developed by CFD Research Corporation (CFDRC) was used to implement the process. This study developed a model for the center section of the A-module, placed in the forward missile launcher of the Arleigh Burke (DDG-51) class destroyer. Two fire scenerios are applied to the aft bulkhead of the launcher. The first fire scenerio is indicative of the high temperature fire caused by unburned Exocet missile propellant experienced by the USS STARK (FFG-31) in the Arabian Gulf. The second fire scenerio applied to the model simulates the conditions caused by a ruptured shipboard F-76 diesel fuel tank, due to a collision at sea. The fire scenerios are used to predict the time and location of the critical cook-off temperatures of the missile's solid and liquid fuel propellants in the CCL.

TABLE OF CONTENTS

I. INTRODUCTION 1

A. DESCRIPTION OF THE PROBLEM 1

B. BACKGROUND 3

C. PREVIOUS WORK 6

D. OBJECTIVES 10

II. COMPUTATIONAL FLUID DYNAMICS PROGRAM 11

A. OVERVIEW 11

B. THEORY 11

III. MODEL 19

A. GEOMETRY 19

1. Selection of CCL Module 19

2. Grid Distribution 19

B. THERMOPHYSICAL MODEL 23

C. FIRE SCENERIOS 28

IV. RESULTS 31

V. CONCLUSIONS 45

VI. RECOMMENDATIONS 49

APPENDIX A. OVERVIEW OF CCL SIMULATIONS 51

APPENDIX B. NODAL DISTRIBUTION IN THE LONGITUDINAL DIRECTION 53

APPENDIX C. CFD-ACE INPUT FILE 59

APPENDIX D. EXOCET FIRE - ROUND 1 73

APPENDIX E. EXOCET FIRE - ROUND 2 83

APPENDIX F. EXOCET FIRE - ROUND 3 93

APPENDIX G. EXOCET FIRE - ROUND 4 103

APPENDIX H. EXOCET FIRE - ROUND 5 113

APPENDIX I. F-76 FIRE - ROUND 1 123

APPENDIX J. F-76 FIRE - ROUND 2 133

APPENDIX K. F-76 FIRE - ROUND 3 143

APPENDIX L. F-76 FIRE - ROUND 4 153

APPENDIX M. F-76 FIRE - ROUND 5 163

APPENDIX N. RESIDUAL ERROR PROFILES 173

APPENDIX O. EXOCET FIRE - CLOSE WALL 177

APPENDIX P. F-76 FIRE - CLOSE WALL 189

LIST OF REFERENCES 201

INITIAL DISTRIBUTION LIST 203

ACKNOWLEDGMENT

I would like to acknowledge the support of NAVSEA Code 03R12 and NAWC China Lake, for providing support for this research. Additionally, I would like to express my sincere appreciation to Professor Kelleher for his guidance and patience during the work performed in this thesis. I'd also like to thank Dave Marco, who was always on hand to help me solve a computer workstation problem, and Richard Thoms, Mark Rist and the other members of the CFDRC software support team who provided me with a working knowledge of the CFD-ACE program and were always quick to respond to a question pertaining to my thesis. And to John Yagla of NSWCDD, for his support and information pertaining to the CCL concept. Most of all I would like to thank the following people: my parents, Michael Null and Sandra Smolenski; Jeffrey and Shannon Smolenski and my wife's parents, Richard and Kathy Maxwell; and my wife Michelle and daughter Courtney for being a continuous source of support and motivation. And finally, I'd like to thank my grandfather, the late Leonard Warner, for constantly watching over me during my research and graduate studies.

I. INTRODUCTION

A. DESCRIPTION OF THE PROBLEM

In the Navy's quest to improve the survivability of the Vertical Launch System (VLS) on U.S. combatants, Naval Surface Warfare Center Dahlgren Division (NSWCDD) has developed the Concentric Canister Launcher (CCL) as an alternative to the current Mk 41 system. [Ref. 1]

The CCL is a ready-to-fire self-contained system that can launch diverse munition types and sizes at any angle (Figure 1). Enhanced survivability measures in the design include a shock collar and passive armor protection. The shock collar is mounted in close proximity to the main deck to allow effective dissipation of an underwater blast away from the keel of the ship. The passive armor protection is provided by two titanium concentric canisters that are connected by interior anti-fragmentation shields. This combination of shields and strong inner and outer shells provides greater survivability of the missiles from enemy weapon penetration into the launcher.

NSWCDD has test fired the NATO Sea Sparrow, Standard Missile (SM-2 Blk IV) and a navalized-version of the Army's Advanced Tactical Missile (ATACM) from the CCL. They have also conducted extensive finite element analyses of imposed stresses on the steel shock collar and CFD simulations of the heat and mass transfer of the missile on the hemispherical lower cap of the canister. [Ref. 2]

To date, NSWCDD has not tested the effects on the CCL magazine due to high temperatures caused by a fire in an adjacent compartment. The first step in fire modeling the CCL system was thesis research performed by Callaham (1996). He conducted a one-

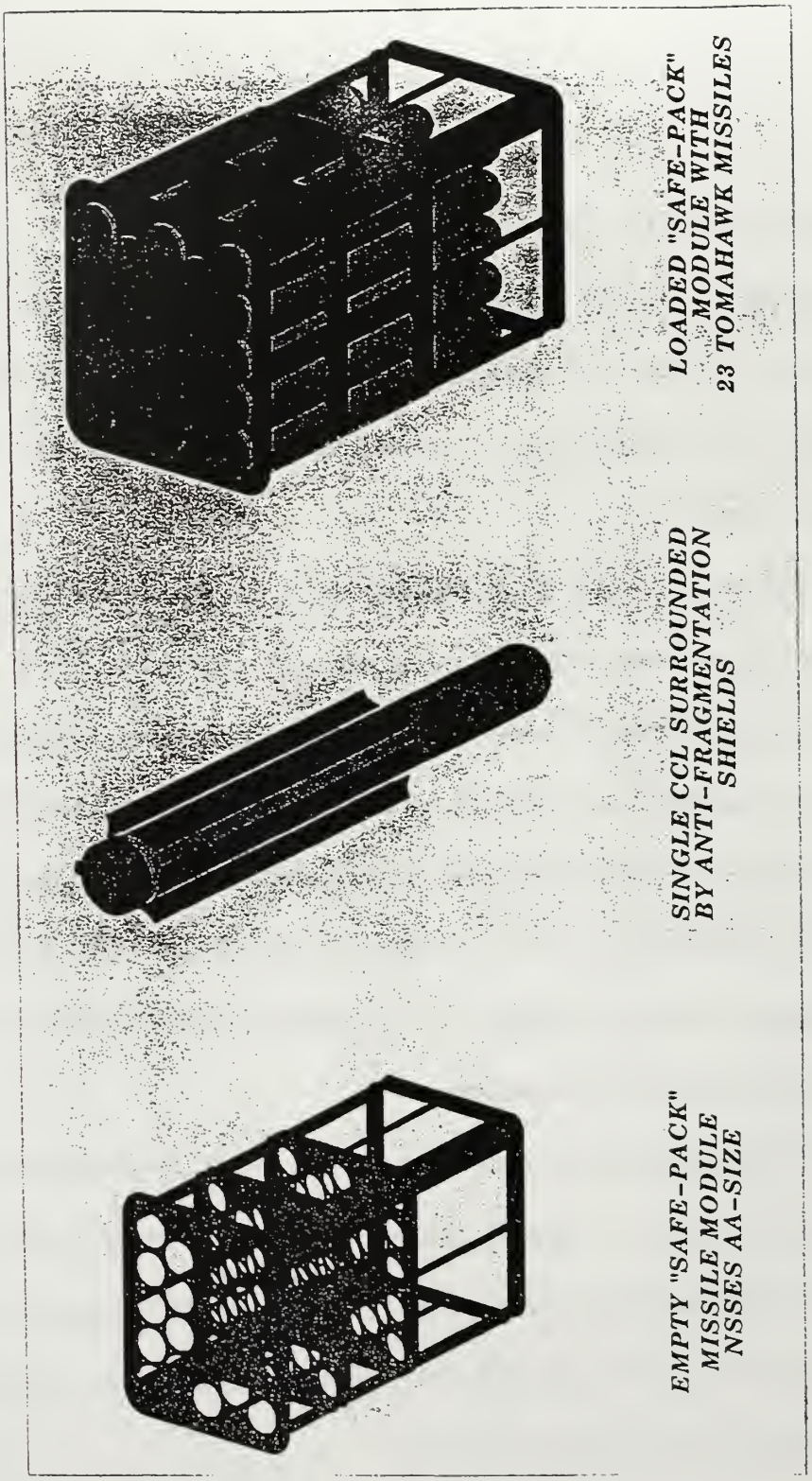

Figure 1. AA-Size Concentric Canister Weapons Module. "From Ref. [4]."

dimensional lumped parameter analysis on a single canister located next to the adjacent hot boundary [Ref. 3]. The fire modeling of the entire launcher is an important step to ensure the CCL meets present survivability criteria.

B. BACKGROUND

Currently, the Mk 41 VLS installed on the Arleigh Burke (DDG-51) class destroyer represents the state of the art in vertical launch design. The DDG-51 has two VLS that are designed to hold Tomahawk (T-LAM B, C, D), Standard (SM-2 Blk II, III, IV) and the Vertical Launch Anti-submarine Rocket (VLA). The forward magazine can carry up to 32 missiles and the aft magazine can carry up to 64. Table 1 shows that the drawback of carrying a large number of missiles onboard is that each contains several hundred pounds of energetic material (i.e., solid propellants, liquid fuels and explosives). A fire in the VLS involving this much energetic material could be catastrophic and result in the loss of the ship.

Weapon System	lb. of propellant	lb. of explosive	lb. of liquid fuel
TLAM - B/C	**304**	**371**	**441**
TLAM - D	**304**	**113**	**441**
SM-2 Blk IV	**297**	**78**	**0**
VLA	**461**	**98**	**88**

Table 1. Munitions Contained in VLS Loadout. "From Ref. [4]."

In 1987, the USS STARK (FFG-331) was struck by two Iraqi Exocet missiles while on patrol in the Arabian Gulf. The missiles failed to detonate upon impact, however, the missiles' solid propellant continued to burn at very high temperatures. Figure 2 shows that although the fire was contained in the midships section, the forward Mk 13 Standard Missile magazine still sustained thermal damage.

The STARK had state of the art fire protection systems, yet due to the high temperatures and damage to parts of these systems, they proved inadequate in fighting a "weapon-induced" fire [Ref. 4]. This type of fire is the most dangerous to the Burke class destroyers. The unburned Exocet fuel produced fires with temperatures in excess of 3000° F (1922 K). The minimum temperature required to melt the steel used in Navy ships is roughly 2800° F (1811 K).

In 1992, the USS INGERSOLL (DD-990) was involved in a major collision at sea with a Singapore merchant vessel. Four of INGERSOLL's forward fuel oil storage tanks were ruptured, which immediately flooded two of the forward compartments with fuel oil. One of the spaces flooded was the five inch gun magazine, while the other was a space immediately adjacent to this compartment. Fortunately, a fire in INGERSOLL was avoided. The crew maintained a thick layer of firefighting foam over the top of the two compartments and shored much of the damaged starboard side, allowing the ship to maintain ten knots enroute to the Singapore shipyard.

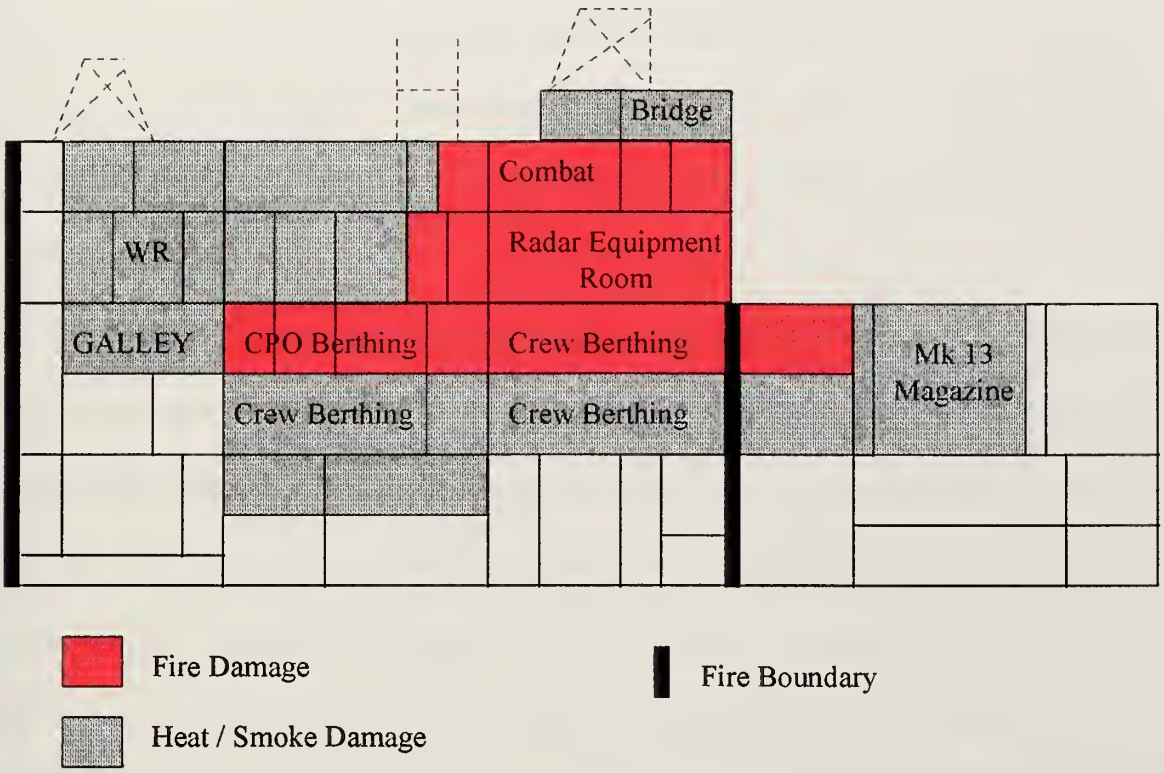

Figure 2. USS STARK (FFG-31). Starboard Side View Summary of Damage. "From Ref. [5]."

C. PREVIOUS WORK

Bowman and Lee developed a one-dimensional heat transfer model to predict the time-temperature profiles in the missile canister of a Mk 41 VLS for the DDG-51. Their scenerios used a fire in an adjacent compartment, which increased temperatures from ambient conditions to 2000°F (1366 K) in a period of five minutes, and then maintained that temperature for the duration of the fire (Figures 3 and 4). [Ref 4] This fire scenerio is indicative of the F-76 fuel oil fire that INGERSOLL potentially faced during her collision in the Straits of Malacca.

The goal of the analysis was to determine the approximate time for the missile's propellants to reach their critical cook-off temperatures. The cook-off temperature for the solid propellants is 300° F (422 K) and 460° F (511 K) is the ignition temperature for the liquid fuel. Bowman and Lees' model predicted that the missile motors and warheads were in danger of self-ignition in approximately 50 minutes, if more than one adacent space was on fire. For a fire in a single adjacent space, the canister temperature was predicted to reach only 245° F (377 K) after 900 minutes. Although this temperature is unlikely to cook-off the solid propellants and warheads, the Otto II fuel in the VLA may be at risk. [Ref 4]

Callaham generated a MATLAB 4.2.c computer algorithm that predicted the time temperature profile in a single CCL canister containing a Tomahawk missile. Using four different fire scenerios, he varied the temperature and heat fluxes applied to the adjacent bulkhead of the CCL compartment to determine the critical value of the cook-off temperature of the propellant at the geometric center of the missile. [Ref 3]

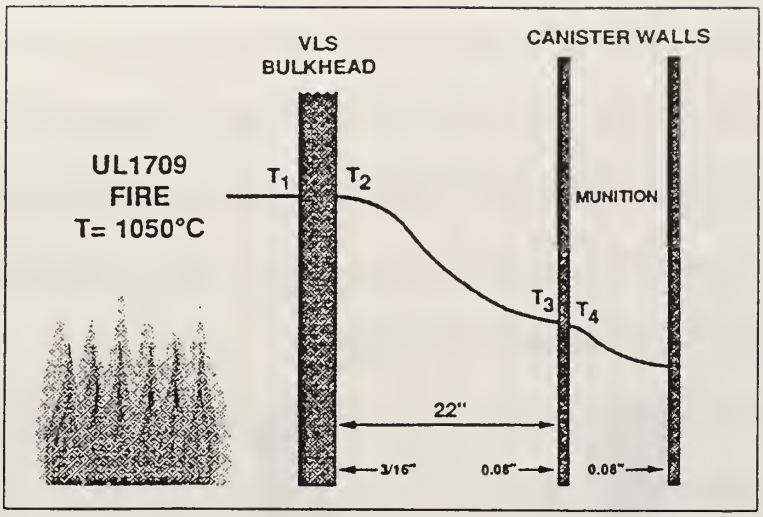

Figure 3. Ship's Structure at VLS Boundary. "From Ref. [4]."

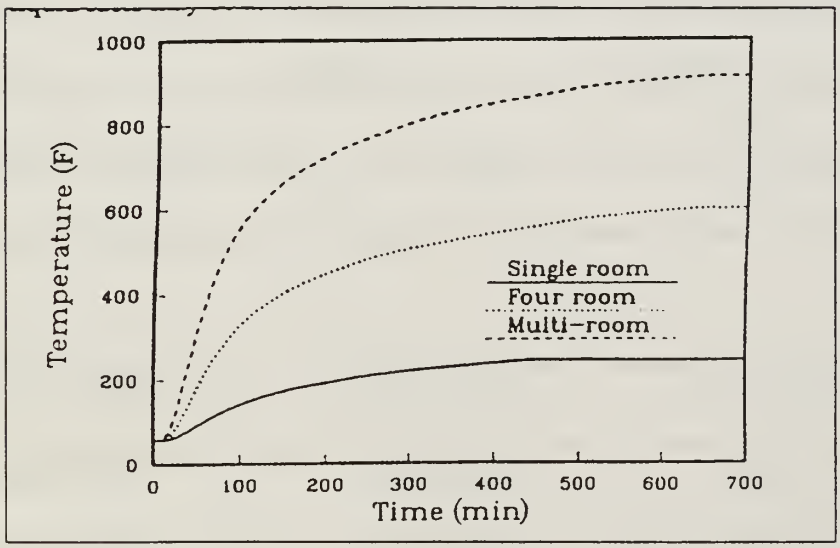

Figure 4. Canister Time Temperature Profile for Various Fire Sizes. "From Ref. [4]."

Callaham's model accounted for a single canister located in the center of the nearest row to the heat affected adjacent bulkhead. He also performed a simulation on a canister located at the corner of the nearest row. Figure 5 shows the thermal resistance network of the CCL canister. The model did not, however, account for the reflected radiation received from two of the four bulkheads, the upper and lower steel supports and canisters in the compartment, as well as, the circulating natural convection on the side of the canister that faced away from the hot boundary.

The most severe scenerio analyzed was one modeled as a fire fueled by a missile's residual solid propellant, as experienced by the STARK. The maximum temperature imposed was 3000° F (1922 K) for a rate of increase of 97.3° F/sec (54 K/sec). Table 2 shows the resultant times for the center of the canister to reach the solid propellant and liquid fuel cook-off temperatures for the STARK scenerio. Table 2 also shows the resultant times for the scenerio used by Bowman and Lee, applied by Callaham to his computer algorithm. Based on his data, he concluded that under the worst case fire scenerio of the STARK, the ship's personnel have approximately 45 minutes to gain control of the fire or cool the weapons in the magazine prior to cook-off. [Ref. 3]

Maximum Temperature	300° F (422 K)	460° F (511 K)
2000° F (1366 K)	**108 minutes**	**152 minutes**
3000° F (1922 K)	**42 minutes**	**53 minutes**

Table 2. Cook-Off and Ignition Times for Callaham Model. "After Ref. [3]."

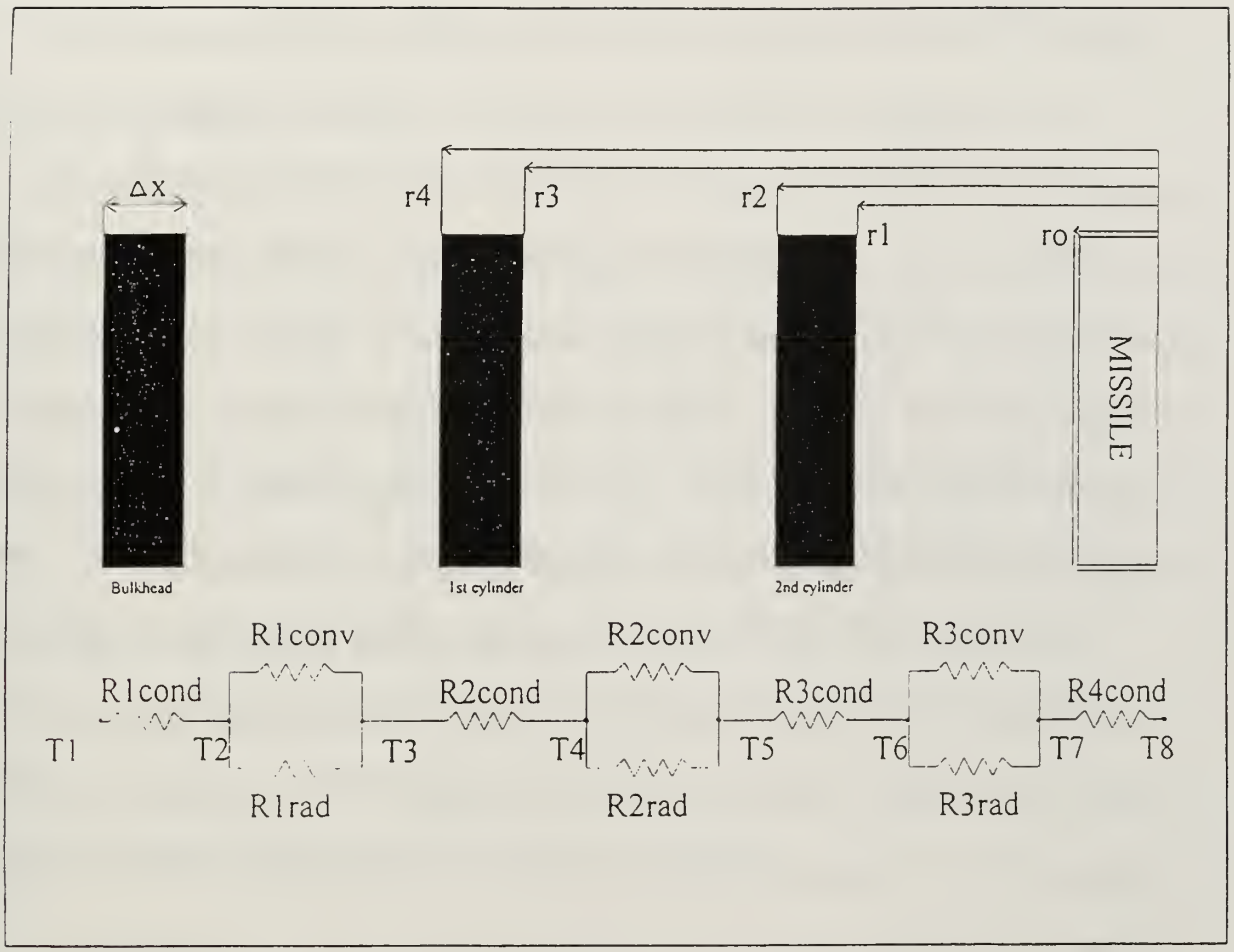

Figure 5. Thermal Resistance Network of the CCL Magazine. "From Ref. [3]."

D. OBJECTIVES

The purpose of this study is to expand upon the previous one-dimensional lumped parameter analysis performed on vertical launch missile magazines, adjacent to a compartment affected by a high temperature shipboard fire. The new three dimensional model includes all of the magazine's bulkheads and the addition of several canisters inside.

The initial step in developing such a model was to generate a meshing code and map it to a finite difference algorithm. The mesh generation code needed to account for the rectangular geometry of the launcher enclosure, as well as, the cylindrical geometry of the canisters and the accompanying radiation shape factors. To develop an accurate finite difference algorithm, the effects of surface radiation, natural convection, and conduction needed to be included in the program. The construction of each of these codes alone was considered to be overly complex given the existence of commercial CFD codes.

The decision was made to procure a commercial CFD program that included a mesh generation pre-processor, as well as, a powerful three dimensional algorithm for solving the continuity, momentum and energy equations. The baseline model is representative of the midsection of an A-module CCL compartment, installed in the forward missile magazine of the DDG-51. Two separate fire scenerios are applied to the affected boundary condition, indicative of a high temperature fire caused by unburned Exocet missile propellant or shipboard F-76 diesel fuel. The data generated by the program can provide a visual representation of the time-temperature profile within the CCL compartment, as a result of a fire in an adjacent compartment, to aid in the development of optimum firefighting systems and procedures for the launcher.

II. COMPUTATIONAL FLUID DYNAMICS PROGRAM

A. OVERVIEW

The CFD program used to analyze the thermal effects in the CCL was developed by CFD Research Corporation (CFDRC). The program incorporates three separate, yet interactive, codes titled CFD-GEOM, CFD-ACE and CFD-VIEW (Figure 6).

CFD-GEOM is the pre-processor geometric modeling and mesh generation code that enables the user to develop the initial architecture of the problem. CFD-ACE allows the user to select the phenomena to be included (i.e., heat transfer, turbulence, radiation), the values for the material properties and initial conditions, and the type of boundary conditions used (i.e., adiabatic, isothermal, inlet etc.). This code also allows the user limited control of the algorithm by enabling the choice of the number of iterations, the type of differencing scheme and the amount of constraint, or relaxation, that the solution can change as it is iterated through each cycle of the nonlinear governing equations. The final code, CFD-VIEW, is a post-processor data visualization tool that enables the user to picture the output through colored planes, vectors or animation.

B. THEORY

CFD-ACE uses a finite volume approach to solve the Favre-averaged Navier Stokes (FANS), continuity and energy equations for velocity, temperature, pressure and density. The geometry is divided into a number of finite volumes, or cells, each generated by a structured grid that uses single I, J, K indices to identify a particular gridpoint and

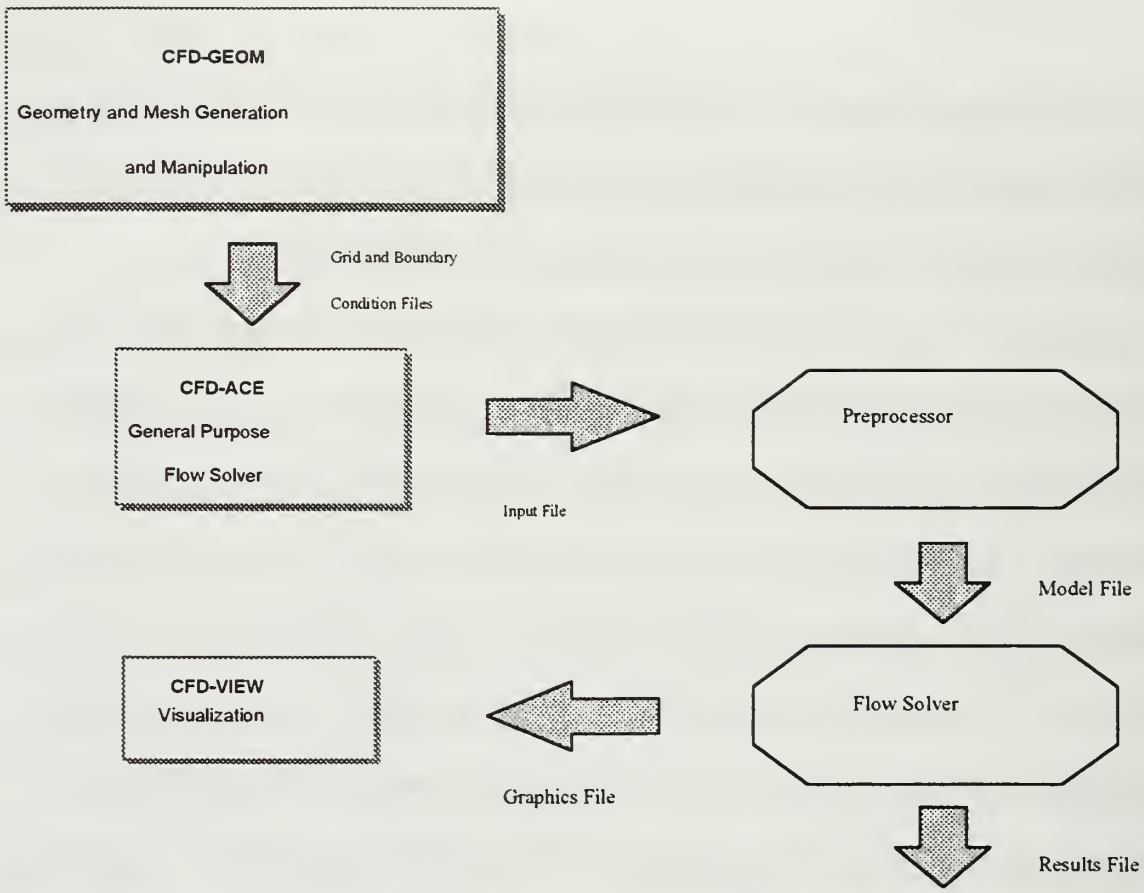

Figure 6. CFDRC Computational Fluid Dynamics Computer Code Overview. "From Ref. [6]."

direction within the finite volume. Each set of cells comprises a domain, which can be combined into a set of sud-domains to facilitate an easier construction of the overall modeled geometry. Since the CCL is a simple parallelepiped with internal cylinders, a cartesian coordinate system is used. The following is a brief summary of the discretization of the governing equations and numerical iterative process used to solve for the unknown variables, as addressed in the CFDRC Theory Manual. A more in-depth discussion of the theory can be found in the manual and its reference section. [Ref. 6, 7]

In CFD programs, the partial differential equations (PDE) that govern the transport of flow quantities are solved using numerical techniques. The techniques involve the discretization of the PDEs on a computational grid, the formation of a set of algebraic equations, and the solution of these equations at each grid point through an iterative algorithm.

The nature of the flow problem in the simulation of thermal effects in the CCL involves turbulent fluid flow and conduction, convection and radiation heat transfer. The standard fluid flow governing equations in tensor form are:

The continuity equation

$$\frac{\partial \rho}{\partial t} + \frac{\partial}{\partial x_j}(\rho u_j) = 0$$

where ρ is the fluid density and u_j is the j^{th} Cartesian component of the instantaneous velocity.

The conservation of momentum equation

$$\frac{\partial}{\partial t}(\rho u_i) + \frac{\partial}{\partial x_j}(\rho u_i u_j) = -\frac{\partial p}{\partial x_i} + \frac{\partial \tau_{ij}}{\partial x_j} + \rho f_i$$

where p is the static pressure, f_i is the body force and τ_{ij} is the viscous stress tensor defined as

$$\tau_{ij} = \mu\left(\frac{\partial u_i}{\partial x_j} + \frac{\partial u_j}{\partial x_i}\right) - \frac{2}{3}\left(\frac{\partial u_k}{\partial x_k}\right)\delta_{ij}$$

where μ is the fluid dynamic viscosity and δ_{ij} is the Kronecker delta.

And the static enthalpy equation

$$\frac{\partial}{\partial t}(\rho h) + \frac{\partial}{\partial x_j}(\rho u_j h) = -\frac{\partial q_j}{\partial x_j} + \frac{\partial p}{\partial t} + u_j\frac{\partial p}{\partial x_j} + \tau_{ij}\frac{\partial u_i}{\partial x_j}$$

where h is the enthalpy and q_j is the j component of the heat flux defined as

$$q_j = -K\frac{\partial T}{\partial x_j}$$

where K is the thermal conductivity.

All of the governing equations possess a common form and can be generalized by the equation

$$\frac{\partial}{\partial t}(\rho\phi) + \frac{\partial}{\partial x_j}(\rho u_j\phi) = \frac{\partial}{\partial x_j}\left(\Gamma\frac{\partial \phi}{\partial x_j}\right) + S_\phi$$

where the symbol ϕ may represent any of the velocity components, enthalpy or the turbulent kinetic energy and dissipation rate. S is the source term and Γ is the diffusion coefficient. For the energy equation, the diffusion coefficient is the effective diffusivity defined as

$$\Gamma = \frac{\mu}{\sigma} + \frac{\mu_t}{\sigma_t} = \frac{K}{c_p}$$

where c_p is the specific heat, σ is the Prandtl number and the subscript t represents turbulent quantities.

The governing equations are discretized using a finite volume approach. As mentioned above, the model is divided into discrete sub-domains, or cells. CFD-ACE employs a co-located cell-centered variable arrangement where all flow variables and fluid properties are stored at the cell center P.

The following equation is derived for each variable in each finite volume

$$a_P\phi_P = a_E\phi_E + a_W\phi_W + a_N\phi_N + a_S\phi_S + a_H\phi_H + a_L\phi_L + S$$

where P is the center location and E, W, N, S, H and L represent values of the center of the six adjacent cells. The variable 'a' represents the effects of convection and diffusion across the cell faces.

Using the east face (E) as an example, the convection and diffusion discretized terms are written as follows:

Convection Term

$$-\rho_E A_E u_E \phi_E$$

Diffusion Term

$$-\Gamma_E \frac{(\phi_P - \phi_E)}{\Delta_E} A_E$$

The source term, S, contains terms other than the convection and diffusion effects, such as the pressure gradient, boundary conditions and other algorithm dependent effects (i.e., under-relaxation). A_E is the area across the east face and Δ_E is the distance from the cell center to the center of the adjacent face.

The differencing scheme determines how the cell face values are calculated. The differencing scheme used in this model is the first-order upwind scheme. In this scheme,

ϕ_E is taken to be the value of ϕ at the upstream grid point, which depends on the flow direction at the cell face E:

$$\phi_E = \phi_P \quad \text{if } u_E \geq 0$$
$$\phi_E = \phi_E \quad \text{if } u_E < 0$$

The continuity equation is not written in the form of the general convection-diffusion equation, as were the conservation of momentum and energy equations. Since, the pressure and velocity terms are strongly coupled in the momentum equation, the pressure gradient term is accounted for differently than the other source terms.

For each iteration, the pressure and velocity terms will equal the current value plus some unknown correction according to the following equation:

$$\mathbf{p} = \mathbf{p}^* + \mathbf{p}'$$
$$\mathbf{u} = \mathbf{u}^* + \mathbf{u}'$$

When the correction approaches zero then we can be reseasonably confident that the value of pressure and velocity are accurate for the given flow field. The values of these corrections are determined by using the momentum equation to develop a functional relationship between the pressure and velocity fields. The pressures are then substituted for the velocities into a discretized continuity equation, and the simultaneous matrix of equations is solved over the entire flow field. The solution procedure is summarized in Figure 7. NITERP is the number of iterations for the continuity equation. NTSTEP is the number of time steps involved. NITER is the number of iterations of the system of equations for each time step.

Figure 7 shows that for each iteration, within a transient time step, a system of equations must be solved for each dependent variable. A benefit to using the structured grid geometry is that it produces a banded matrix of coefficients for each dependent

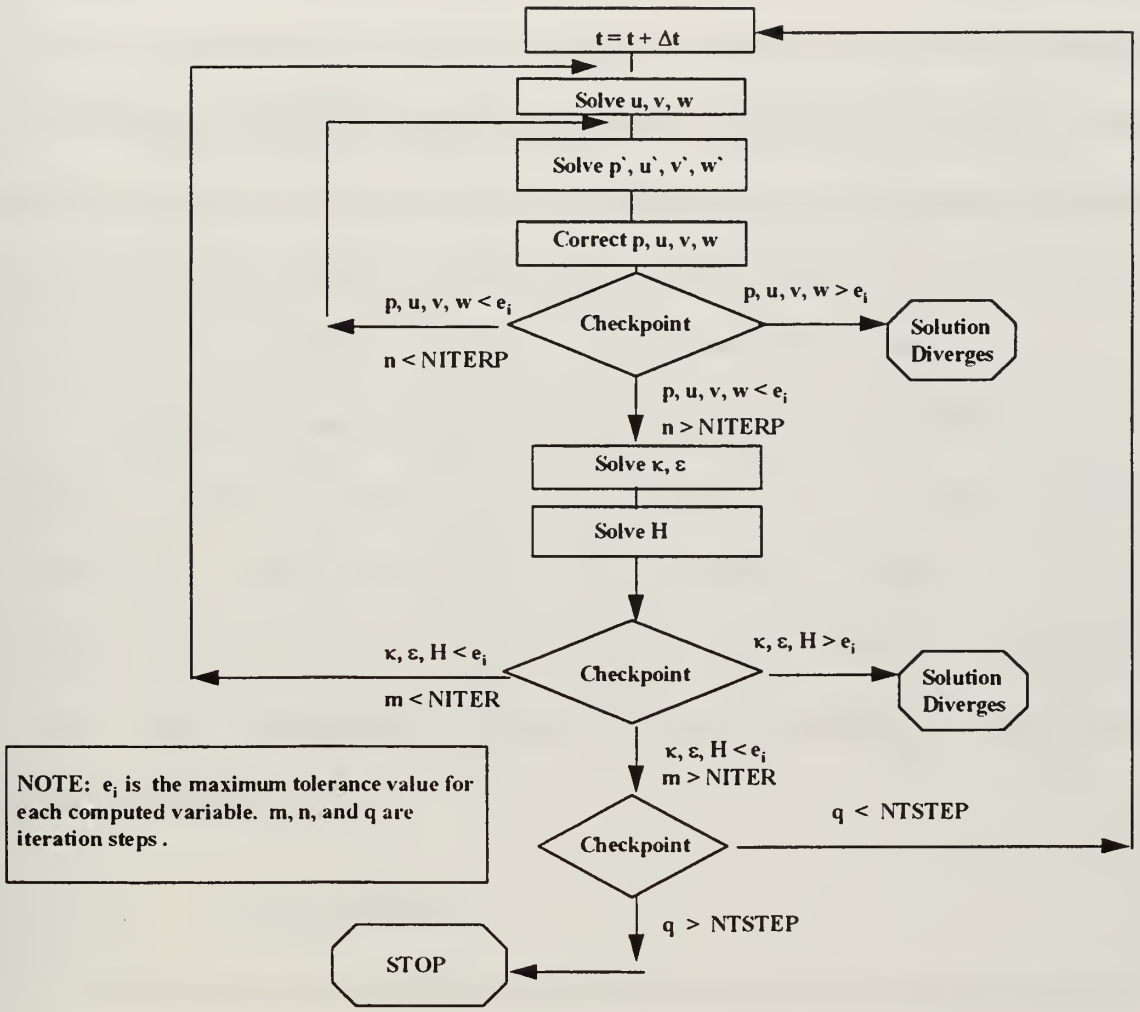

Figure 7. CFD-ACE Flow Solver Solution Procedure. "After Ref. [6]."

variable. The solution methods for each system of equations are Backward Euler and a version of the Forward Differencing Technique.

In order to ensure that the solution for each iteration does not diverge, under-relaxation must be applied to the dependent and auxiliary variables. Under-relaxation constrains the amount that each variable can change from one iteration to the next. The dependent variables (u, v, w, k, ε, H) are modified using an Inertial Factor. A linear under-relaxation technique is applied to the auxiliary variables (p, T, μ, ρ).

III. MODEL

A. GEOMETRY

1. Selection of CCL Module

Since the CCL Concept is under development as an alternative weapons system for the Surface Combatant of the 21st century (DD-21), the DDG-51 Flight II destroyer was used as the platform for construction of the CCL model in CFD-GEOM. The A-module standard size was selected since it is designed to hold 35 Tomahawk missiles and thus fit in the DDG-51's forward missile launcher. Figure 8 shows the dimensions of the A-module and an equidistant distribution of 35 Tomahawk missiles inside.

In order to develop a credible fire scenerio for the forward launcher, the fire was placed in a single compartment, aft of the forward launcher, to simulate the same conditions experienced by the STARK mass conflagration (Figure 9). The six compartments, adjacent to the common bulkhead of the CCL enclosure, are assumed to occupy an entire deck, without any intermediate longitudinal bulkheads or partitions to further contain the fire.

2. Grid Distribution

The simulations were carried out through the use of a Silicon Graphics Indigo XS-4000 workstation with 96 megabytes of RAM and an external 9 gigabyte hard drive to supplement the internal hard drive. The limitations of the computations using this workstation and the CFD-ACE version 2.0 program, updated as of 01 March 1997, were 65,000 grid points and 500 boundary conditions per domain.

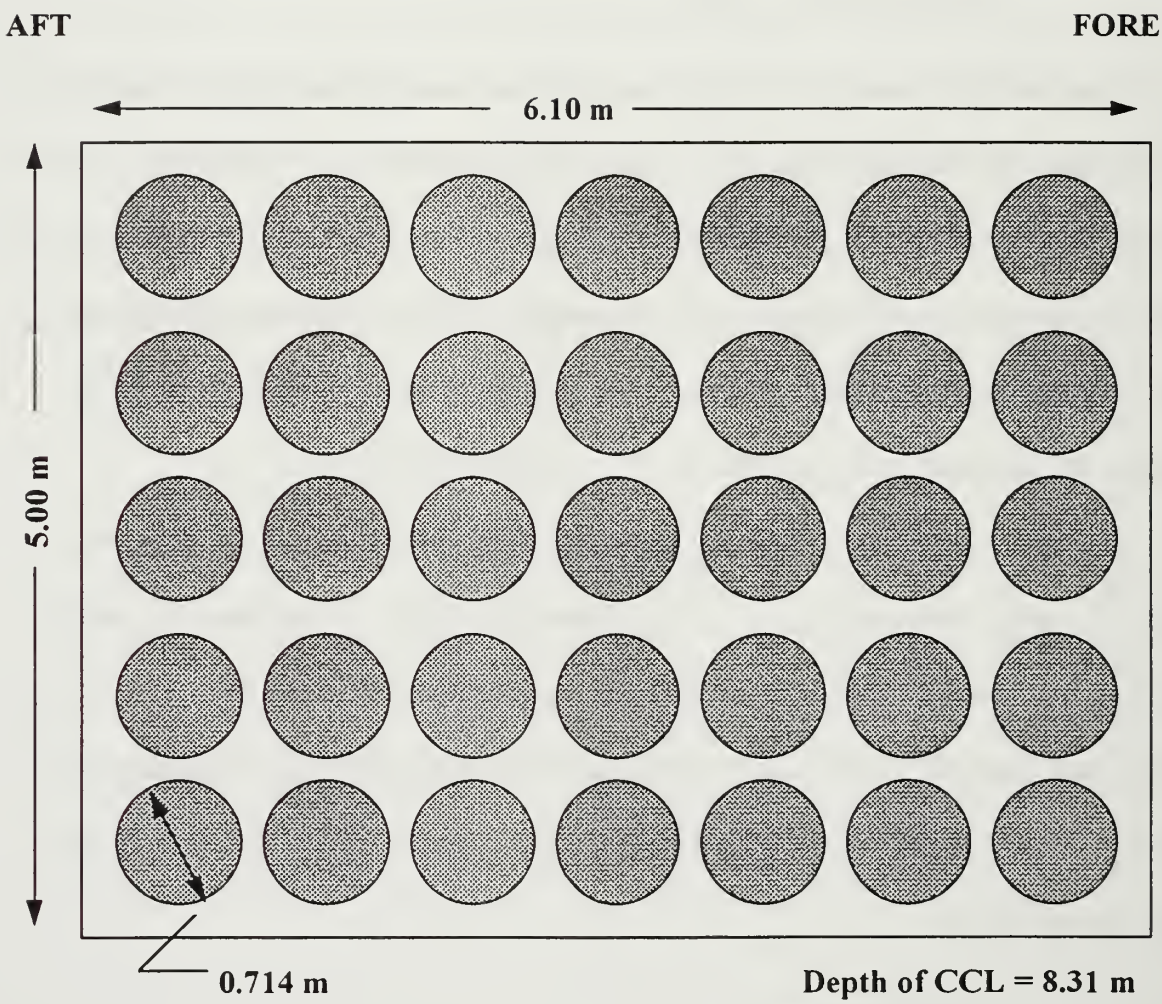

Figure 8. A-Module Standard Size with 35 Tomahawk Missiles.

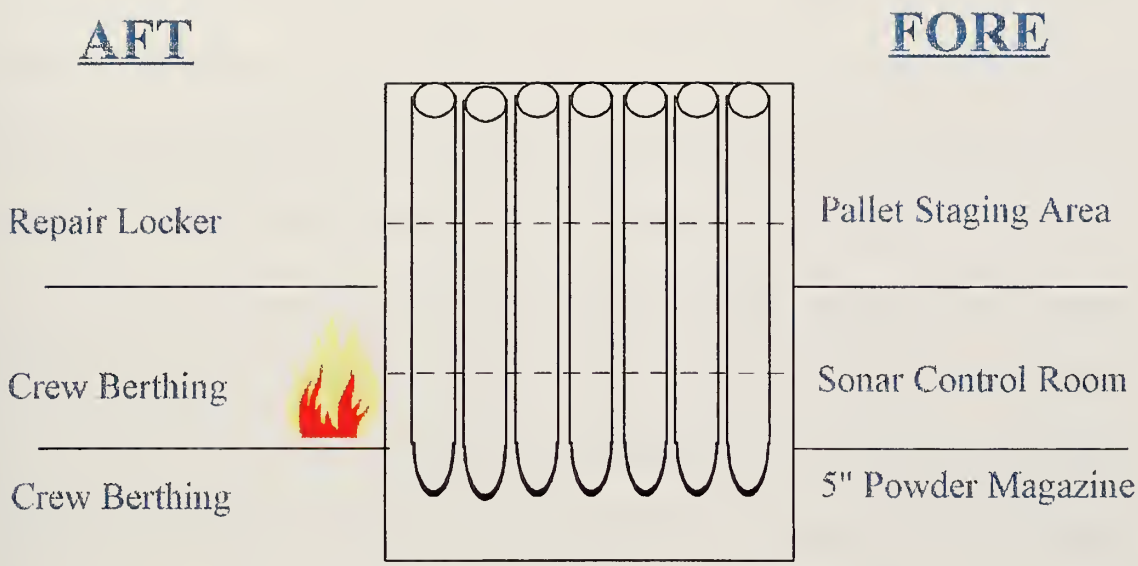

Figure 9. Sideview of the DDG-51 Forward Missile Launcher.

The initial simulations on the A-module involved a geometric model of the entire launcher, including the correct dimensions and material specifications of the HY-80 horizontal steel supports. The canister geometry initially included two concentric titanium cylinders, separated by air, and an internal aluminum core. This overall geometry exceeded the allowable number of grid points and boundary conditions, and was therefore reduced to the center one-third of the missile launcher, located between the two steel supports, with the canister geometry changed to include only an outer cylinder of solid titanium. The height of the center section is 2.33 meters.

The geometry included in the model was reduced for the following reasons. Initial simulations on the entire missile launcher, involving only a single mode of heat transfer (i.e., conduction or convection) showed that the sections of the canisters located adjacent to the fire were directly affected by the thermal effects, as expected, and those sections that were separated by a steel support received only minor residual effects. Therefore, since the fire was located in the center compartment aft of the launcher, the decision was made to model only the center section of the CCL. Additionally, this selection was made because it tended to accurately model the location of the solid and liquid propellants of the missiles contained in the launcher. The selection of solid canisters was based entirely on the conservation of nodal points, and the determination that the effects between the canister walls were minimal in comparison to the large scale of the CCL model.

Based on the updated reduced model of the CCL, the first simulations were conducted on a launcher that contained only the single aft row of canisters immediately adjacent to the affected fire boundary. Figure 10 shows the distribution of nodal points along the edges of this model. The vertical edges each contained 15 nodal points and the

transverse edges each contained 34.

A second row of canisters was then added directly behind the first row to gain an understanding of how the buildup of canisters affected the row immediately adjacent to the affected fire boundary. Figure 11 shows the distribution of nodal points along the edges of this model, with the vertical and transverse edges containing the same number of nodal points as Figure 10.

In the construction of the single- and double-row models, a high level of accuracy was not anticipated for the initial simulations due to the small number of nodal points, and hence large nodal point spacing. A crude method used to verify the accuracy of the output data was to vary the number of nodal points in the longitudinal direction. A single direction was chosen in order to maintain consistency throughout the computer runs. The longitudinal direction was the one chosen because it reflected the greatest change in the temperature gradients.

Figure 12 shows the distribution of nodal points in the longitudinal direction for the single- and double-row models. Note, the grid points within the canisters were monitored by the CFD-ACE flow solver program and thus never altered.

B. THERMOPHYSICAL MODEL

Once CFD-GEOM has determined the grid and boundary condition locations and generated files containing this information, the files are then read into the CFD-ACE code. The CFD-ACE flow solver code allows the user to choose thermophysical properties, modes of heat transfer, boundary condition values, turbulent flow models and numerical solution methods.

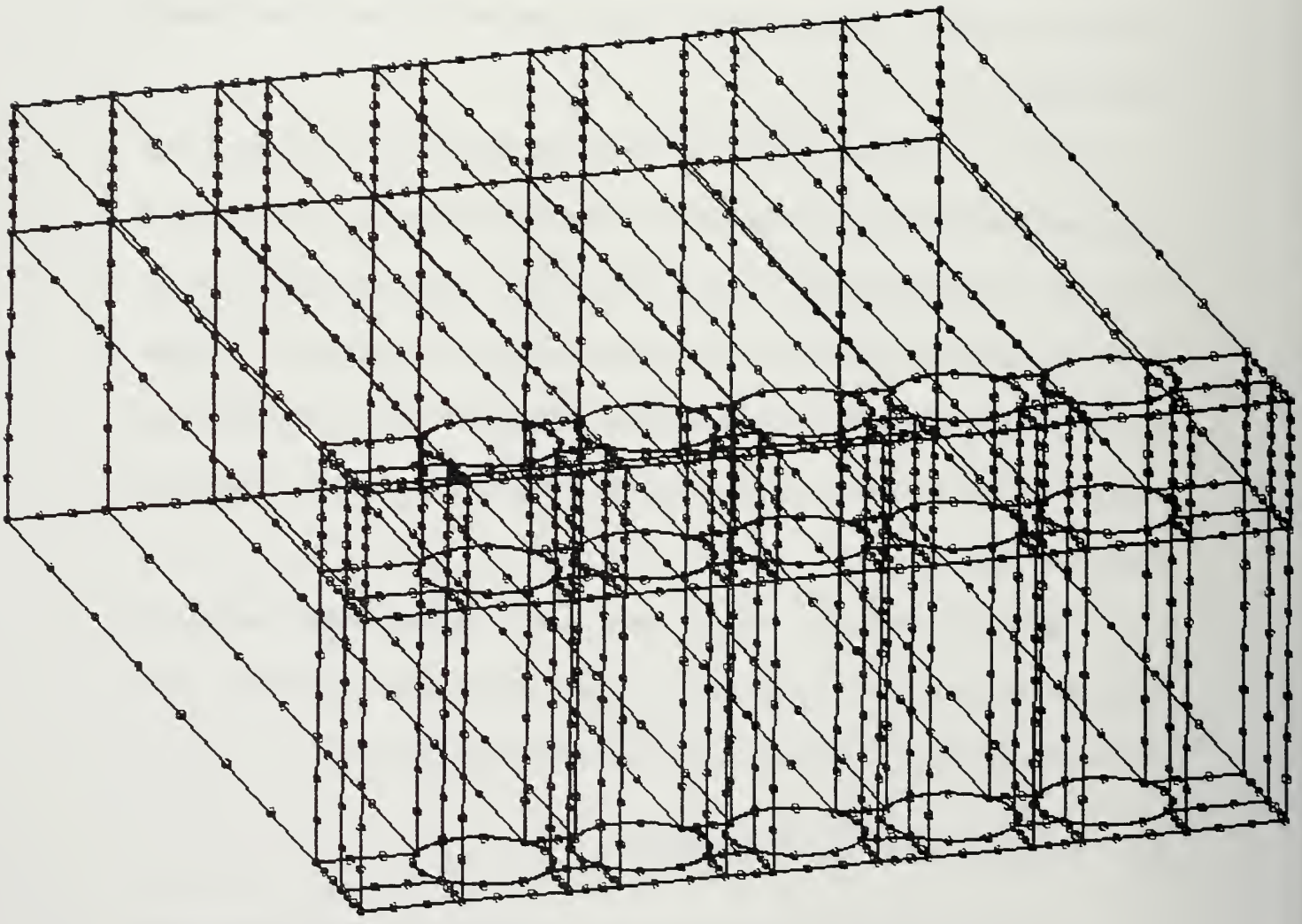

Figure 10. Grid Distribution for a Single Row of CCL Canisters.

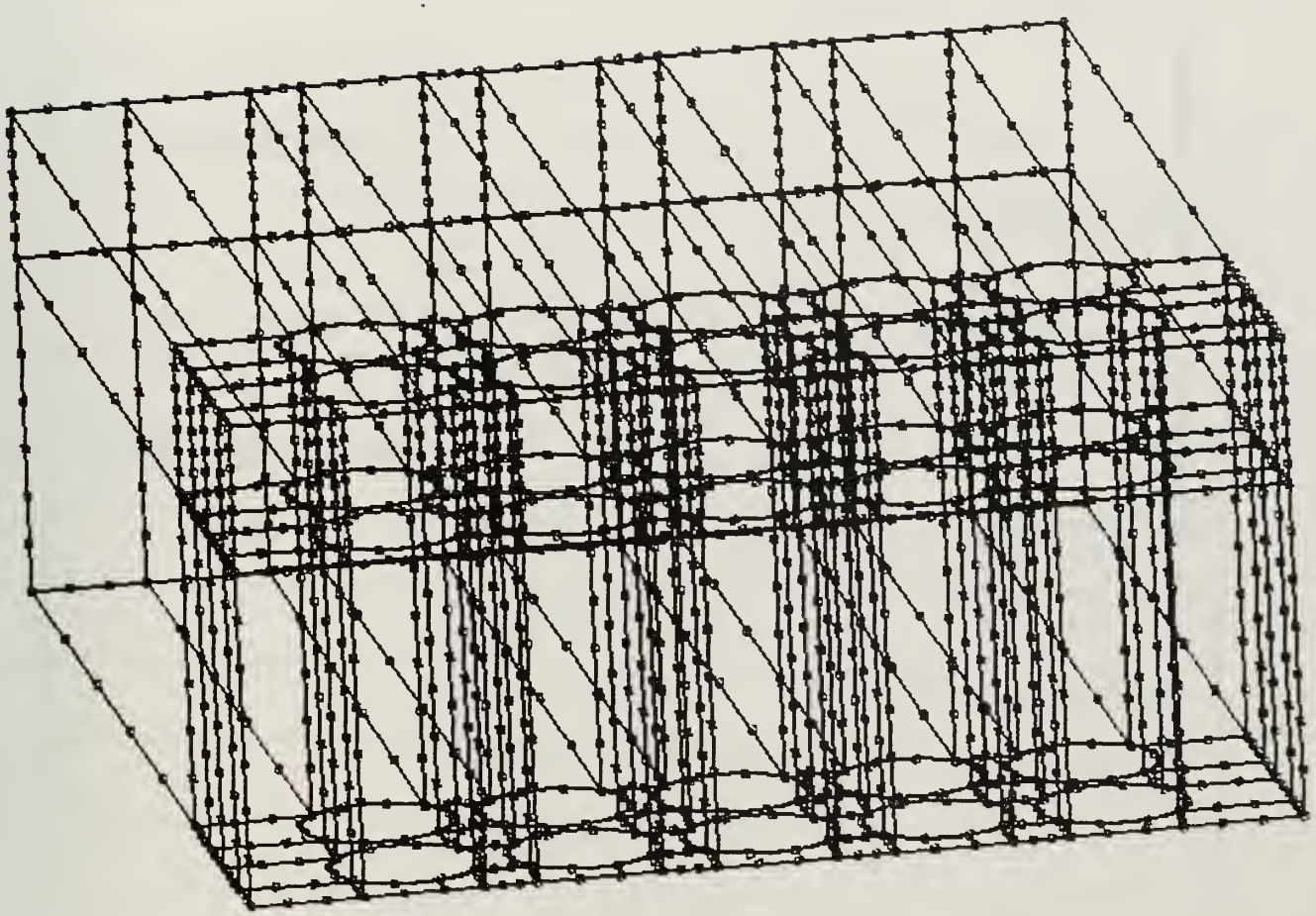

Figure 11. Grid Distribution for Two Rows of CCL Canisters.

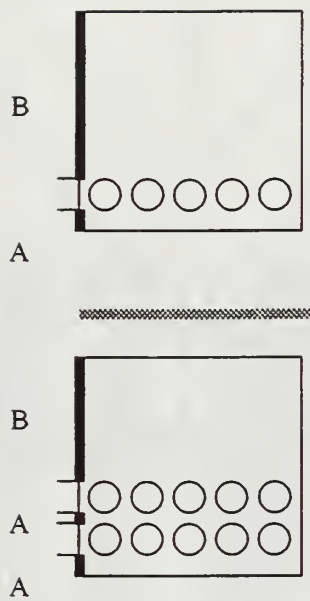

	A Segments	Segment B
Round 1 (Total 14)	4	8
Round 2 (Total 18)	4	12
Round 3 (Total 28)	6	20
Round 4 (Total 18)	2	4
Round 5 (Total 24)	3	8

Figure 12. The Total Number of Nodal Points on Each Longitudinal Edge.

The goal of the computations was to input enough data into the flow solver algorithm to accurately visualize the thermal effects within the CCL and to determine the elapsed time until propellant cook-off, while keeping the model simple, so as to limit the time required to run each simulation. Therefore, the canisters were modeled as solid titanium cylinders and the steel bulkheads and supports were given an emissivity equivalent to HY-80 steel [Ref. 8]. Table 3 lists the material property information used in all of the CFD-ACE simulations.

TITANIUM CANISTERS	CONDUCTIVITY	21.9 W / m K
	SPECIFIC HEAT	522 J / kg K
	DENSITY	4930 kg / m^3
	EMISSIVITY	0.6
STEEL STRUCTURES	EMISSIVITY	0.82
AIR	KINEMATIC VISCOSITY	1.71 E-5 m^2 / sec
	SPECIFIC HEAT	1000 J / kg K
	DENSITY	Temperature Dependent
	MOLECULAR WEIGHT	29 kg / kmol
	PRANDTL NUMBER	0.7
	SCATTERING	0.0
	ABSORPTIVITY	0.0

Table 3. Thermophysical Property Data

Each simulation was carried out as a turbulent incompressible flow with surface radiation, conduction and non-Boussinesq natural convection heat transfer. Table 4 lists additional information used in the CFD-ACE simulations. The input file is contained in Appendix C.

TIME DEPENDENCE		TRANSIENT
TURBULENCE		K-EPSILON MODEL
		$Pr_t = 1.0$
BODY FORCES		$g = -9.81\ m / sec^2$
INITIAL CONDITIONS	TEMPERATURE	300 K
	TURBULENT KINETIC ENERGY	5
	DISSIPATION RATE	25
SPATIAL METHOD		UPWIND
TIME METHOD		BACKWARD EULER

Table 4. CFD-ACE Input Data

C. FIRE SCENERIOS

The simulated fire scenerios applied to the CCL model represent two of the most severe mass conflagrations that face our warships today. In order to realistically apply each of these boundary conditions, the maximum temperature and rate of temperature increase from ambient conditions must be included in the input file of the computer program.

The first scenerio analyzed is indicative of the severe inferno fueled by an anti-ship missile's unburned solid propellant, as experienced by the STARK in 1987. The maximum temperature used to model this fire is 3000° F (1922 K), and climbs rapidly from ambient conditions to this maximum temperature in 30 seconds, where it is maintained for the duration of the simulation (Figure 13) [Ref. 3].

The second scenerio represents a less severe, though more likely to occur, fire fueled by a ruptured or leaking fuel oil storage tank, as faced by the INGERSOLL in 1992. The maximum temperature used to model this fire is 2000° F (1366 K), and climbs from ambient to this maximum temperature in a relatively slower rate of five minutes [Ref. 3]. Figure 14 shows the plot of this fire scenerio, in addition to the points along the curve that are added to the CFD-ACE input file.

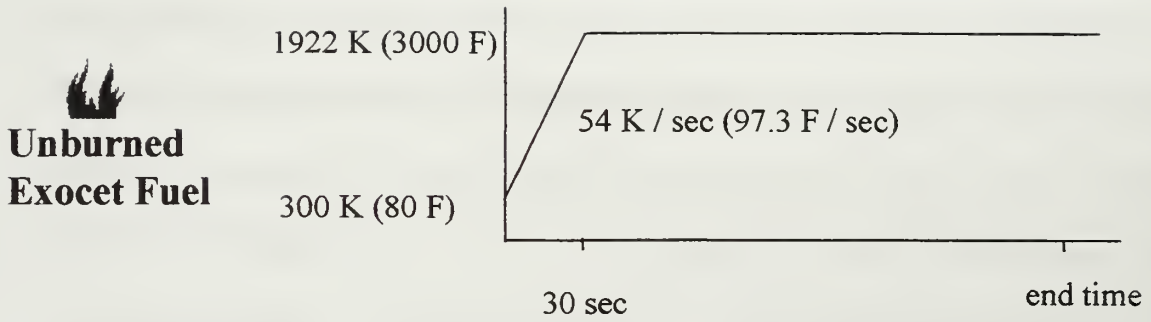

Time (sec)	0	12	24	36
Temperature (K)	300	649	1298	1922

Figure 13. Unburned Exocet Missile Rocket Propellant Fire Scenerio. "After Ref. [3]."

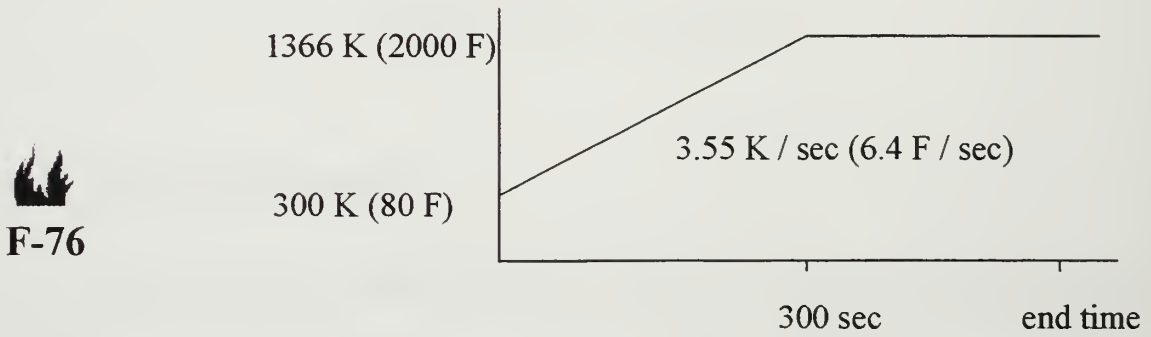

Time (sec)	0	100	200	300
Temperature (K)	300	655	1010	1365

Figure 14. Common Shipboard Fuel Fire Scenerio. "After Ref. [3]."

IV. RESULTS

This study models the thermal effects on the center section of a single-row and two-row CCL module using the CFD-ACE program. An unburned Exocet missile propellant fire and an F-76 shipboard fuel fire are used to simulate the scenerios along the affected boundary. The remaining three walls and upper and lower steel supports are modeled as adiabatic boundaries since the amount of heat conducted through them is negligible to the amount of heat transfer within the center section.

Once the geometric, thermophysical and flow models are determined in the CFD-ACE and CFD-GEOM programs, the remaining challenge is to decide on the length of time for the processor to run and the size of the time step to use. Using the nodal distribution of round 1 (see Figure 12), a comparison was made between the following four runs:

1. Time Interval: 0 - 60 seconds, Time Step: 1 second
2. Time Interval: 0 - 600 seconds, Time Step: 10 seconds
3. Time Interval: 0 - 1800 seconds, Time Step: 10 seconds
4. Time Interval: 0 - 3600 seconds, Time Step: 60 seconds

The decision was made to use a time interval of 600 seconds (10 minutes) with a time step of 10 seconds for all of the simulations. The larger time intervals and time step produced poor residual plots and ran for an extensive amount of time. None of the simulations reached the critical cook-off temperatures in less than one minute, therefore this time interval was determined to be too short.

Although a time step of 10 seconds may have been judged to be too long for an accurate solution, the amount of time that these simulations took under this condition was roughly 3 to 4.5 days of continous processing. Decreasing the size of the time step would have been unproductive to this study.

CFD-ACE allows the user to input a set of locations that the code monitors for changes in selected variables during each simulation (see Appendix C). The value is monitored at the center of each cell, and is identified in the input file by its domain and the indices of the top left nodal point of the cell. An example of the code used in the input file can be found at the end of Appendix C.

In the CCL simulations, the temperatures within the center canister of the row adjacent to the fire boundary were monitored at a height of 0.69 meters (2 nodal points) above the bottom support, at three internal locations. This height was determined to roughly estimate the location of the missile's propellant within the canister. Figure 15 shows the resultant times to reach the critical cook-off temperatures of the solid and liquid propellants for rounds three and five of the Exocet and F-76 fire scenerios. The time-temperature profiles for all five rounds of the two fire scenerios can be found in Appendices D through M.

Additional aspects of the temperature profiles at a height of 0.69 meters are also generated using the CFD-VIEW program. One profile uses a line probe that is sliced through the center canister of the front row, just left of centerline, to display the temperature as a function of longitudinal displacement from the fire boundary. Figures 16 through 20 show these images for the Exocet fire scenerios and Figures 21 through 25 show the F-76 fire scenerios.

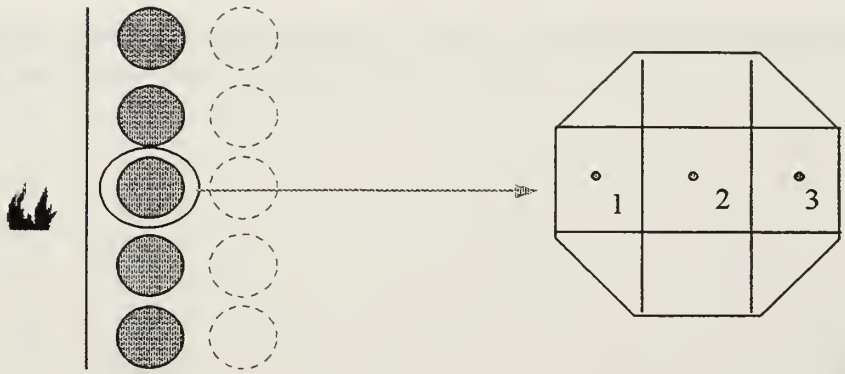

F-76

		422 K	511 K
1 Row	1	6.7 min	10.8 min
	2	17.9 min	28.3 min
	3	Undetermined	Undetermined
2 Rows	1	10.0 min	15.4 min
	2	10.7 min	15.6 min
	3	50.0 min	82.9 min

Exocet

		422 K	511 K
1 Row	1	1.5 min	3.0 min
	2	5.8 min	9.2 min
	3	49.0 min	82.0 min
2 Rows	1	2.5 min	4.2 min
	2	3.0 min	4.2 min
	3	13.5 min	22.0 min

NOTE: 422 K = Cook-off Temperature of the Solid Propellant. 511 K = Ignition Temperature of the Liquid Fuel

Figure 15. Elapsed Times to Cook-Off for CCL Simulation Rounds Three and Five.

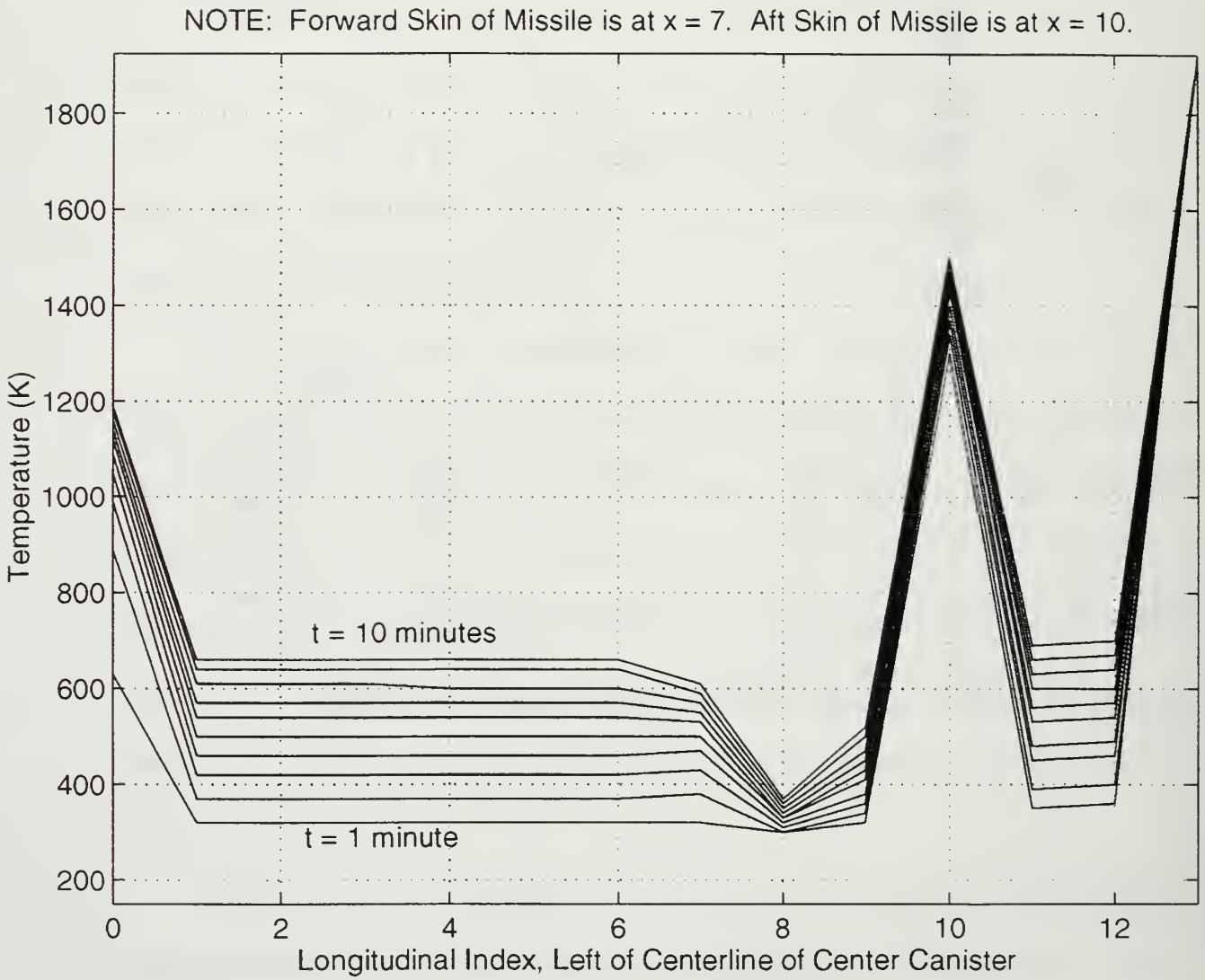

Figure 16. Temperature vs. Longitudinal Index, Displaced One Nodal Point Left of Centerline for Round 1 of the Exocet Fire Scenerio.

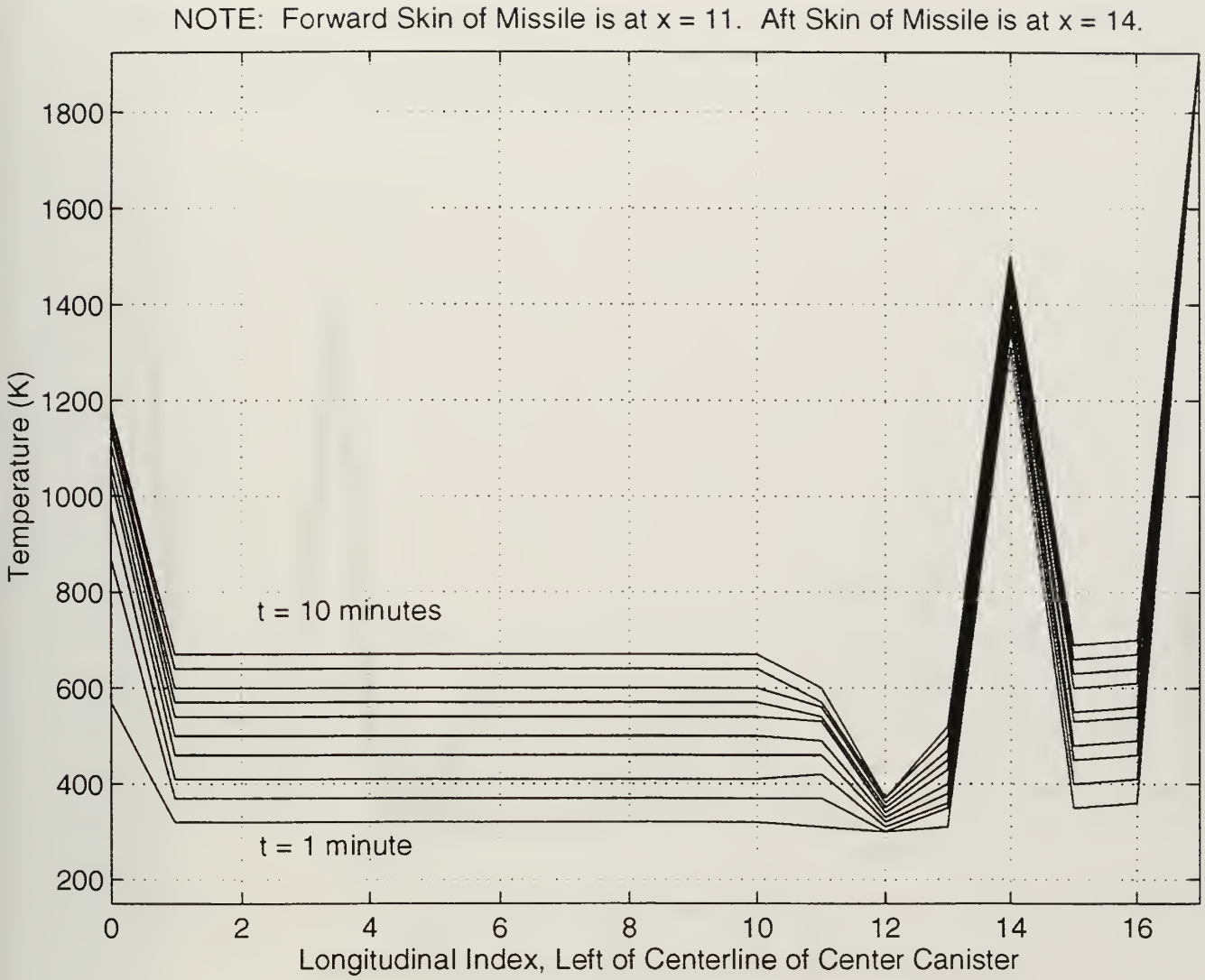

Figure 17. Temperature vs. Longitudinal Index, Displaced One Nodal Point Left of Centerline for Round 2 of the Exocet Fire Scenerio.

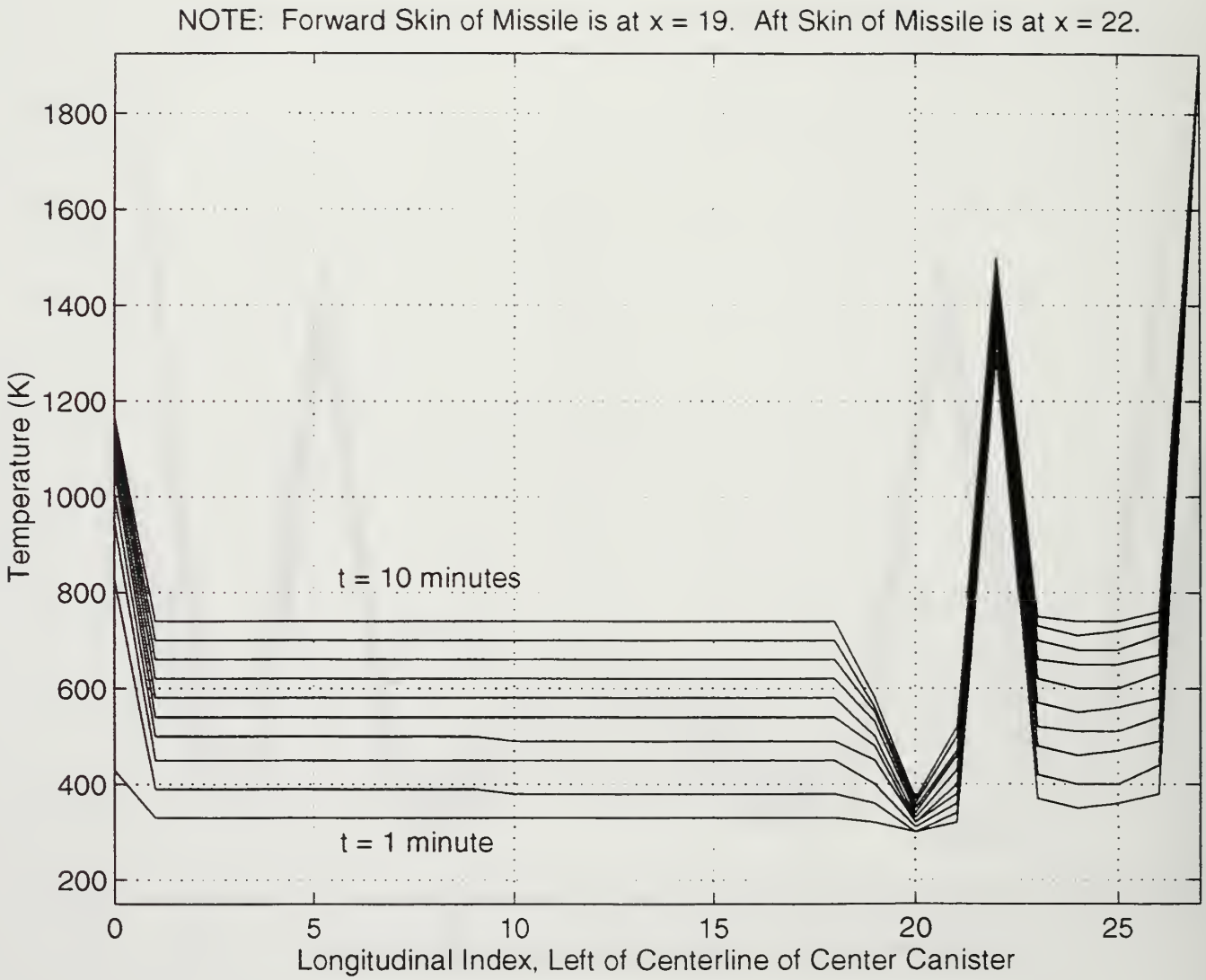

Figure 18. Temperature vs. Longitudinal Index, Displaced One Nodal Point Left of Centerline for Round 3 of the Exocet Fire Scenerio.

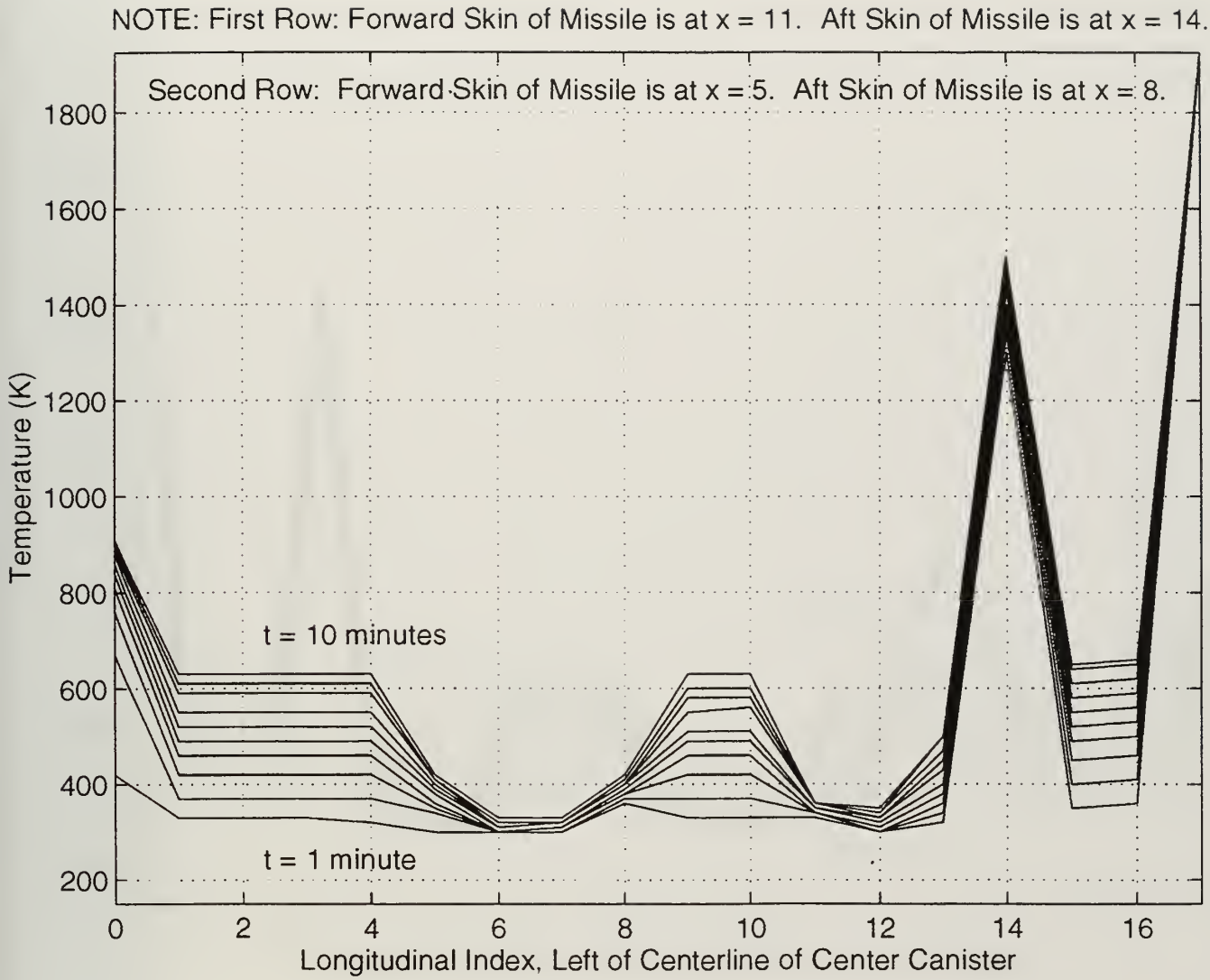

Figure 19. Temperature vs. Longitudinal Index, Displaced One Nodal Point Left of Centerline for Round 4 of the Exocet Fire Scenerio.

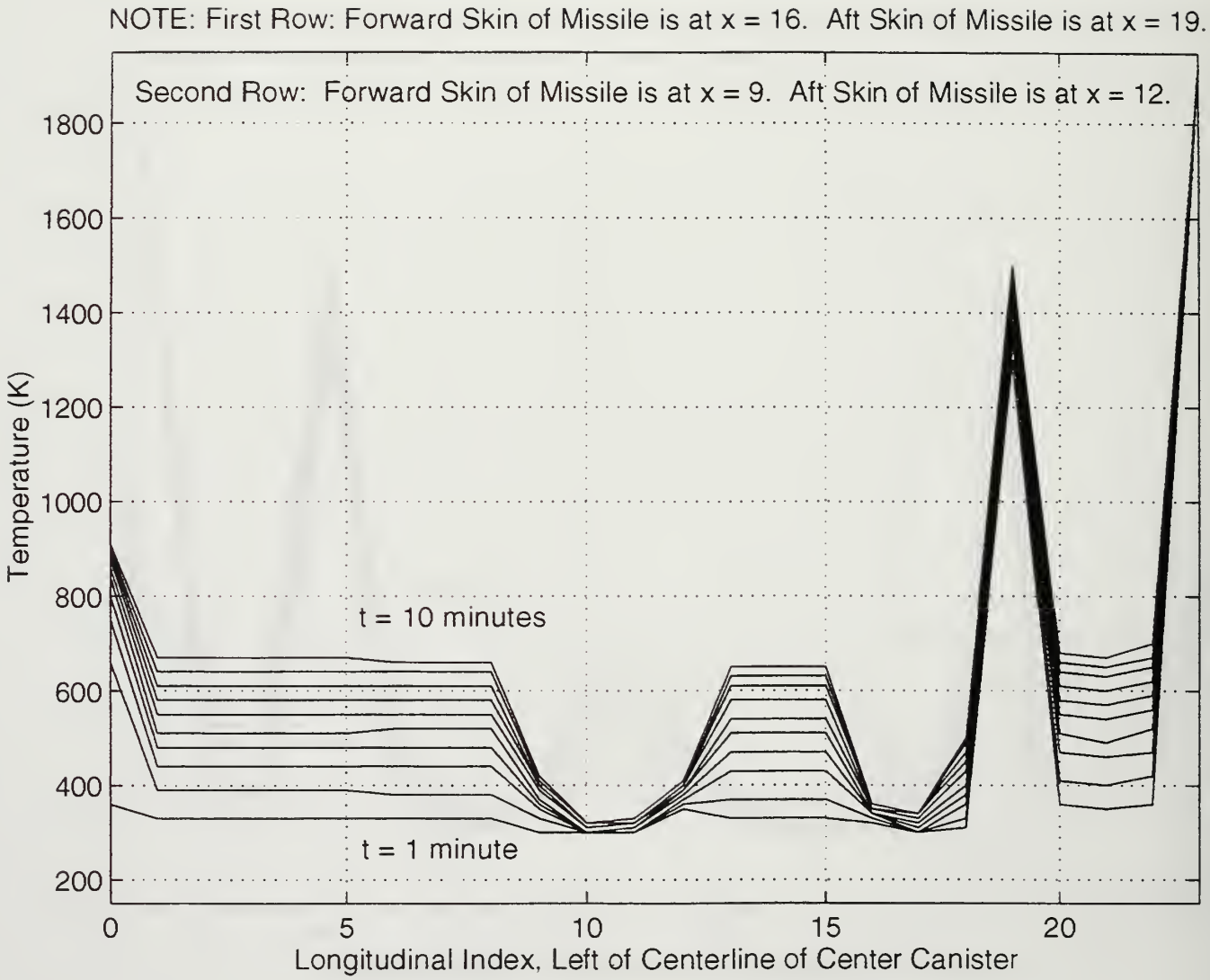

Figure 20. Temperature vs. Longitudinal Index, Displaced One Nodal Point Left of Centerline for Round 5 of the Exocet Fire Scenerio.

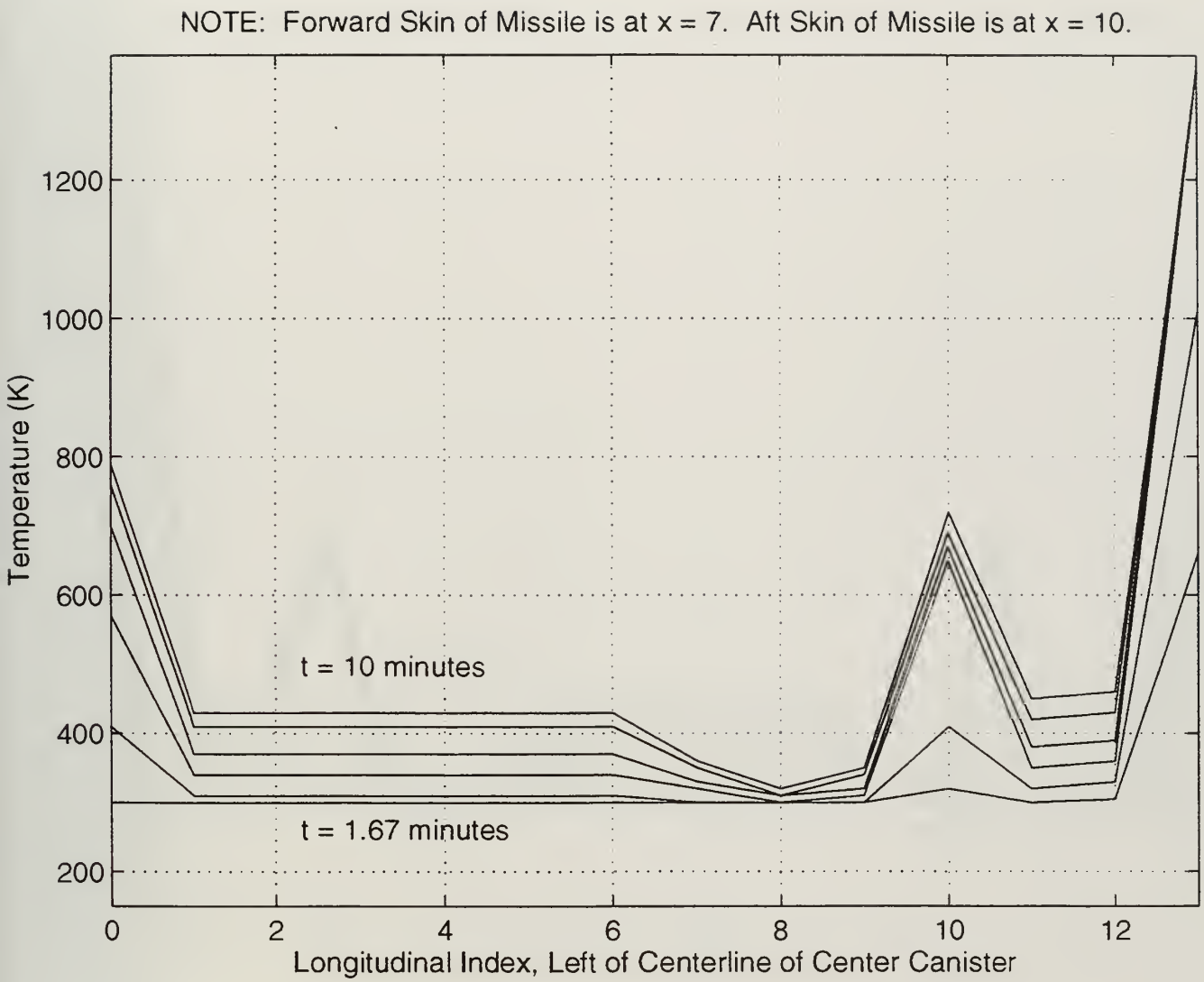

Figure 21. Temperature vs. Longitudinal Index, Displaced One Nodal Point Left of Centerline for Round 1 of the F-76 Fire Scenerio.

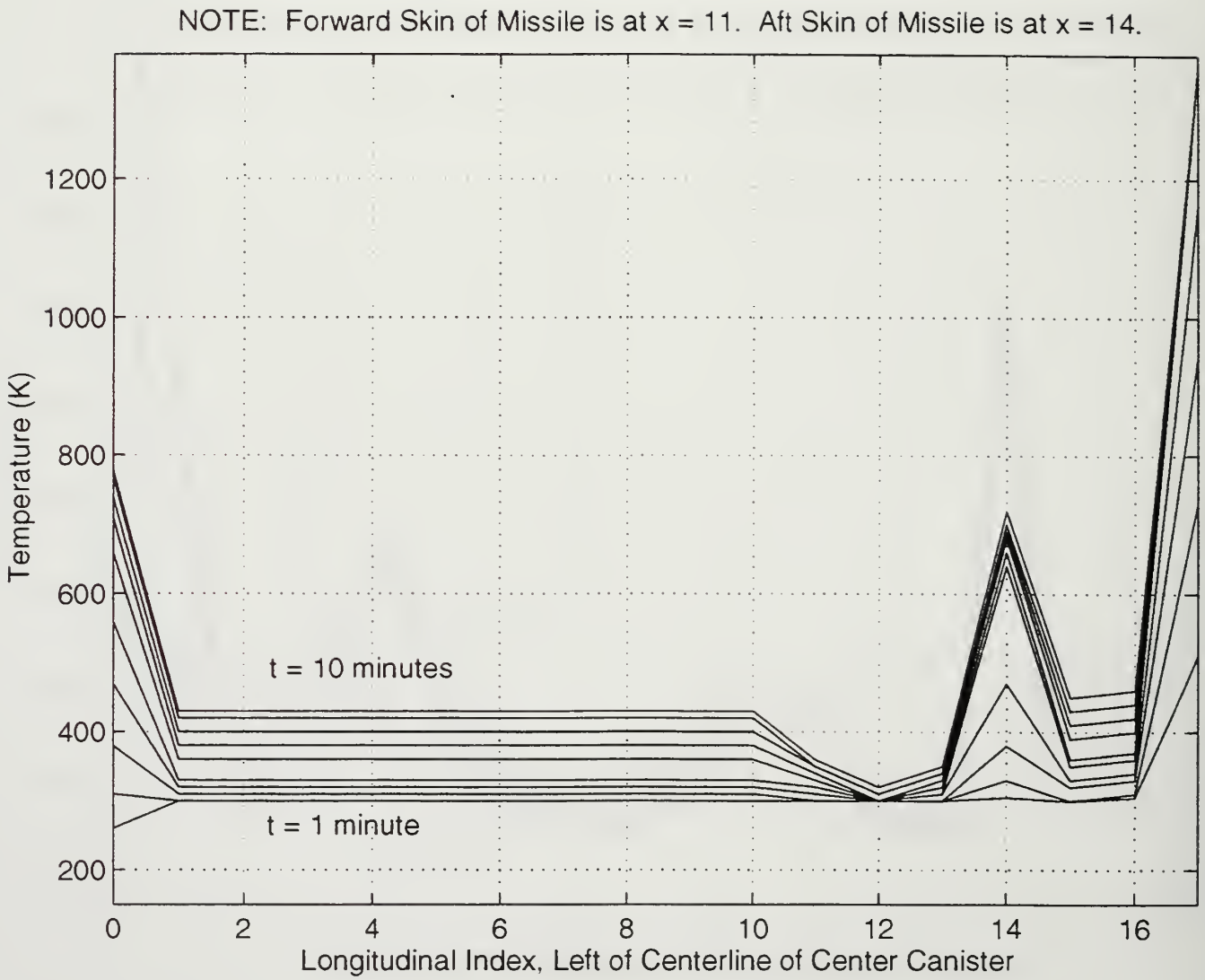

Figure 22. Temperature vs. Longitudinal Index, Displaced One Nodal Point Left of Centerline for Round 2 of the F-76 Fire Scenerio.

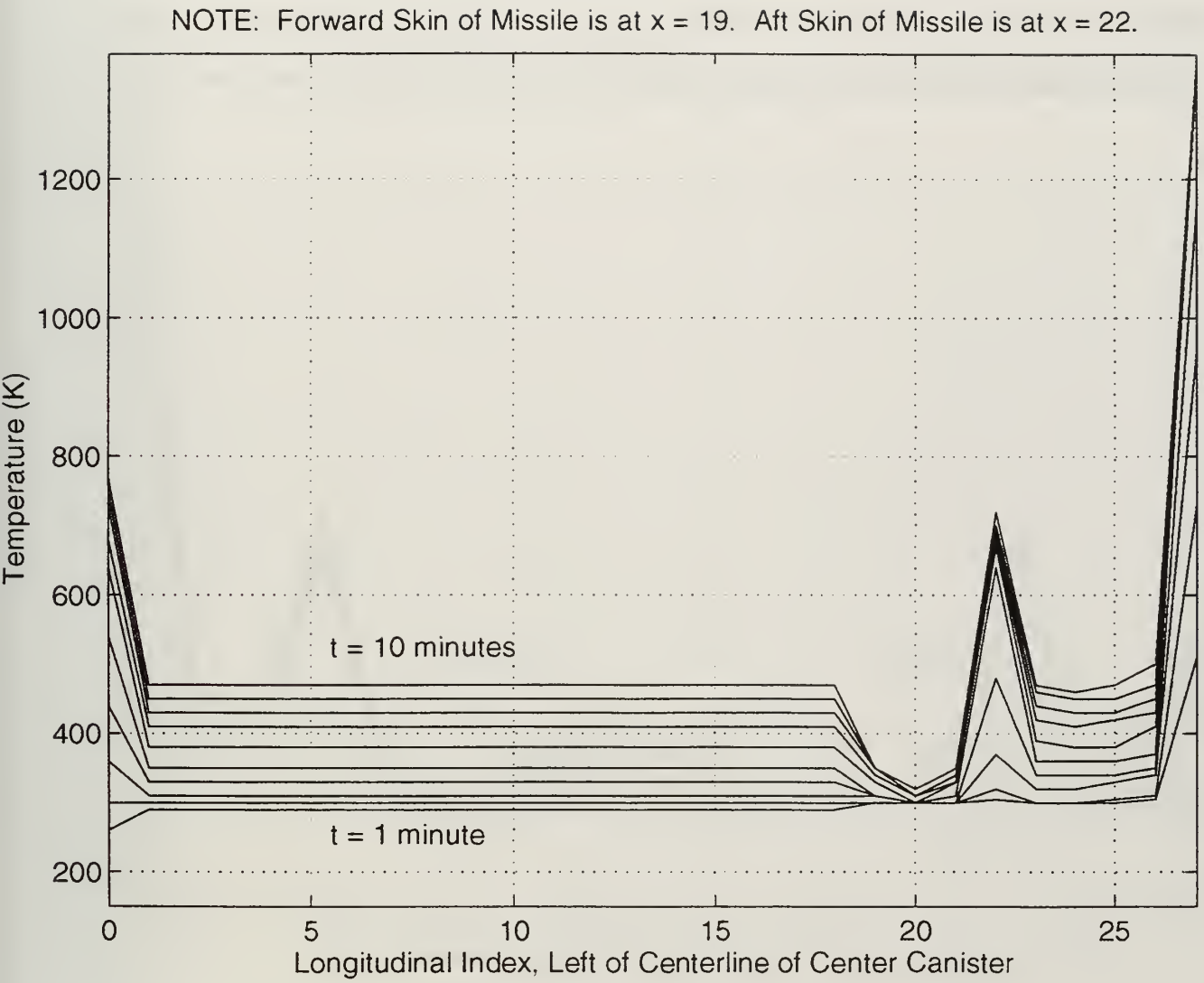

Figure 23. Temperature vs. Longitudinal Index, Displaced One Nodal Point Left of Centerline for Round 3 of the F-76 Fire Scenerio.

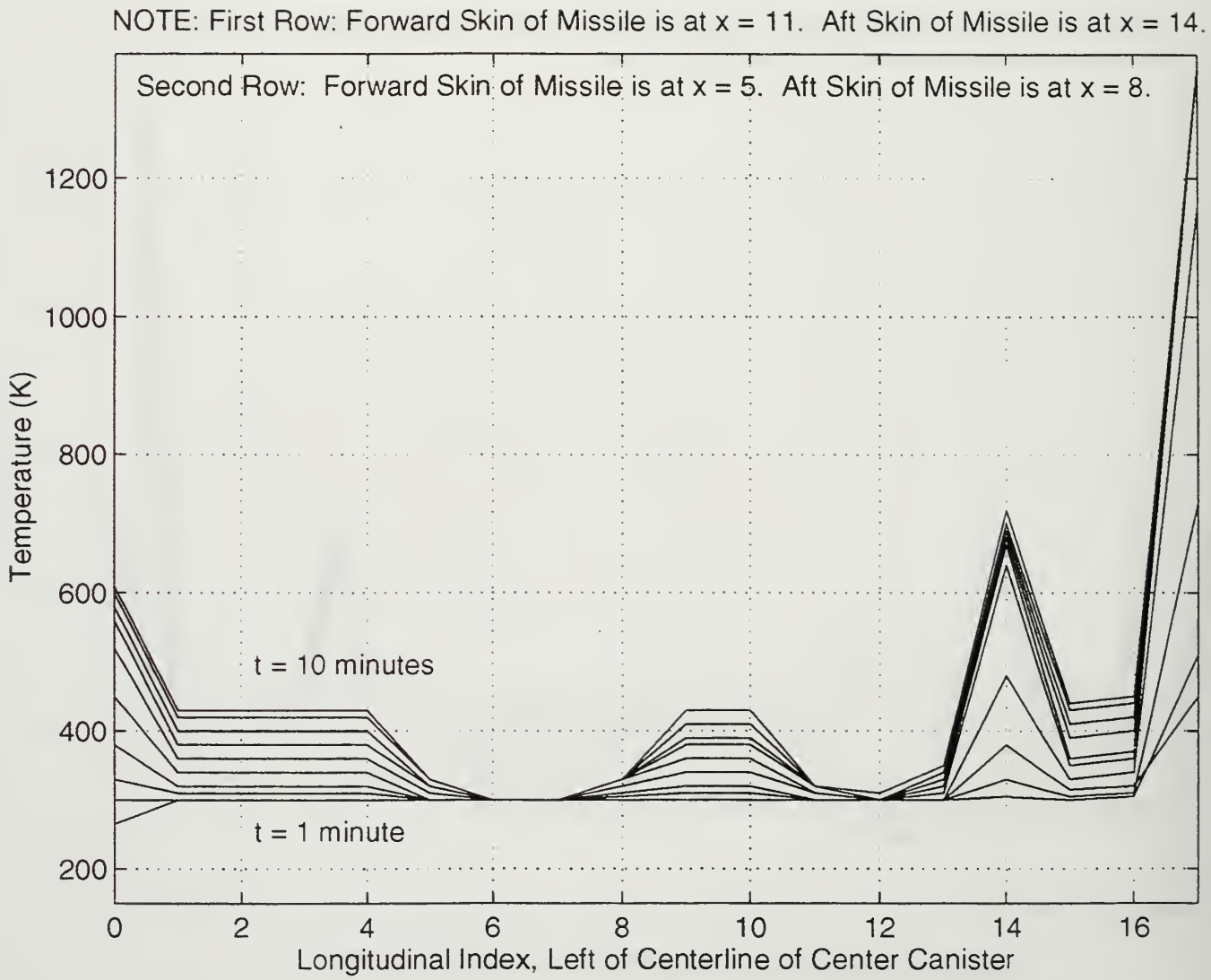

Figure 24. Temperature vs. Longitudinal Index, Displaced One Nodal Point Left of Centerline for Round 4 of the F-76 Fire Scenerio.

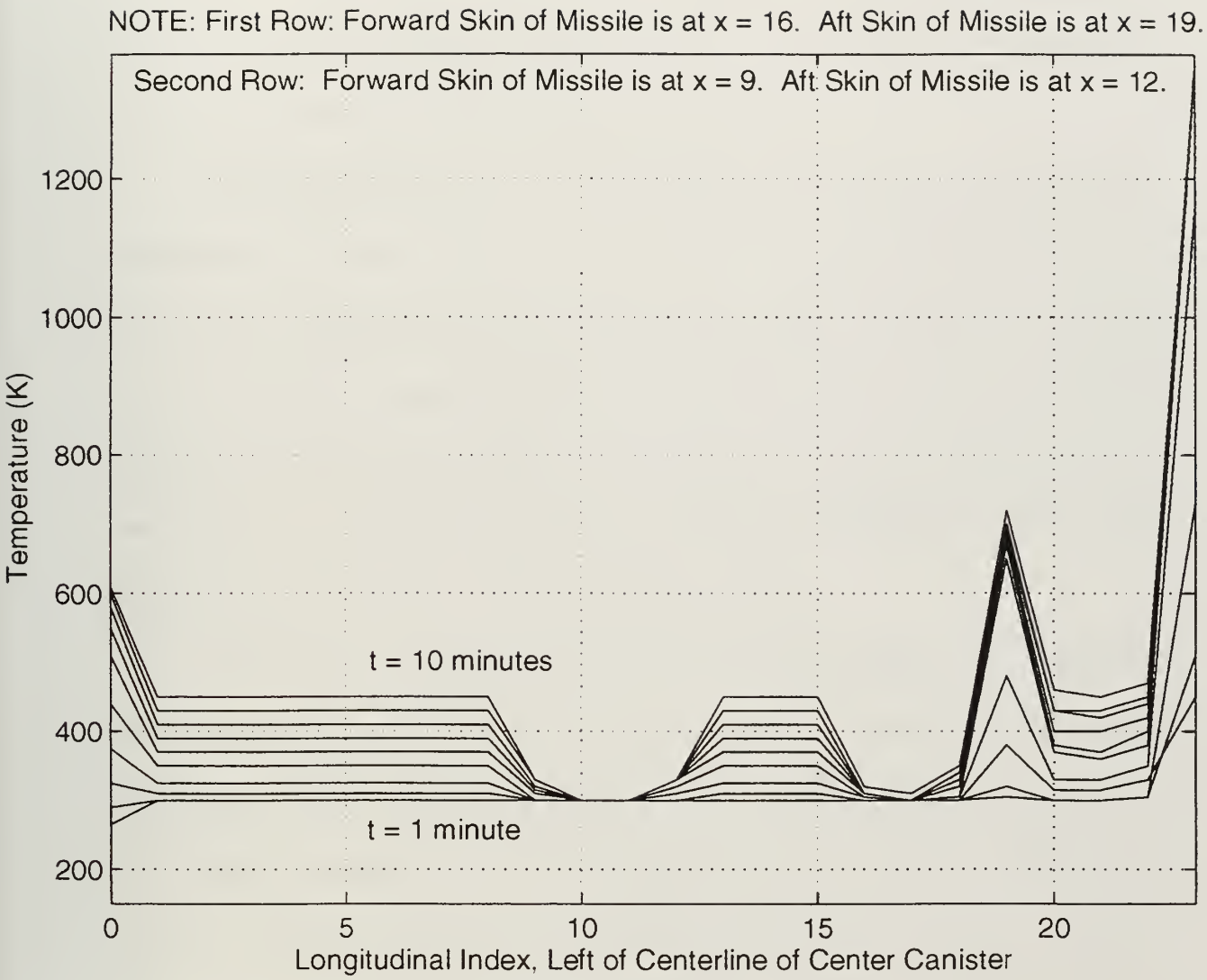

Figure 25. Temperature vs. Longitudinal Index, Displaced One Nodal Point Left of Centerline for Round 5 of the F-76 Fire Scenerio.

V. CONCLUSIONS

A main objective of this research was to use a commercially-available CFD program to develop a three-dimensional model of the thermal effects within a CCL compartment. The results could then be compared to previous one-dimensional algorithms to achieve a realistic method for non-destructively determining the elapsed time for missile cook-off due to a fire in an adjacent compartment.

The results achieved in these simulations appeared to vary from Callaham's predictions by one order of magnitude. One reason that the one-dimensional model's times are long is that they did not account for reflected radiation received from two of the four side bulkheads, the upper and lower steel supports, and off of the other canisters within the launcher. On the other hand, the elapsed times to cook-off in this study could be short due to the fact that the canisters were modeled as solid titanium cylinders with a higher thermal diffusivity than the actual concentric canisters.

One method to determine the accuracy of the CFD results is by viewing the residual plots produced by CFD-ACE during the simulation (Appendix N). The software developers at CFDRC recommend a five order of magnitude drop in the residuals of all of the calculated variables (i.e., velocity, turbulence quantities, radiation, enthalpy and pressure). Appendix N shows that this was only achieved for the turbulence quantities, and even then, only in the first time step. The enthalpy managed to drop three orders of magnitude, which is not entirely unacceptable.

The number of input items that could have been changed to achieve this uniform drop in residual errors is infinite. For example, changes could have been made in the

relaxation values, the size of the time step, the distribution of the nodal points, or even in the types of differencing techniques used. However, the decision was made to vary only the longitudinal distribution of nodes in the geometric model and leave all other input data the same for every simulation.

Another possible method to determine the accuracy of the data is by increasing the nodal distribution. This is the motive for the multiple rounds of each single-row and two-row fire scenerio. The temperature profiles in Appendices D through M show consistent values of temperature distribution and elapsed time to cook-off as the grid distribution is increased in the longitudinal direction.

Although the value for the elapsed time to cook-off, as predicted in this study, may not be precise, the figures given in the back of this report clearly show an accurate temperature profile for the simulated fire scenerios. The three dimensional profiles accurately depict the relative size and direction of the circulation of air generated by the hot fire boundary. The planar cutaway and temperature-index plots of these profiles provide a visualization of the temperature distribution across the launcher. These pictures show the immediate radiative heat transfer occurring on all metal surfaces and the relatively slow conductive heat transfer through the titanium canisters. The planar cutaway of the temperature distribution also shows how the single-row of canisters is cooled by the circulating air flow (i.e., the extended blue area overlapping the canister circle), and how this effect is negated by the placement of a second row of canisters directly behind the first row, with a shift in the convection to the backside of the second row.

The time-temperature results also depict accurate descriptions of the phenomena within the center CCL canister of the first row. Figure 15 shows the increase in the time it takes to heat the front of the canister as the second row is added. With only one row in the CCL enclosure, the radiation intensity is strong on the front skin of the canister wall since the radiation does not strike a second surface until it is has reached the forward bulkhead of the enclosure. The distance from the aft bulkhead of the launcher to the second row of canisters is much closer than it is to the forward bulkhead of the enclosure, therefore, the radiation no longer intensely strikes only the front row, but is now able to also intensely strike the closer second row.

Furthermore, Figure 15 shows the decrease in the time it takes to heat the back of the center canister of the front row, as a second row is added. With only one row in the CCL enclosure, the circulation of air cooled the back skin of the canisters, that were receiving reflected radiation from the forward bulkhead of the enclosure. Now, with the addition of a second row of canisters, the back skin of the second row receives this cooling effect, leaving a relatively stagnant air gap between the two rows. Additionally, the reflected radiation off of the front skin of the second row of canisters is much stronger on the back skin of the first row, because the distance between the canisters is closer than the distance between the back skin of the first row and the forward bulkhead of the enclosure (see Figures 8 and 9).

Appendices O and P contain the results of an additional geometric model of the CCL enclosure using the F-76 and Exocet fire scenerios. This model also contained two rows of canisters, however, the forward bulkhead of the launcher was placed directly

behind the second row of cylinders, at the same distance that separated the aft bulkhead from the first row. The purpose of this simulation was to gain an understanding of how the temperatures in the two rows of canisters were affected by removing the large volume of excess space that the original model contained.

As expected, Appendices O and P show that the reflected radiation from the forward bulkhead of the enclosure increased as the distance between it and the second row of canisters was decreased. Additionally, the tighter enclosure reduced the amount of circulation within the space, and thus the back skin of the second row of canisters does not receive a cooling effect as shown in the original two-row model. The time-temperature results plotted for the front row monitored points show that only the front skin of the canisters are affected by the decrease in the longitudinal distance between the aft and forward bulkheads of the enclosure. The cook-off times for the front skin in the reduced geometric launcher are decreased by approximately one-half the values in the full-size intermediate-level CCL compartment, due to an increase in the radiation intensity on the front skin of the canisters in the first row.

In general, this study attempted to pioneer the use of today's CFD technology to simulate the effects of shipboard fires, for the development of improved firefighting detection and extinguishing systems and procedures. The visual profiles produced by the CFD-VIEW program have proven to accurately predict the temperature profiles in the modeling of the thermal effects in a CCL caused by a fire in an adjacent compartment. As the power of the computer and accuracy of CFD programs improve, this method of shipboard fire simulation will one day become the norm for system design and engineering.

VI. RECOMMENDATIONS

The following recommendations are made in the continuation of this study:

- The first step that needs to be taken is to run the software on a faster and more powerful computer system, such as a Cray.

- Decrease the time step below 0.37 seconds. Callaham's algorithm required a time step below this value in order to satisfy stability requirements. It would be interesting to see how this value effects the three-dimensional CFD model, especially in the residual plots.

- Increase the geometry of the model to include the remaining five rows of canisters. Add one row at a time to see how each additional row affects the temperature distribution and elapsed time to propellant cook-off.

- Completely model a single concentric canister, placing the minimum cook-off temperatures on the canister's skin to determine the effects they have on the internal propellant.

- The CFD-ACE package includes a combustion algorithm. Use this algorithm to model the effects of an actual shipboard fire, to develop optimum firefighting procedures and systems.

- The CFD-ACE package also includes a spray algorithm. Use this algorithm to model the effects of sprinkler location, in comparison to the location of possible fire sources in a main engine room or magazine.

APPENDIX A. OVERVIEW OF CCL SIMULATIONS

This matrix shows the five rounds of simulations used to model the Exocet and F-76 fire scenerios. The one row model used three increments of nodal distribution in the longitudinal direction and the two row model used two increments.

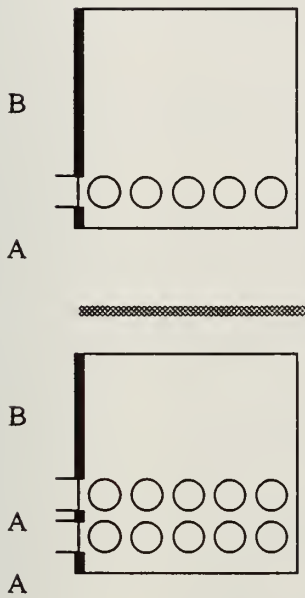

(A, B)	Exocet Fire	F-76 Fire
Round 1 (4, 8) = 14	X	X
Round 2 (4, 12)= 18	X	X
Round 3 (6, 20) = 28	X	X
Round 4 (2, 4) = 18	X	X
Round 5 (3, 8) = 24	X	X

Figure 26. Overview of CCL Simulations.

APPENDIX B. NODAL DISTRIBUTION IN THE LONGITUDINAL DIRECTION

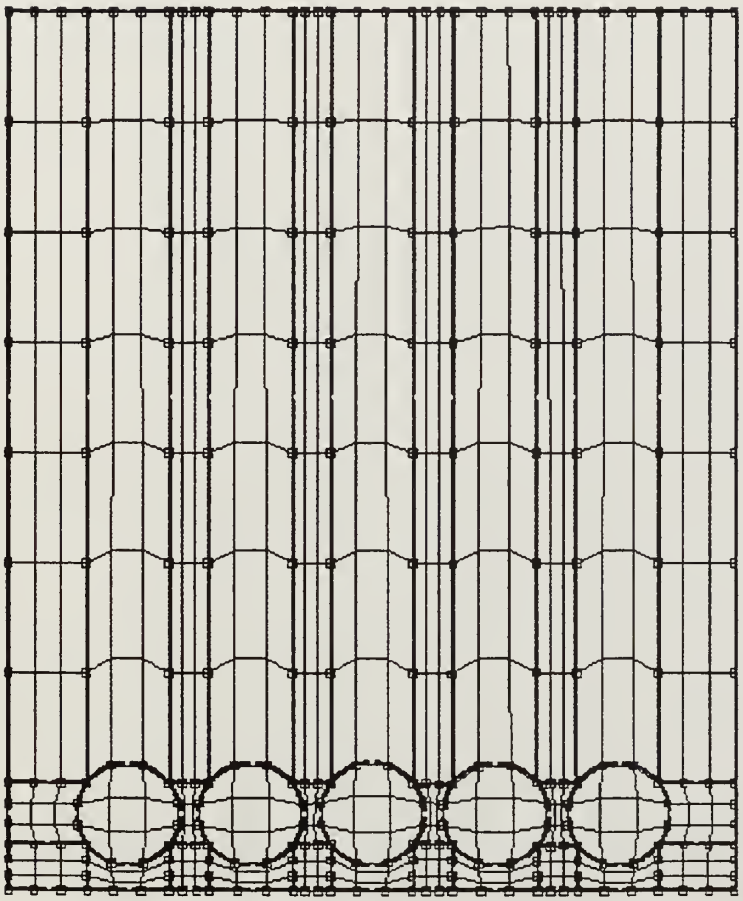

Figure 27. Horizontal Grid Distribution for Round 1.

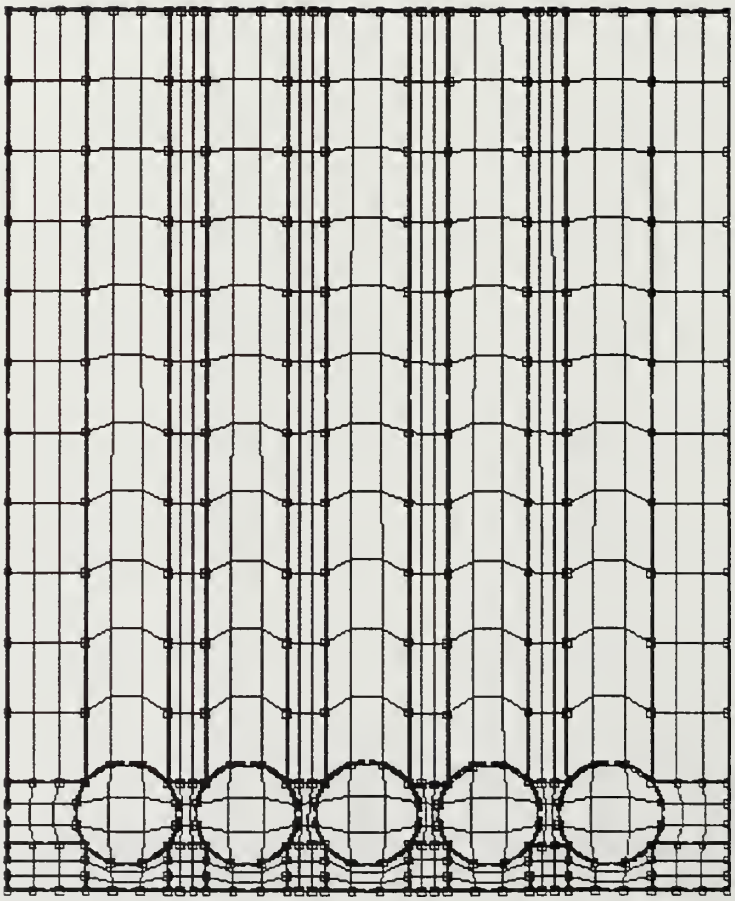

Figure 28. Horizontal Grid Distribution for Round 2.

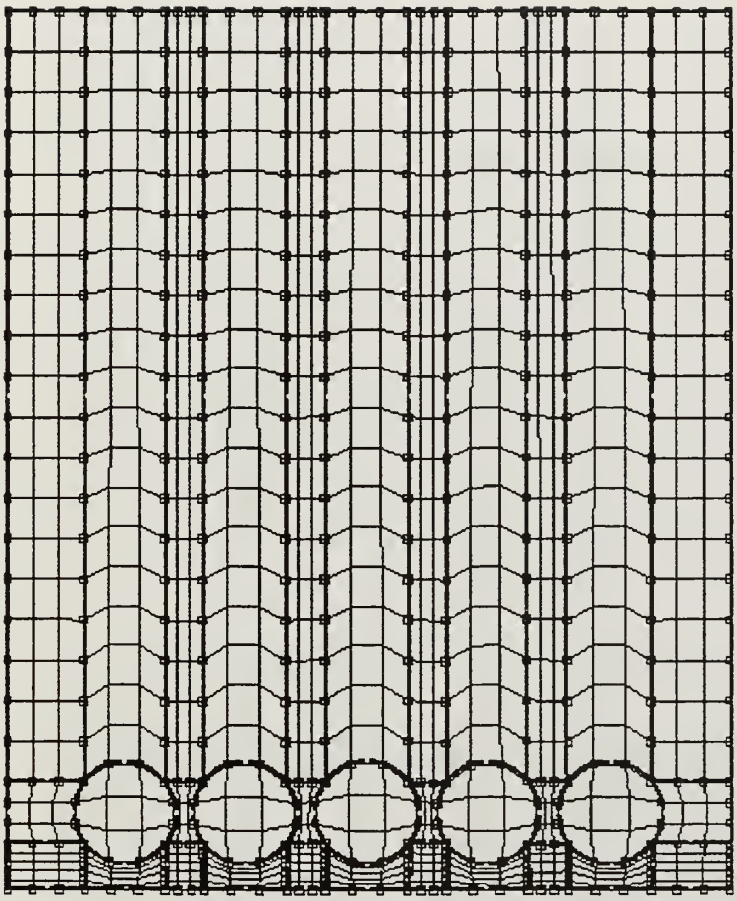

Figure 29. Horizontal Grid Distribution for Round 3.

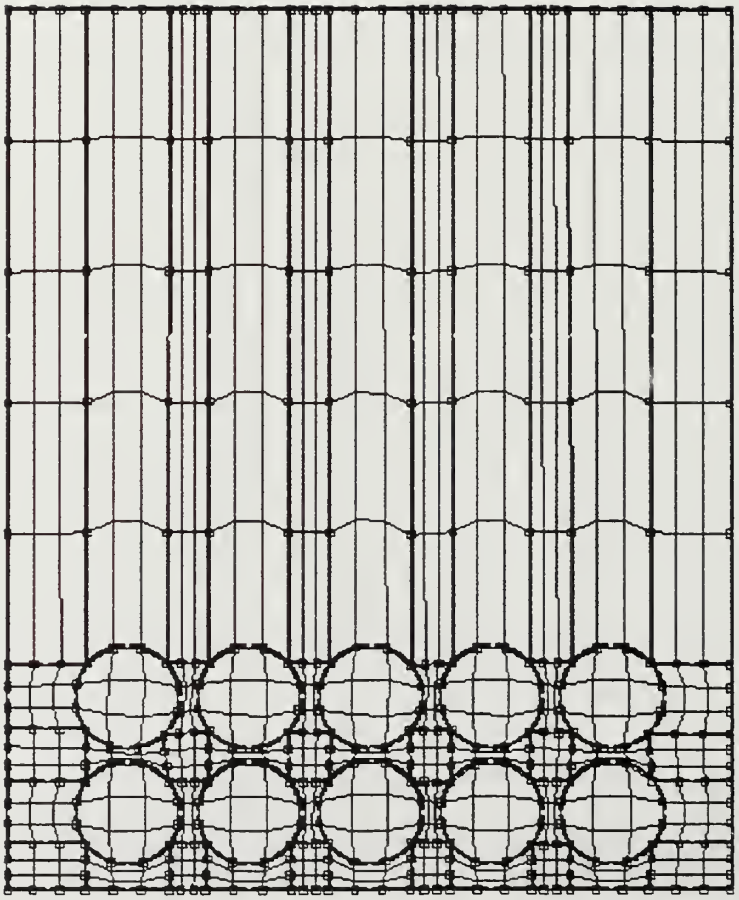

Figure 30. Horizontal Grid Distribution for Round 4.

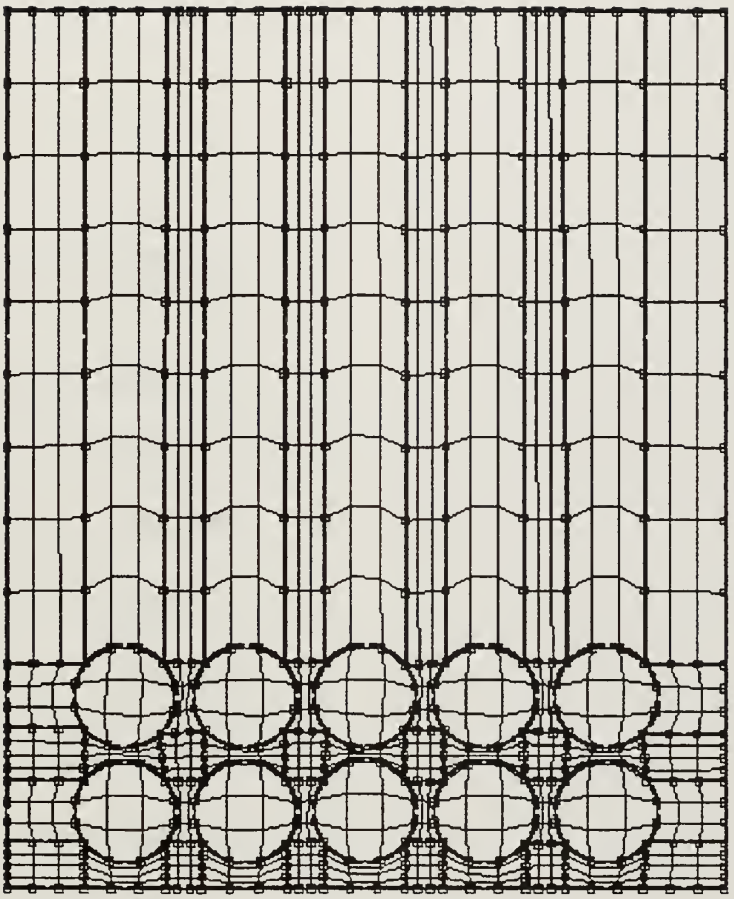

Figure 31. Horizontal Grid Distribution for Round 5.

APPENDIX C. CFD-ACE INPUT FILE.

This is a sample CFD-ACE input file used to run the CCL simulations. All of the experiments used the same general format. The only two differences in the input files for each of the runs is in the number of longitudinal nodes and the number of canisters (ie. five for the single row runs and ten for the two row runs.). This particular file is for an F-76 fire scenerio involving a single row of canisters.

```
MODEL Round_3
*
GEOMETRY
  GRID 3D BFC
  READ GRID FROM Round_3.PFG
* Cell Types
* name: tomahawk
    SOLID titanium 4 6 8 14 20 22
* name: tomahawk
    SOLID titanium 4 6 1 7 20 22
* name: tomahawk
    SOLID titanium 10 12 8 14 20 22
* name: tomahawk
    SOLID titanium 10 12 1 7 20 22
* name: tomahawk
    SOLID titanium 16 18 8 14 20 22
* name: tomahawk
    SOLID titanium 16 18 1 7 20 22
* name: tomahawk
    SOLID titanium 22 24 8 14 20 22
* name: tomahawk
    SOLID titanium 22 24 1 7 20 22
* name: tomahawk
    SOLID titanium 28 30 8 14 20 22
* name: tomahawk
    SOLID titanium 28 30 1 7 20 22
END
*
PROBLEM_TYPE
  SOLVE FLOW TURBULENCE HEAT RADIATION
  UNSTEADY TF = 0 TL = 600 STEPS = 60
```

```
END
*
PROPERTIES
 DENSITY INVERSE_T
 VISCOSITY CONSTANT_KINEMATIC 1.71e-05
 CONDUCTIVITY PRANDTL 0.7
 SPECIFIC_HEAT 1000
 PRT 1
 SOLID_PROPERTIES titanium K = 21.9 CP = 522 RHO = 4930  EMISS = 0.6
 RADIATION EMISS = 0.82 ABSOR = 0 SCATTER = 0
END
*
MODELS
 TURBULENCE_MODEL KE
END
*
*** Boundary Conditions ***
*
BOUNDARY_CONDITIONS
*  Gravity boundary condition specified
  GRAV_X 0
  GRAV_Y -9.81
  RHOREF AUTO
  GRAV_Z 0
*  boundary condition: Default
  WALL 1 1 8 14 1 19  WEST
  U = 0 V = 0 W = 0
*  boundary condition: top_deck
  WALL 1 3 14 14 1 19  NORTH
  U = 0 V = 0 W = 0
*  boundary condition: Default
  WALL 1 3 8 14 1 1  LOW
  U = 0 V = 0 W = 0
*  boundary condition: Default
  WALL 1 1 1 7 1 19  WEST
  U = 0 V = 0 W = 0
*  boundary condition: Default
  WALL 1 3 1 1 1 19  SOUTH
  U = 0 V = 0 W = 0
*  boundary condition: Default
  WALL 1 3 1 7 1 1  LOW
  U = 0 V = 0 W = 0
*  boundary condition: top_deck
  WALL 4 6 14 14 1 19  NORTH
  U = 0 V = 0 W = 0
```

```
* boundary condition: Default
  WALL 4 6 8 14 1 1  LOW
  U = 0 V = 0 W = 0
* boundary condition: Default_10
* boundary condition: Default
  WALL 4 6 1 1 1 19  SOUTH
  U = 0 V = 0 W = 0
* boundary condition: Default
  WALL 4 6 1 7 1 1  LOW
  U = 0 V = 0 W = 0
* boundary condition: Default_10
* boundary condition: top_deck
  WALL 7 9 14 14 1 19  NORTH
  U = 0 V = 0 W = 0
* boundary condition: Default
  WALL 7 9 8 14 1 1  LOW
  U = 0 V = 0 W = 0
* boundary condition: Default
  WALL 7 9 1 1 1 19  SOUTH
  U = 0 V = 0 W = 0
* boundary condition: Default
  WALL 7 9 1 7 1 1  LOW
  U = 0 V = 0 W = 0
* boundary condition: top_deck
  WALL 10 12 14 14 1 19  NORTH
  U = 0 V = 0 W = 0
* boundary condition: Default
  WALL 10 12 8 14 1 1  LOW
  U = 0 V = 0 W = 0
* boundary condition: Default_10
* boundary condition: Default
  WALL 10 12 1 1 1 19  SOUTH
  U = 0 V = 0 W = 0
* boundary condition: Default
  WALL 10 12 1 7 1 1  LOW
  U = 0 V = 0 W = 0
* boundary condition: Default_10
* boundary condition: top_deck
  WALL 13 15 14 14 1 19  NORTH
  U = 0 V = 0 W = 0
* boundary condition: Default
  WALL 13 15 8 14 1 1  LOW
  U = 0 V = 0 W = 0
* boundary condition: Default
  WALL 13 15 1 1 1 19  SOUTH
```

U = 0 V = 0 W = 0
* boundary condition: Default
WALL 13 15 1 7 1 1 LOW
U = 0 V = 0 W = 0
* boundary condition: top_deck
WALL 16 18 14 14 1 19 NORTH
U = 0 V = 0 W = 0
* boundary condition: Default
WALL 16 18 8 14 1 1 LOW
U = 0 V = 0 W = 0
* boundary condition: Default_10
* boundary condition: Default
WALL 16 18 1 1 1 19 SOUTH
U = 0 V = 0 W = 0
* boundary condition: Default
WALL 16 18 1 7 1 1 LOW
U = 0 V = 0 W = 0
* boundary condition: Default_10
* boundary condition: top_deck
WALL 19 21 14 14 1 19 NORTH
U = 0 V = 0 W = 0
* boundary condition: Default
WALL 19 21 8 14 1 1 LOW
U = 0 V = 0 W = 0
* boundary condition: Default
WALL 19 21 1 1 1 19 SOUTH
U = 0 V = 0 W = 0
* boundary condition: Default
WALL 19 21 1 7 1 1 LOW
U = 0 V = 0 W = 0
* boundary condition: top_deck
WALL 22 24 14 14 1 19 NORTH
U = 0 V = 0 W = 0
* boundary condition: Default
WALL 22 24 8 14 1 1 LOW
U = 0 V = 0 W = 0
* boundary condition: Default_10
* boundary condition: Default
WALL 22 24 1 1 1 19 SOUTH
U = 0 V = 0 W = 0
* boundary condition: Default
WALL 22 24 1 7 1 1 LOW
U = 0 V = 0 W = 0
* boundary condition: Default_10
* boundary condition: top_deck

WALL 25 27 14 14 1 19 NORTH
U = 0 V = 0 W = 0
* boundary condition: Default
WALL 25 27 8 14 1 1 LOW
U = 0 V = 0 W = 0
* boundary condition: Default
WALL 25 27 1 1 1 19 SOUTH
U = 0 V = 0 W = 0
* boundary condition: Default
WALL 25 27 1 7 1 1 LOW
U = 0 V = 0 W = 0
* boundary condition: top_deck
WALL 28 30 14 14 1 19 NORTH
U = 0 V = 0 W = 0
* boundary condition: Default
WALL 28 30 8 14 1 1 LOW
U = 0 V = 0 W = 0
* boundary condition: Default_10
* boundary condition: Default
WALL 28 30 1 1 1 19 SOUTH
U = 0 V = 0 W = 0
* boundary condition: Default
WALL 28 30 1 7 1 1 LOW
U = 0 V = 0 W = 0
* boundary condition: Default_10
* boundary condition: Default
WALL 33 33 8 14 1 19 EAST
U = 0 V = 0 W = 0
* boundary condition: top_deck
WALL 31 33 14 14 1 19 NORTH
U = 0 V = 0 W = 0
* boundary condition: Default
WALL 31 33 8 14 1 1 LOW
U = 0 V = 0 W = 0
* boundary condition: Default
WALL 33 33 1 7 1 19 EAST
U = 0 V = 0 W = 0
* boundary condition: Default
WALL 31 33 1 1 1 19 SOUTH
U = 0 V = 0 W = 0
* boundary condition: Default
WALL 31 33 1 7 1 1 LOW
U = 0 V = 0 W = 0
* boundary condition: Default
WALL 1 1 8 14 20 22 WEST

U = 0 V = 0 W = 0
* boundary condition: Default_10
* boundary condition: top_deck
WALL 1 3 14 14 20 22 NORTH
U = 0 V = 0 W = 0
* boundary condition: Default
WALL 1 1 1 7 20 22 WEST
U = 0 V = 0 W = 0
* boundary condition: Default_10
* boundary condition: Default
WALL 1 3 1 1 20 22 SOUTH
U = 0 V = 0 W = 0
* boundary condition: Default_10
* boundary condition: Default_10
* boundary condition: top_deck
WALL 4 6 14 14 20 22 NORTH
U = 0 V = 0 W = 0
* boundary condition: Wall_10
* boundary condition: Wall_10
* boundary condition: Default
WALL 4 6 1 1 20 22 SOUTH
U = 0 V = 0 W = 0
* boundary condition: Default_10
* boundary condition: Default_10
* boundary condition: top_deck
WALL 7 9 14 14 20 22 NORTH
U = 0 V = 0 W = 0
* boundary condition: Wall_10
* boundary condition: Default
WALL 7 9 1 1 20 22 SOUTH
U = 0 V = 0 W = 0
* boundary condition: Default_10
* boundary condition: Default_10
* boundary condition: top_deck
WALL 10 12 14 14 20 22 NORTH
U = 0 V = 0 W = 0
* boundary condition: Wall_10
* boundary condition: Wall_10
* boundary condition: Default
WALL 10 12 1 1 20 22 SOUTH
U = 0 V = 0 W = 0
* boundary condition: Default_10
* boundary condition: Default_10
* boundary condition: top_deck
WALL 13 15 14 14 20 22 NORTH

U = 0 V = 0 W = 0
* boundary condition: Wall_10
* boundary condition: Default
WALL 13 15 1 1 20 22 SOUTH
U = 0 V = 0 W = 0
* boundary condition: Default_10
* boundary condition: Default_10
* boundary condition: top_deck
WALL 16 18 14 14 20 22 NORTH
U = 0 V = 0 W = 0
* boundary condition: Wall_10
* boundary condition: Wall_10
* boundary condition: Default
WALL 16 18 1 1 20 22 SOUTH
U = 0 V = 0 W = 0
* boundary condition: Default_10
* boundary condition: Default_10
* boundary condition: top_deck
WALL 19 21 14 14 20 22 NORTH
U = 0 V = 0 W = 0
* boundary condition: Wall_10
* boundary condition: Default
WALL 19 21 1 1 20 22 SOUTH
U = 0 V = 0 W = 0
* boundary condition: Default_10
* boundary condition: Default_10
* boundary condition: top_deck
WALL 22 24 14 14 20 22 NORTH
U = 0 V = 0 W = 0
* boundary condition: Wall_10
* boundary condition: Wall_10
* boundary condition: Default
WALL 22 24 1 1 20 22 SOUTH
U = 0 V = 0 W = 0
* boundary condition: Default_10
* boundary condition: Default_10
* boundary condition: top_deck
WALL 25 27 14 14 20 22 NORTH
U = 0 V = 0 W = 0
* boundary condition: Wall_10
* boundary condition: Default
WALL 25 27 1 1 20 22 SOUTH
U = 0 V = 0 W = 0
* boundary condition: Default_10
* boundary condition: Default_10

```
* boundary condition: top_deck
  WALL 28 30 14 14 20 22  NORTH
  U = 0 V = 0 W = 0
* boundary condition: Wall_10
* boundary condition: Wall_10
* boundary condition: Default
  WALL 28 30 1 1 20 22  SOUTH
  U = 0 V = 0 W = 0
* boundary condition: Default_10
* boundary condition: Default
  WALL 33 33 8 14 20 22  EAST
  U = 0 V = 0 W = 0
* boundary condition: top_deck
  WALL 31 33 14 14 20 22  NORTH
  U = 0 V = 0 W = 0
* boundary condition: Default
  WALL 33 33 1 7 20 22  EAST
  U = 0 V = 0 W = 0
* boundary condition: Default
  WALL 31 33 1 1 20 22  SOUTH
  U = 0 V = 0 W = 0
* boundary condition: Default
  WALL 1 1 8 14 23 27  WEST
  U = 0 V = 0 W = 0
* boundary condition: top_deck
  WALL 1 3 14 14 23 27  NORTH
  U = 0 V = 0 W = 0
* boundary condition: Fire_bulkhead
  WALL 1 3 8 14 27 27  HIGH
  U = 0 V = 0 W = 0
* boundary condition: Default
  WALL 1 1 1 7 23 27  WEST
  U = 0 V = 0 W = 0
* boundary condition: Default
  WALL 1 3 1 1 23 27  SOUTH
  U = 0 V = 0 W = 0
* boundary condition: Fire_bulkhead
  WALL 1 3 1 7 27 27  HIGH
  U = 0 V = 0 W = 0 T = PROF_T
  T 4
  0 100 200 300
  300 655 1010 1365
* boundary condition: top_deck
  WALL 4 6 14 14 23 27  NORTH
  U = 0 V = 0 W = 0
```

```
* boundary condition: Fire_bulkhead
  WALL 4 6 8 14 27 27  HIGH
  U = 0 V = 0 W = 0
* boundary condition: Default
  WALL 4 6 1 1 23 27  SOUTH
  U = 0 V = 0 W = 0
* boundary condition: Fire_bulkhead
  WALL 4 6 1 7 27 27  HIGH
  U = 0 V = 0 W = 0 T = PROF_T
  T 4
  0 100 200 300
  300 655 1010 1365
* boundary condition: top_deck
  WALL 7 9 14 14 23 27  NORTH
  U = 0 V = 0 W = 0
* boundary condition: Fire_bulkhead
  WALL 7 9 8 14 27 27  HIGH
  U = 0 V = 0 W = 0
* boundary condition: Default
  WALL 7 9 1 1 23 27  SOUTH
  U = 0 V = 0 W = 0
* boundary condition: Fire_bulkhead
  WALL 7 9 1 7 27 27  HIGH
  U = 0 V = 0 W = 0 T = PROF_T
  T 4
  0 100 200 300
  300 655 1010 1365
* boundary condition: top_deck
  WALL 10 12 14 14 23 27  NORTH
  U = 0 V = 0 W = 0
* boundary condition: Fire_bulkhead
  WALL 10 12 8 14 27 27  HIGH
  U = 0 V = 0 W = 0
* boundary condition: Default
  WALL 10 12 1 1 23 27  SOUTH
  U = 0 V = 0 W = 0
* boundary condition: Fire_bulkhead
  WALL 10 12 1 7 27 27  HIGH
  U = 0 V = 0 W = 0 T = PROF_T
  T 4
  0 100 200 300
  300 655 1010 1365
* boundary condition: top_deck
  WALL 13 15 14 14 23 27  NORTH
  U = 0 V = 0 W = 0
```

```
*  boundary condition: Fire_bulkhead
   WALL 13 15 8 14 27 27  HIGH
   U = 0 V = 0 W = 0
*  boundary condition: Default
   WALL 13 15 1 1 23 27  SOUTH
   U = 0 V = 0 W = 0
*  boundary condition: Fire_bulkhead
   WALL 13 15 1 7 27 27  HIGH
   U = 0 V = 0 W = 0 T = PROF_T
   T 4
   0 100 200 300
   300 655 1010 1365
*  boundary condition: top_deck
   WALL 16 18 14 14 23 27  NORTH
   U = 0 V = 0 W = 0
*  boundary condition: Fire_bulkhead
   WALL 16 18 8 14 27 27  HIGH
   U = 0 V = 0 W = 0
*  boundary condition: Default
   WALL 16 18 1 1 23 27  SOUTH
   U = 0 V = 0 W = 0
*  boundary condition: Fire_bulkhead
   WALL 16 18 1 7 27 27  HIGH
   U = 0 V = 0 W = 0 T = PROF_T
   T 4
   0 100 200 300
   300 655 1010 1365
*  boundary condition: top_deck
   WALL 19 21 14 14 23 27  NORTH
   U = 0 V = 0 W = 0
*  boundary condition: Fire_bulkhead
   WALL 19 21 8 14 27 27  HIGH
   U = 0 V = 0 W = 0
*  boundary condition: Default
   WALL 19 21 1 1 23 27  SOUTH
   U = 0 V = 0 W = 0
*  boundary condition: Fire_bulkhead
   WALL 19 21 1 7 27 27  HIGH
   U = 0 V = 0 W = 0 T = PROF_T
   T 4
   0 100 200 300
   300 655 1010 1365
*  boundary condition: top_deck
   WALL 22 24 14 14 23 27  NORTH
   U = 0 V = 0 W = 0
```

```
* boundary condition: Fire_bulkhead
  WALL 22 24 8 14 27 27  HIGH
  U = 0 V = 0 W = 0
* boundary condition: Default
  WALL 22 24 1 1 23 27  SOUTH
  U = 0 V = 0 W = 0
* boundary condition: Fire_bulkhead
  WALL 22 24 1 7 27 27  HIGH
  U = 0 V = 0 W = 0 T = PROF_T
  T 4
  0 100 200 300
  300 655 1010 1365
* boundary condition: top_deck
  WALL 25 27 14 14 23 27  NORTH
  U = 0 V = 0 W = 0
* boundary condition: Fire_bulkhead
  WALL 25 27 8 14 27 27  HIGH
  U = 0 V = 0 W = 0
* boundary condition: Default
  WALL 25 27 1 1 23 27  SOUTH
  U = 0 V = 0 W = 0
* boundary condition: Fire_bulkhead
  WALL 25 27 1 7 27 27  HIGH
  U = 0 V = 0 W = 0 T = PROF_T
  T 4
  0 100 200 300
  300 655 1010 1365
* boundary condition: top_deck
  WALL 28 30 14 14 23 27  NORTH
  U = 0 V = 0 W = 0
* boundary condition: Fire_bulkhead
  WALL 28 30 8 14 27 27  HIGH
  U = 0 V = 0 W = 0
* boundary condition: Default
  WALL 28 30 1 1 23 27  SOUTH
  U = 0 V = 0 W = 0
* boundary condition: Fire_bulkhead
  WALL 28 30 1 7 27 27  HIGH
  U = 0 V = 0 W = 0 T = PROF_T
  T 4
  0 100 200 300
  300 655 1010 1365
* boundary condition: Default
  WALL 33 33 8 14 23 27  EAST
  U = 0 V = 0 W = 0
```

```
*  boundary condition: top_deck
   WALL 31 33 14 14 23 27  NORTH
   U = 0 V = 0 W = 0
*  boundary condition: Fire_bulkhead
   WALL 31 33 8 14 27 27  HIGH
   U = 0 V = 0 W = 0
*  boundary condition: Default
   WALL 33 33 1 7 23 27  EAST
   U = 0 V = 0 W = 0
*  boundary condition: Default
   WALL 31 33 1 1 23 27  SOUTH
   U = 0 V = 0 W = 0
*  boundary condition: Fire_bulkhead
   WALL 31 33 1 7 27 27  HIGH
   U = 0 V = 0 W = 0 T = PROF_T
   T 4
   0 100 200 300
   300 655 1010 1365
END
*
INITIAL_CONDITIONS
* Full field initial conditions
  U = 0 V = 0 W = 0 P = 0 T = 300 K = 5 D = 25 L = 0
END
*
********************** Solve **********************
*
*
SOLUTION_CONTROL
  ALGORITHM SIMPLEC
  S_SCHEME UPWIND U V W RHO K D H
  T_SCHEME EULER
  ITERATIONS 100
  C_ITERATIONS 1
  SOLVER WHOLE_J U V W PP K D
  SOLVER CG H
  S_ITERATIONS 8 U V W
  S_ITERATIONS 30 PP
  S_ITERATIONS 5 K D
  S_ITERATIONS 1000 H
  INERTIAL_FACTOR 1 U V W
  INERTIAL_FACTOR 0.2 K D
  INERTIAL_FACTOR 0.1 H
  RELAX 0.8 P
  RELAX 1 RHO
```

```
  RELAX 0.3 T
  RELAX 1 VIS
  RELAX 0.1 RAD
  MINVAL -1e+20 U V W
  MINVAL -1e+20 P
  MINVAL 1e-06 RHO
  MINVAL 1e-10 T VIS
  MINVAL 1e-10 K D
  MINVAL -1e+20 H
  MAXVAL 1e+20 U V W
  MAXVAL 1e+20 P RHO
  MAXVAL 5000 T
  MAXVAL 1e+20 VIS
  MAXVAL 1e+20 K D
  MAXVAL 1e+20 H
END
*
OUTPUT
  PLOT3D ON FORMATTED
  SCALAR_FILE 1 RHO P T K D
  DIAGNOSTICS OFF
*  inside left of far tube wall
MONITOR 1 17 3 21 T
*  inside right of far tube wall
MONITOR 1 18 3 21 T
*  inside left of near tube wall
MONITOR 1 17 3 22 T
*  inside right of near tube wall
MONITOR 1 18 3 22 T
*  left of far tube wall
MONITOR 1 17 3 20 T
*  right of far tube wall
MONITOR 1 18 3 20 T
*  left of near tube wall
MONITOR 1 17 3 23 T
*  right of near tube wall
MONITOR 1 18 3 23 T
  TIME_SAVE 6
  UNIQUE_NAME ON
```

END

APPENDIX D. EXOCET FIRE - ROUND 1

The following data corresponds to the round 1 simulation of the Exocet fire scenerio, including:

(1) 3-dimensional temperature profile at a time of 1 minute.
(2) 3-dimensional temperature profile at a time of 10 minutes.
(3) Horizontal temperature profile at a time of 1 minute.
(4) Horizontal temperature profile at a time of 10 minutes.
(5) Temperature vs. index profile at a time of 1 minute.
(6) Temperature vs. index profile at a time of 10 minutes.
(7) Temperature vs. time plot for monitor point 2.
(8) Temperature vs. time plot for monitor point 3.

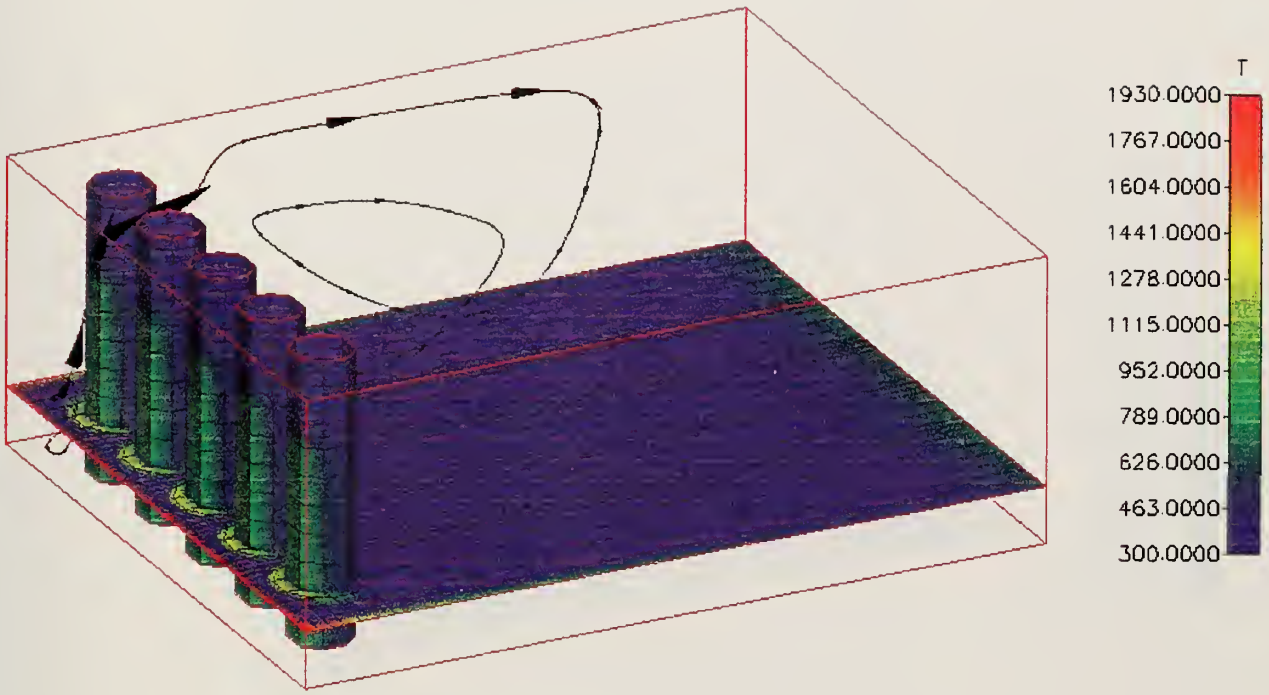

Figure 32. Exocet Fire - Round 1. 3-Dimensional Temperature Profile at a Time of 1 Minute.

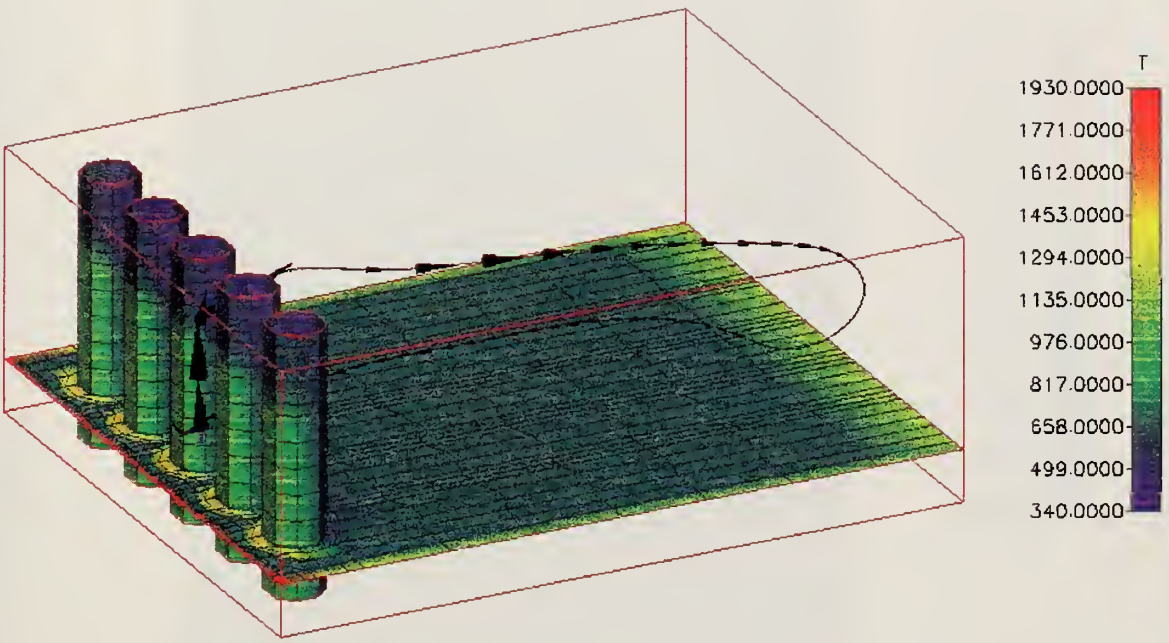

Figure 33. Exocet Fire - Round 1. 3-Dimensional Temperature Profile at a Time of 10 Minutes.

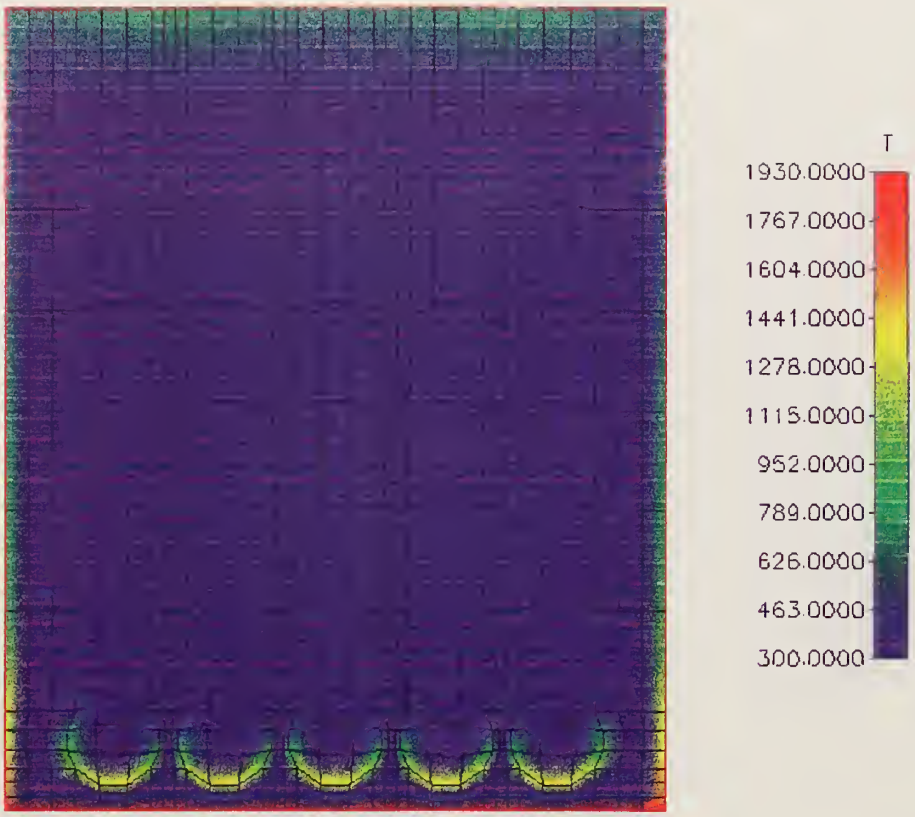

Figure 34. Exocet Fire - Round 1. Horizontal Temperature Profile at a Time of 1 Minute.

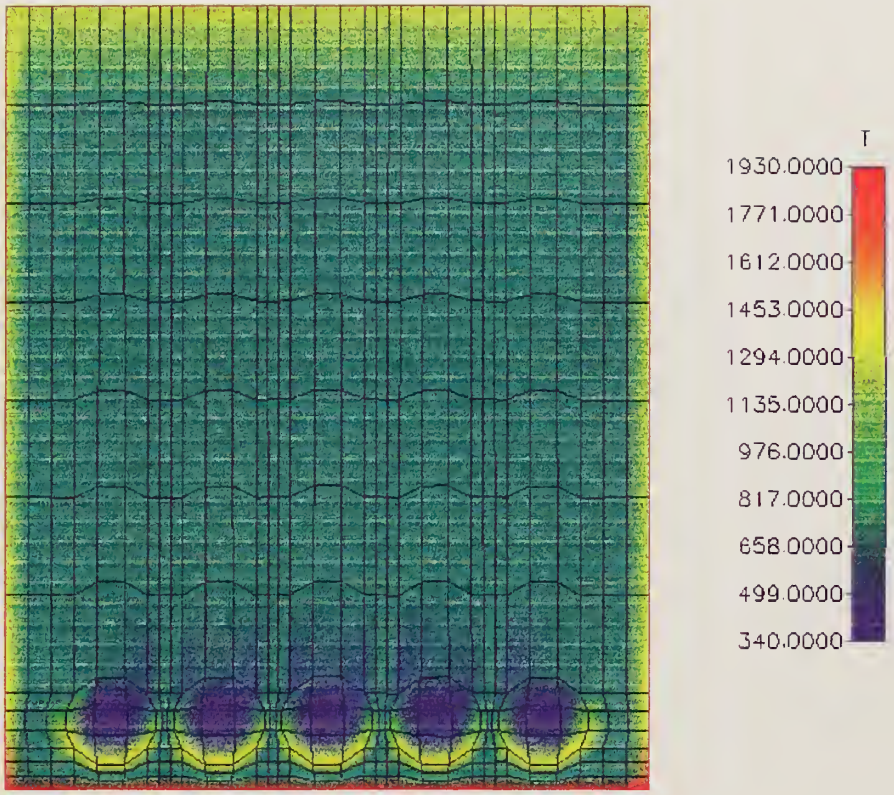

Figure 35. Exocet Fire - Round 1. Horizontal Temperature Profile at a Time of 10 Minutes.

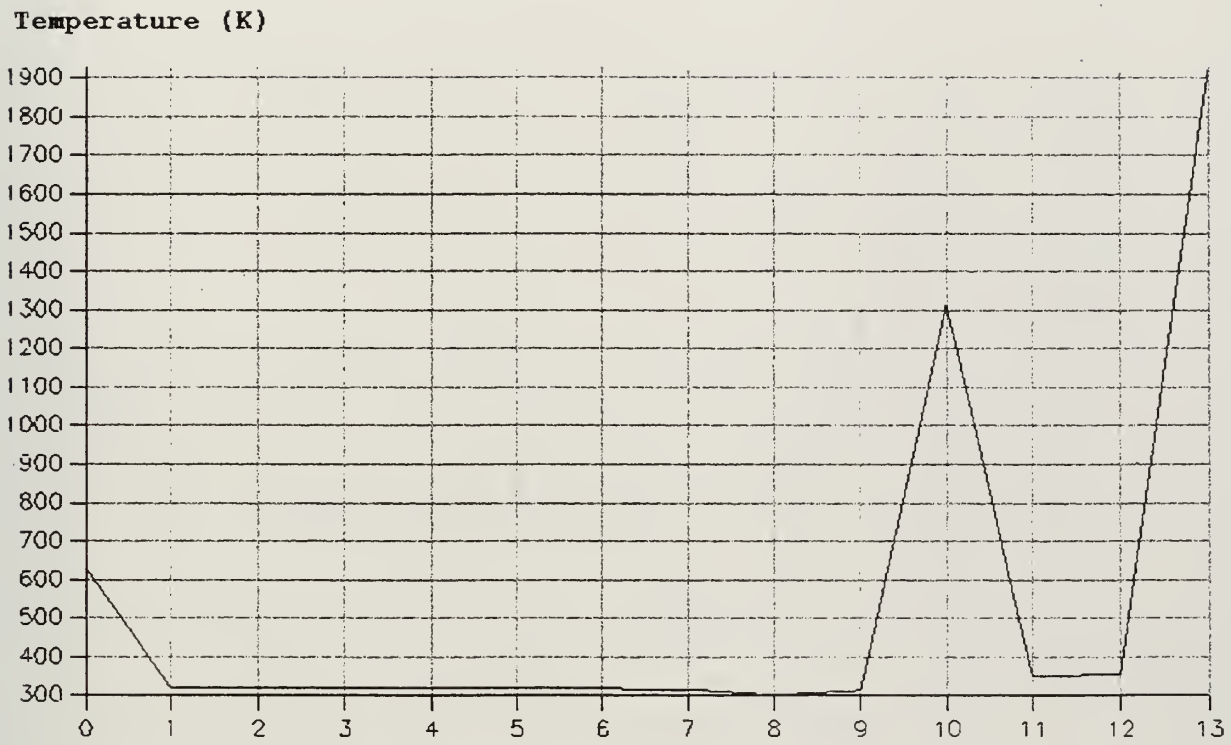

Figure 36. Exocet Fire - Round 1. Temperature vs. Index Profile at a Time of 1 Minute.

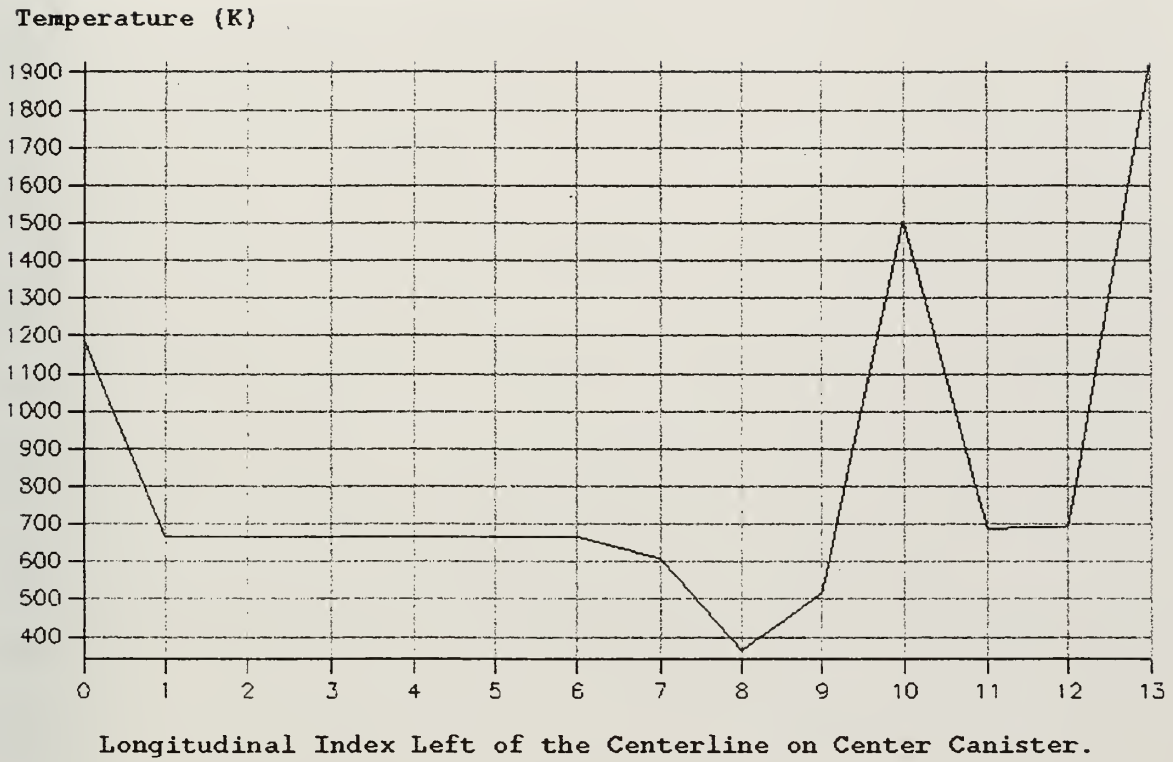

Figure 37. Exocet Fire - Round 1. Temperature vs. Index Profile at a Time of 10 Minutes.

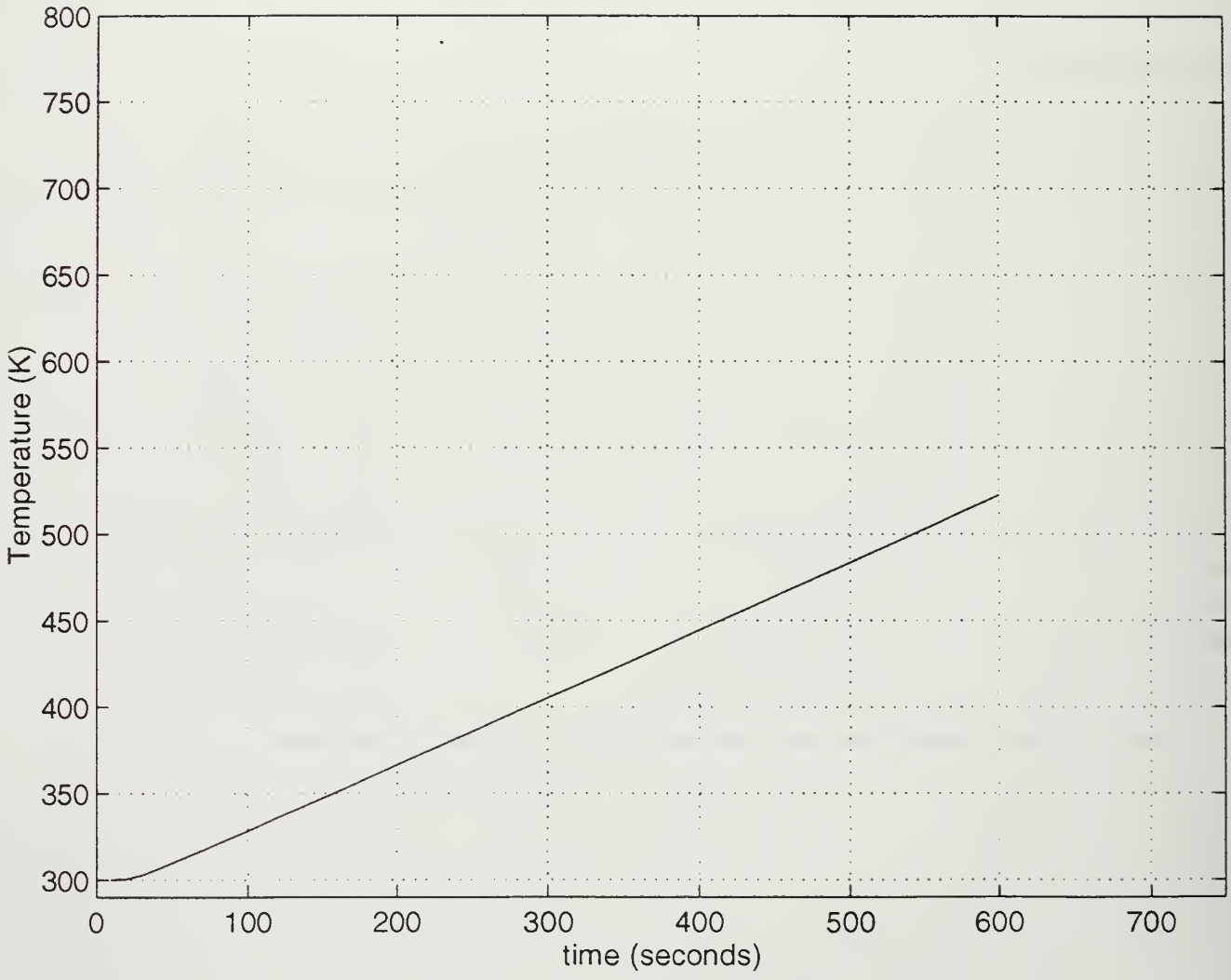

Figure 38. Exocet Fire - Round 1. Temperature vs. Time Plot for Monitor Point 2.

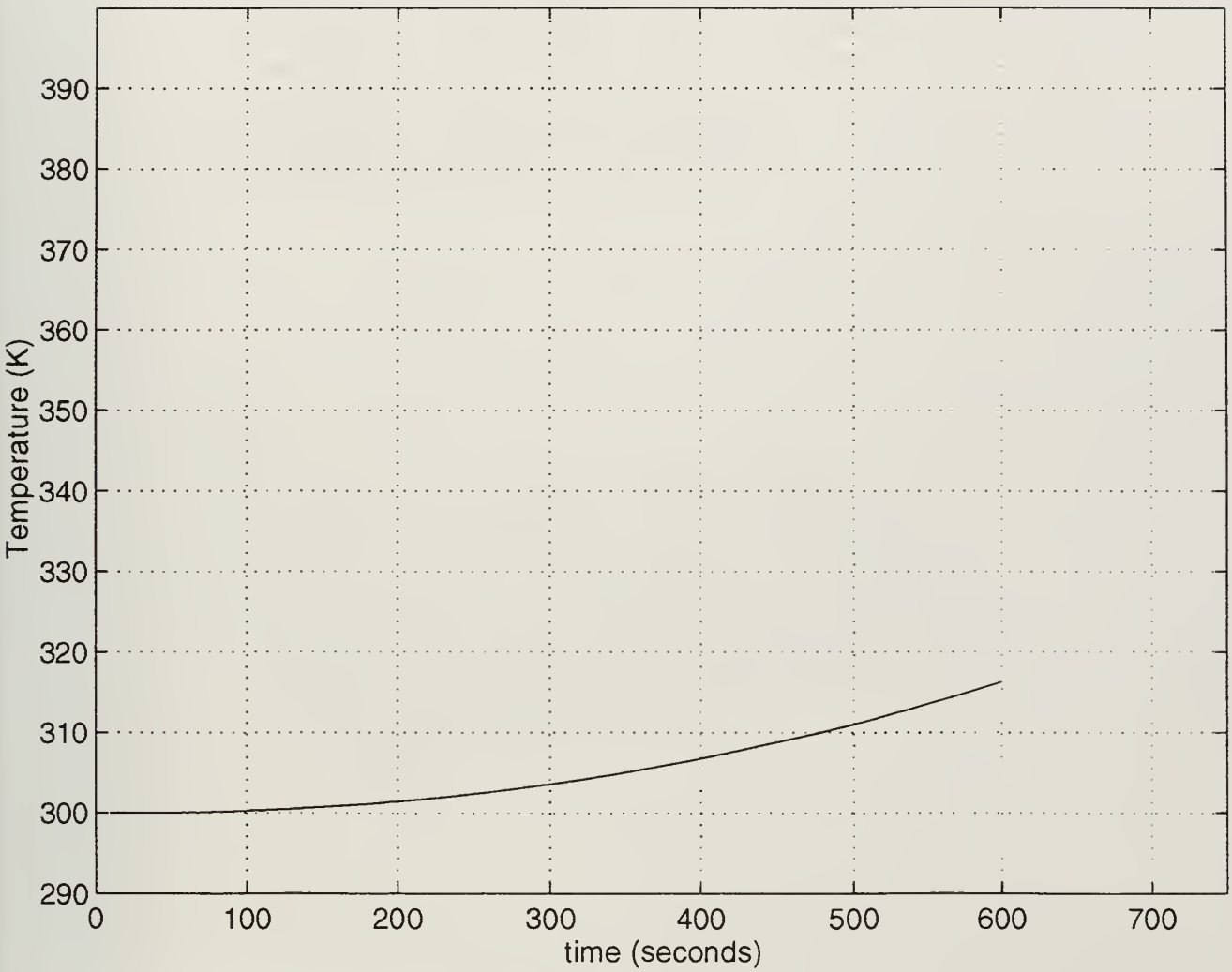

Figure 39. Exocet Fire - Round 1. Temperature vs. Time Plot for Monitor Point 3.

APPENDIX E. EXOCET FIRE - ROUND 2

The following data corresponds to the round 2 simulation of the Exocet fire scenerio, including:

(1) 3-dimensional temperature profile at a time of one minute.
(2) 3-dimensional temperature profile at a time of 10 minutes.
(3) Horizontal temperature profile at a time of one minute.
(4) Horizontal temperature profile at a time of 10 minutes.
(5) Temperature vs. index profile at a time of one minute.
(6) Temperature vs. index profile at a time of 10 minutes.
(7) Temperature vs. time plot for monitor point 1.
(8) Temperature vs. time plot for monitor point 2.
(9) Temperature vs. time plot for monitor point 3.

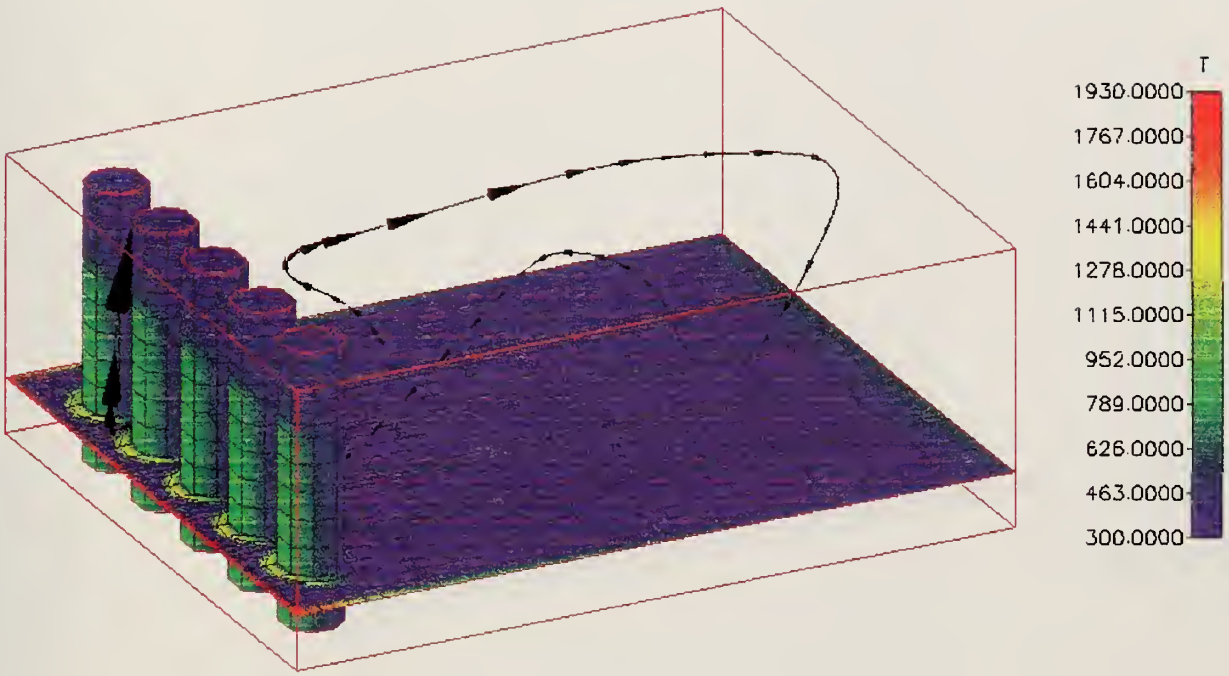

Figure 40. Exocet Fire - Round 2. 3-Dimensional Temperature Profile at a Time of 1 Minute.

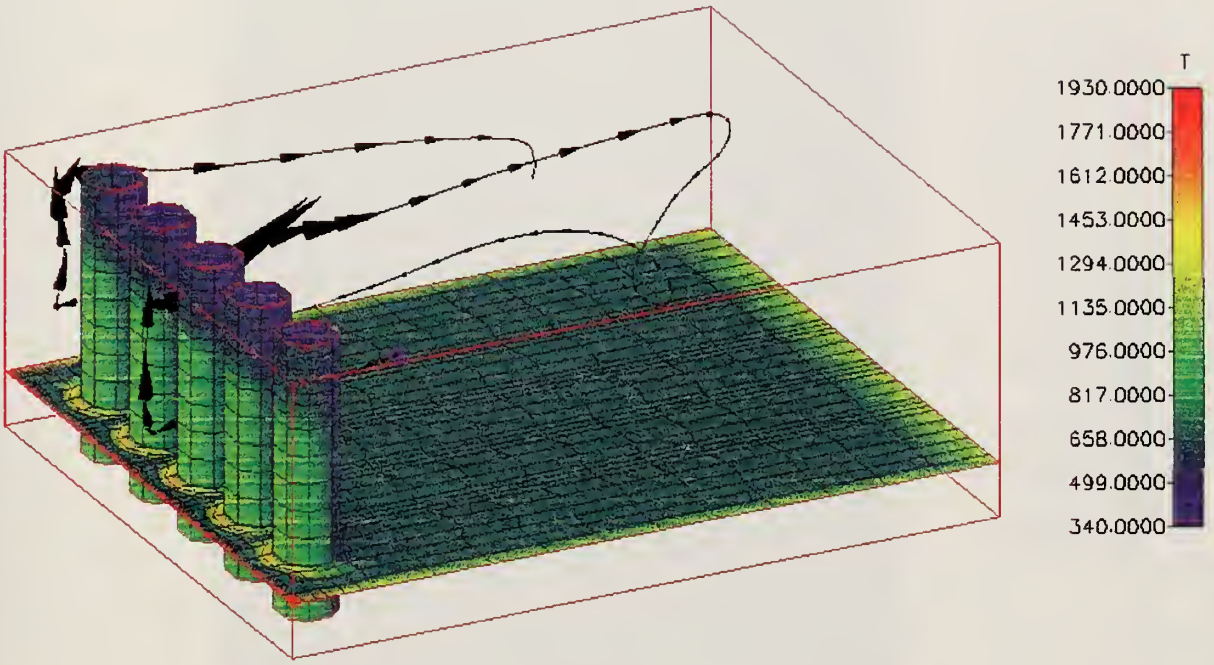

Figure 41. Exocet Fire - Round 2. 3-Dimensional Temperature Profile at a Time of 10 Minutes.

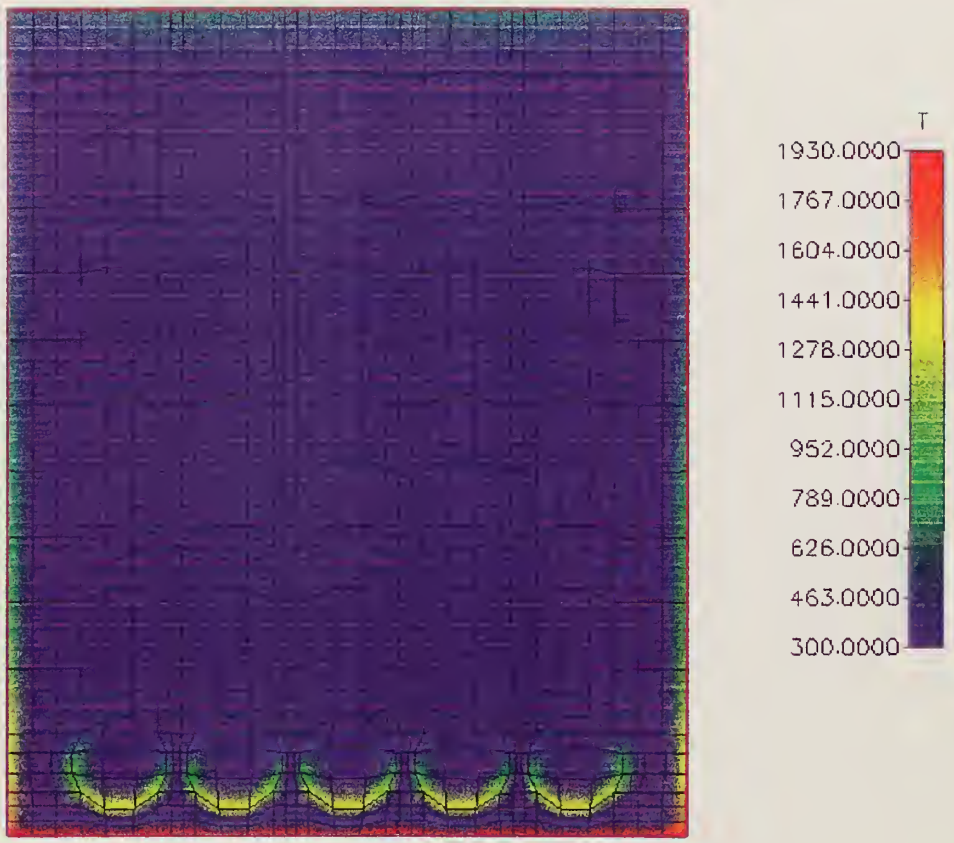

Figure 42. Exocet Fire - Round 2. Horizontal Temperature Profile at a Time of 1 Minute.

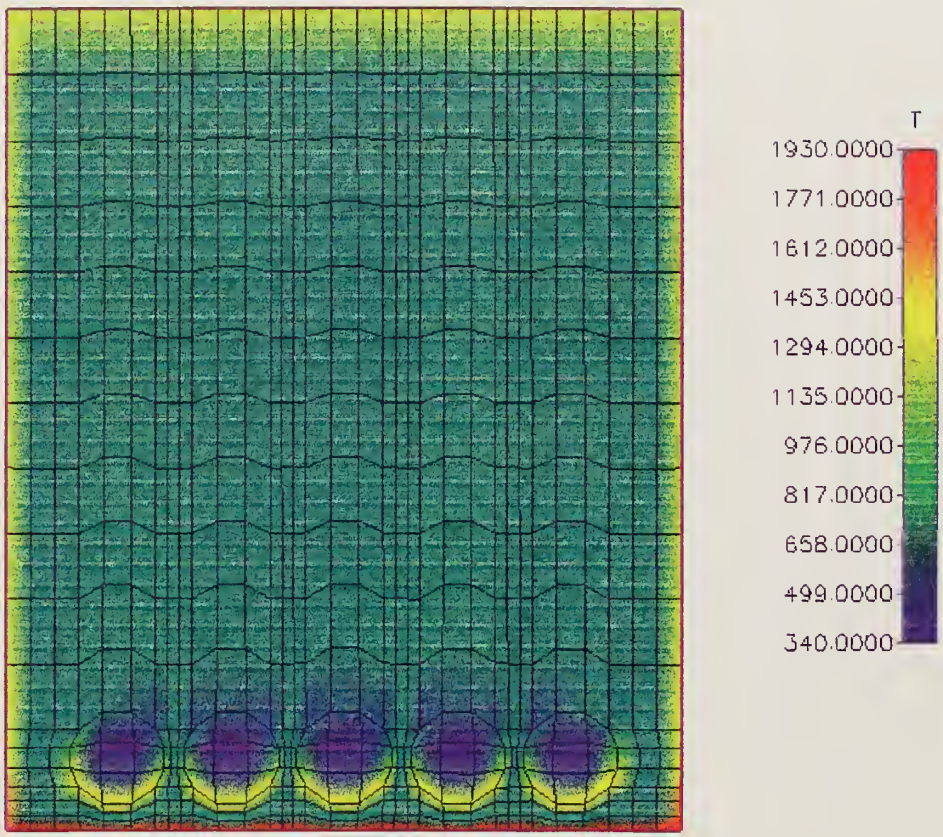

Figure 43. Exocet Fire - Round 2. Horizontal Temperature Profile at a Time of 10 Minutes.

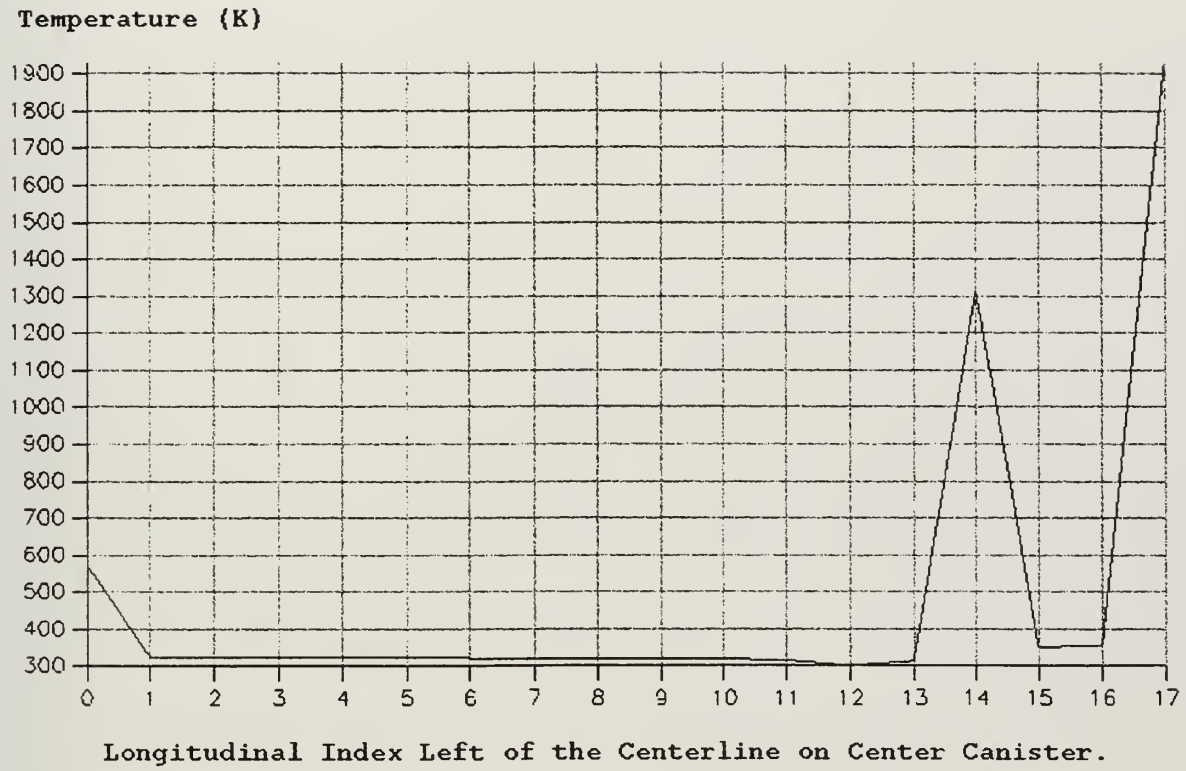

Figure 44. Exocet Fire - Round 2. Temperature vs. Index Profile at a Time of 1 Minute.

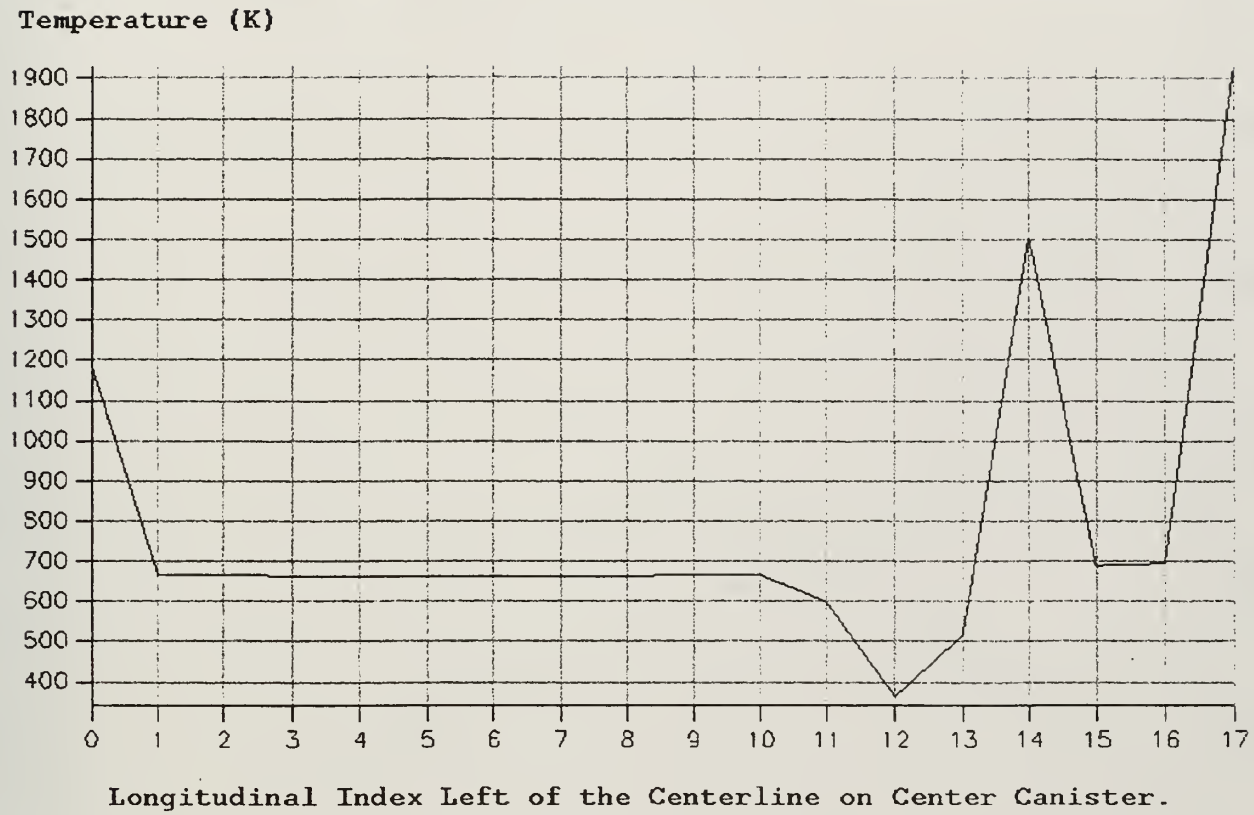

Figure 45. Exocet Fire - Round 2. Temperature vs. Index Profile at a Time of 10 Minutes.

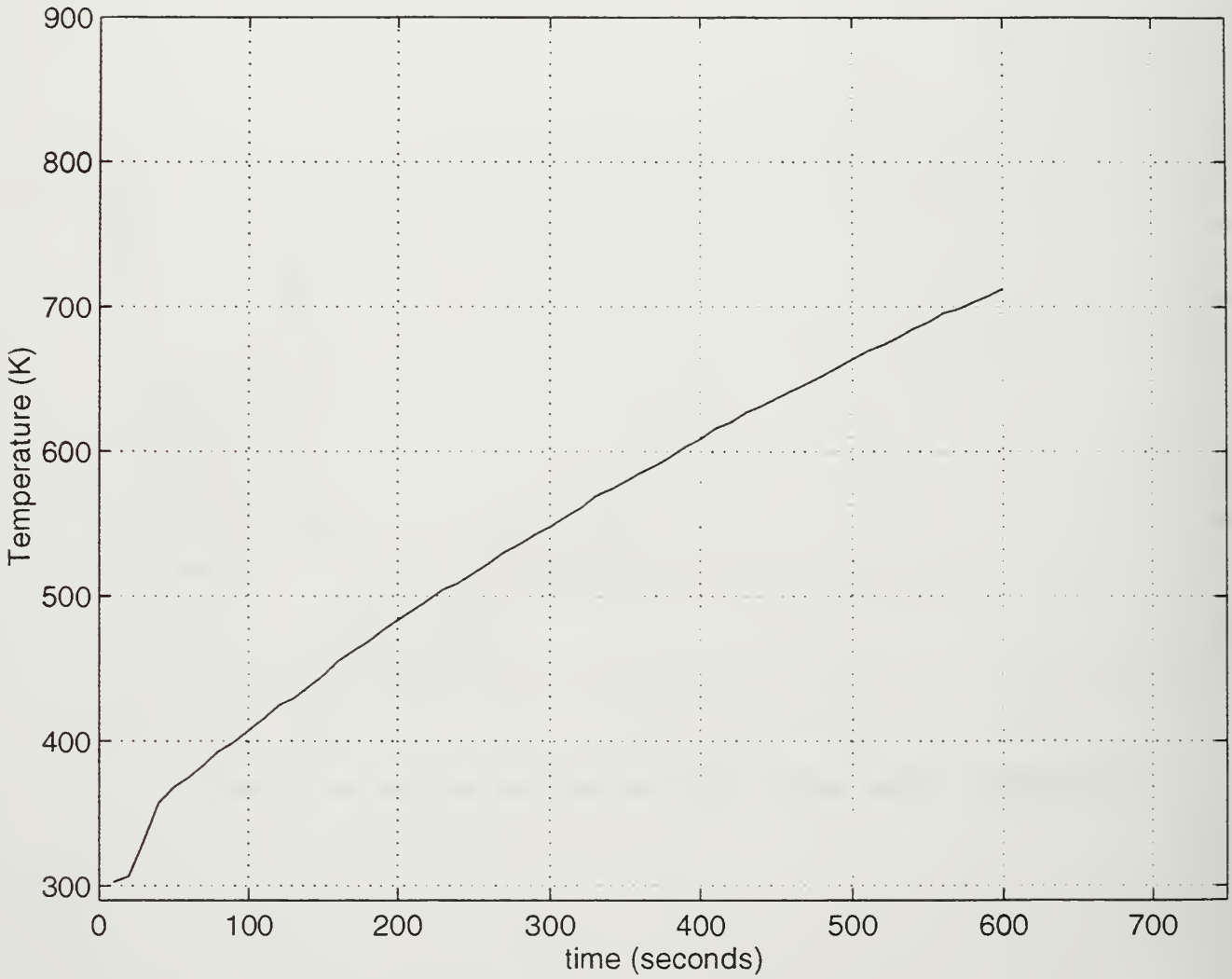

Figure 46. Exocet Fire - Round 2. Temperature vs. Time Plot for Monitor Point 1.

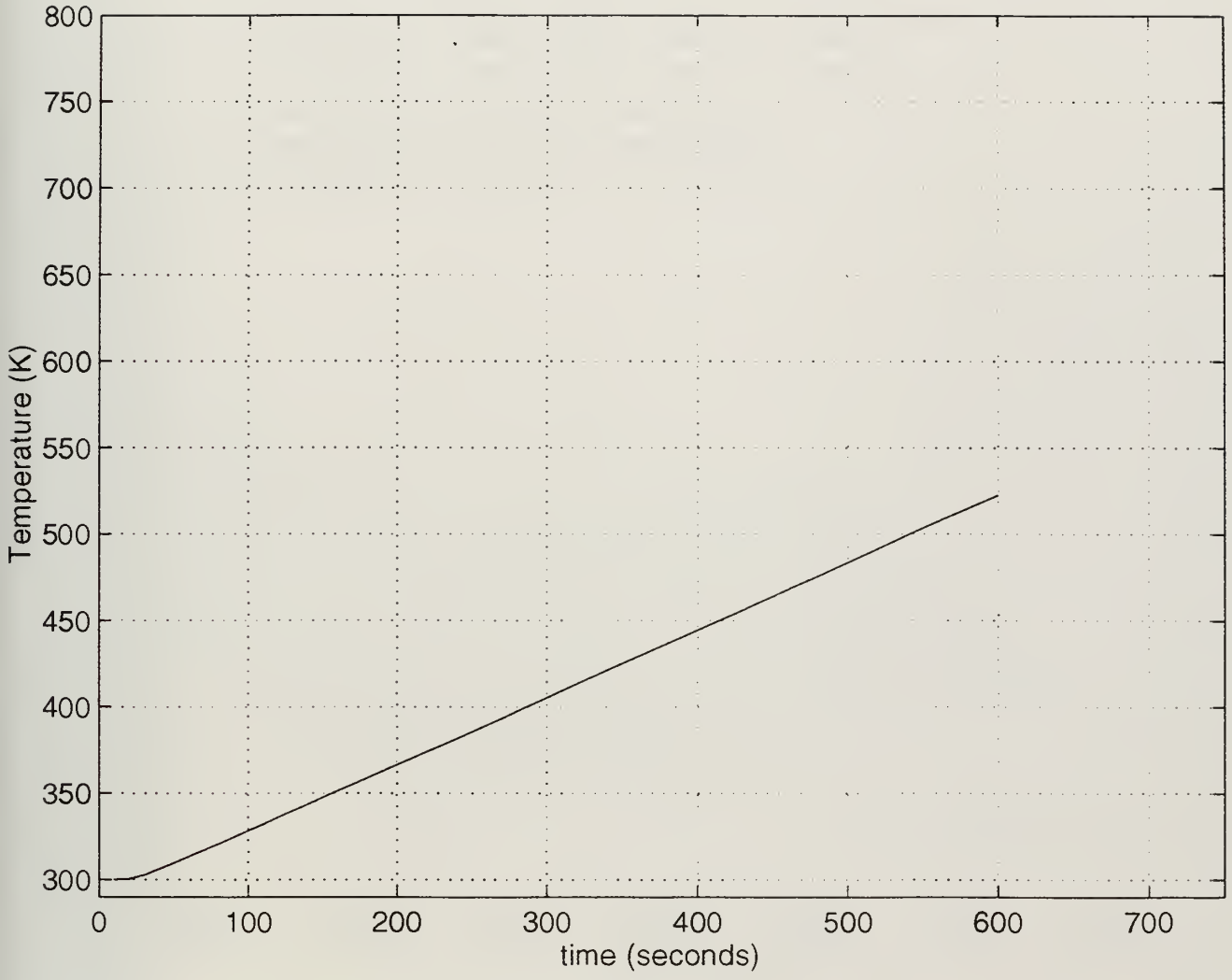

Figure 47. Exocet Fire - Round 2. Temperature vs. Time Plot for Monitor Point 2.

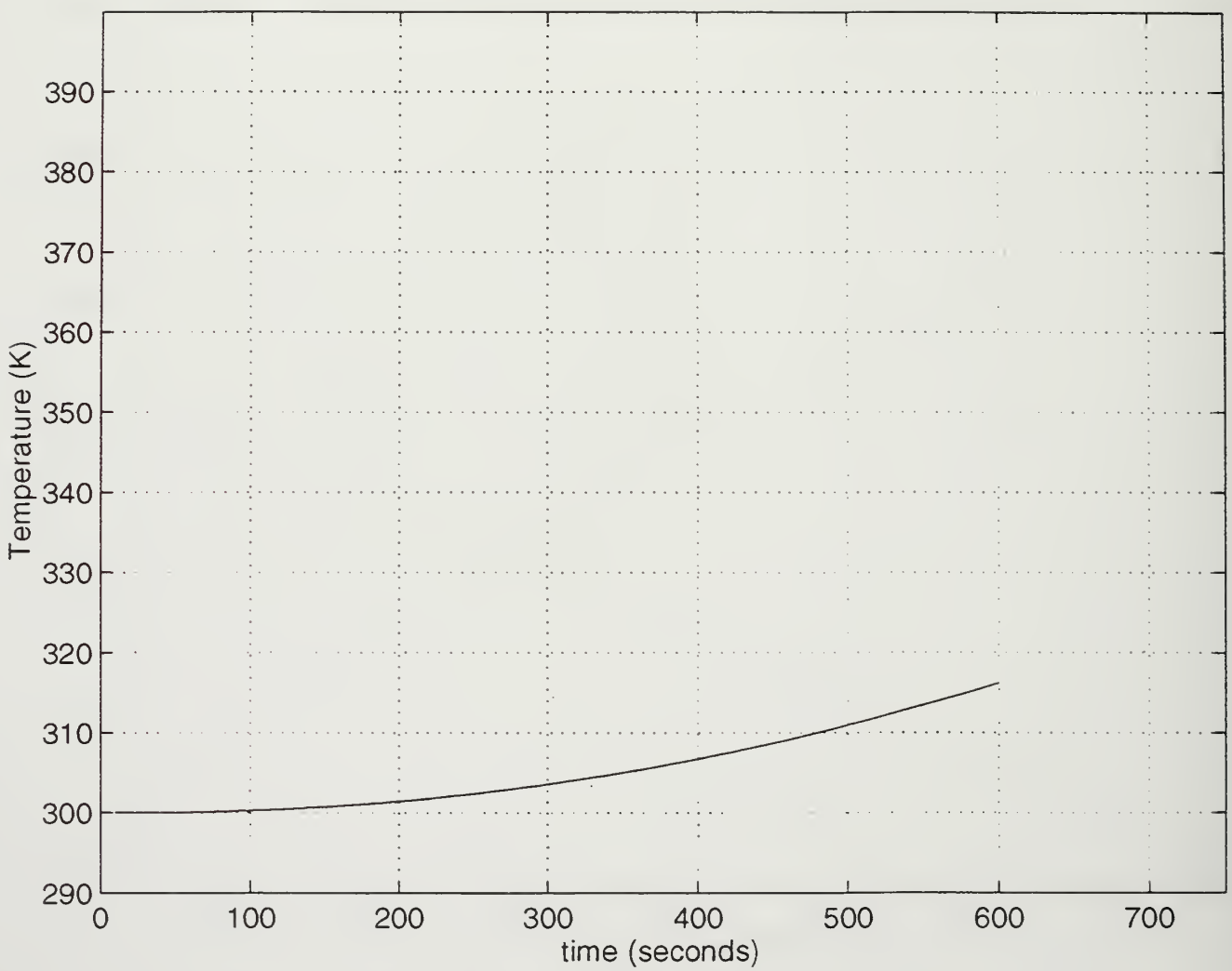

Figure 48. Exocet Fire - Round 2. Temperature vs. Time Plot for Monitor Point 3.

APPENDIX F. EXOCET FIRE - ROUND 3

The following data corresponds to the round 3 simulation of the Exocet fire scenerio, including:

(1) 3-dimensional temperature profile at a time of one minute.
(2) 3-dimensional temperature profile at a time of 10 minutes.
(3) Horizontal temperature profile at a time of one minute.
(4) Horizontal temperature profile at a time of 10 minutes.
(5) Temperature vs. index profile at a time of one minute.
(6) Temperature vs. index profile at a time of 10 minutes.
(7) Temperature vs. time plot for monitor point 1.
(8) Temperature vs. time plot for monitor point 2.
(9) Temperature vs. time plot for monitor point 3.

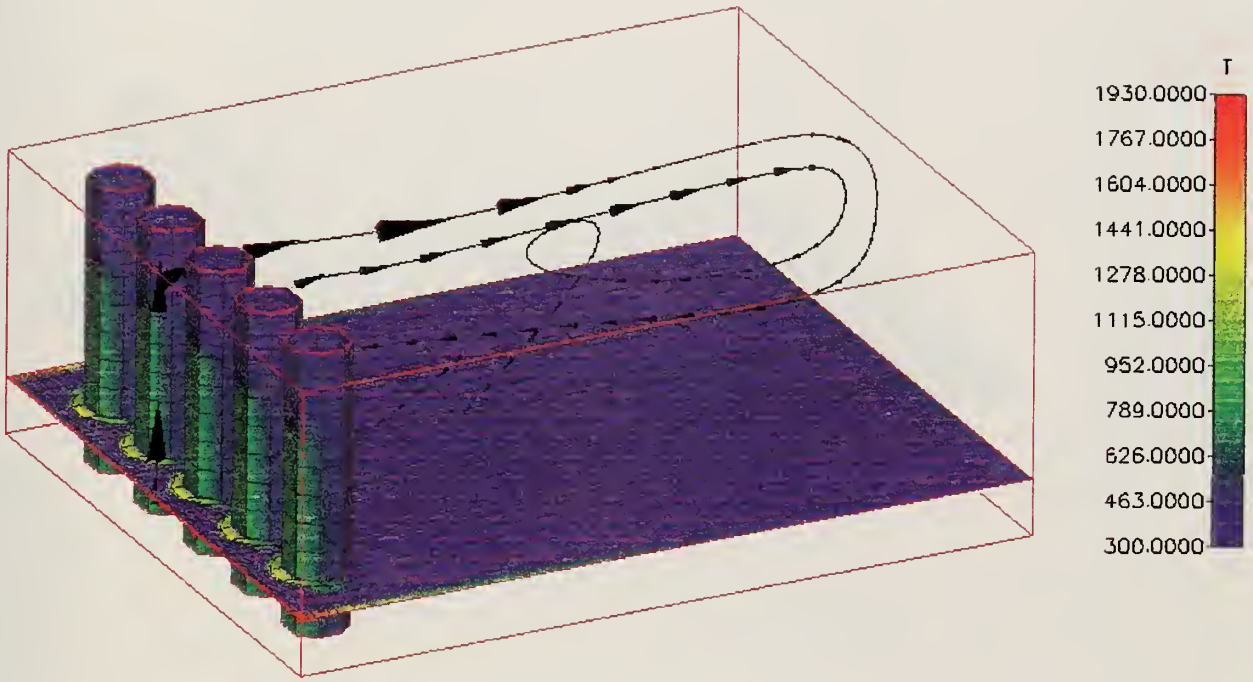

Figure 49. Exocet Fire - Round 3. 3-Dimensional Temperature Profile at a Time of 1 Minute.

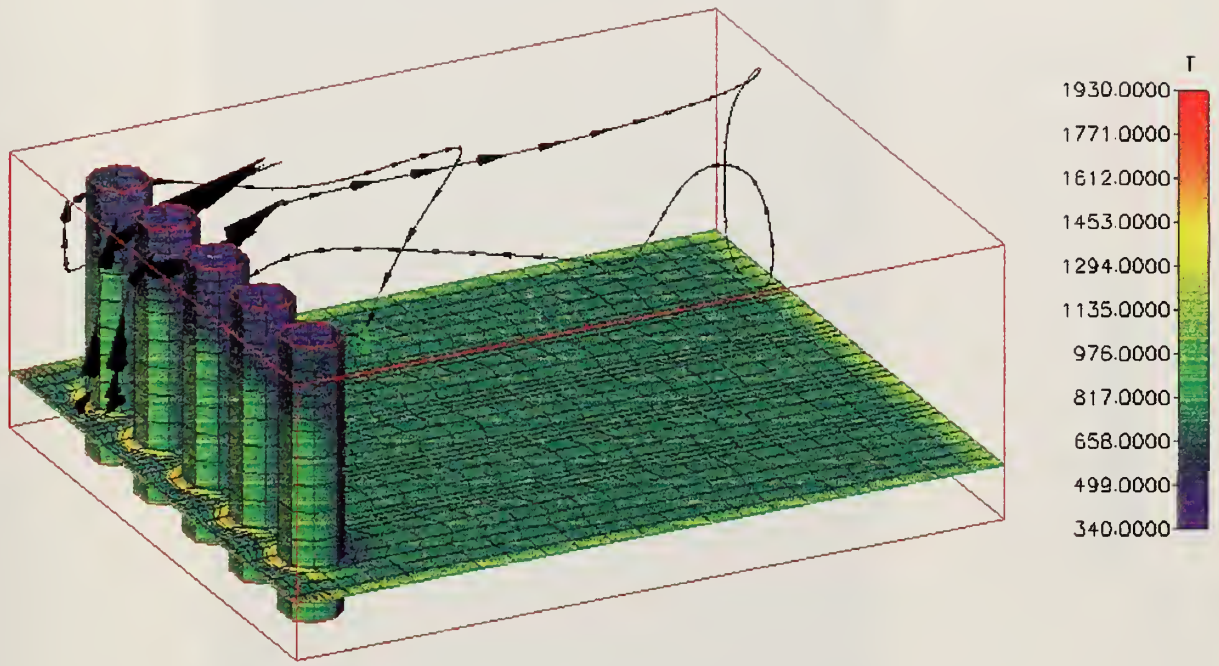

Figure 50. Exocet Fire - Round 3. 3-Dimensional Temperature Profile at a Time of 10 Minutes.

Figure 51. Exocet Fire - Round 3. Horizontal Temperature Profile at a Time of 1 Minute.

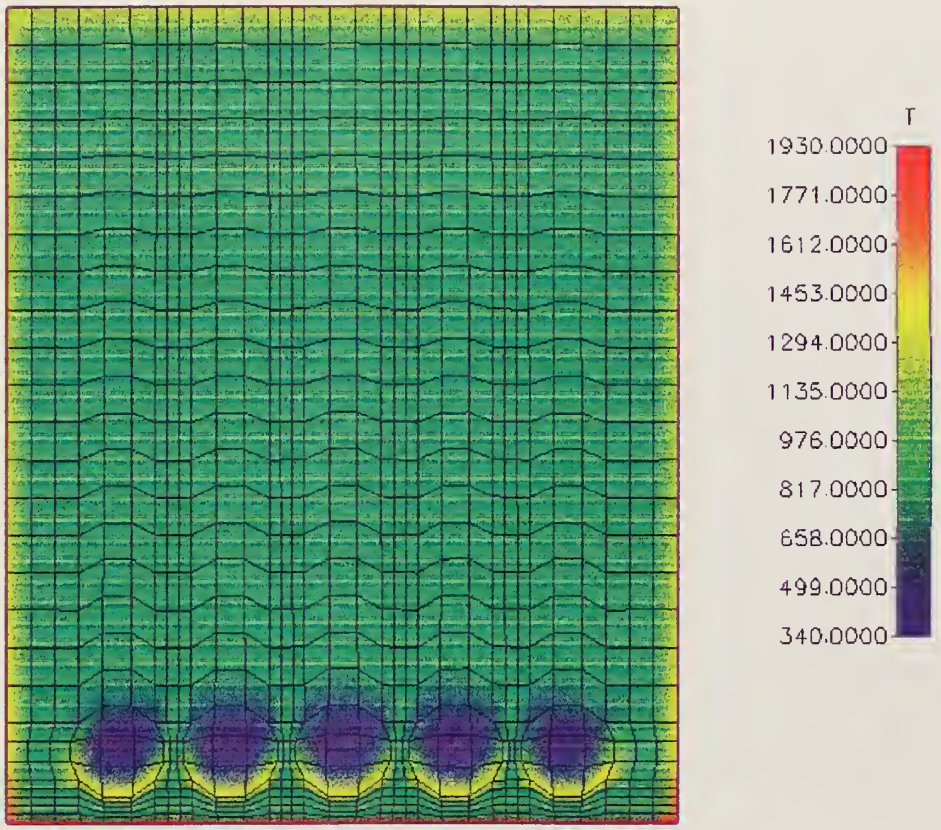

Figure 52. Exocet Fire - Round 3. Horizontal Temperature Profile at a Time of 10 Minutes.

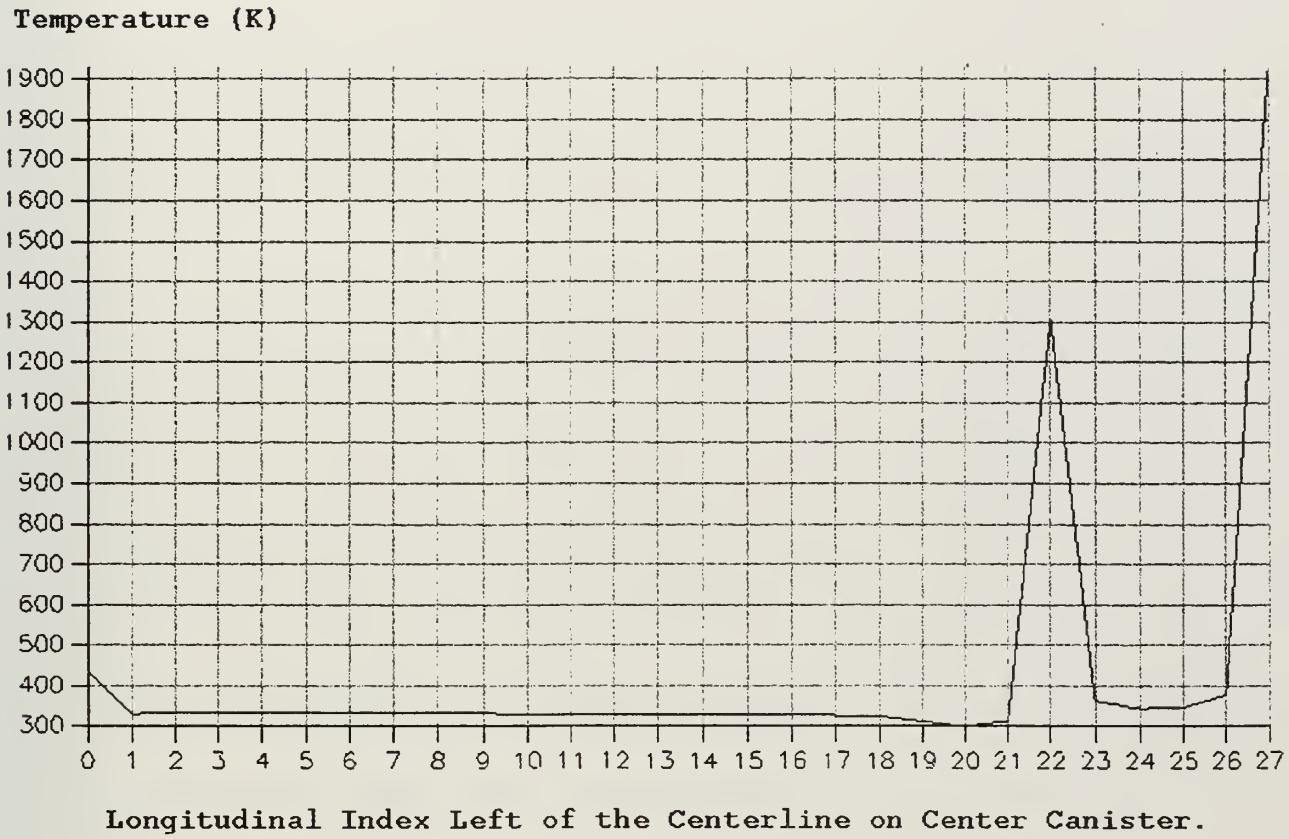

Figure 53. Exocet Fire - Round 3. Temperature vs. Index Profile at a Time of 1 Minute.

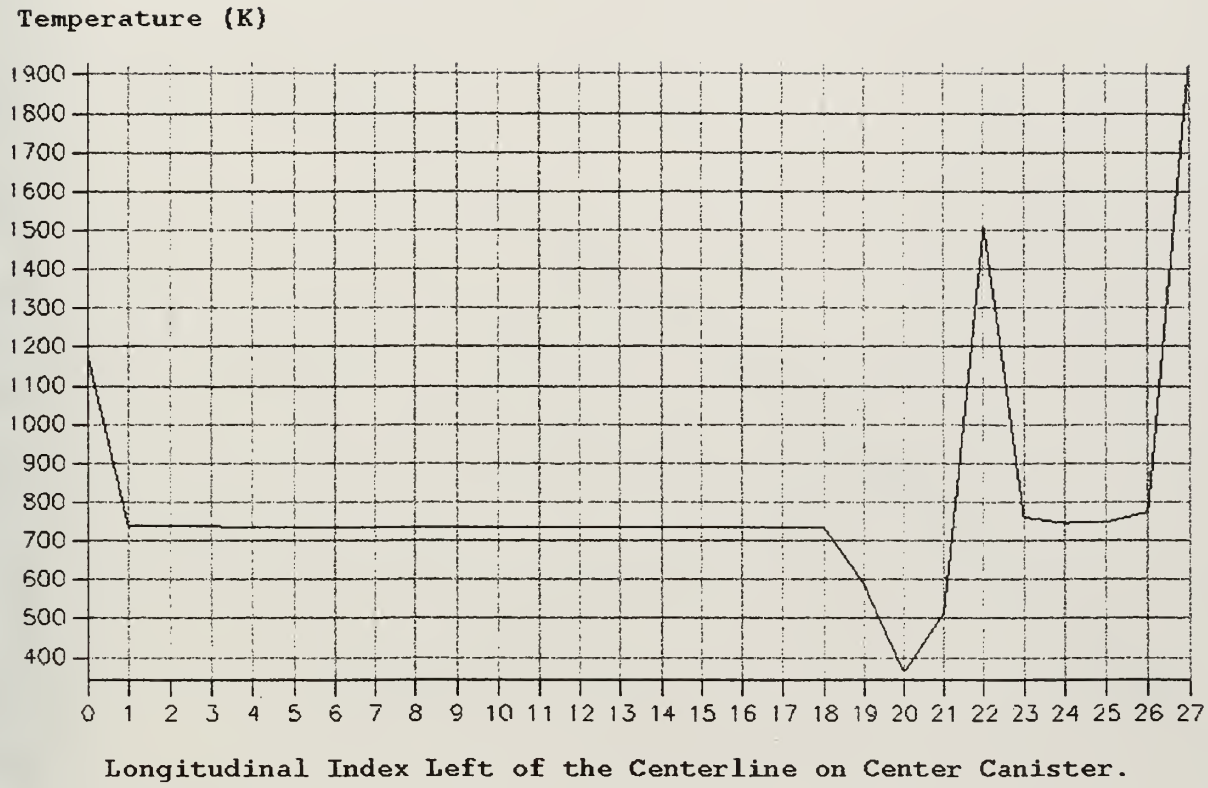

Figure 54. Exocet Fire - Round 3. Temperature vs. Index Profile at a Time of 10 Minutes.

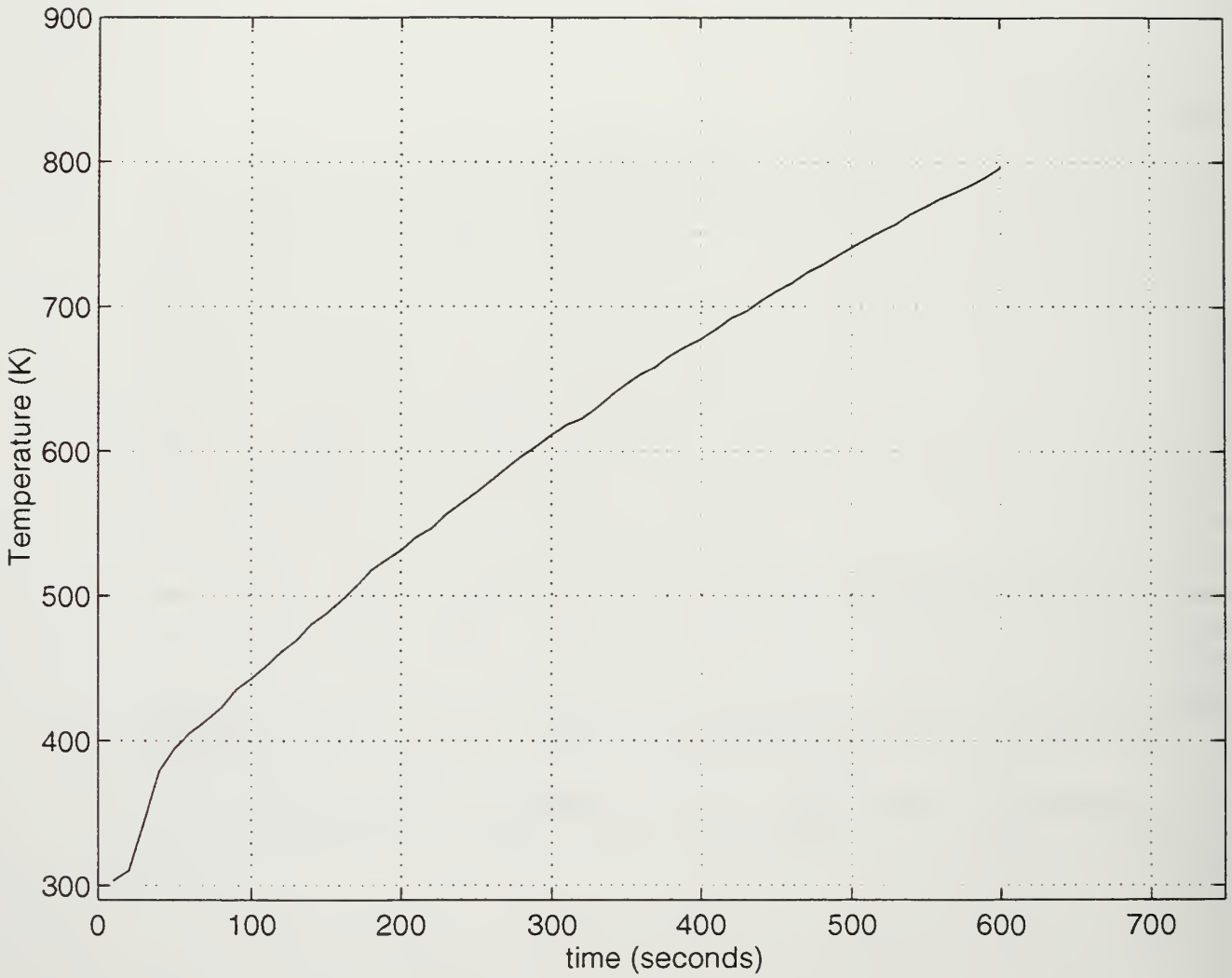

Figure 55. Exocet Fire - Round 3. Temperature vs. Time Plot for Monitor Point 1.

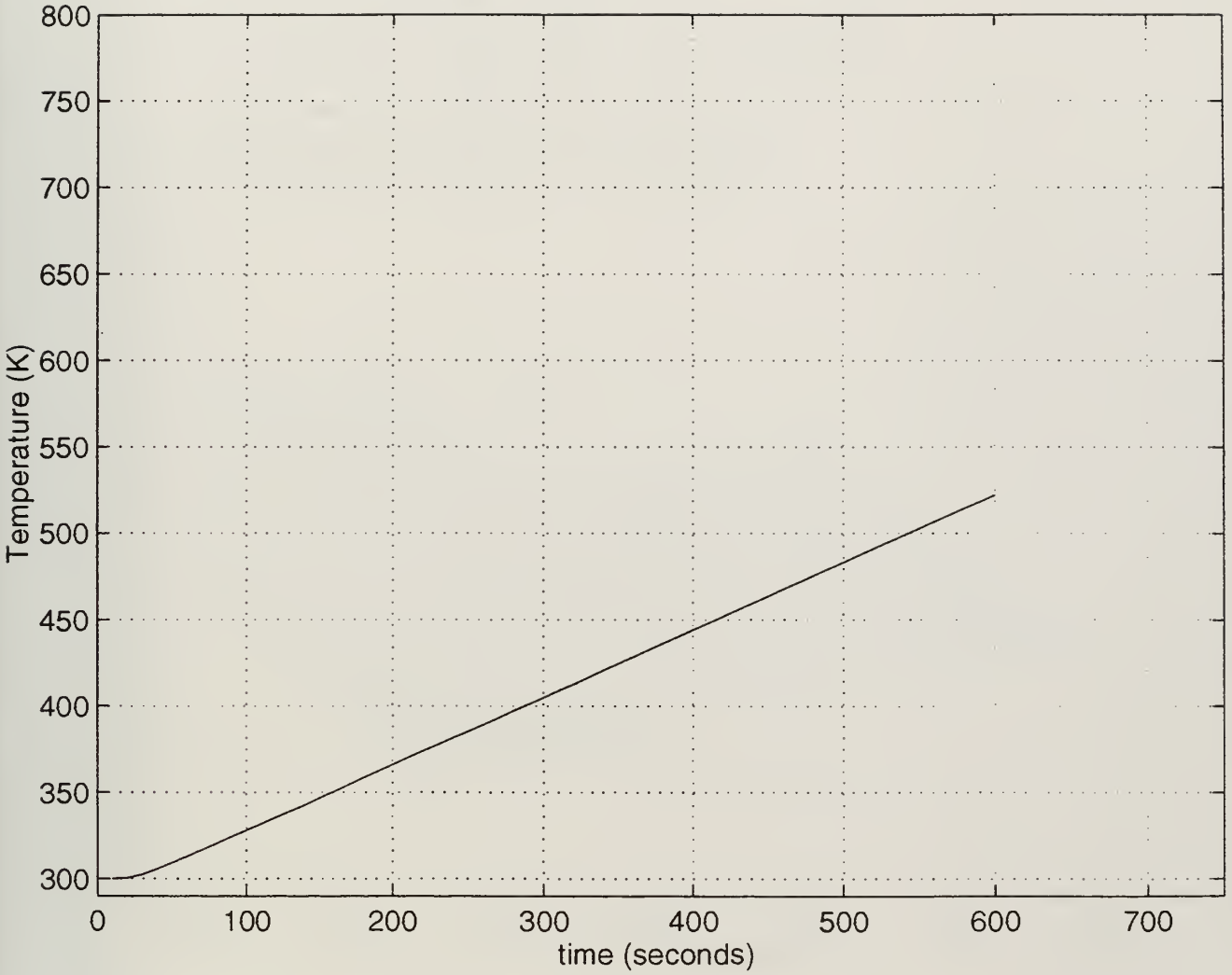

Figure 56. Exocet Fire - Round 3. Temperature vs. Time Plot for Monitor Point 2.

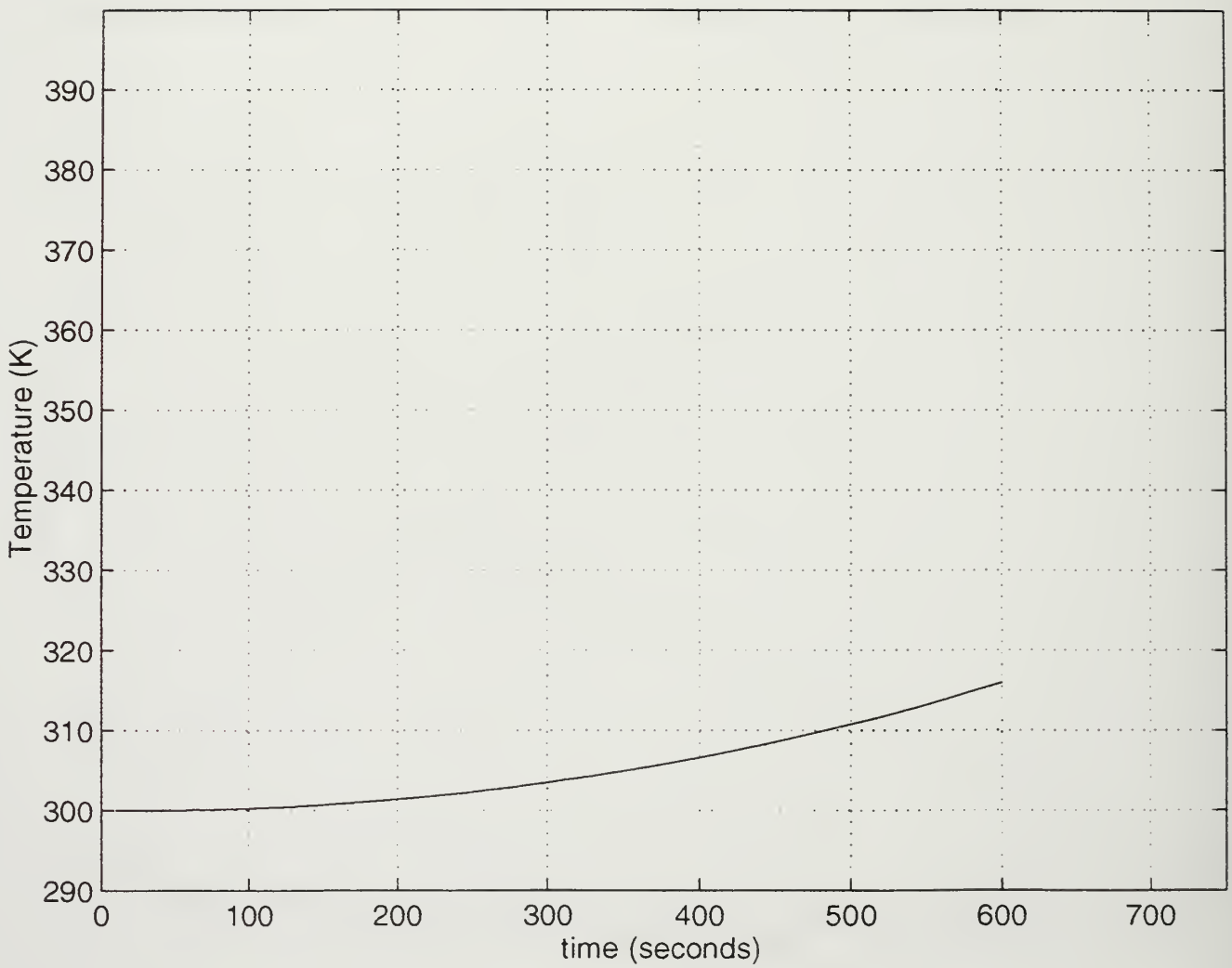

Figure 57. Exocet Fire - Round 3. Temperature vs. Time Plot for Monitor Point 3.

APPENDIX G. EXOCET FIRE - ROUND 4

The following data corresponds to the round 4 simulation of the Exocet fire scenerio, including:

(1) 3-dimensional temperature profile at a time of one minute.
(2) 3-dimensional temperature profile at a time of 10 minutes.
(3) Horizontal temperature profile at a time of one minute.
(4) Horizontal temperature profile at a time of 10 minutes.
(5) Temperature vs. index profile at a time of one minute.
(6) Temperature vs. index profile at a time of 10 minutes.
(7) Temperature vs. time plot for monitor point 1.
(8) Temperature vs. time plot for monitor point 2.
(9) Temperature vs. time plot for monitor point 3.

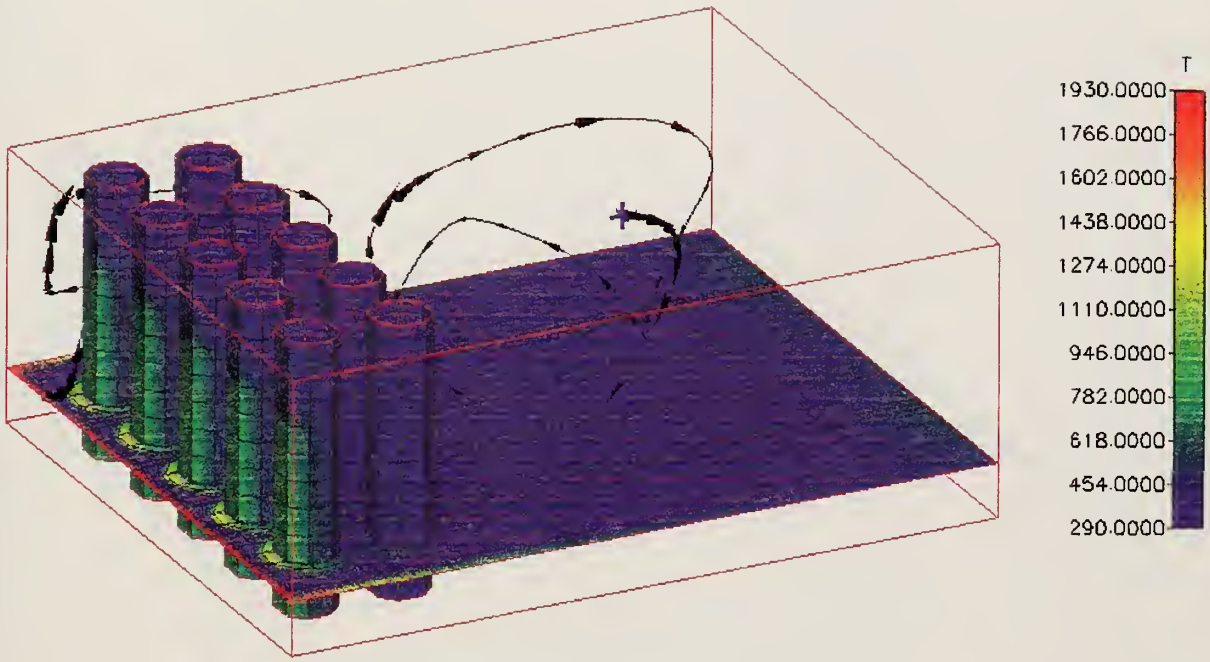

Figure 58. Exocet Fire - Round 4. 3-Dimensional Temperature Profile at a Time of 1 Minute.

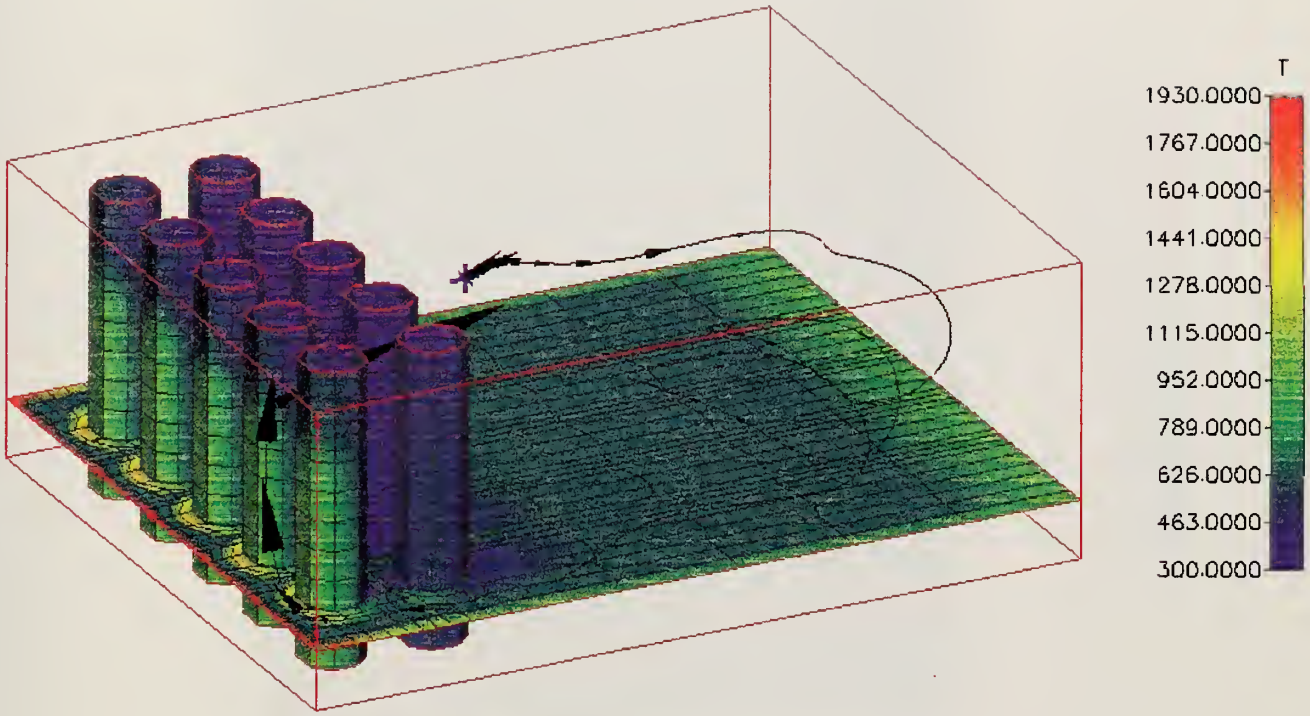

Figure 59. Exocet Fire - Round 4. 3-Dimensional Temperature Profile at a Time of 10 Minutes.

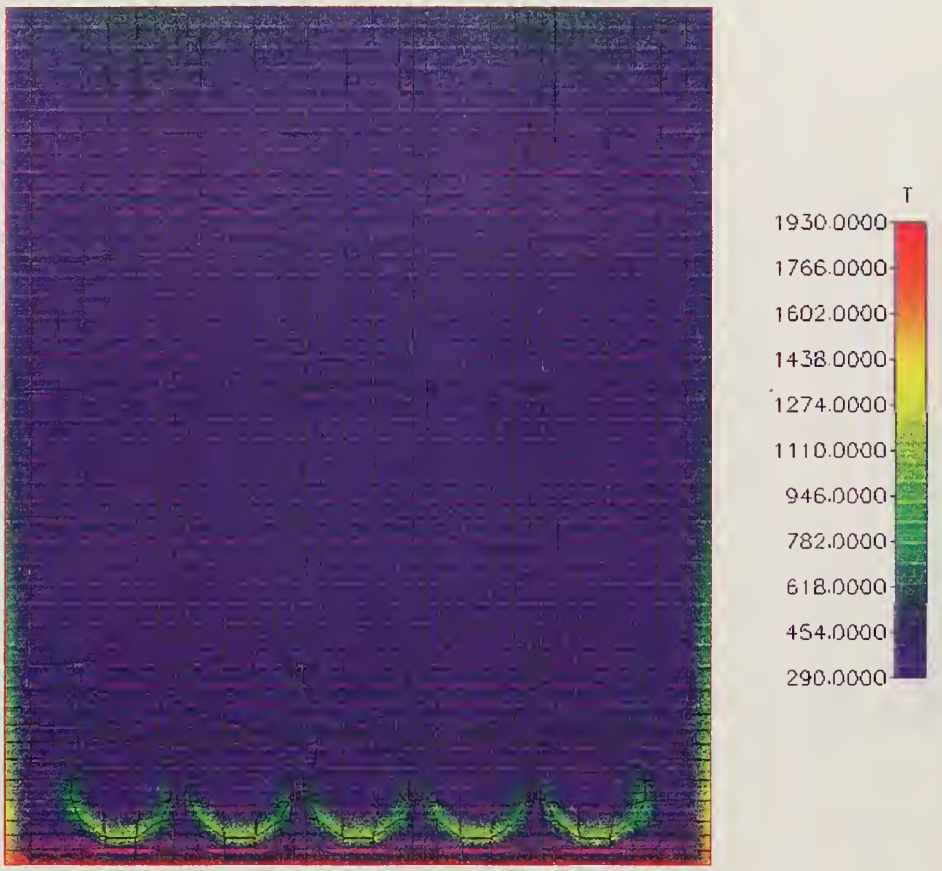

Figure 60. Exocet Fire - Round 4. Horizontal Temperature Profile at a Time of 1 Minute.

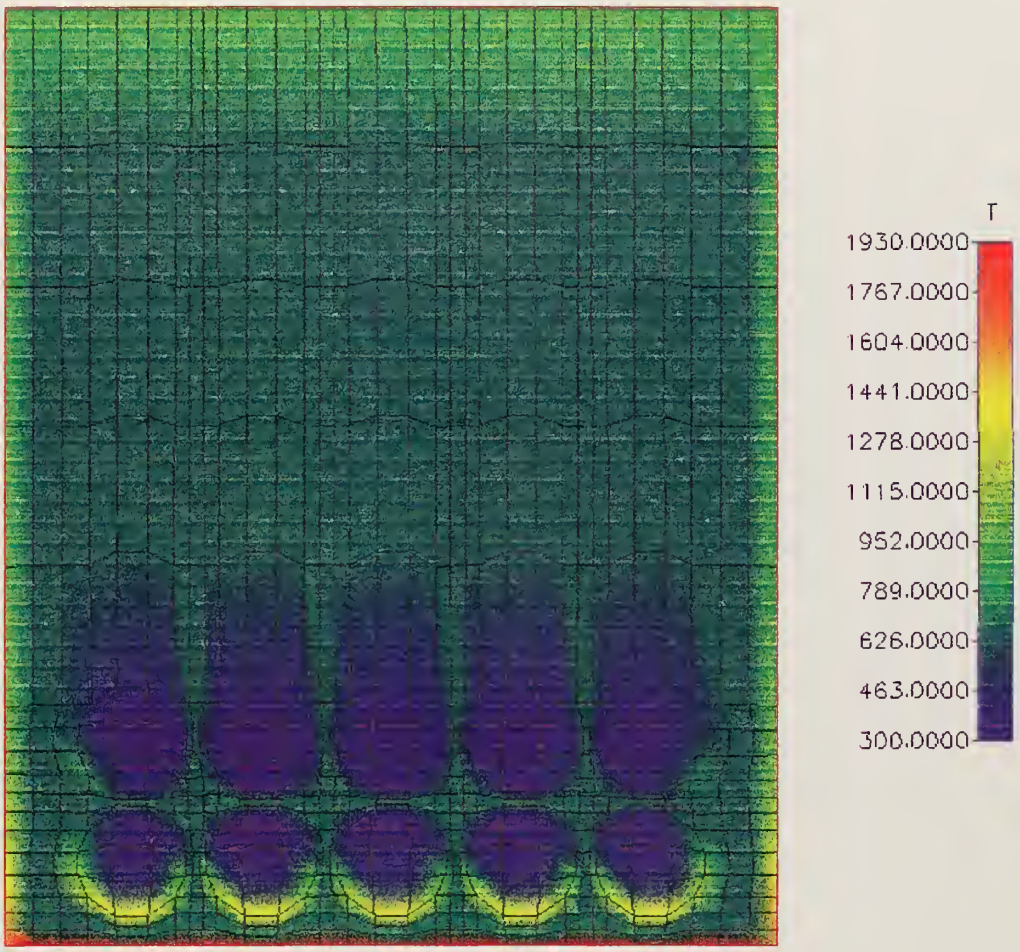

Figure 61. Exocet Fire - Round 4. Horizontal Temperature Profile at a Time of 10 Minutes.

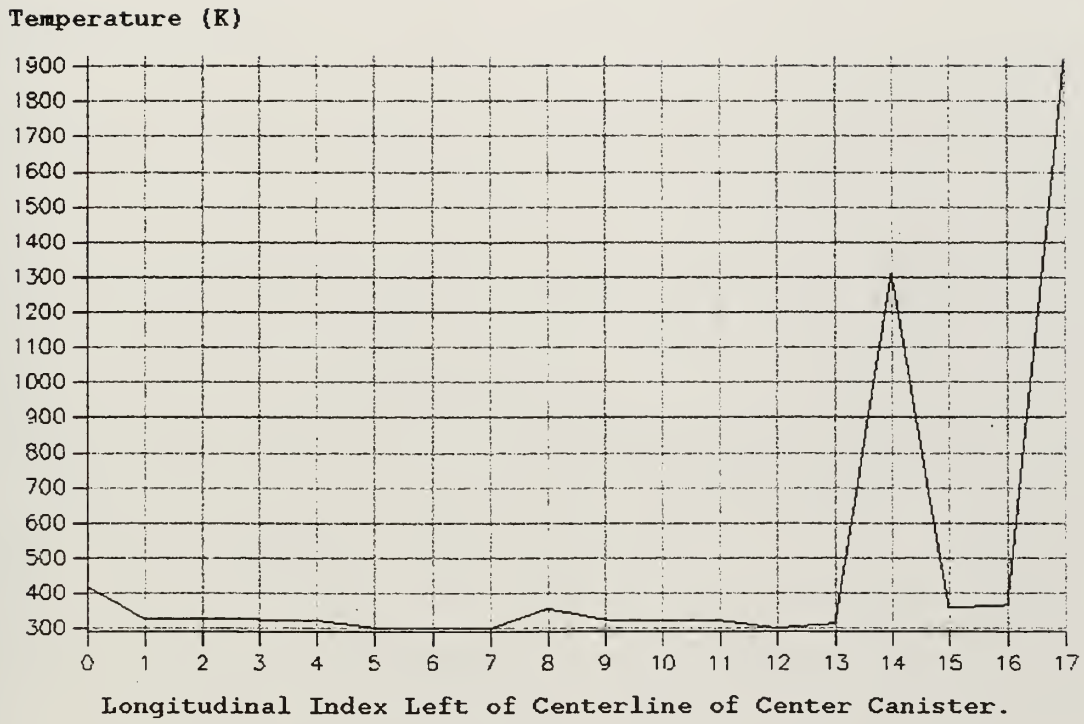

Figure 62. Exocet Fire - Round 4. Temperature vs. Index Profile at a Time of 1 Minute.

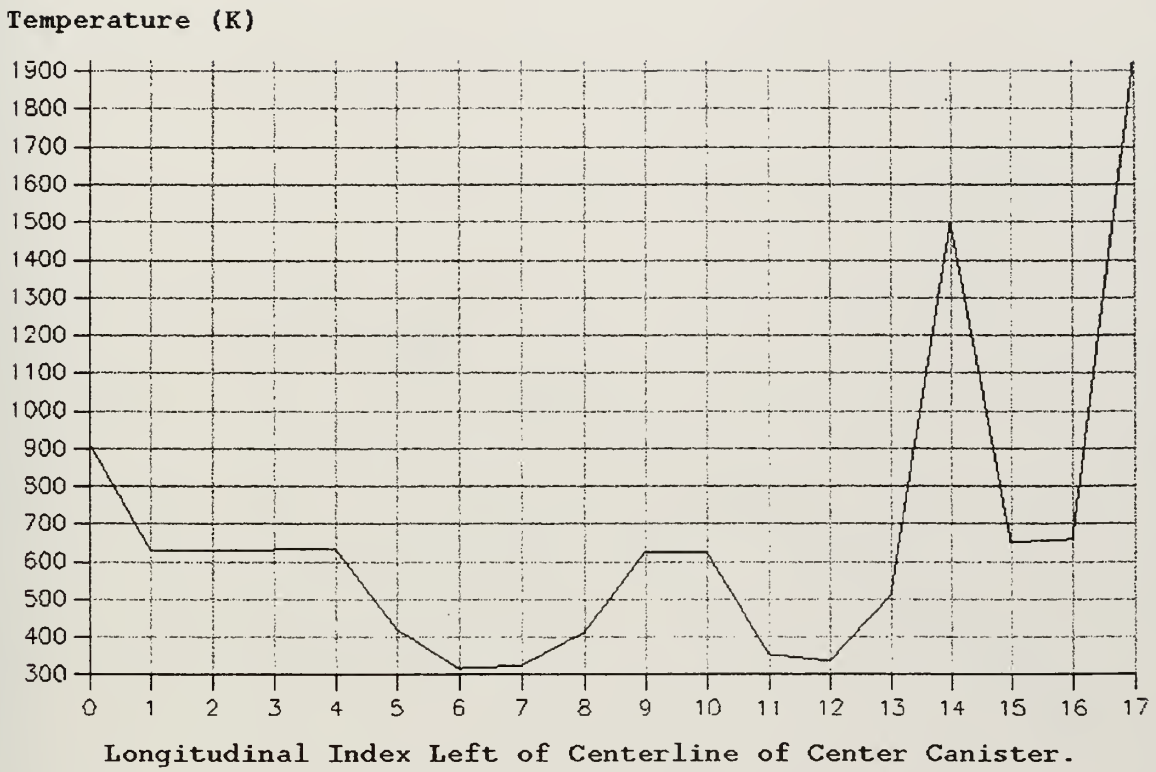

Figure 63. Exocet Fire - Round 4. Temperature vs. Index Profile at a Time of 10 Minutes.

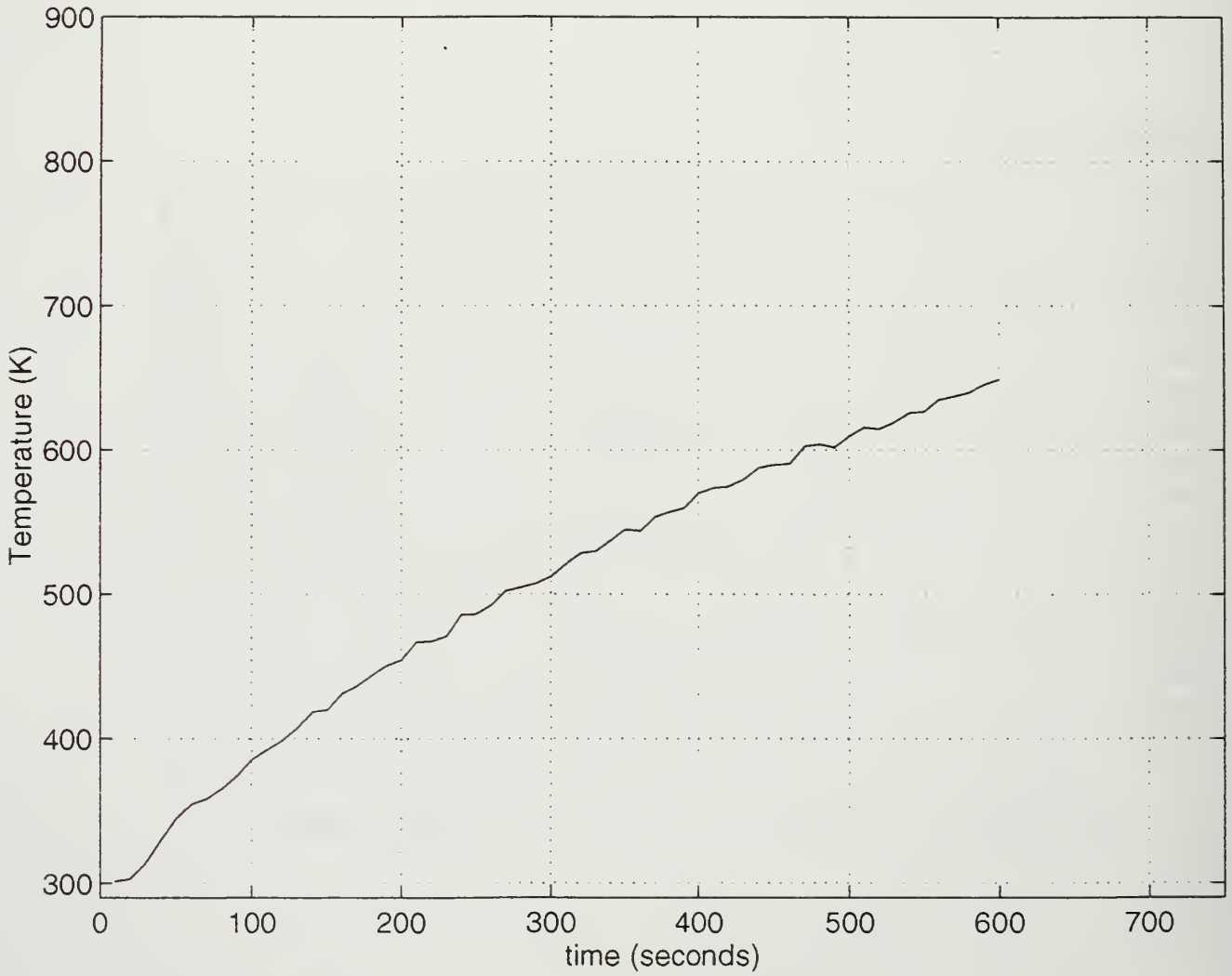

Figure 64. Exocet Fire - Round 4. Temperature vs. Time Plot for Monitor Point 1.

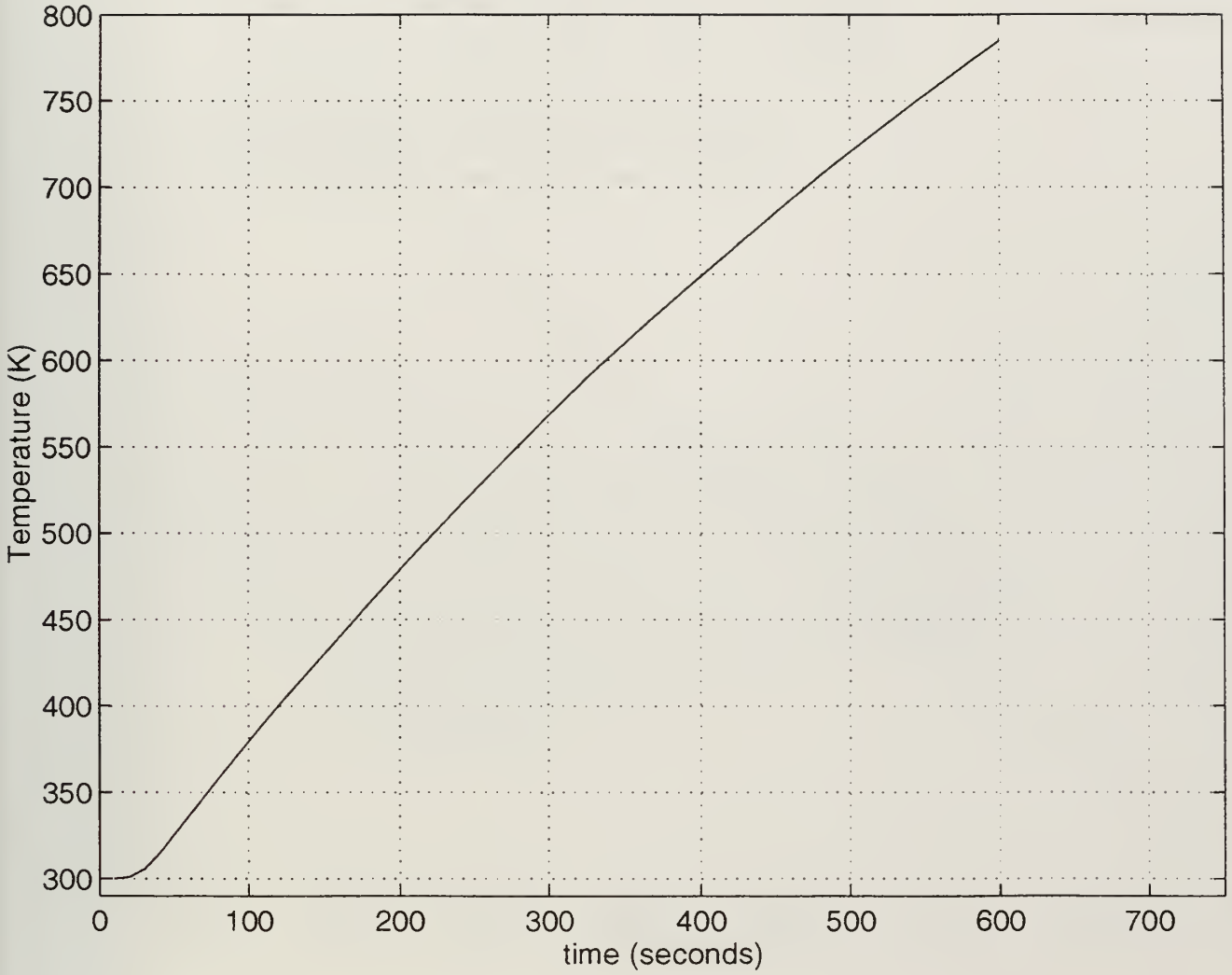

Figure 65. Exocet Fire - Round 4. Temperature vs. Time Plot for Monitor Point 2.

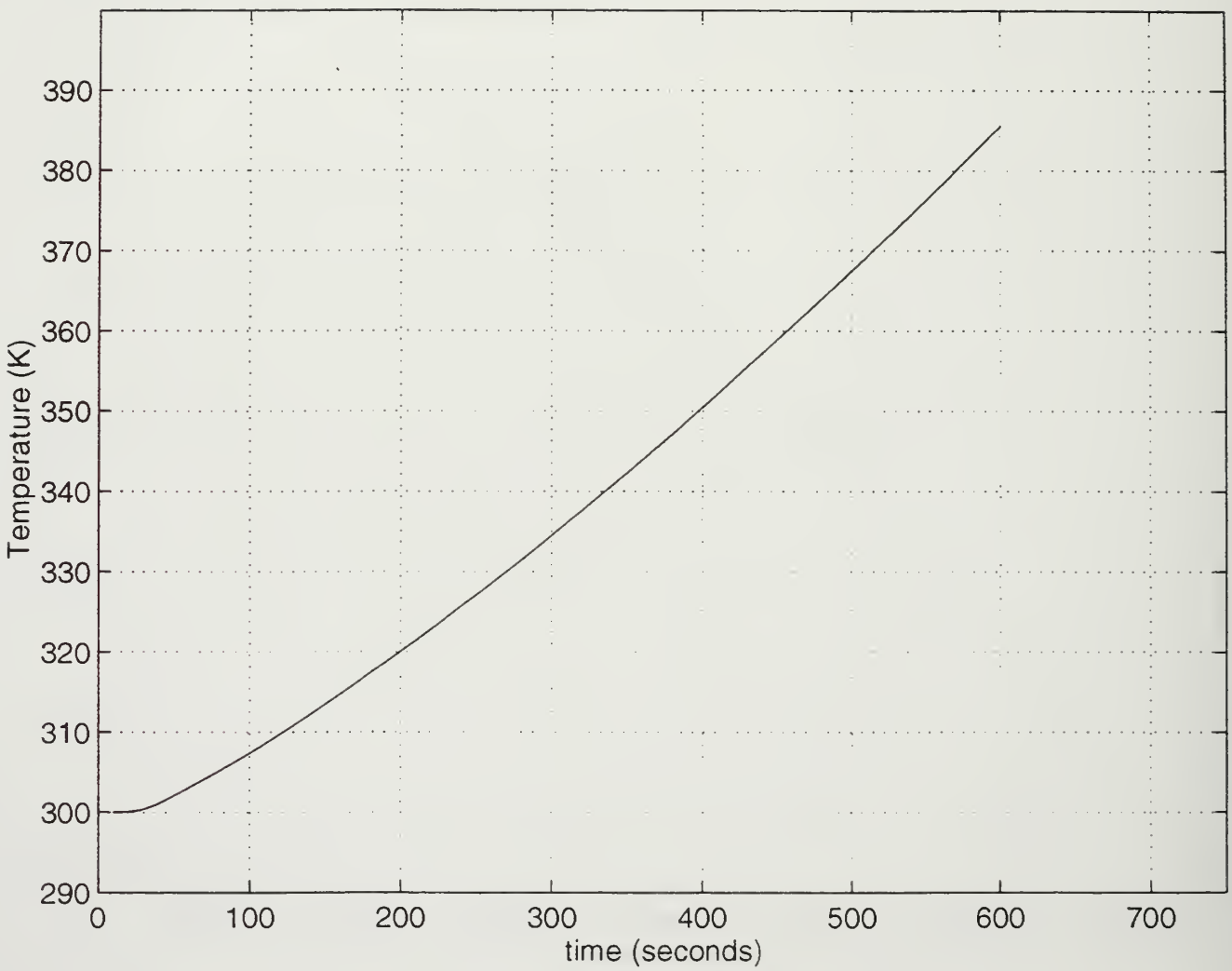

Figure 66. Exocet Fire - Round 4. Temperature vs. Time Plot for Monitor Point 3.

APPENDIX H. EXOCET FIRE - ROUND 5

The following data corresponds to the round 5 simulation of the Exocet fire scenerio, including:

(1) 3-dimensional temperature profile at a time of one minute.
(2) 3-dimensional temperature profile at a time of 10 minutes.
(3) Horizontal temperature profile at a time of one minute.
(4) Horizontal temperature profile at a time of 10 minutes.
(5) Temperature vs. index profile at a time of one minute.
(6) Temperature vs. index profile at a time of 10 minutes.
(7) Temperature vs. time plot for monitor point 1.
(8) Temperature vs. time plot for monitor point 2.
(9) Temperature vs. time plot for monitor point 3.

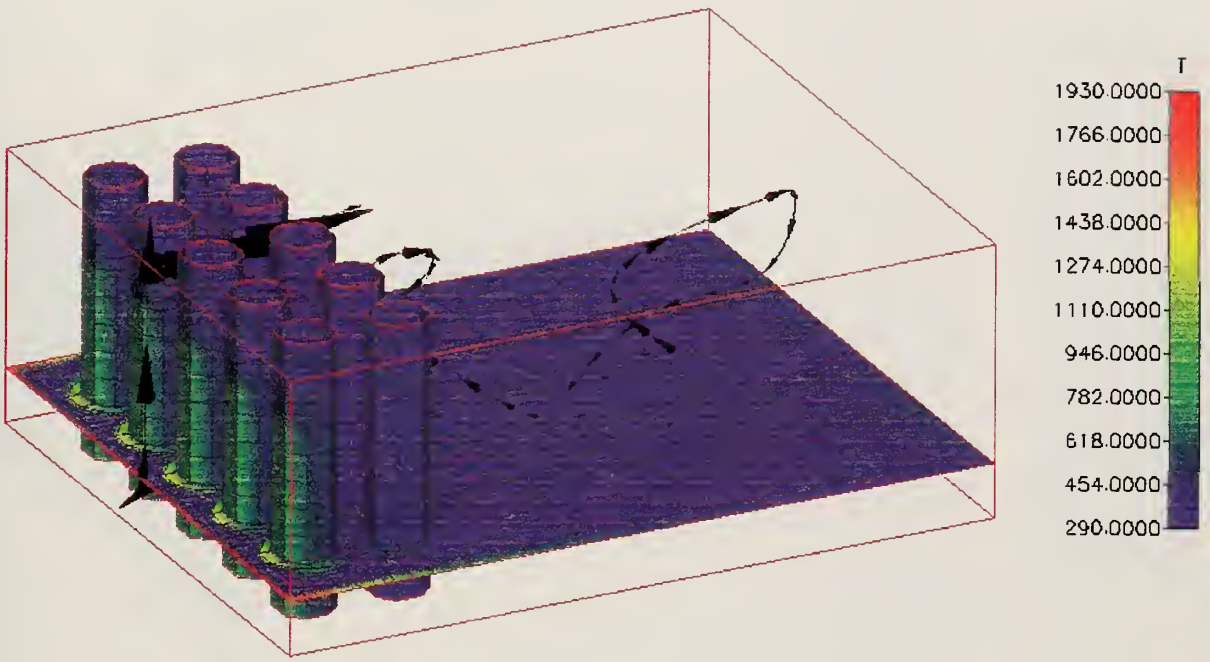

Figure 67. Exocet Fire - Round 5. 3-Dimensional Temperature Profile at a Time of 1 Minute.

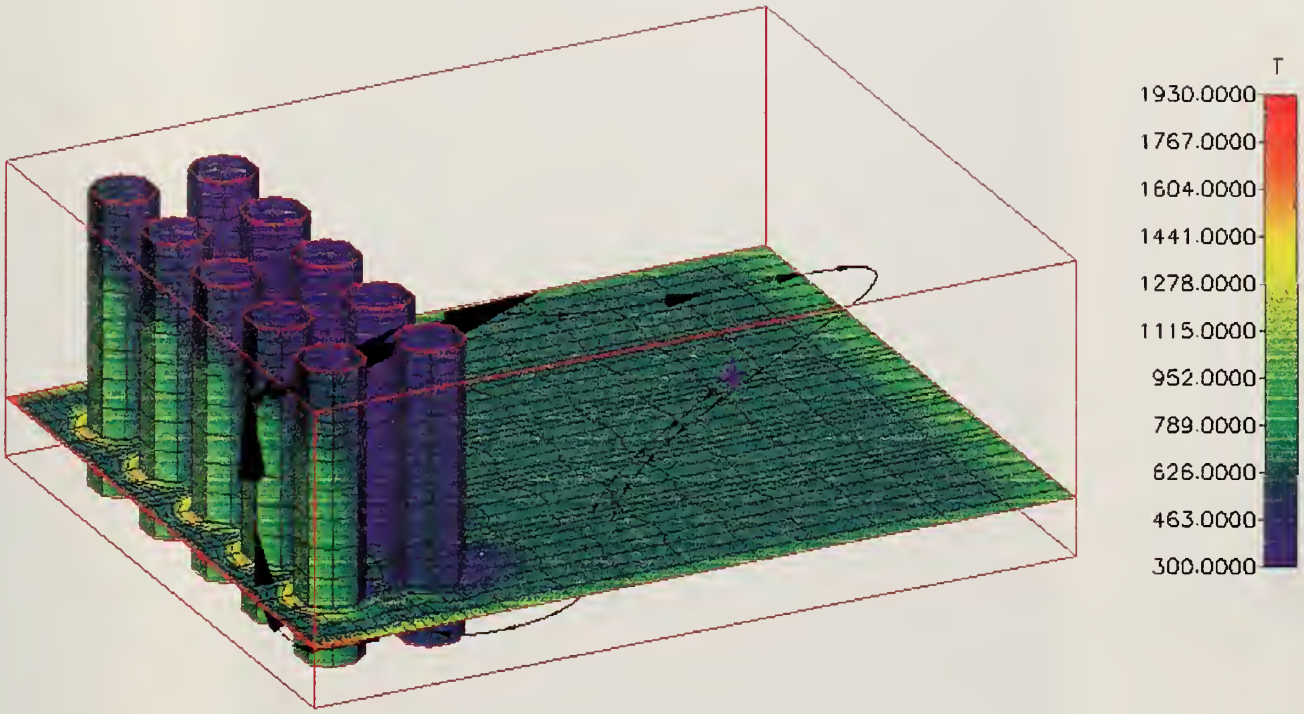

Figure 68. Exocet Fire - Round 5. 3-Dimensional Temperature Profile at a Time of 10 Minutes.

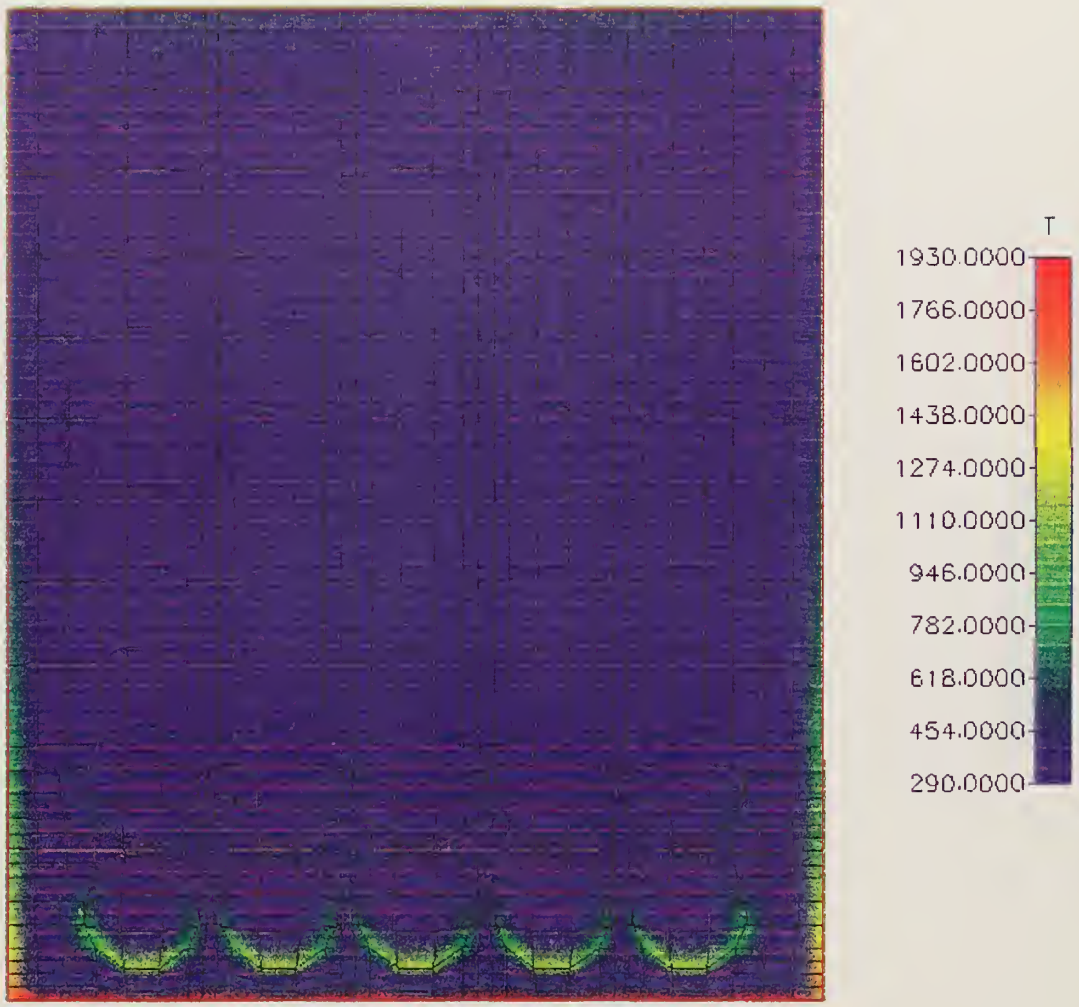

Figure 69. Exocet Fire - Round 5. Horizontal Temperature Profile at a Time of 1 Minute.

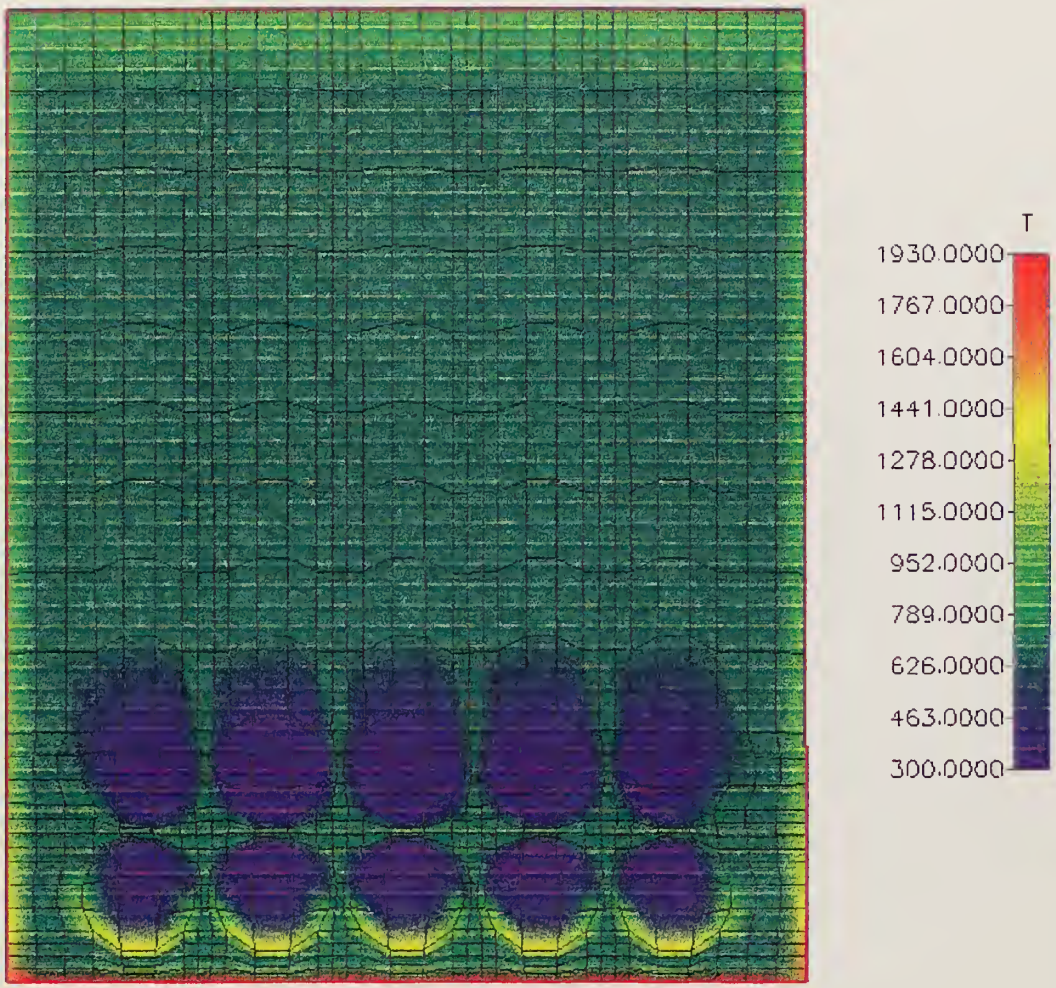

Figure 70. Exocet Fire - Round 5. Horizontal Temperature Profile at a Time of 10 Minutes.

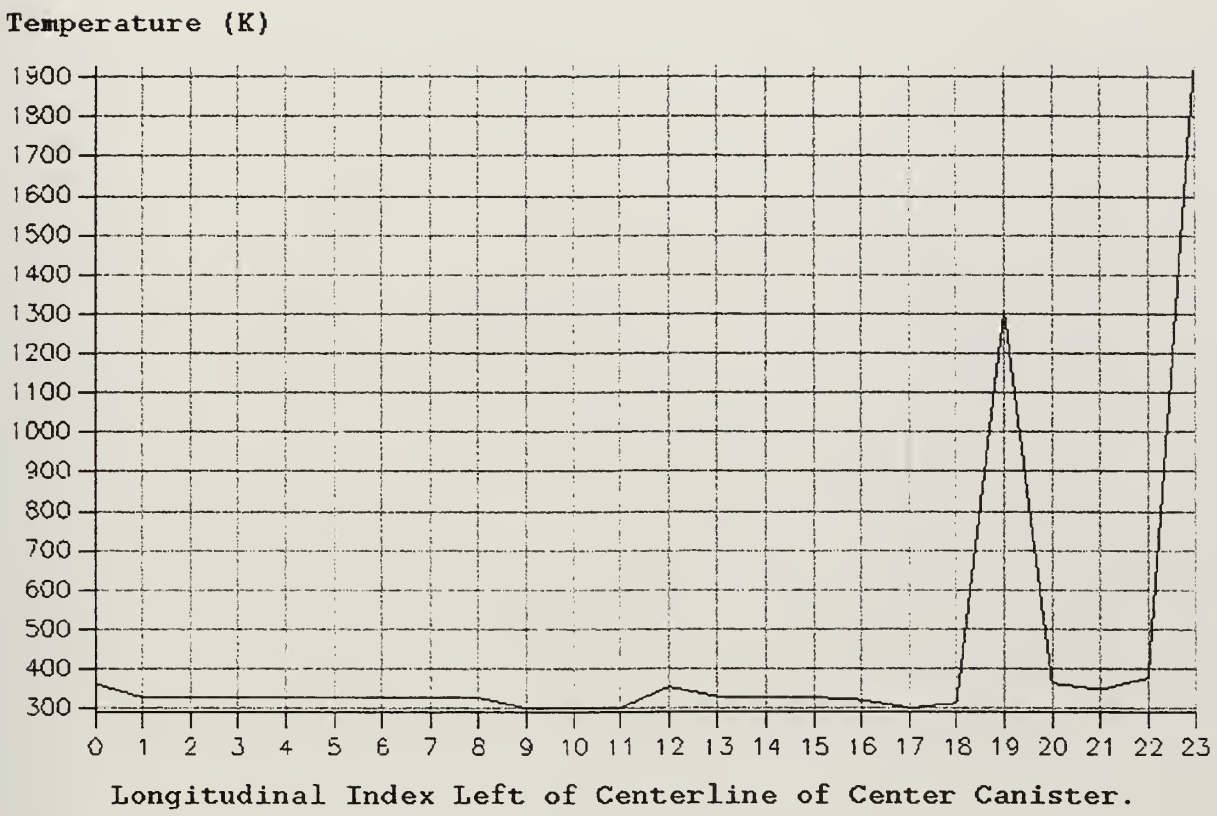

Figure 71. Exocet Fire - Round 5. Temperature vs. Index Profile at a Time of 1 Minute.

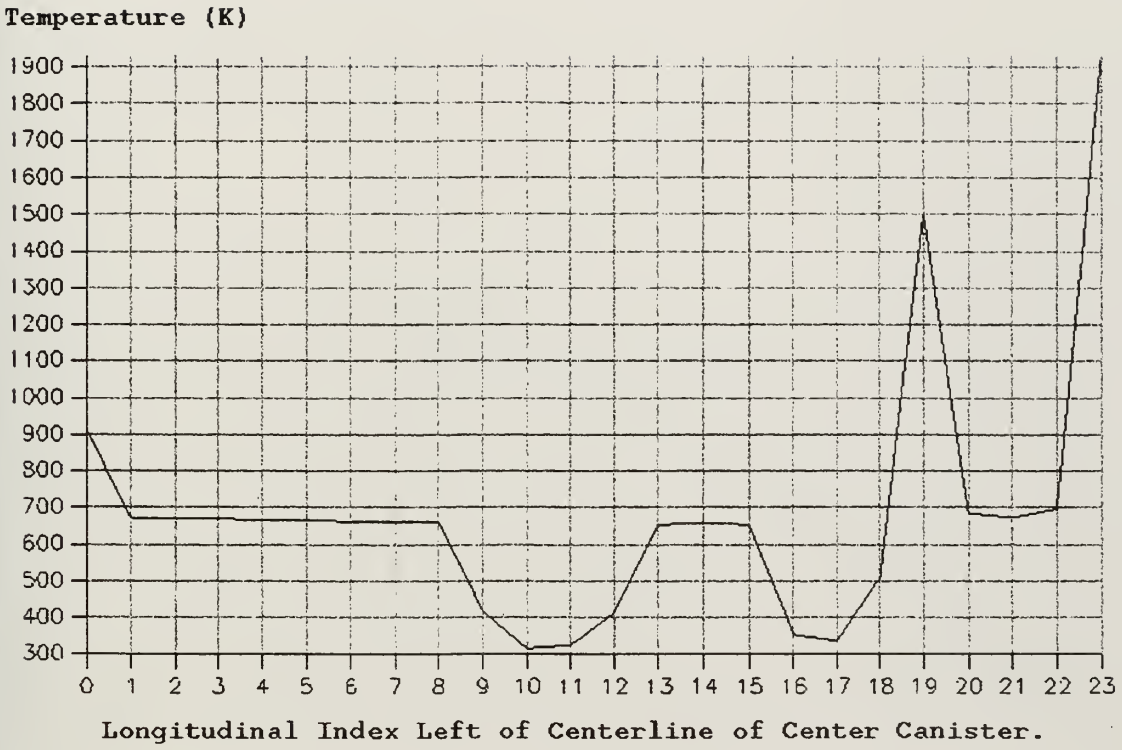

Figure 72. Exocet Fire - Round 5. Temperature vs. Index Profile at a Time of 10 Minutes.

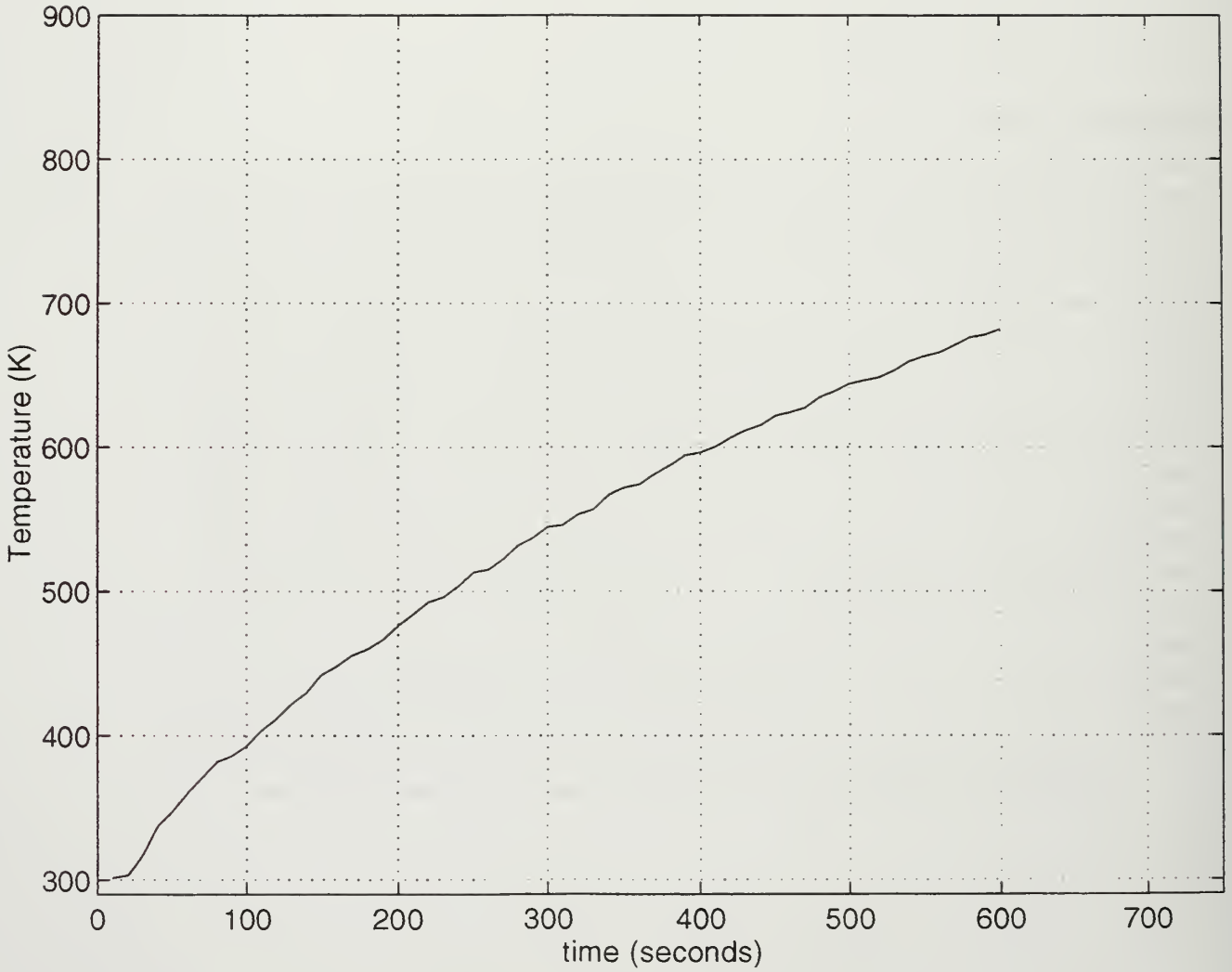

Figure 73. Exocet Fire - Round 5. Temperature vs. Time Plot for Monitor Point 1.

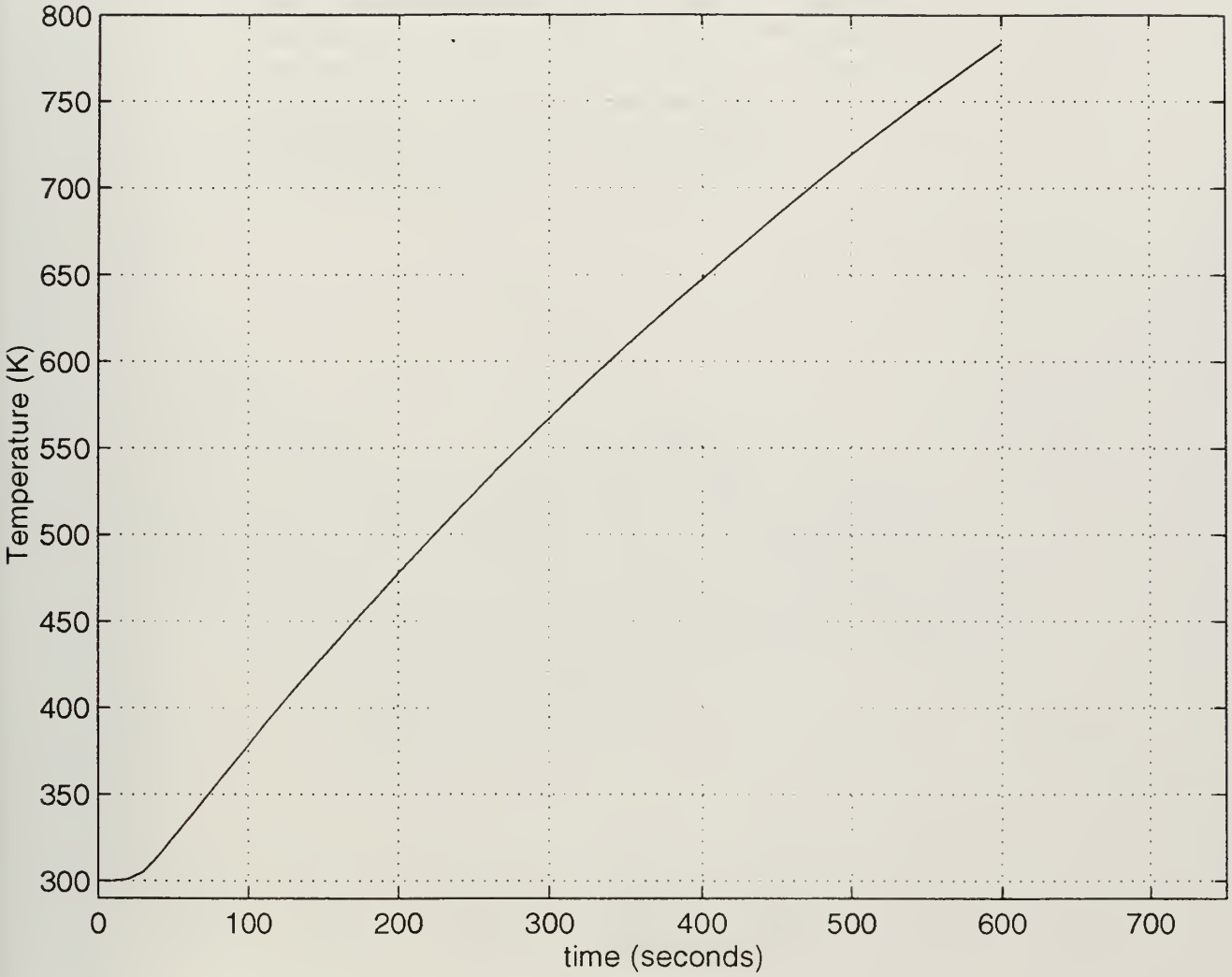

Figure 74. Exocet Fire - Round 5. Temperature vs. Time Plot for Monitor Point 2.

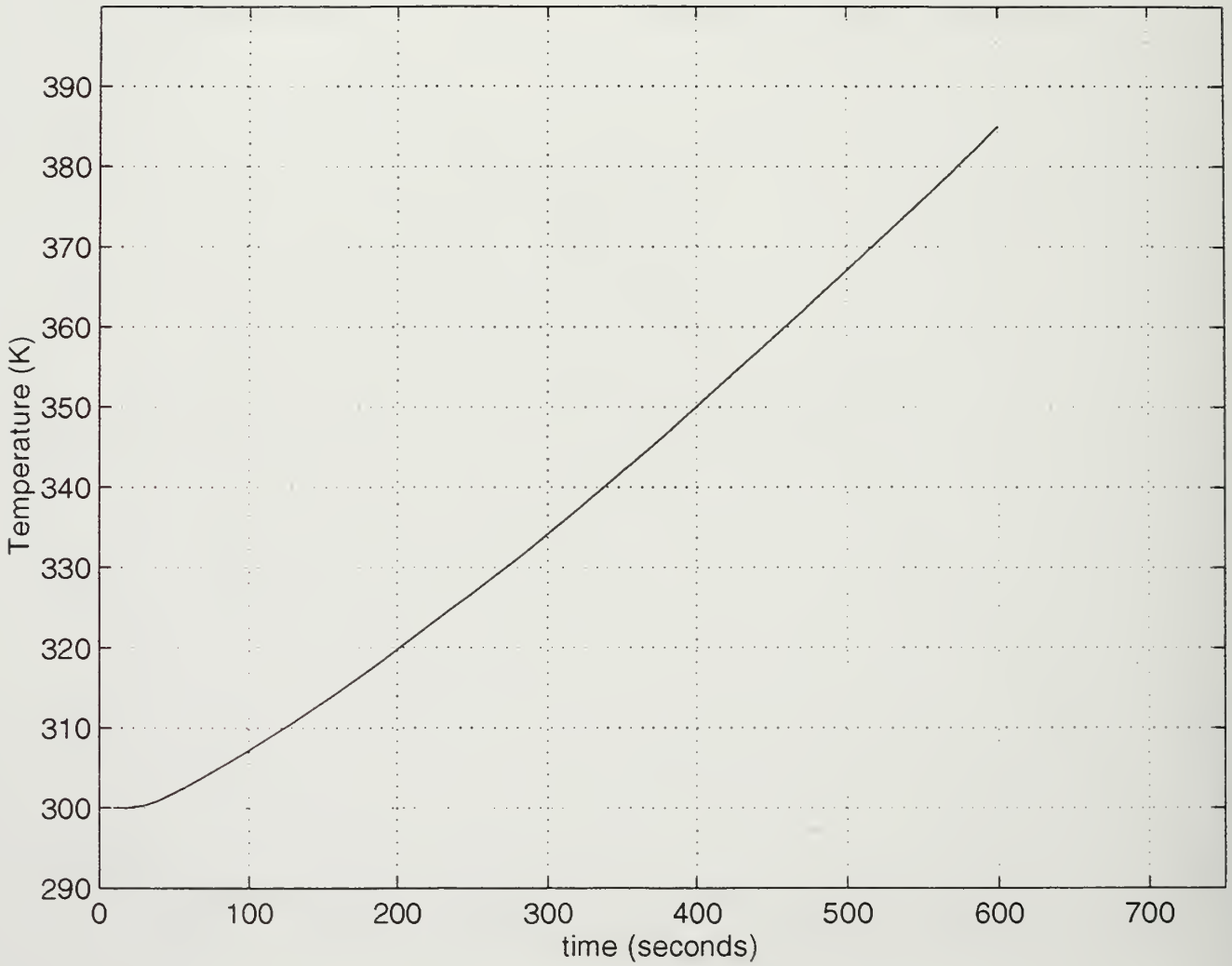

Figure 75. Exocet Fire - Round 5. Temperature vs. Time Plot for Monitor Point 3.

APPENDIX I. F-76 FIRE - ROUND 1

The following data corresponds to the round 1 simulation of the F-76 fire scenerio, including:

(1) 3-dimensional temperature profile at a time of 1.67 minutes.
(2) 3-dimensional temperature profile at a time of 10 minutes.
(3) Horizontal temperature profile at a time of 1.67 minutes.
(4) Horizontal temperature profile at a time of 10 minutes.
(5) Temperature vs. index profile at a time of 1.67 minutes.
(6) Temperature vs. index profile at a time of 10 minutes.
(7) Temperature vs. time plot for monitor point 1.
(8) Temperature vs. time plot for monitor point 2.
(9) Temperature vs. time plot for monitor point 3.

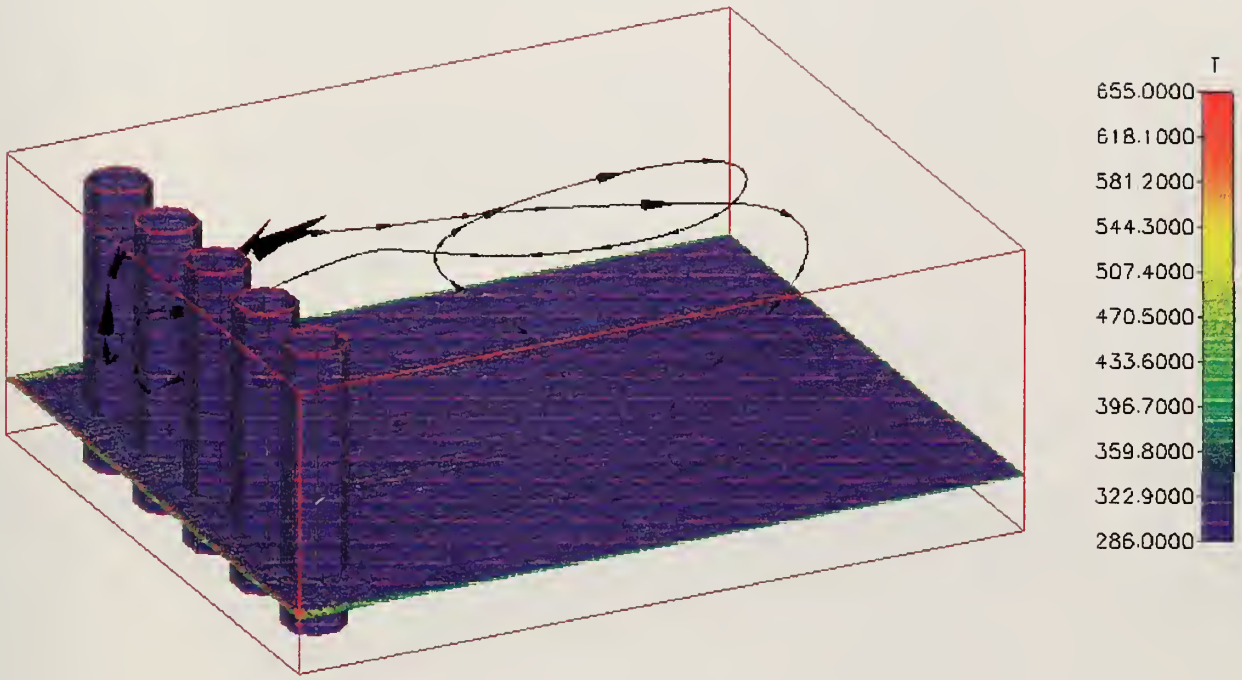

Figure 76. F-76 Fire - Round 1. 3-Dimensional Temperature Profile at a Time of 1.67 Minutes.

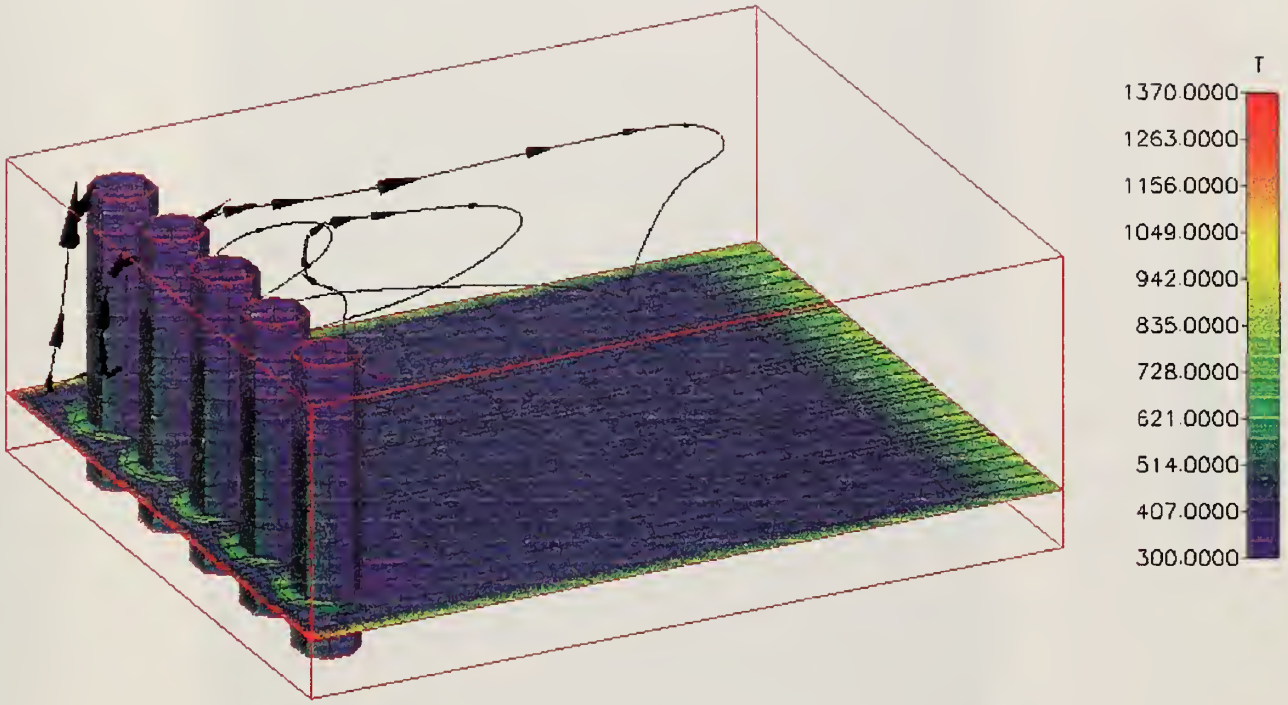

Figure 77. F-76 Fire - Round 1. 3-Dimensional Temperature Profile at a Time of 10 Minutes.

Figure 78. F-76 Fire - Round 1. Horizontal Temperature Profile at a Time of 1.67 Minutes.

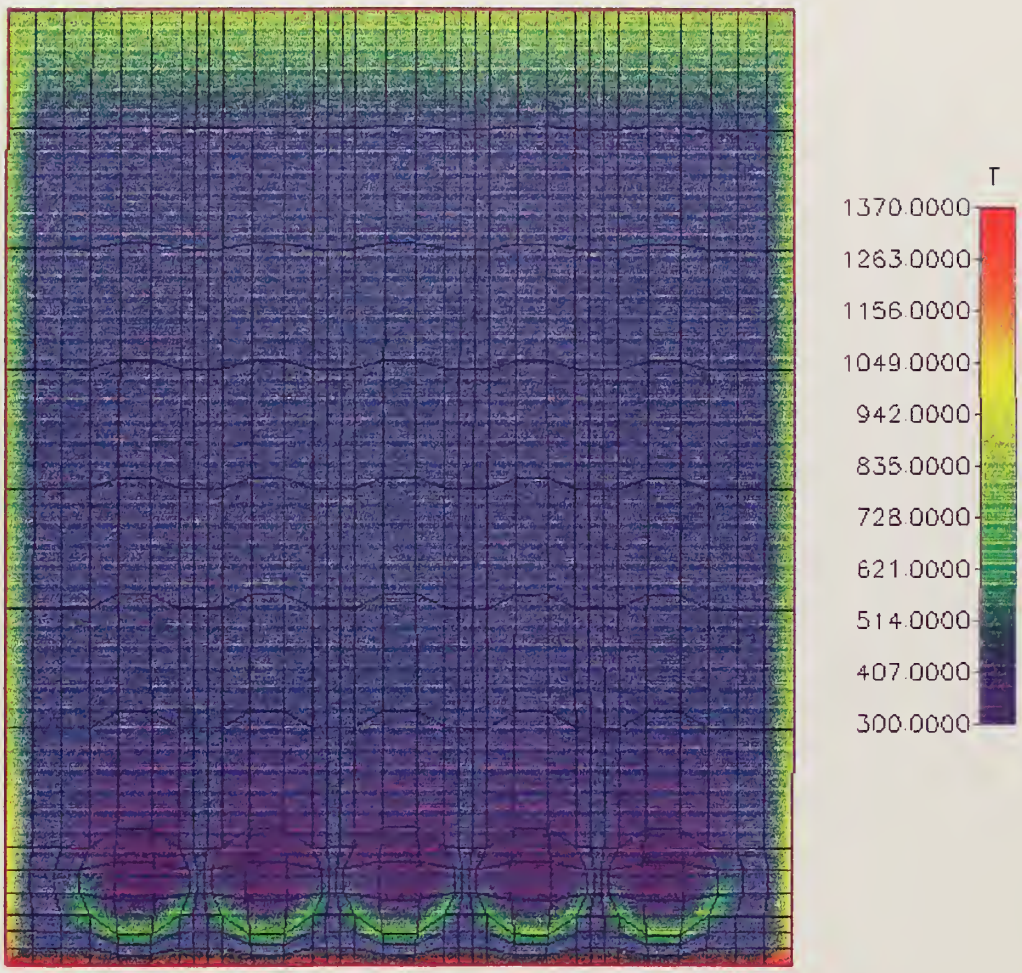

Figure 79. F-76 Fire - Round 1. Horizontal Temperature Profile at a Time of 10 Minutes.

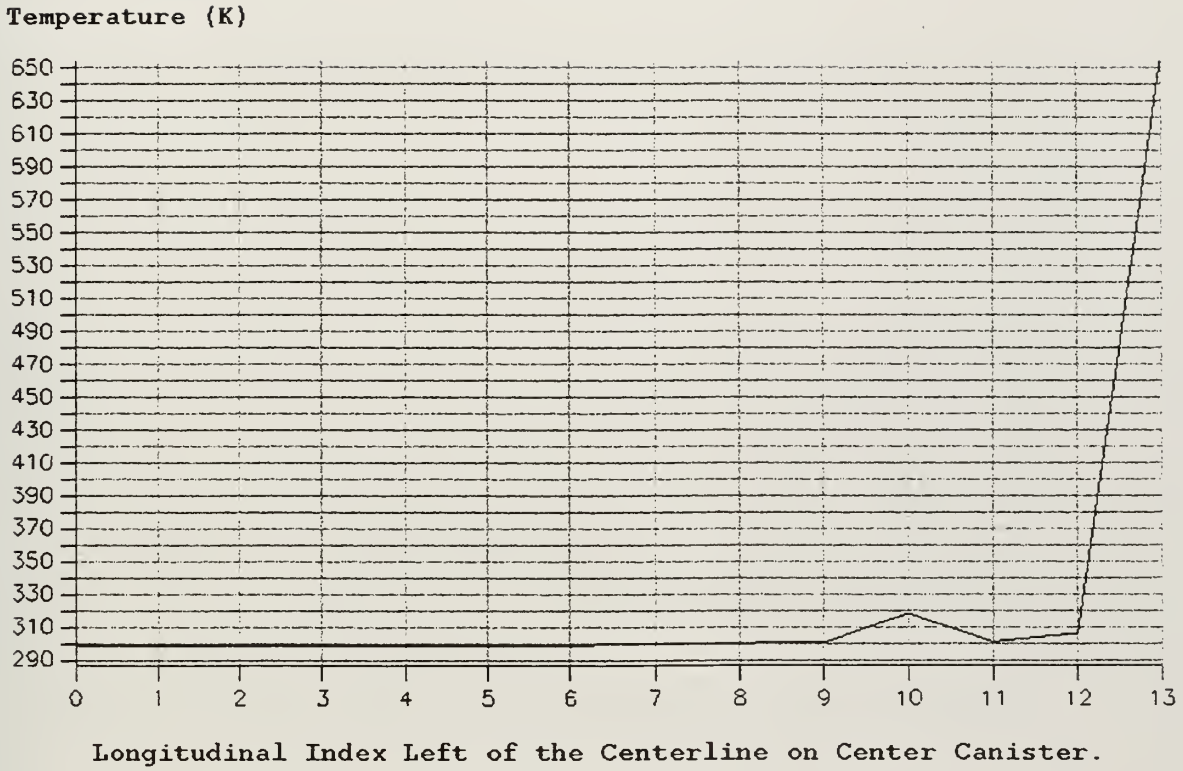

Figure 80. F-76 Fire - Round 1. Temperature vs. Index Profile at a Time of 1.67 Minutes.

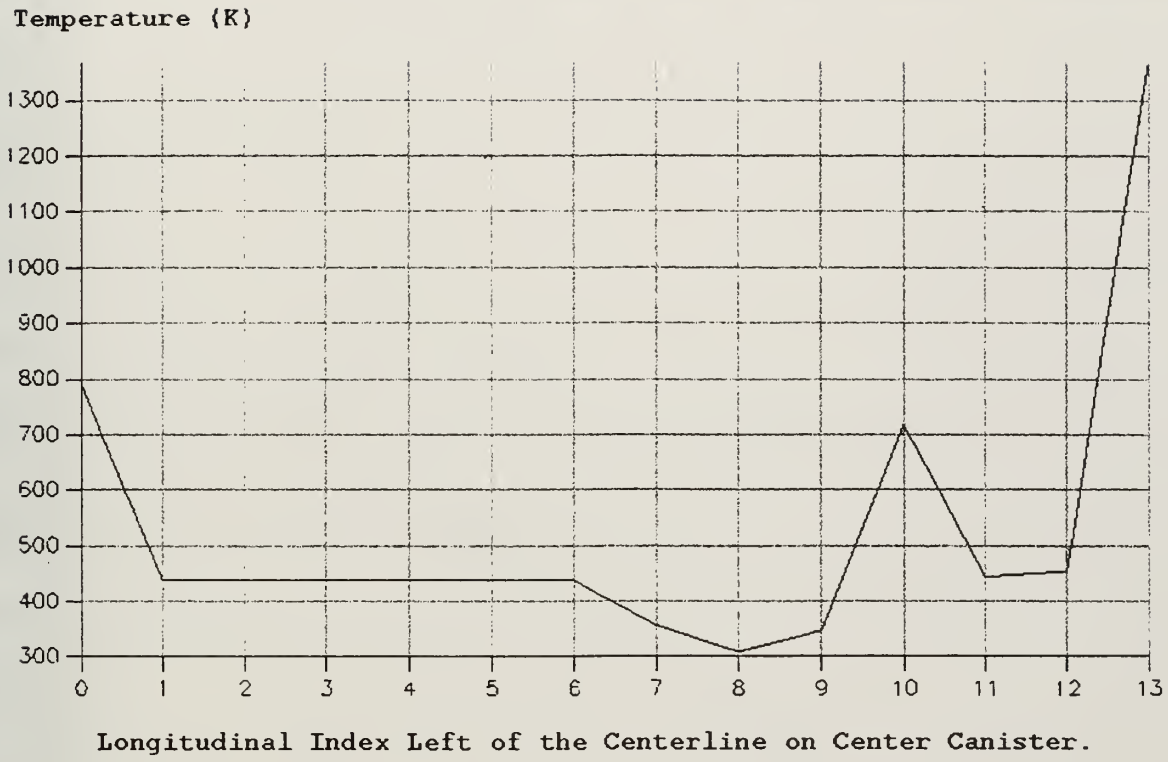

Figure 81. F-76 Fire - Round 1. Temperature vs. Index Profile at a Time of 10 Minutes.

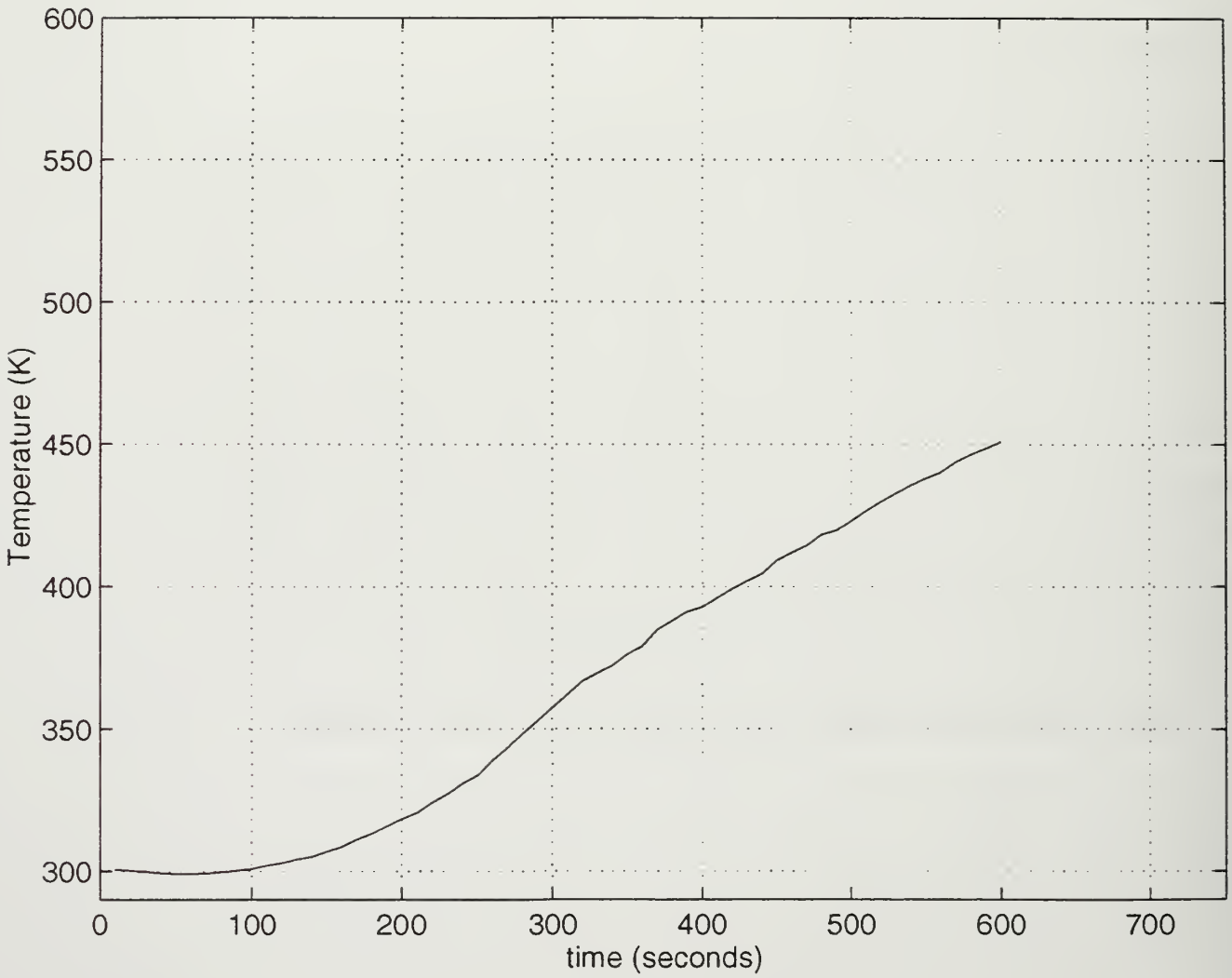

Figure 82. F-76 Fire - Round 1. Temperature vs. Time Plot for Monitor Point 1.

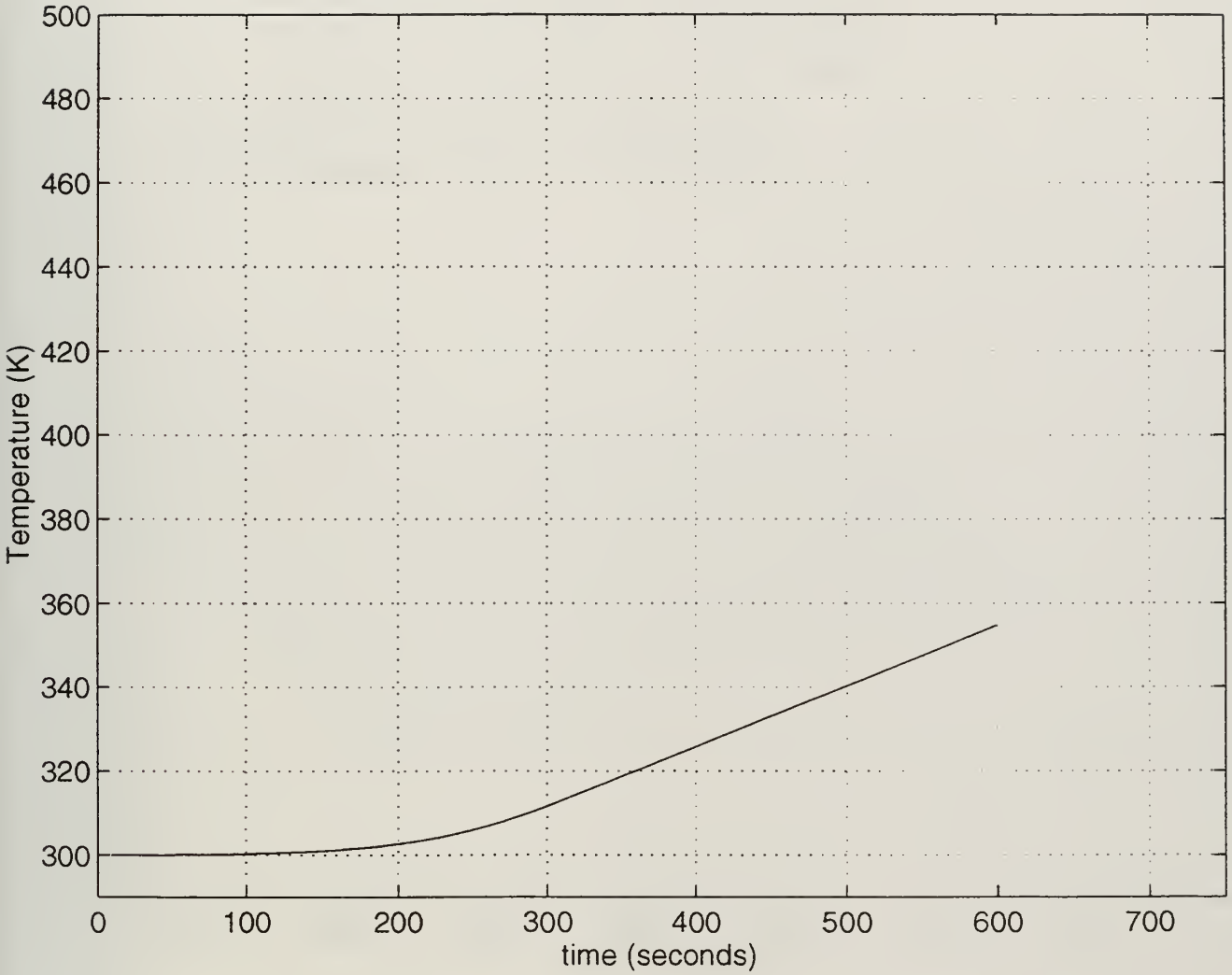

Figure 83. F-76 Fire - Round 1. Temperature vs. Time Plot for Monitor Point 2.

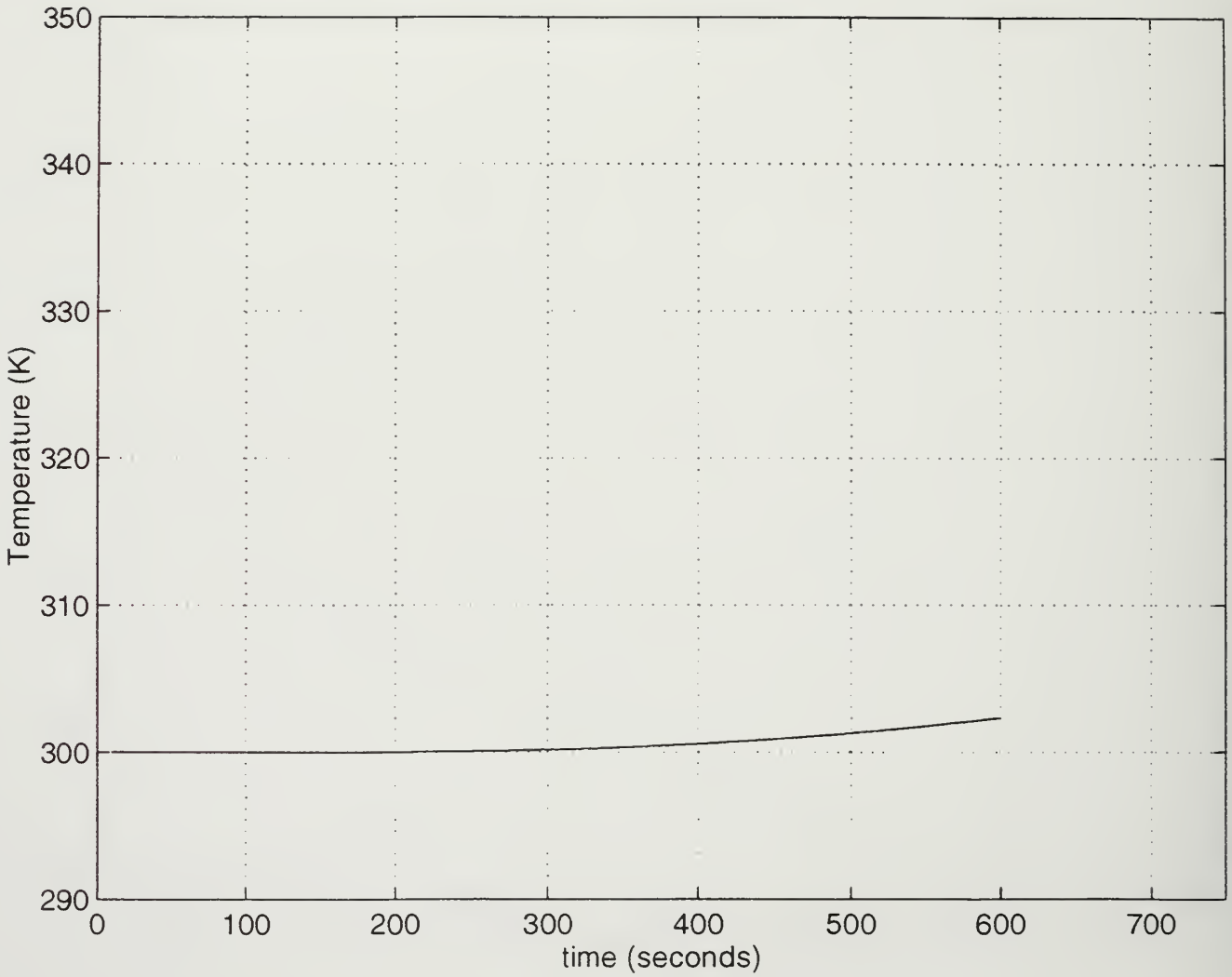

Figure 84. F-76 Fire - Round 1. Temperature vs. Time Plot for Monitor Point 3.

APPENDIX J. F-76 FIRE - ROUND 2

The following data corresponds to the round 2 simulation of the F-76 fire scenerio, including:

(1) 3-dimensional temperature profile at a time of one minute.
(2) 3-dimensional temperature profile at a time of 10 minutes.
(3) Horizontal temperature profile at a time of one minute.
(4) Horizontal temperature profile at a time of 10 minutes.
(5) Temperature vs. index profile at a time of one minute.
(6) Temperature vs. index profile at a time of 10 minutes.
(7) Temperature vs. time plot for monitor point 1.
(8) Temperature vs. time plot for monitor point 2.
(9) Temperature vs. time plot for monitor point 3.

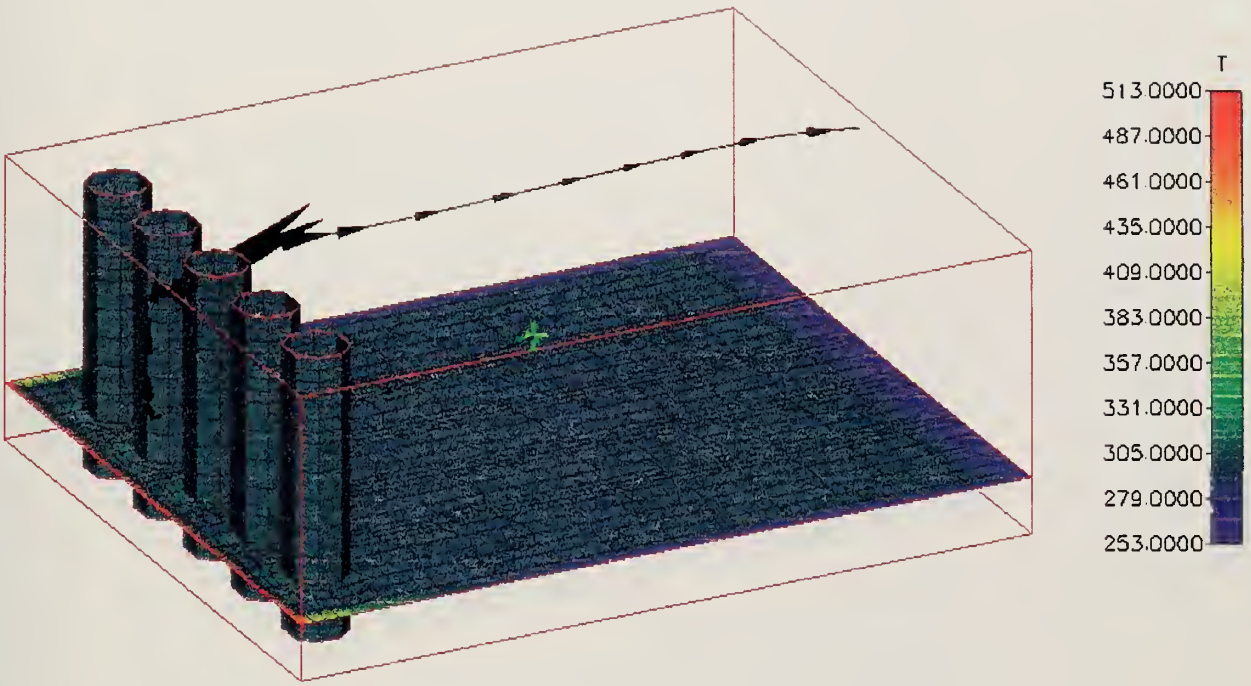

Figure 85. F-76 Fire - Round 2. 3-Dimensional Temperature Profile at a Time of 1 Minute.

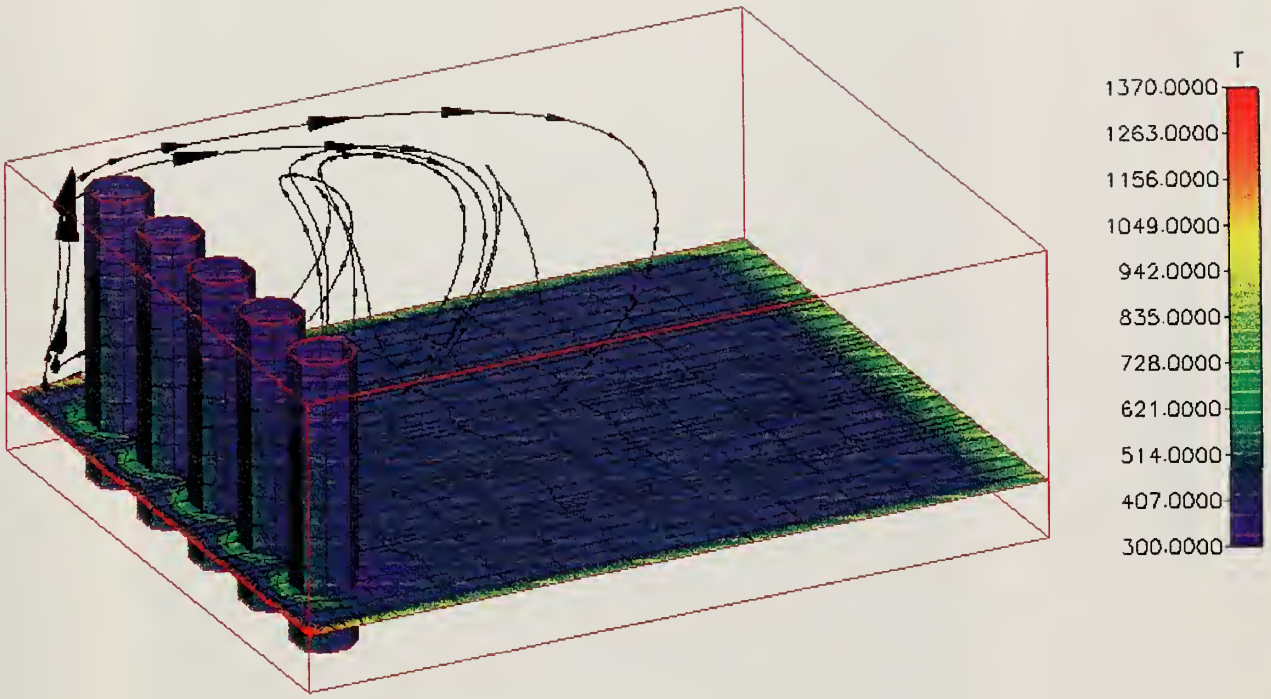

Figure 86. F-76 Fire - Round 2. 3-Dimensional Temperature Profile at a Time of 10 Minutes.

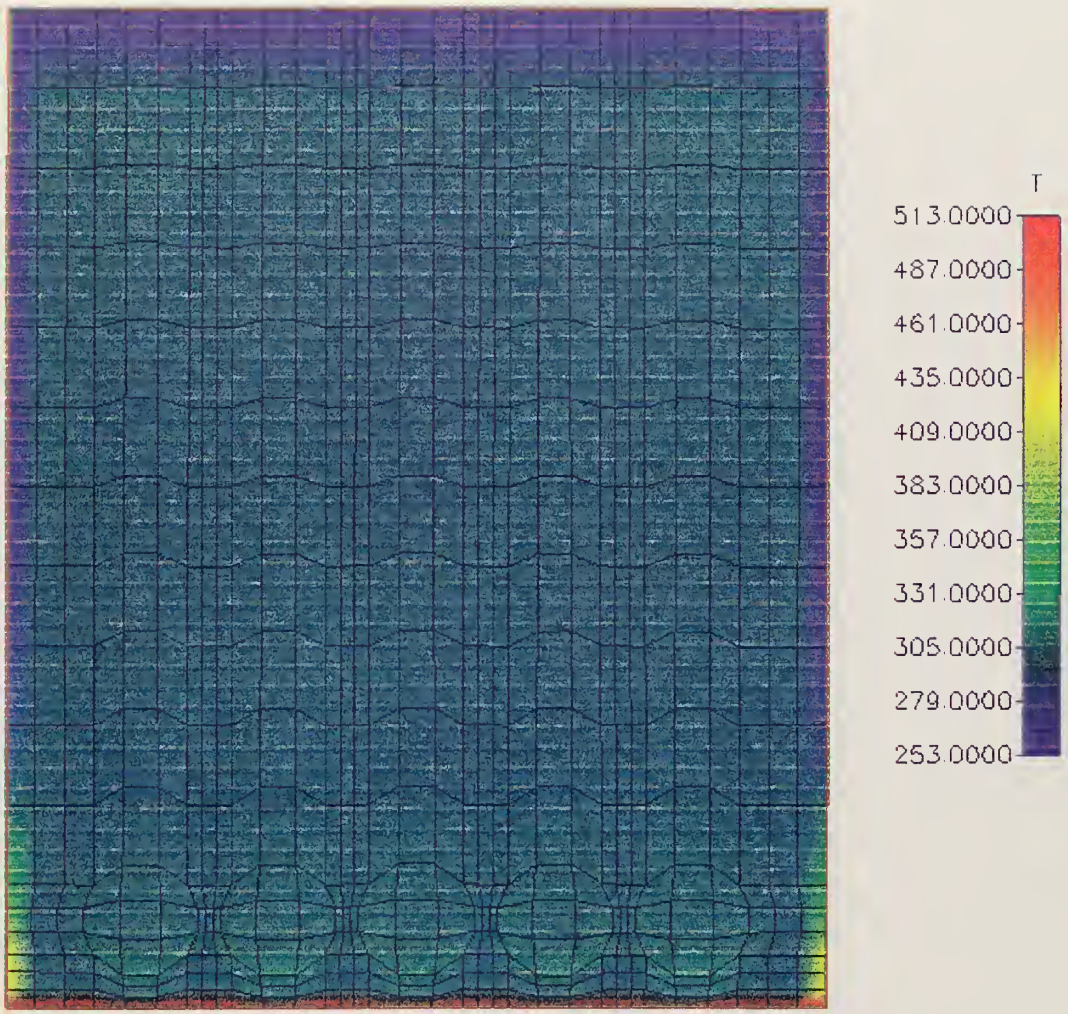

Figure 87. F-76 Fire - Round 2. Horizontal Temperature Profile at a Time of 1 Minute.

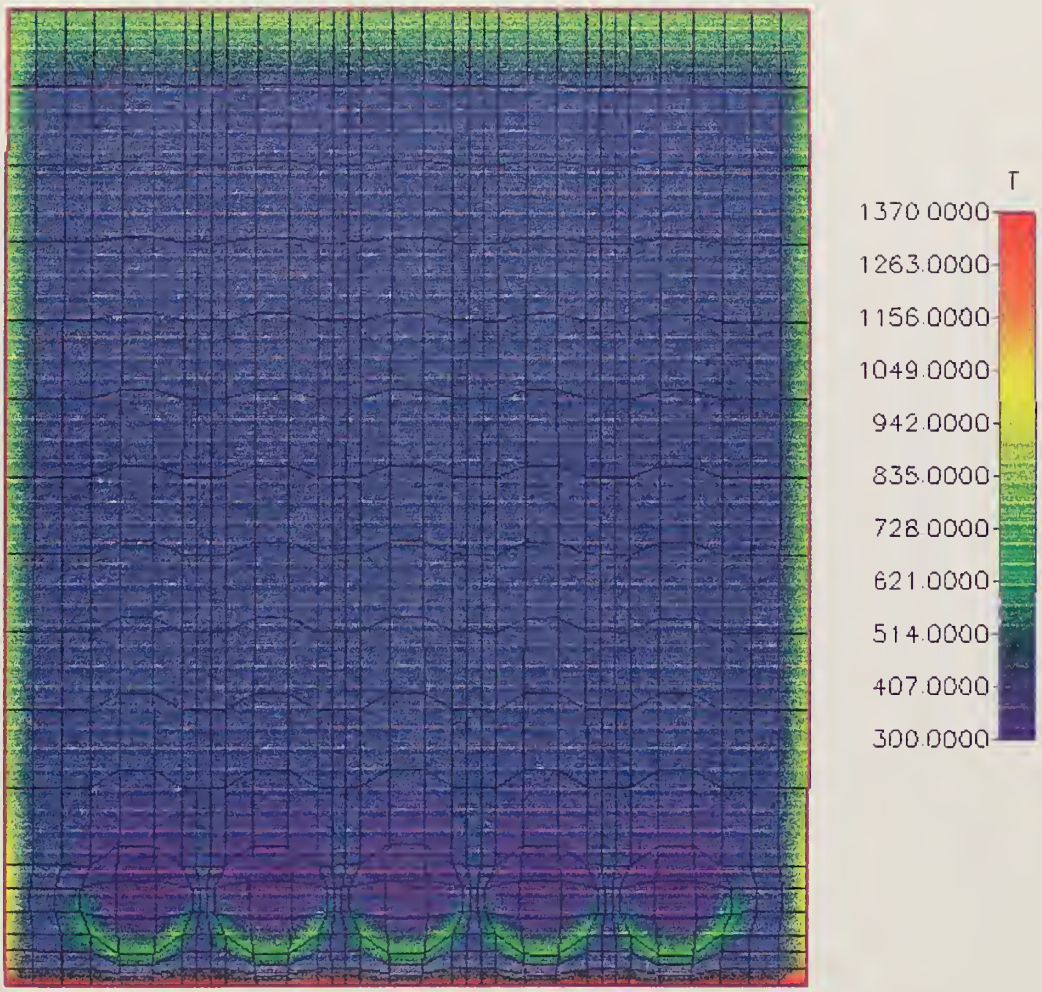

Figure 88. F-76 Fire - Round 2. Horizontal Temperature Profile at a Time of 10 Minutes.

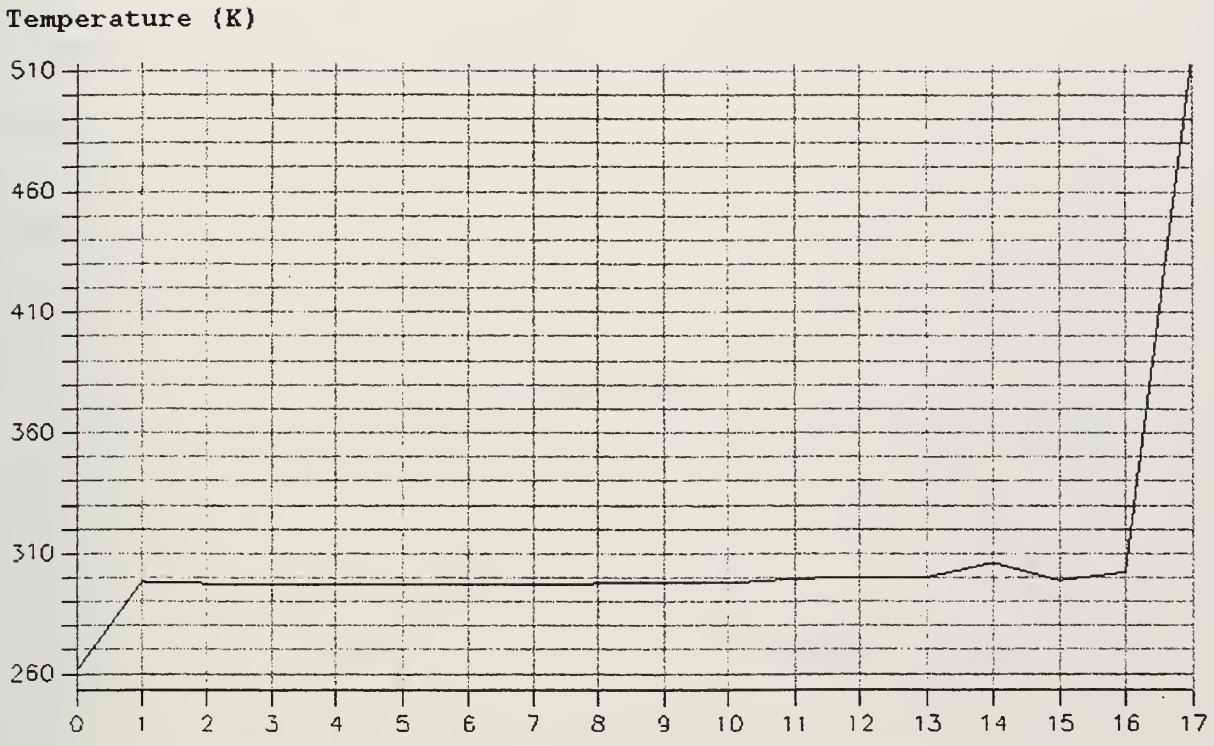

Figure 89. F-76 Fire - Round 2. Temperature vs. Index Profile at a Time of 1 Minute.

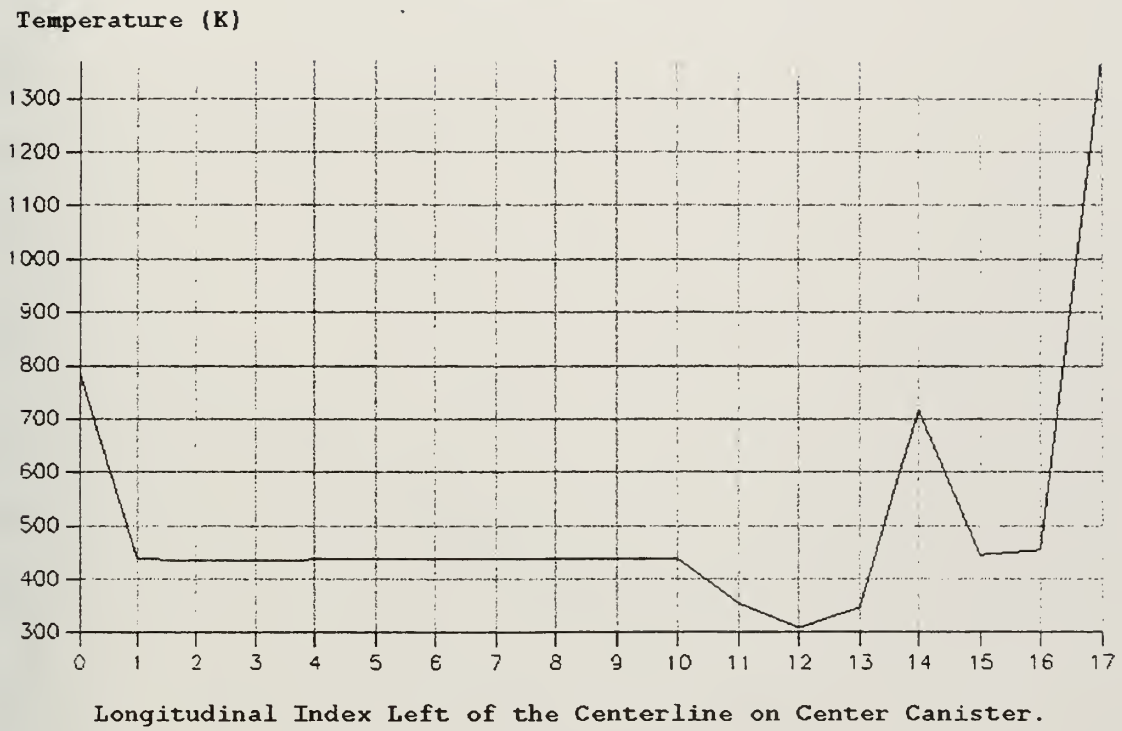

Figure 90. F-76 Fire - Round 2. Temperature vs. Index Profile at a Time of 10 Minutes.

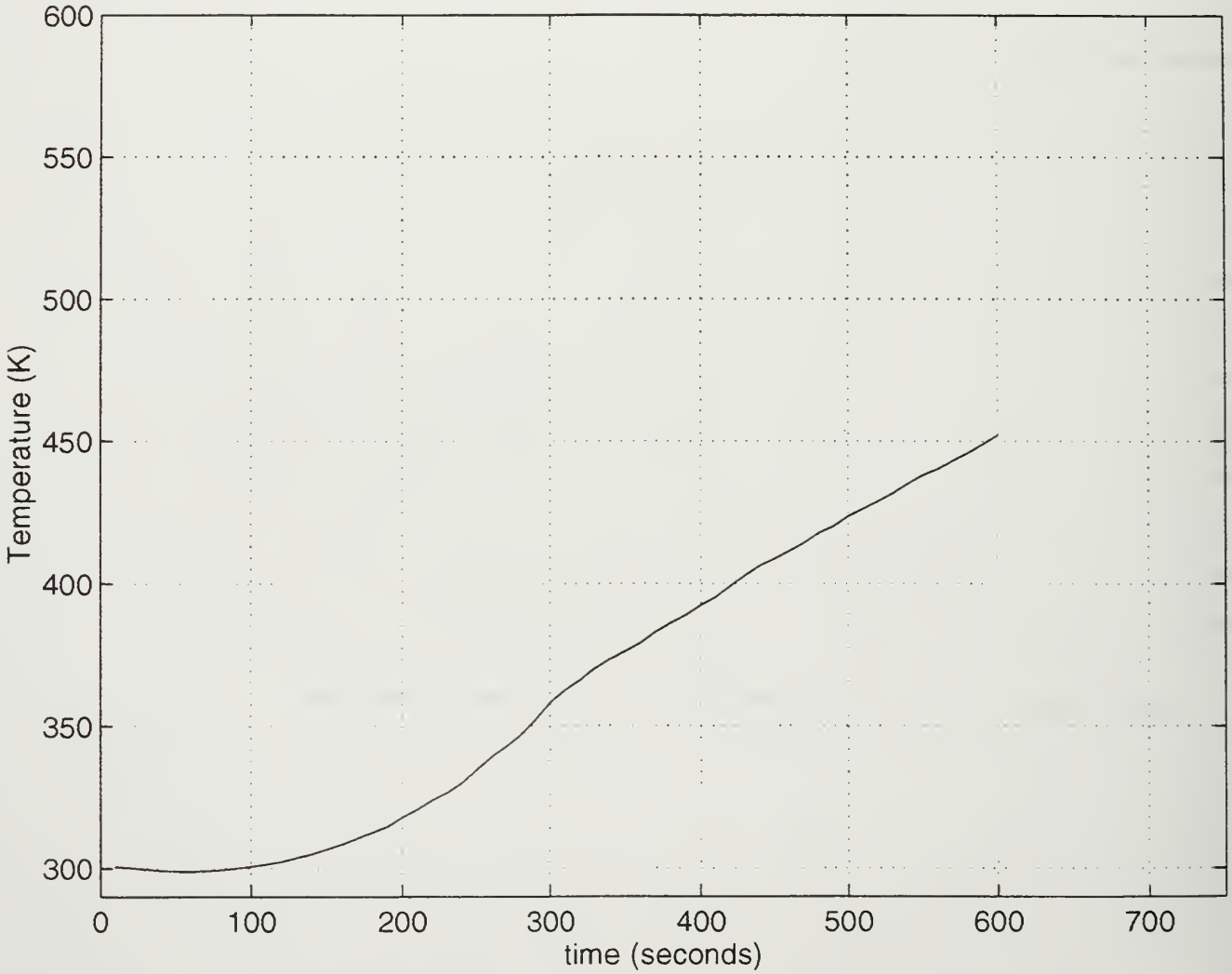

Figure 91. F-76 Fire - Round 2. Temperature vs. Time Plot for Monitor Point 1.

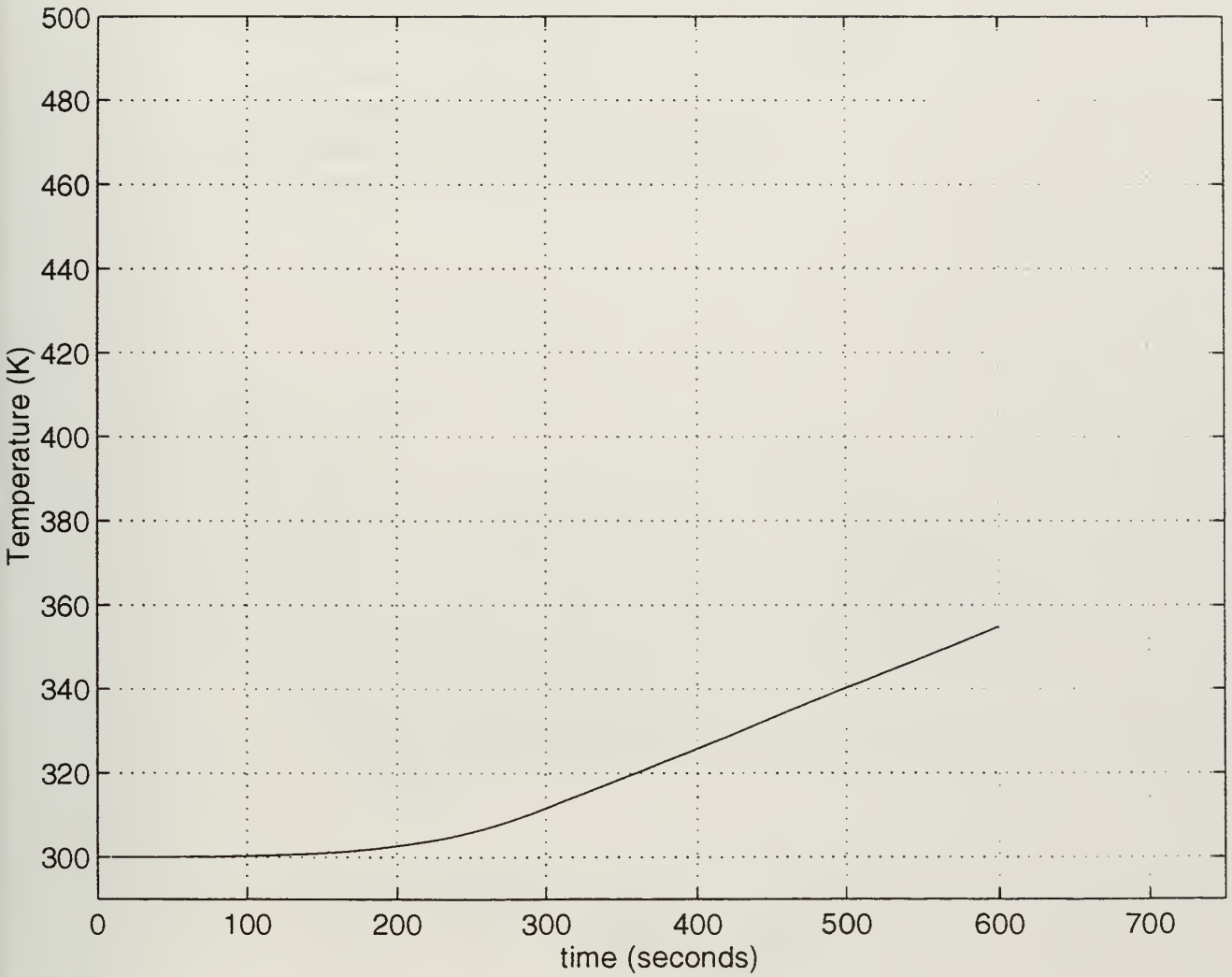

Figure 92. F-76 Fire - Round 2. Temperature vs. Time Plot for Monitor Point 2.

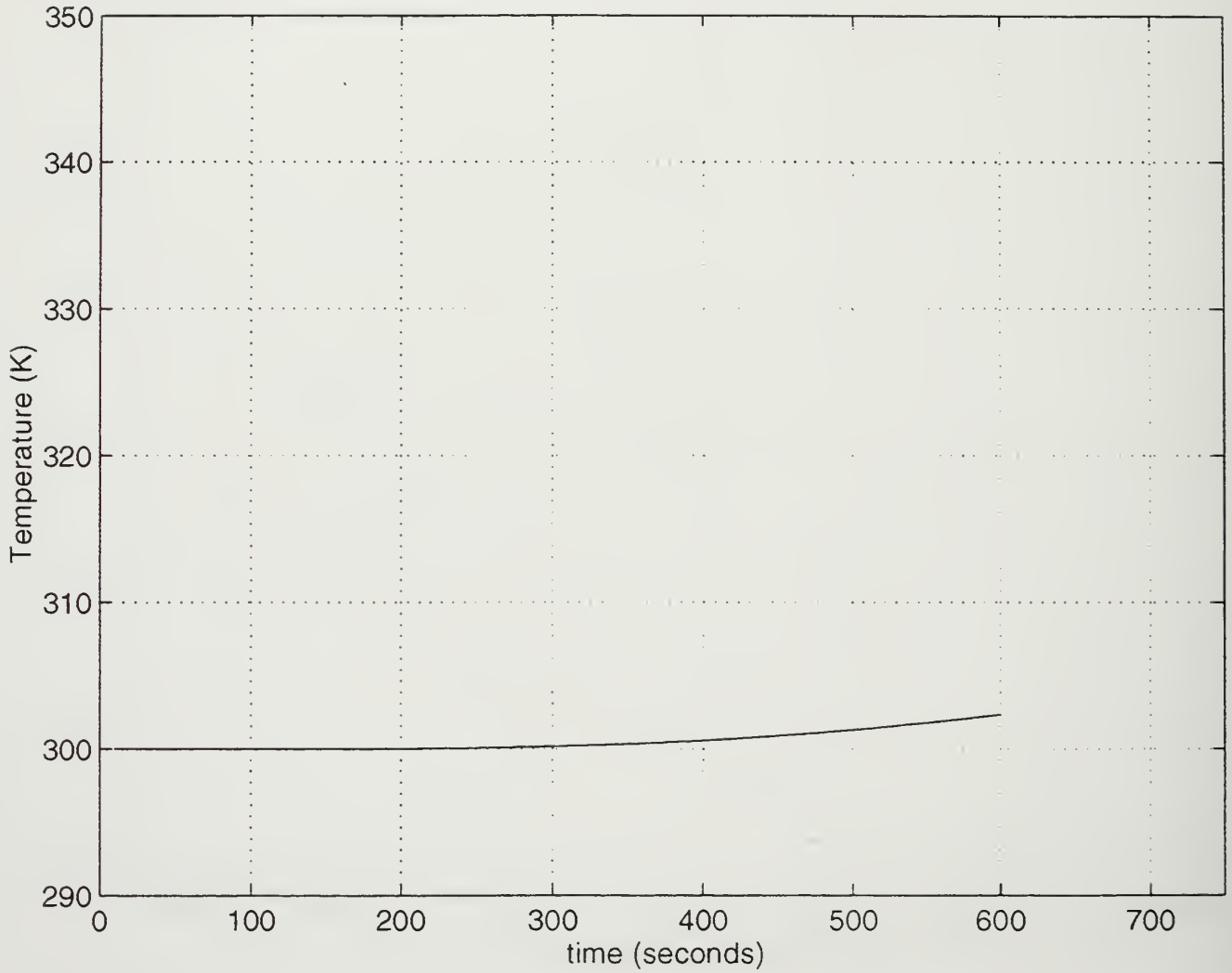

Figure 93. F-76 Fire - Round 2. Temperature vs. Time Plot for Monitor Point 3.

APPENDIX K. F-76 FIRE - ROUND 3

The following data corresponds to the round 3 simulation of the F-76 fire scenerio, including:

(1) 3-dimensional temperature profile at a time of one minute.
(2) 3-dimensional temperature profile at a time of 10 minutes.
(3) Horizontal temperature profile at a time of one minute.
(4) Horizontal temperature profile at a time of 10 minutes.
(5) Temperature vs. index profile at a time of one minute.
(6) Temperature vs. index profile at a time of 10 minutes.
(7) Temperature vs. time plot for monitor point 1.
(8) Temperature vs. time plot for monitor point 2.
(9) Temperature vs. time plot for monitor point 3.

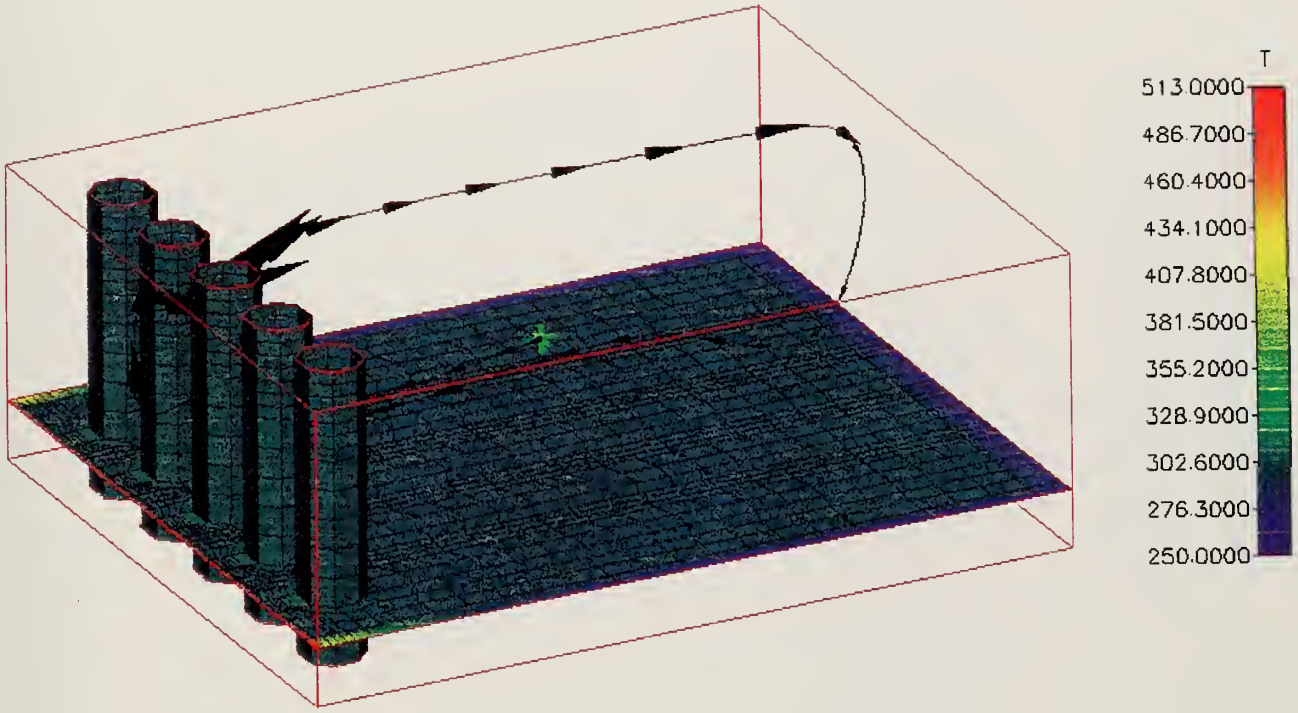

Figure 94. F-76 Fire - Round 3. 3-Dimensional Temperature Profile at a Time of 1 Minute.

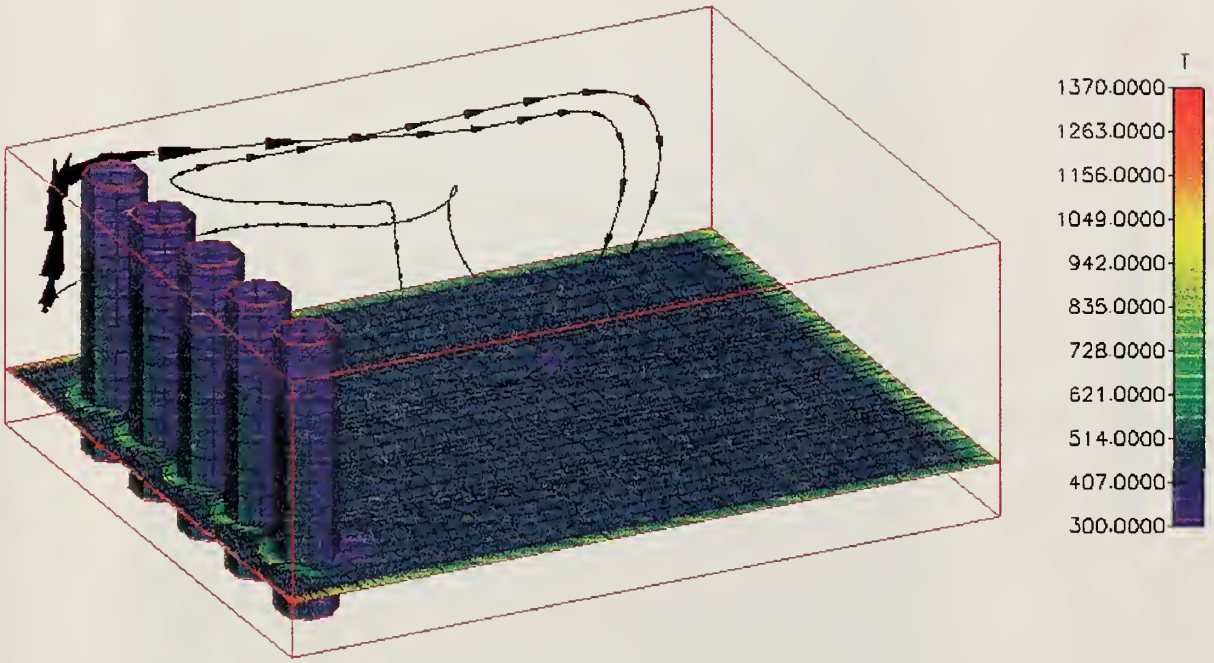

Figure 95. F-76 Fire - Round 3. 3-Dimensional Temperature Profile at a Time of 10 Minutes.

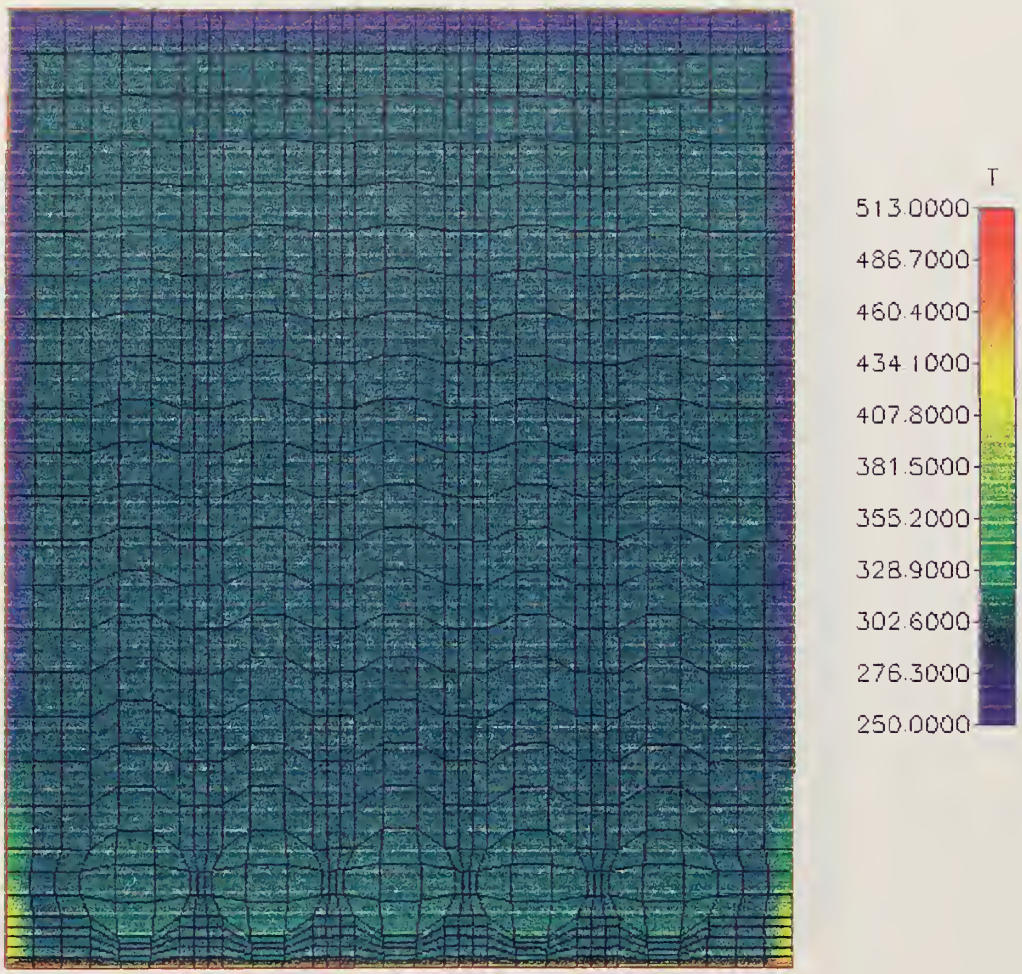

Figure 96. F-76 Fire - Round 3. Horizontal Temperature Profile at a Time of 1 Minute.

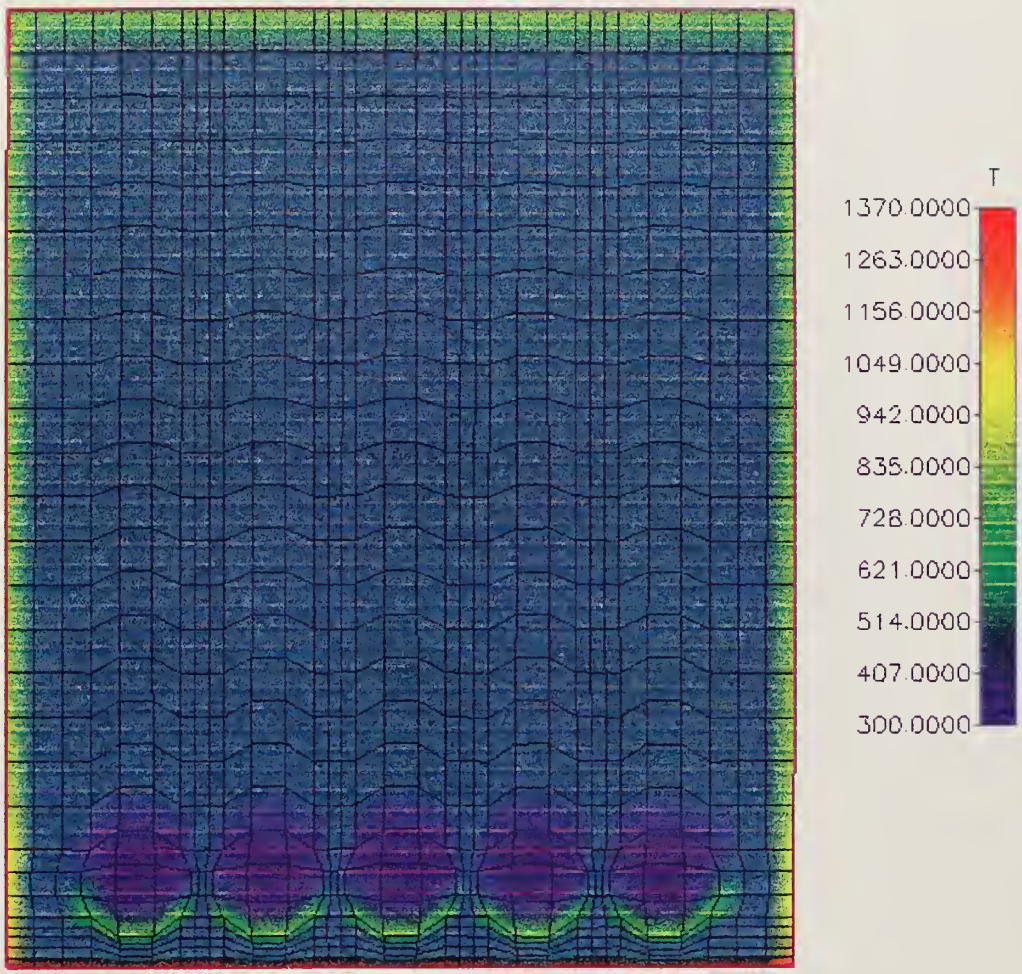

Figure 97. F-76 Fire - Round 3. Horizontal Temperature Profile at a Time of 10 Minutes.

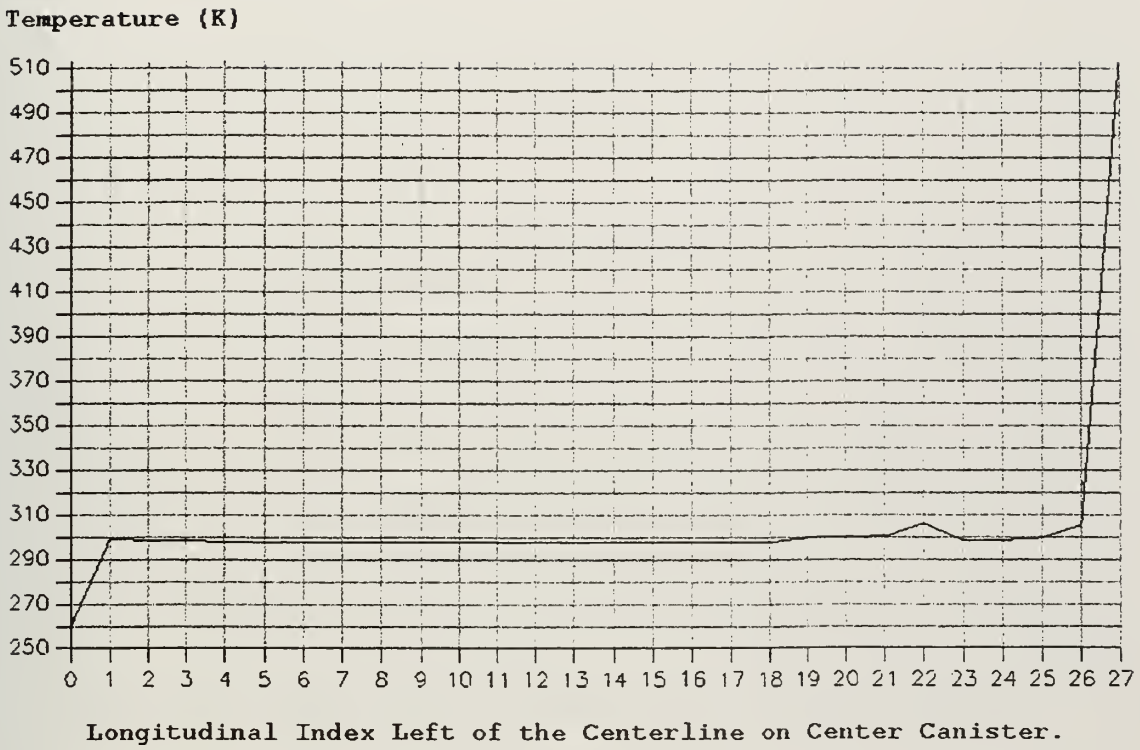

Figure 98. F-76 Fire - Round 3. Temperature vs. Index Profile at a Time of 1 Minute.

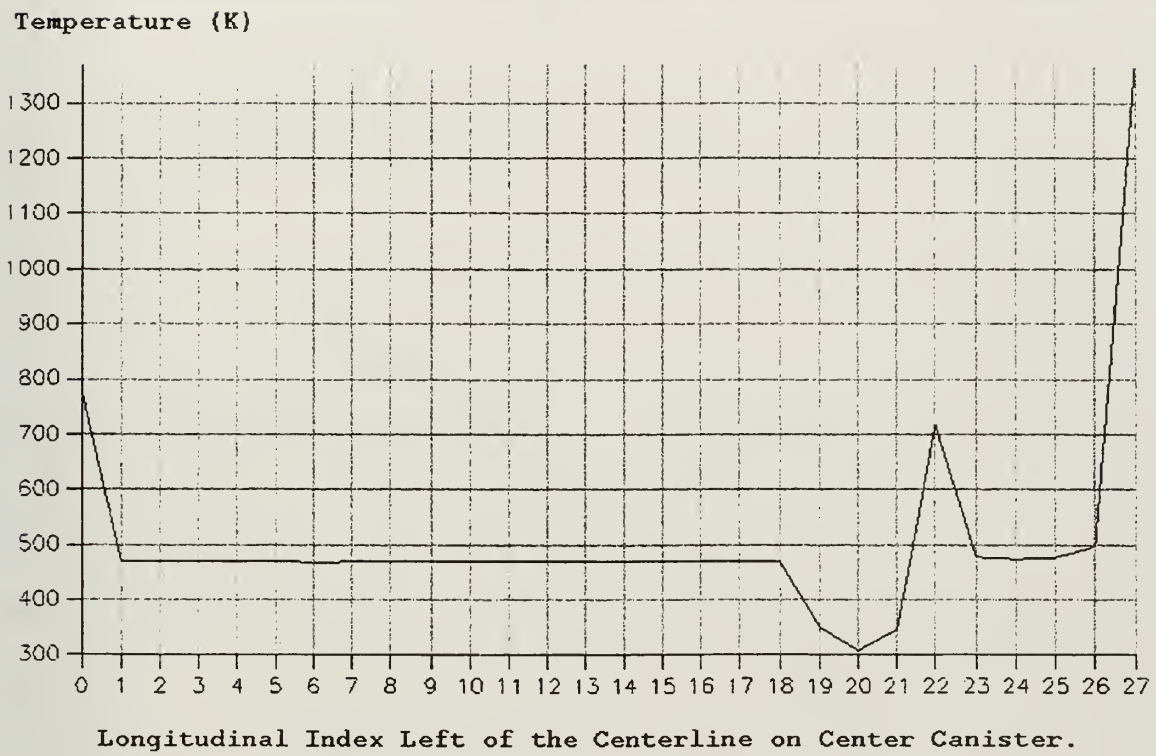

Figure 99. F-76 Fire - Round 3. Temperature vs. Index Profile at a Time of 10 Minutes.

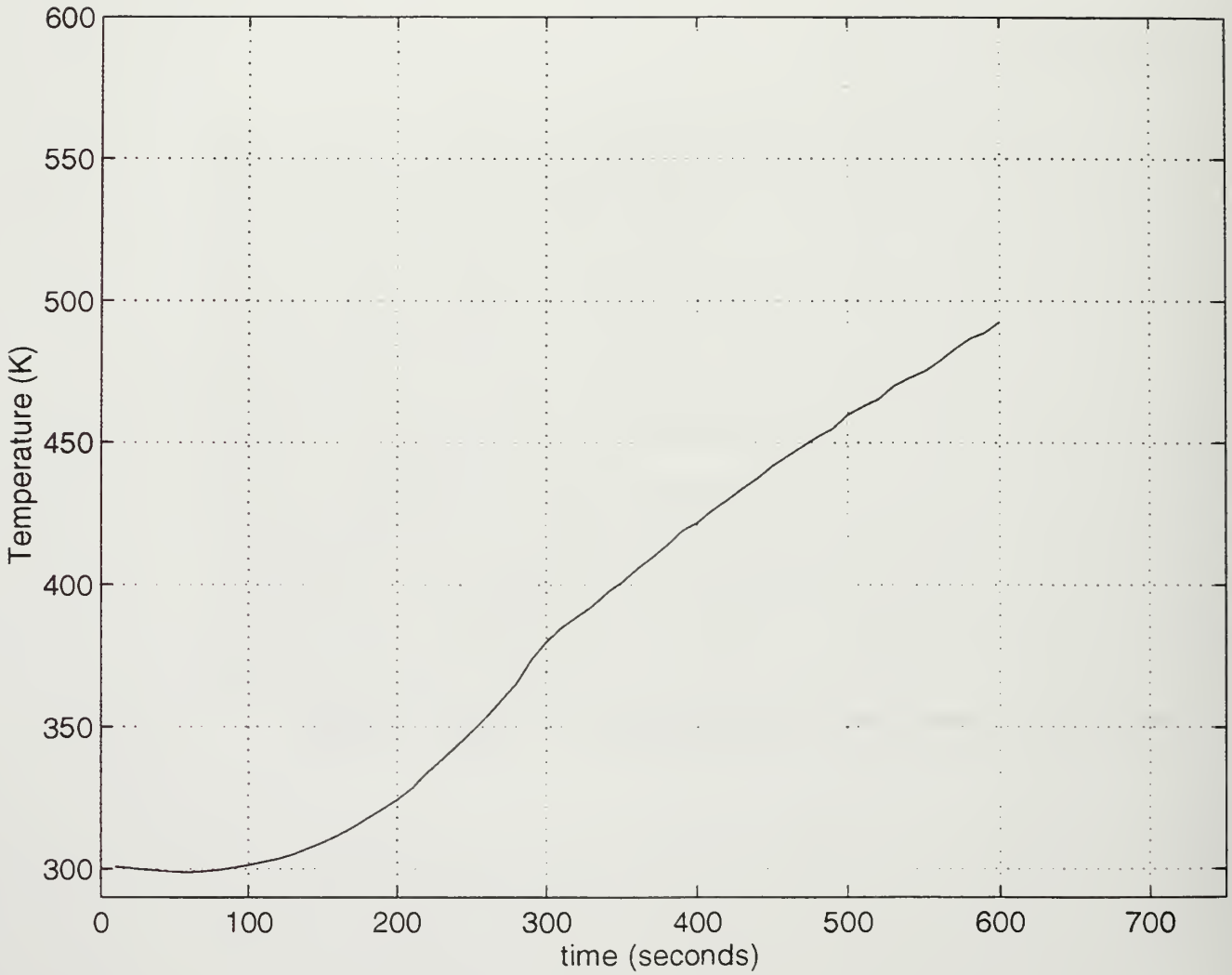

Figure 100. F-76 Fire - Round 3. Temperature vs. Time Plot for Monitor Point 1.

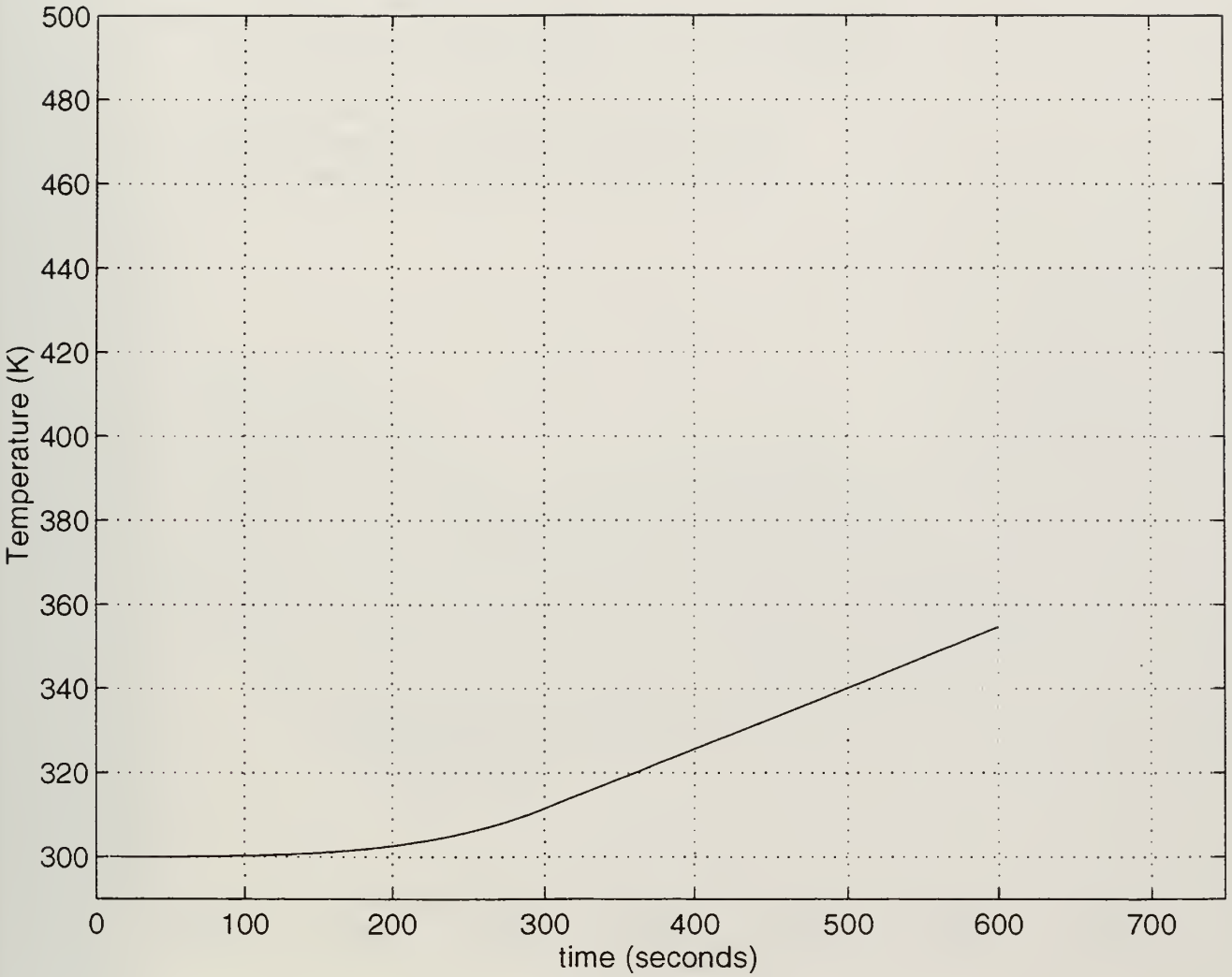

Figure 101. F-76 Fire - Round 3. Temperature vs. Time Plot for Monitor Point 2.

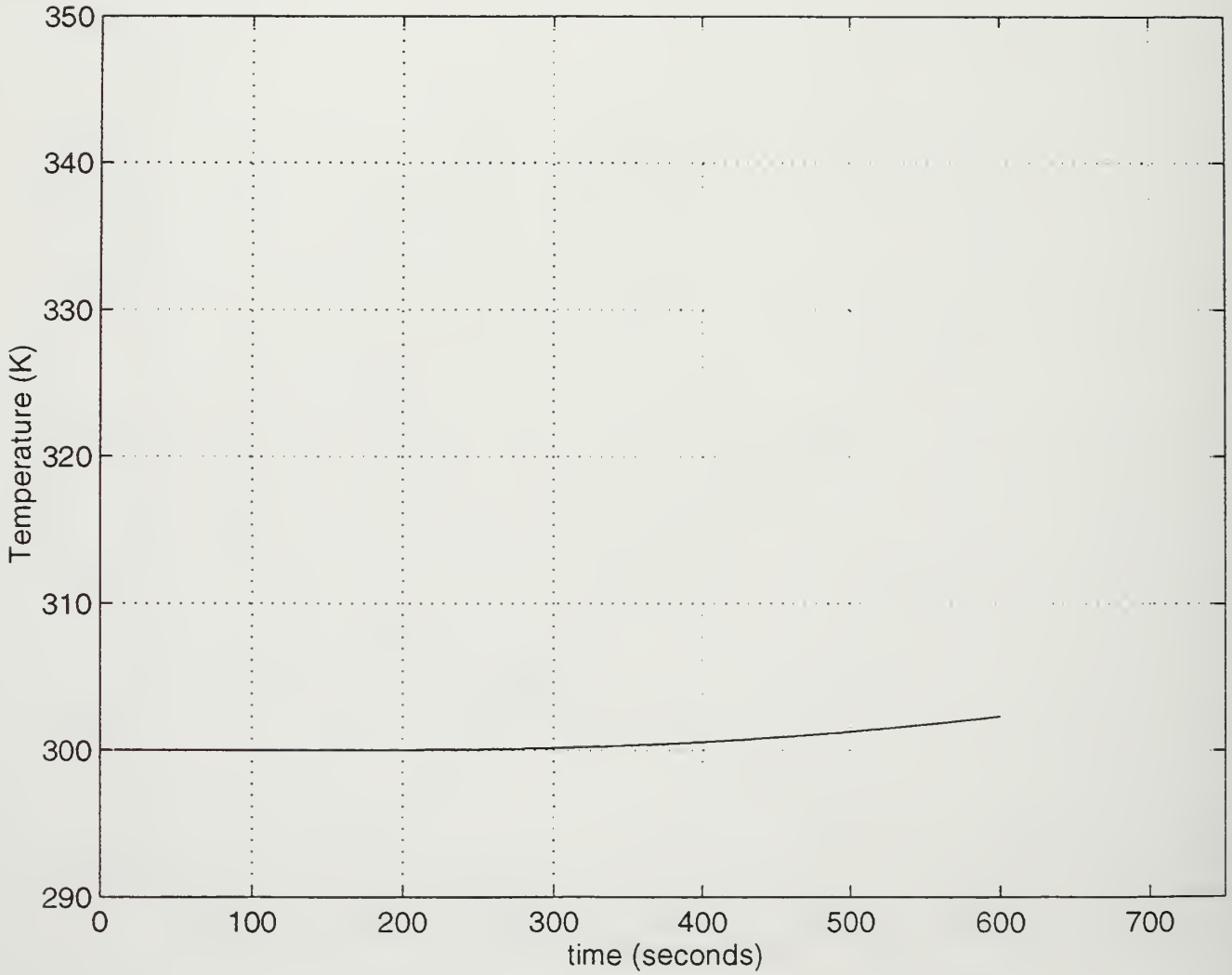

Figure 102. F-76 Fire - Round 3. Temperature vs. Time Plot for Monitor Point 3.

APPENDIX L. F-76 FIRE - ROUND 4

The following data corresponds to the round 4 simulation of the F-76 fire scenerio, including:

(1) 3-dimensional temperature profile at a time of one minute.
(2) 3-dimensional temperature profile at a time of 10 minutes.
(3) Horizontal temperature profile at a time of one minute.
(4) Horizontal temperature profile at a time of 10 minutes.
(5) Temperature vs. index profile at a time of one minute.
(6) Temperature vs. index profile at a time of 10 minutes.
(7) Temperature vs. time plot for monitor point 1.
(8) Temperature vs. time plot for monitor point 2.
(9) Temperature vs. time plot for monitor point 3.

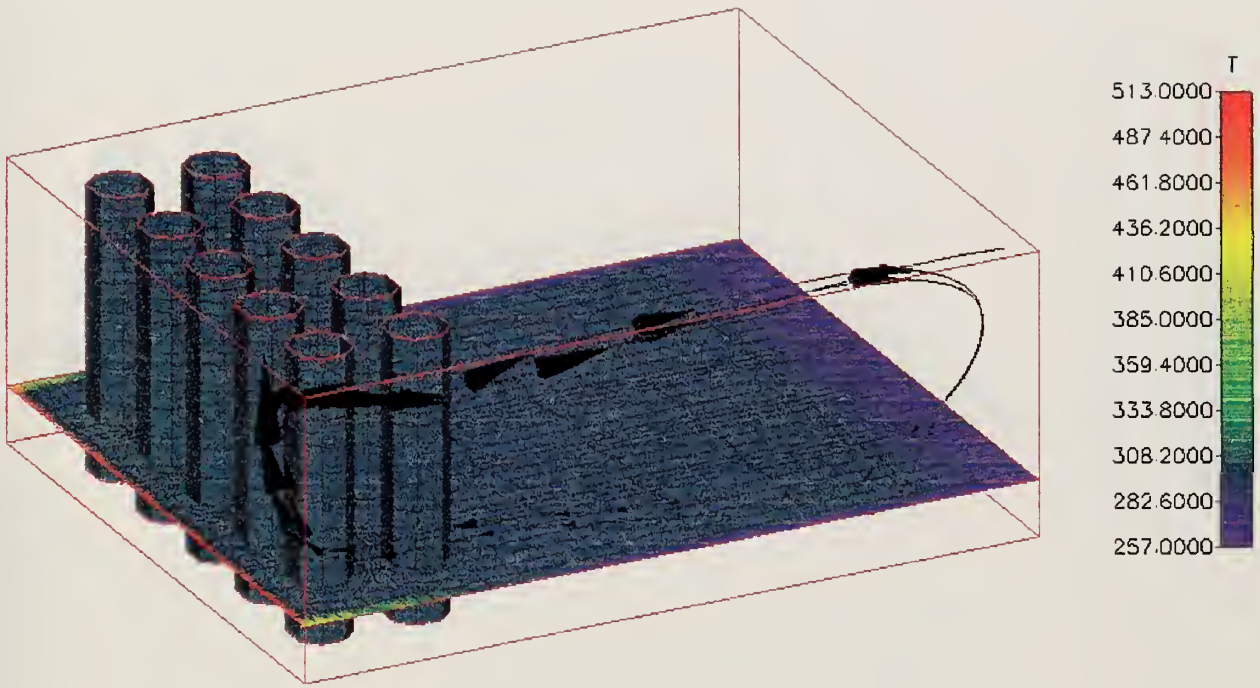

Figure 103. F-76 Fire - Round 4. 3-Dimensional Temperature Profile at a Time of 1 Minute.

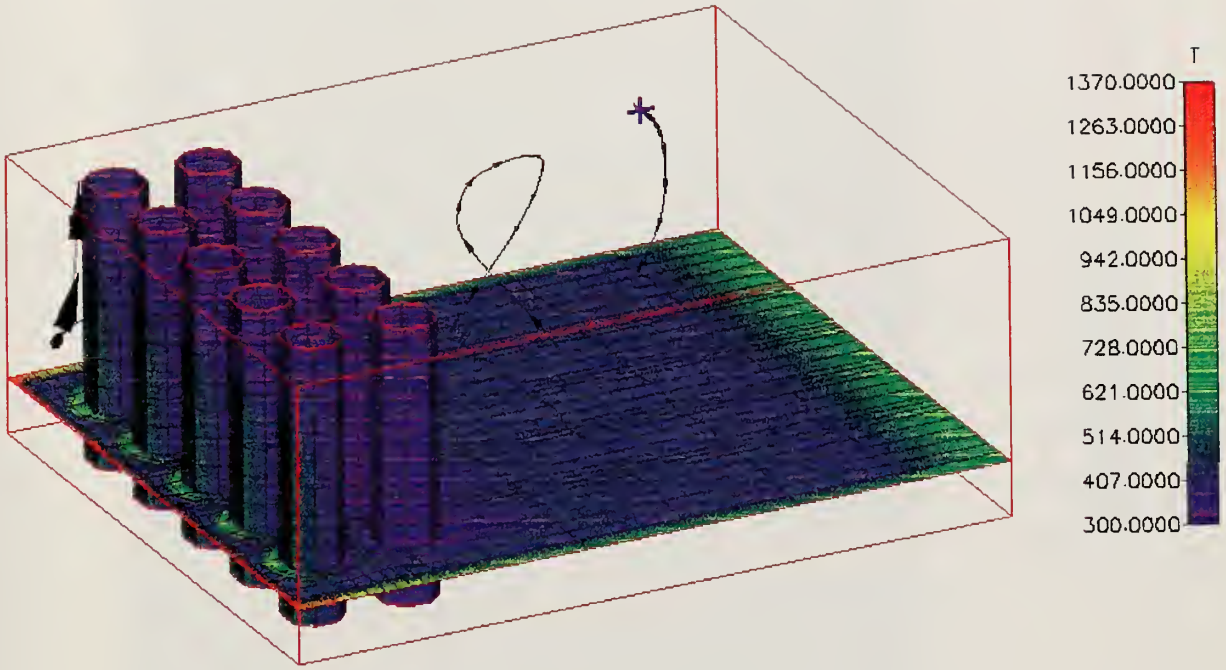

Figure 104. F-76 Fire - Round 4. 3-Dimensional Temperature Profile at a Time of 10 Minutes.

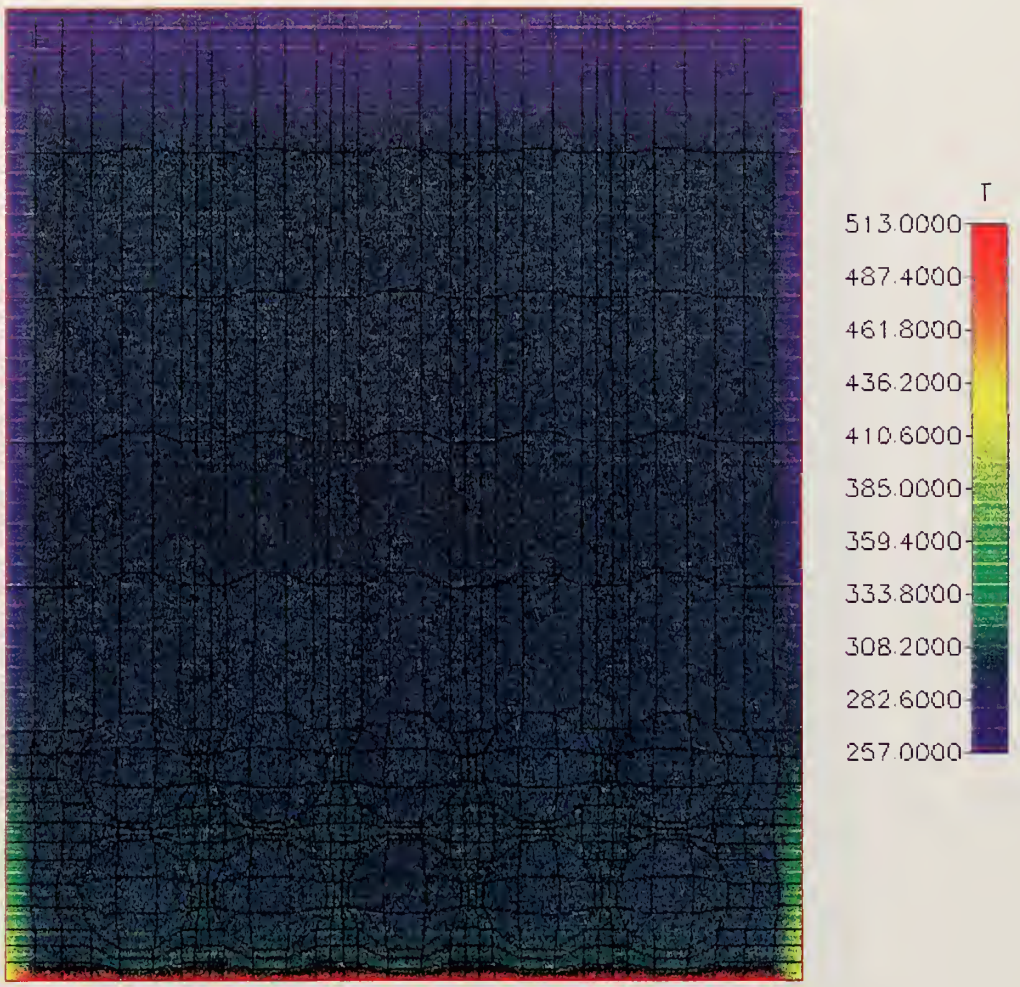

Figure 105. F-76 Fire - Round 4. Horizontal Temperature Profile at a Time of 1 Minute.

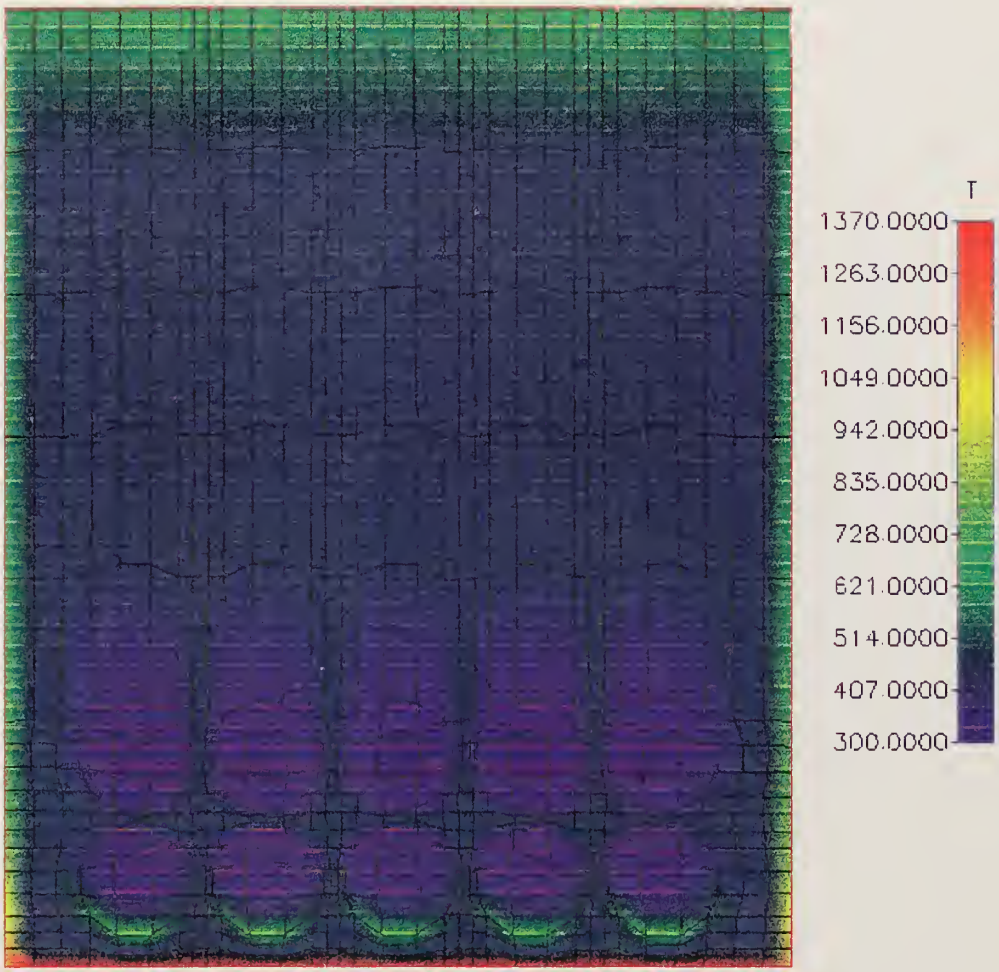

Figure 106. F-76 Fire - Round 4. Horizontal Temperature Profile at a Time of 10 Minutes.

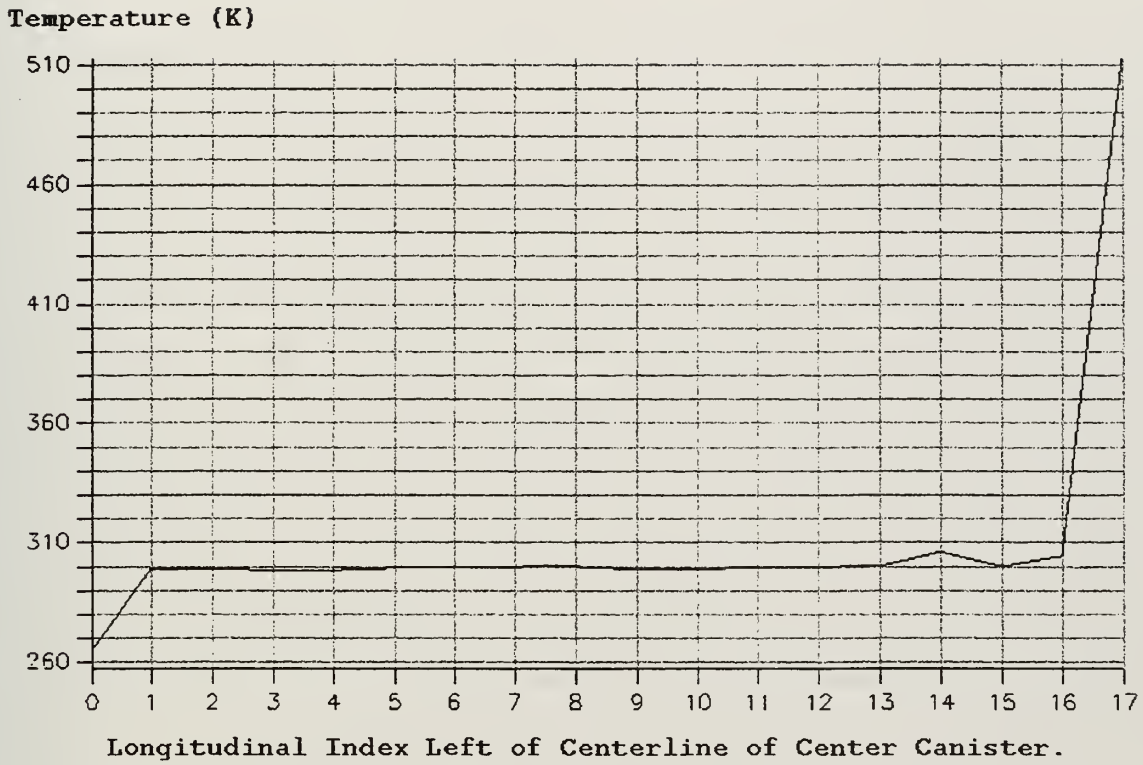

Figure 107. F-76 Fire - Round 4. Temperature vs. Index Profile at a Time of 1 Minute.

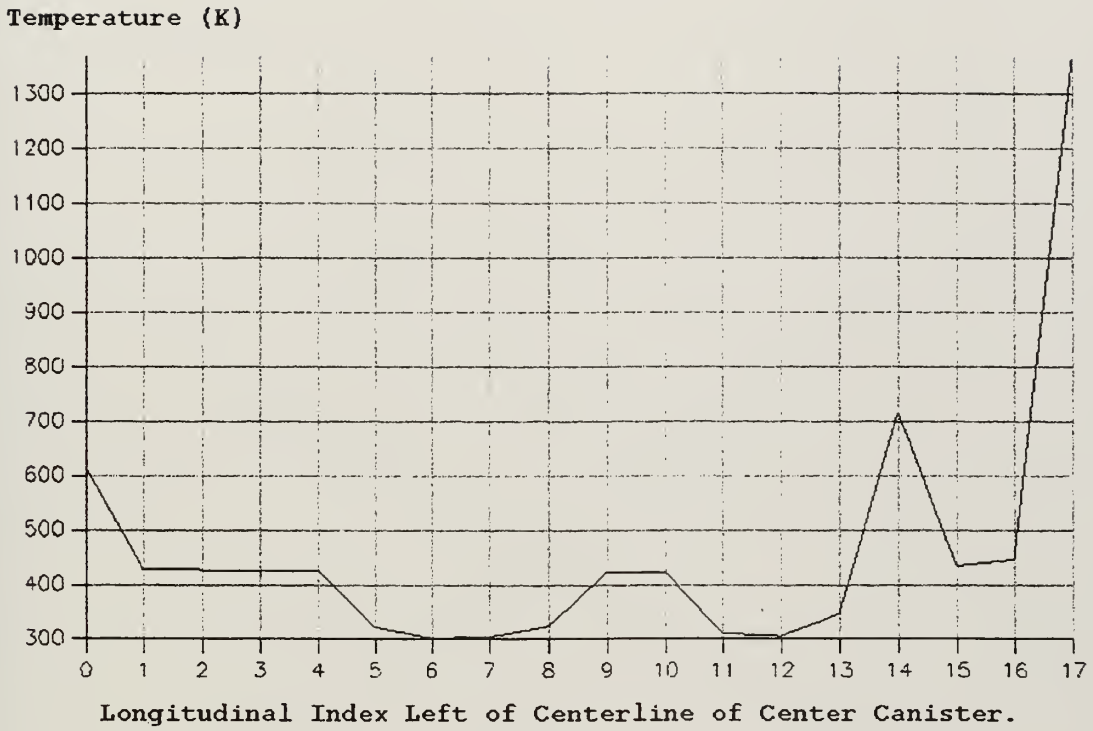

Figure 108. F-76 Fire - Round 4. Temperature vs. Index Profile at a Time of 10 Minutes.

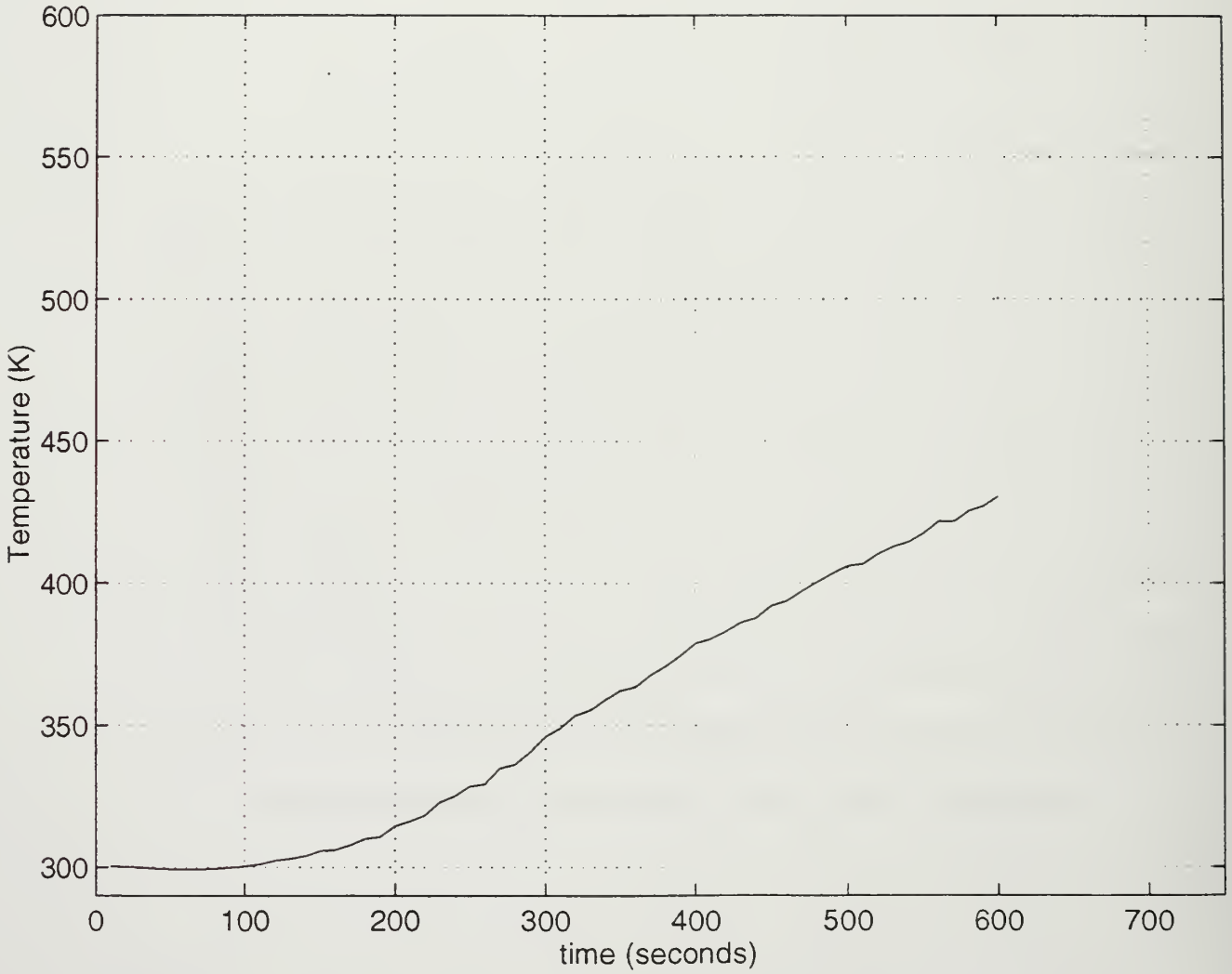

Figure 109. F-76 Fire - Round 4. Temperature vs. Time Plot for Monitor Point 1.

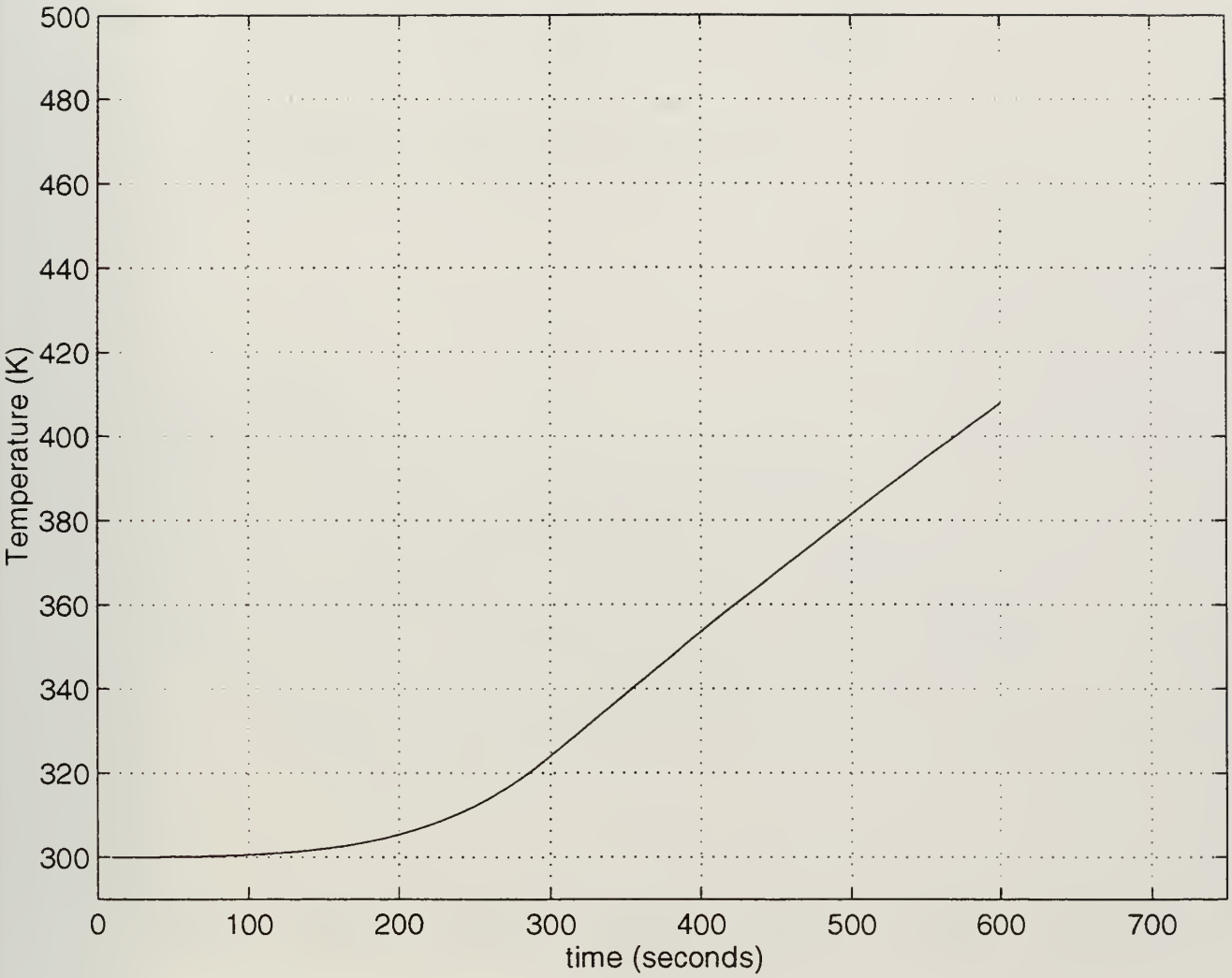

Figure 110. F-76 Fire - Round 4. Temperature vs. Time Plot for Monitor Point 2.

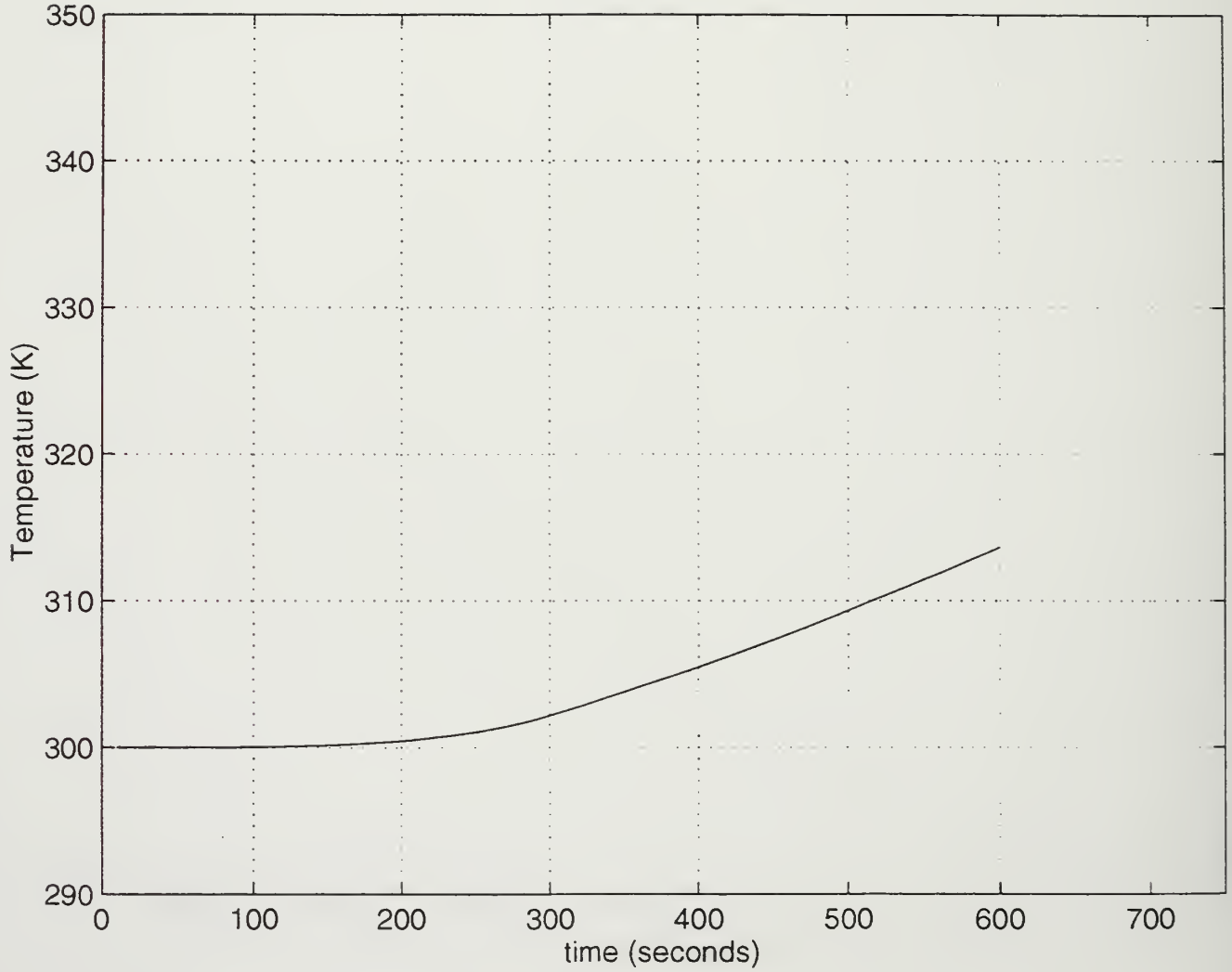

Figure 111. F-76 Fire - Round 4. Temperature vs. Time Plot for Monitor Point 3.

APPENDIX M. F-76 FIRE - ROUND 5

The following data corresponds to the round 5 simulation of the F-76 fire scenerio, including:

(1) 3-dimensional temperature profile at a time of one minute.
(2) 3-dimensional temperature profile at a time of 10 minutes.
(3) Horizontal temperature profile at a time of one minute.
(4) Horizontal temperature profile at a time of 10 minutes.
(5) Temperature vs. index profile at a time of one minute.
(6) Temperature vs. index profile at a time of 10 minutes.
(7) Temperature vs. time plot for monitor point 1.
(8) Temperature vs. time plot for monitor point 2.
(9) Temperature vs. time plot for monitor point 3.

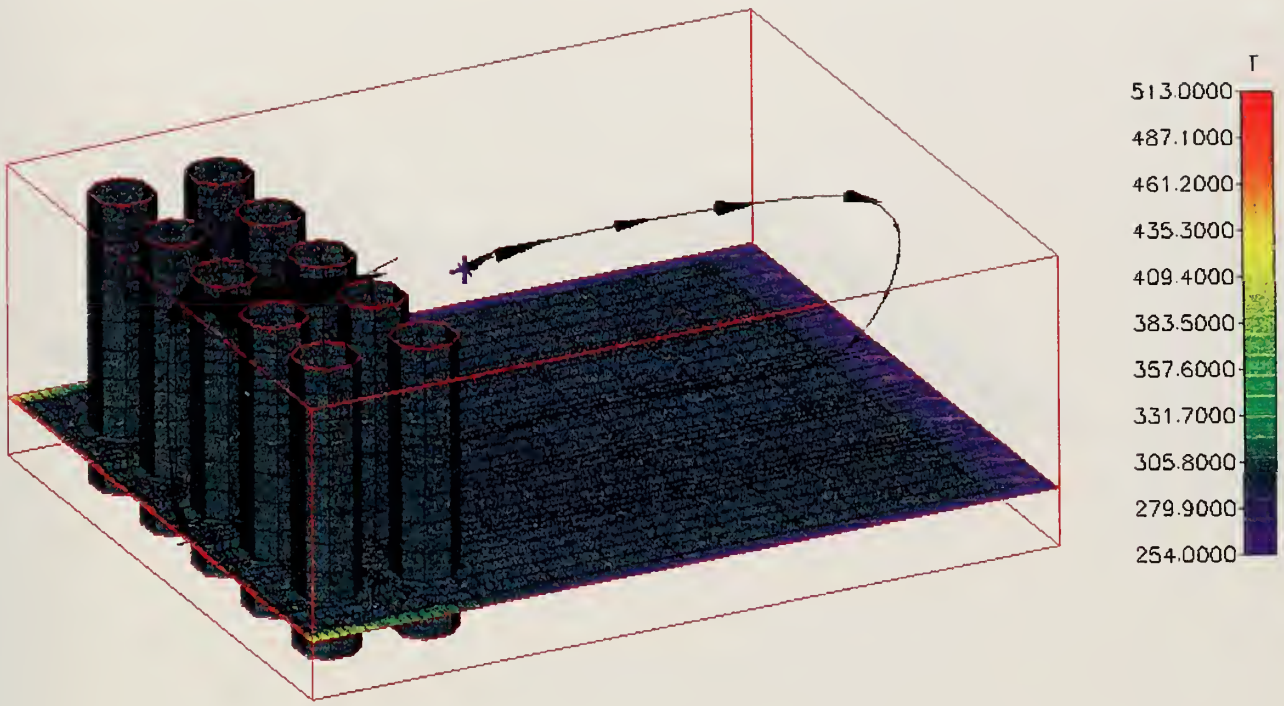

Figure 112. F-76 Fire - Round 5. 3-Dimensional Temperature Profile at a Time of 1 Minute.

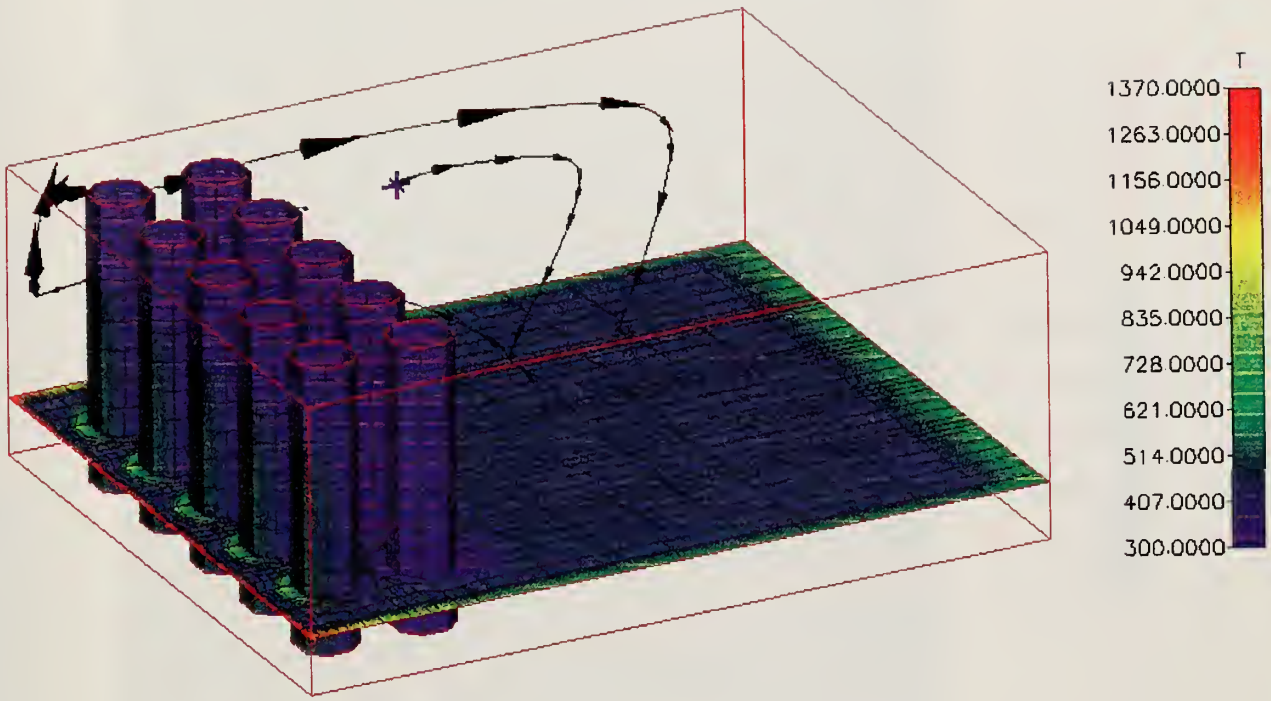

Figure 113. F-76 Fire - Round 5. 3-Dimensional Temperature Profile at a Time of 10 Minutes.

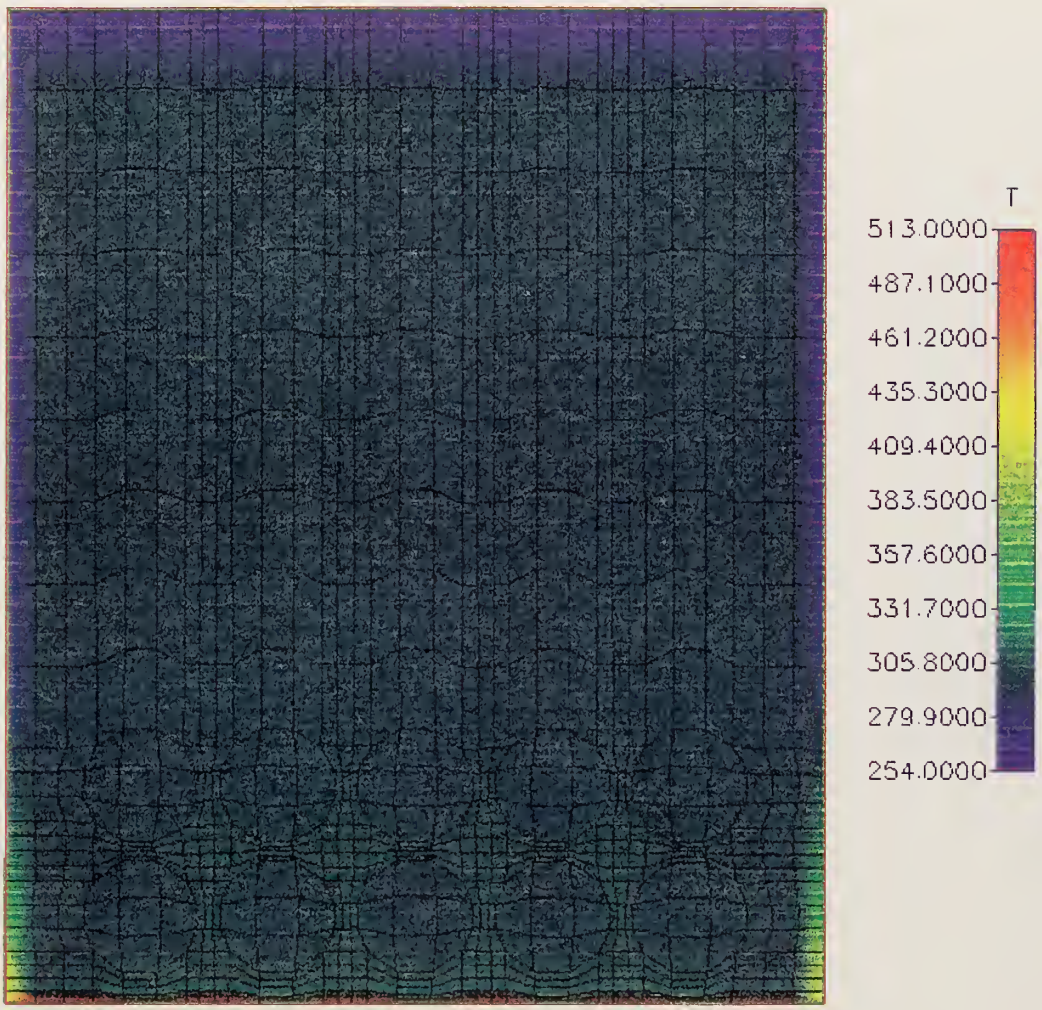

Figure 114. F-76 Fire - Round 5. Horizontal Temperature Profile at a Time of 1 Minute.

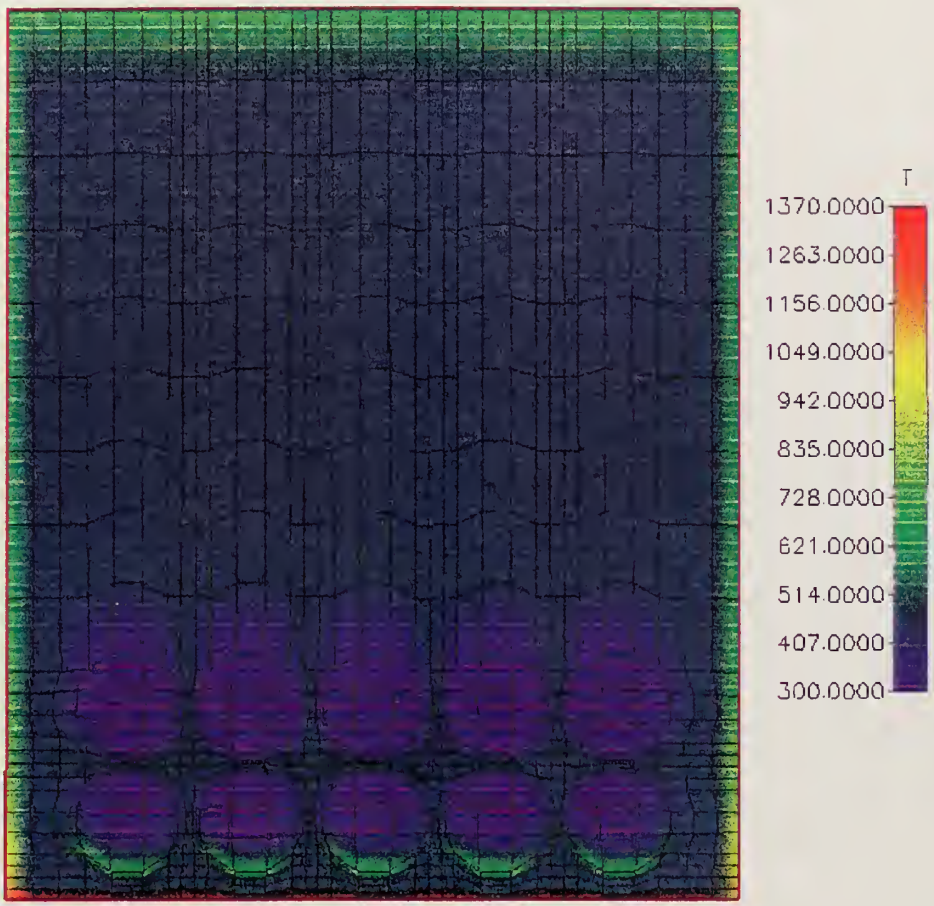

Figure 115. F-76 Fire - Round 5. Horizontal Temperature Profile at a Time of 10 Minutes.

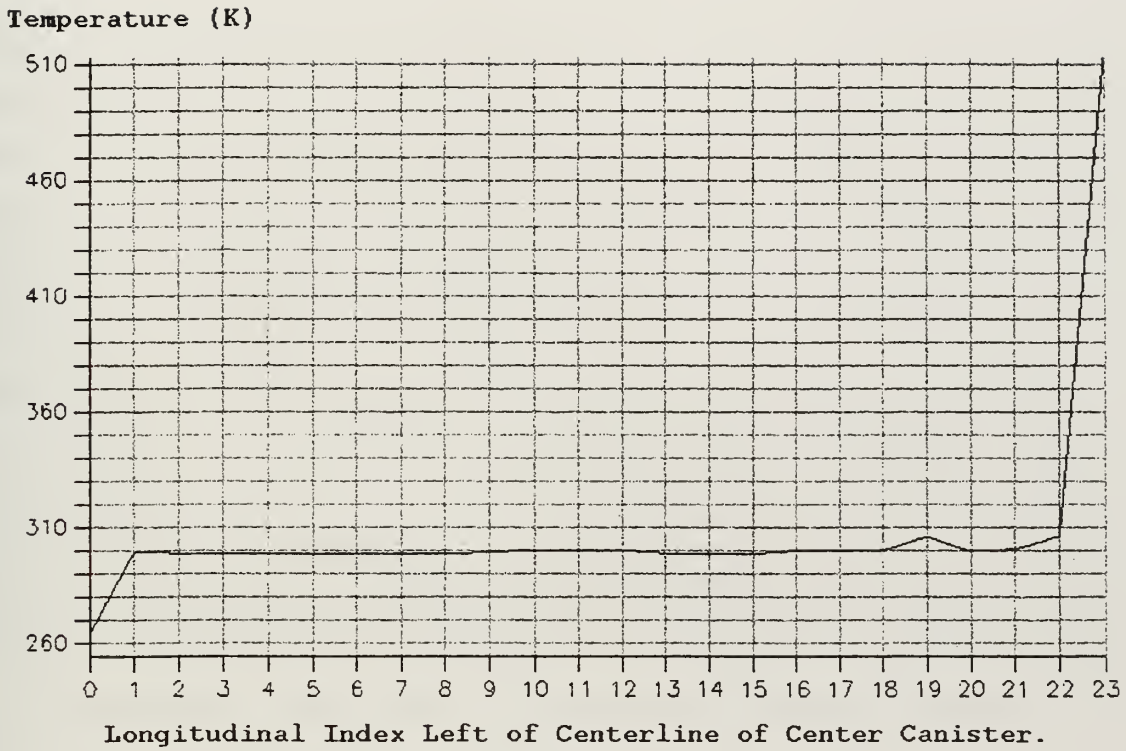

Figure 116. F-76 Fire - Round 5. Temperature vs. Index Profile at a Time of 1 Minute.

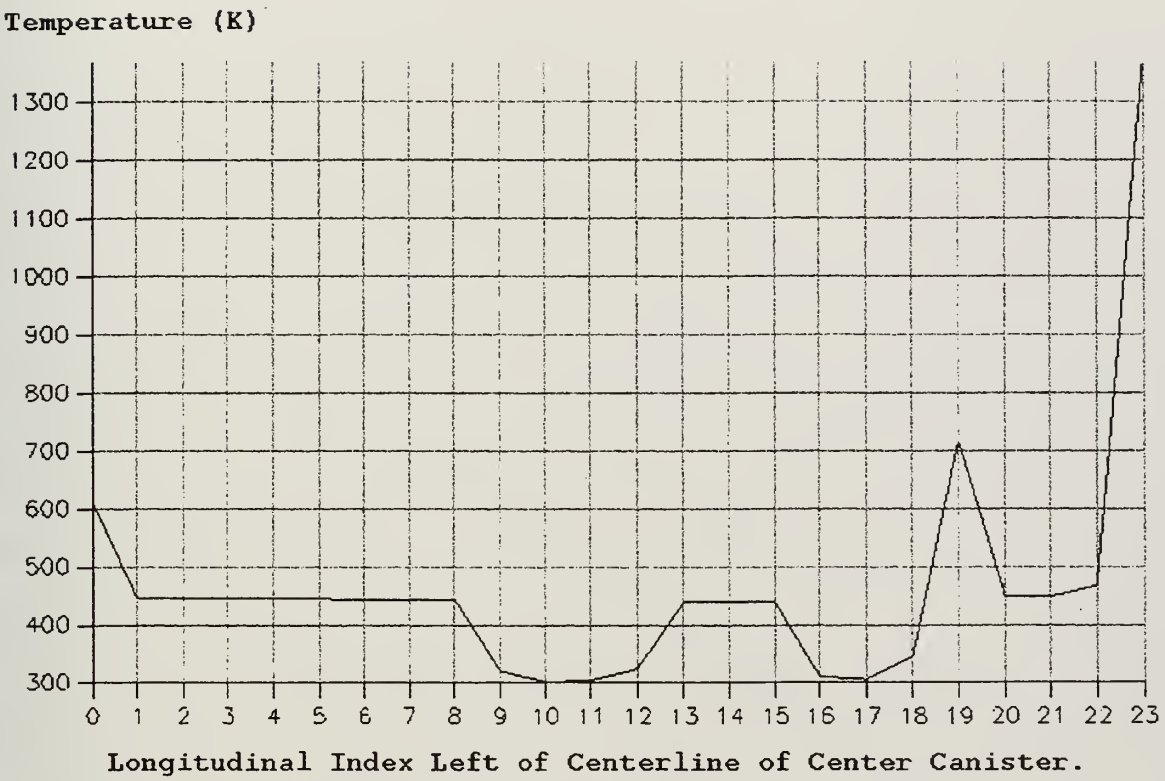

Figure 117. F-76 Fire - Round 5. Temperature vs. Index Profile at a Time of 10 Minutes.

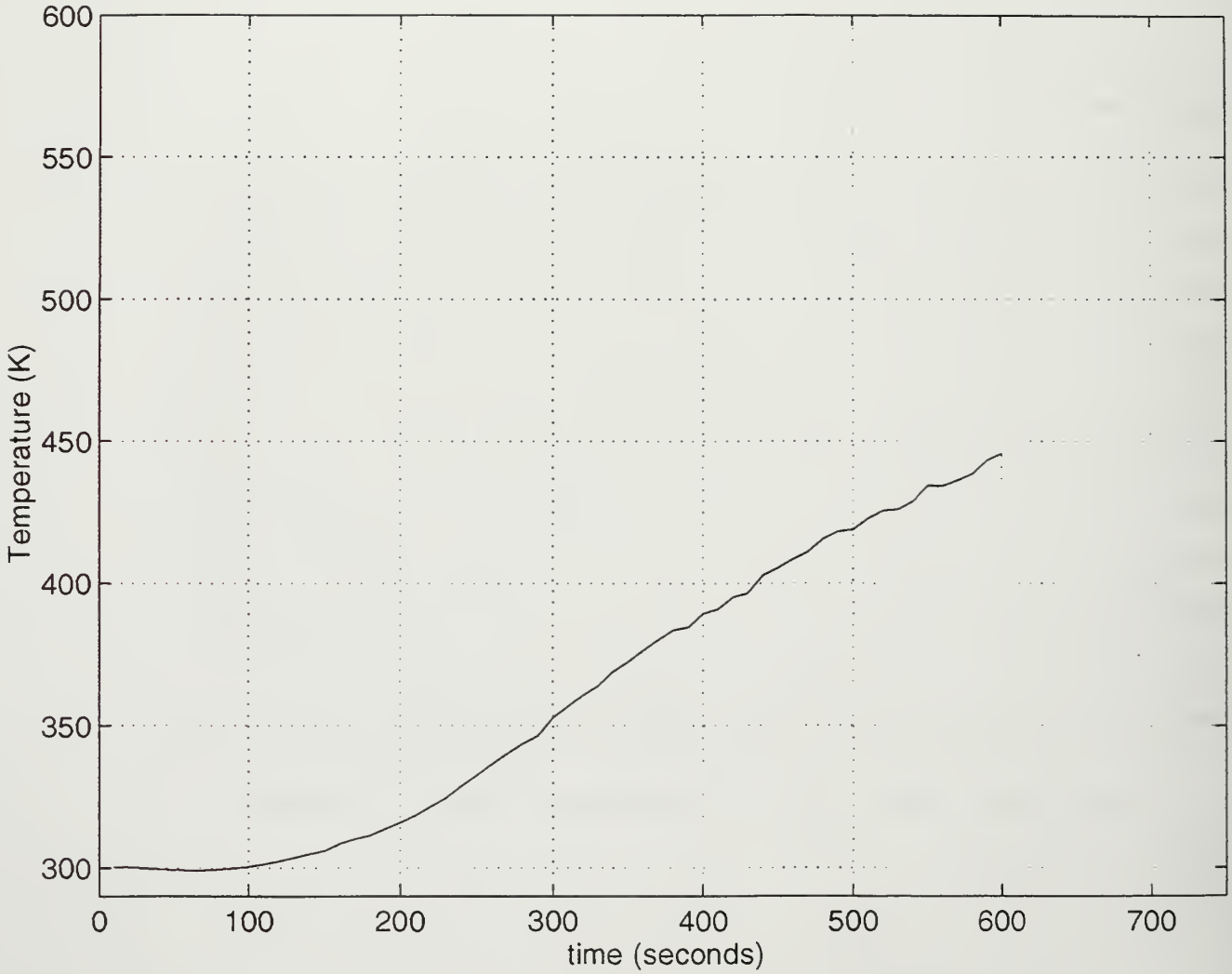

Figure 118. F-76 Fire - Round 5. Temperature vs. Time Plot for Monitor Point 1.

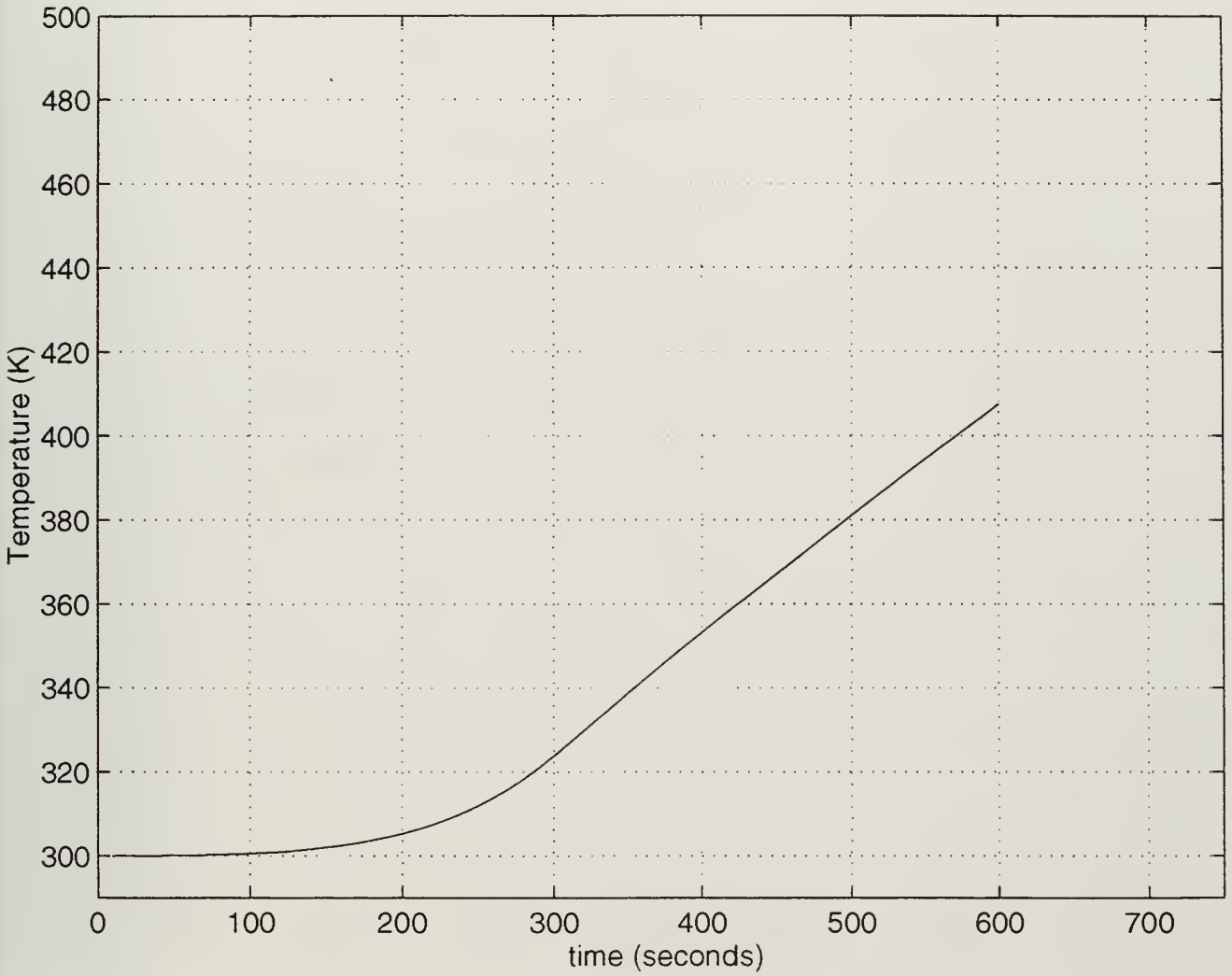

Figure 119. F-76 Fire - Round 5. Temperature vs. Time Plot for Monitor Point 2.

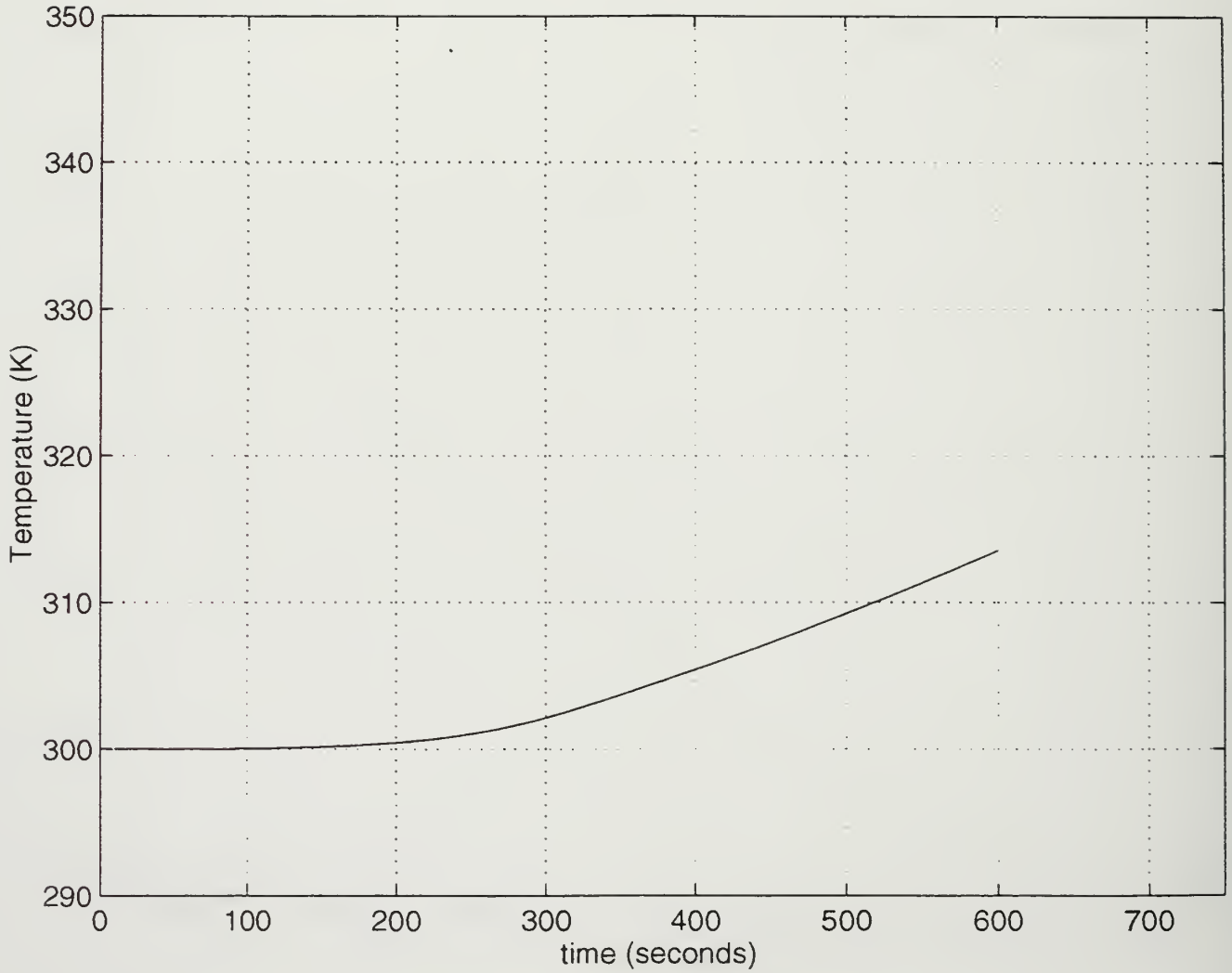

Figure 120. F-76 Fire - Round 5. Temperature vs. Time Plot for Monitor Point 3.

APPENDIX N. RESIDUAL ERROR PROFILES.

The following residual error figures are representative of all Exocet and F-76 fire scenerios at time steps of 1 (i.e., t = 10 sec) and 60 (i.e., t = 10 min). The variables are:

u = velocity component in the I-direction.

v = velocity component in the J-direction.

w = velocity component in the K-direction.

PP = pressure.

K = turbulent kinetic energy.

D = dissipation rate of turbulent kinetic energy.

H = enthalpy.

RX = radiation.

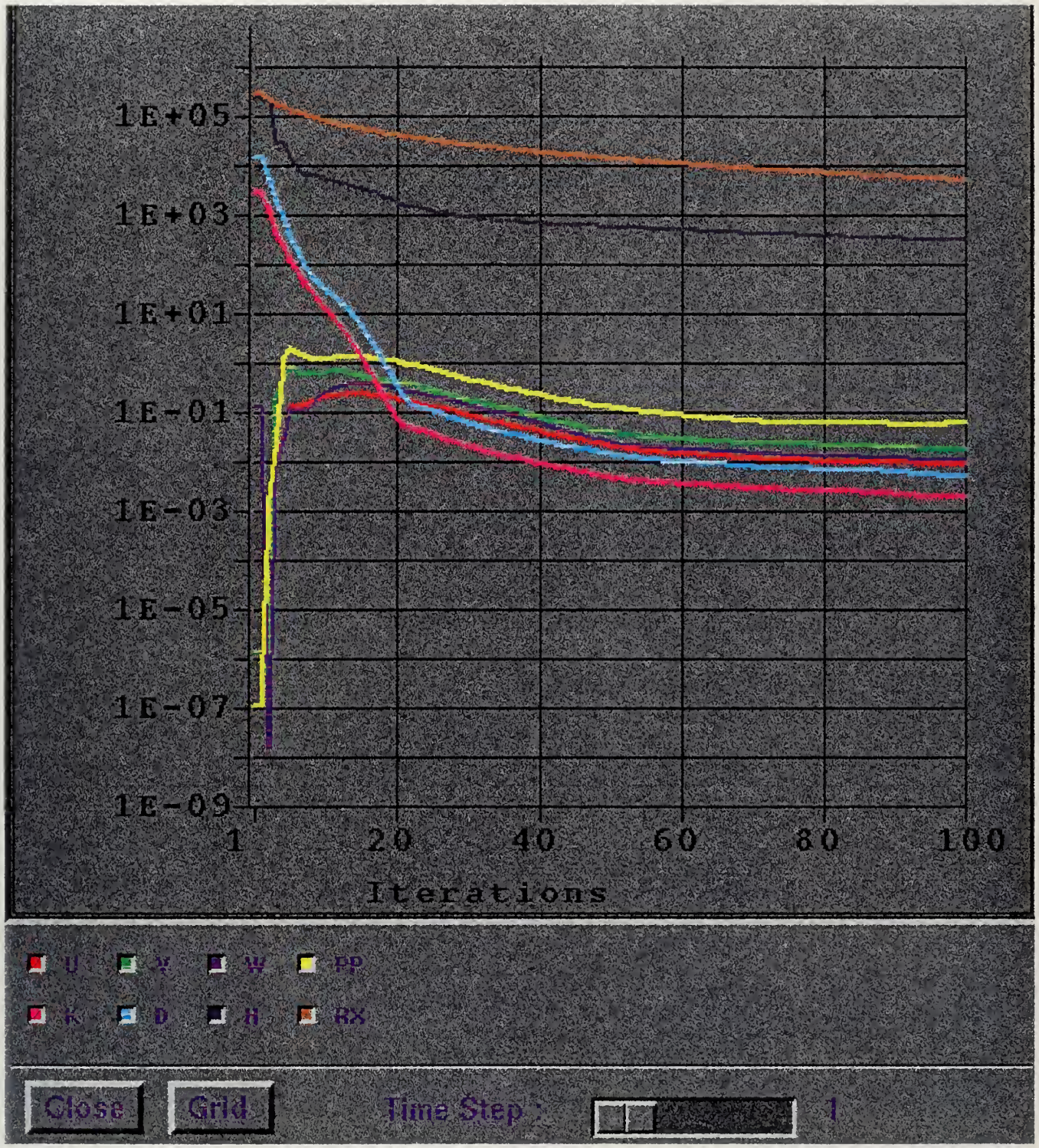

Figure 121. Residual Profile at Time Step 1 (10 seconds).

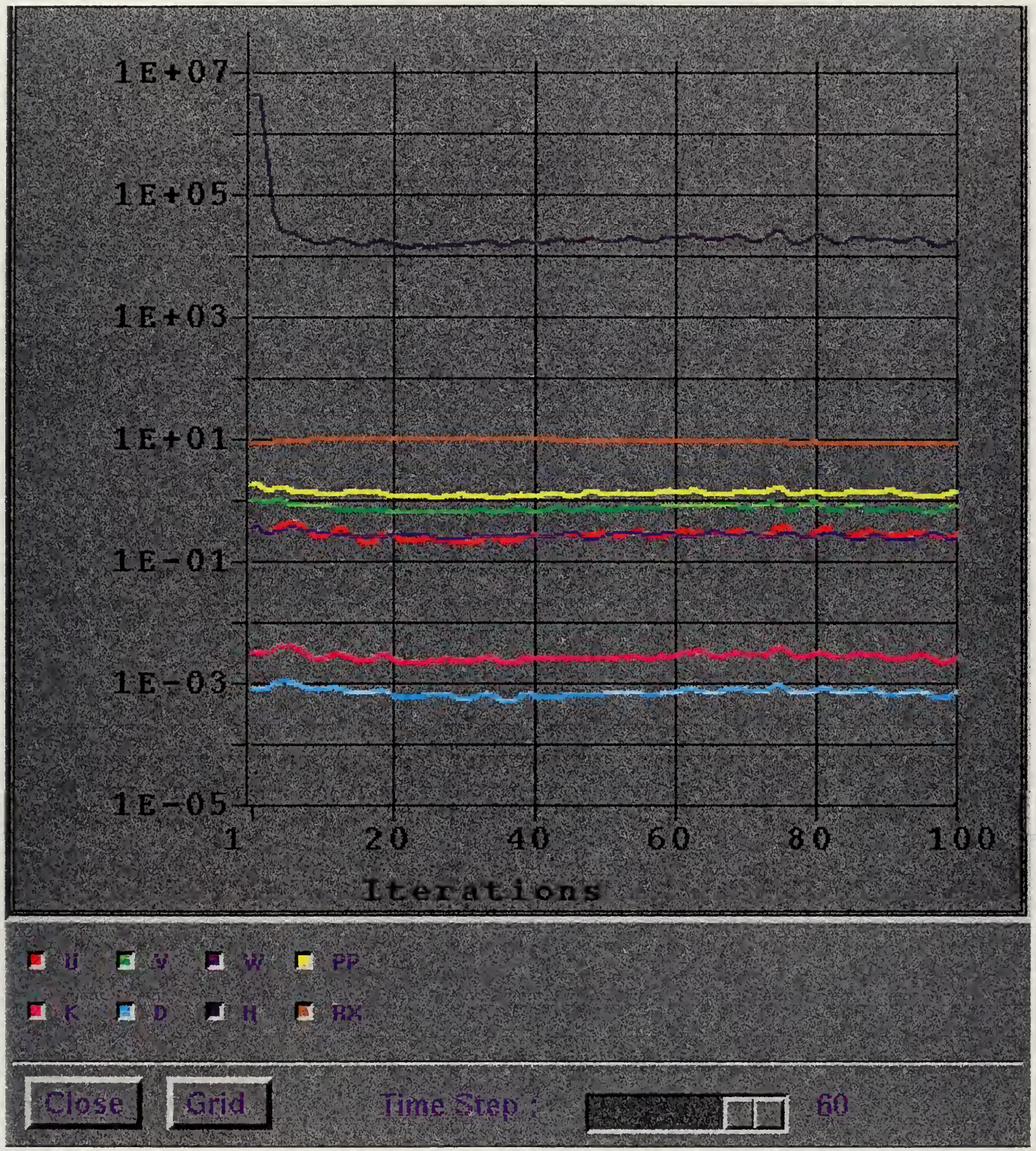

Figure 122. Residual Profile at Time Step 60 (10 minutes).

APPENDIX O. EXOCET FIRE - CLOSE WALL

The following data corresponds to a close wall simulation of the Exocet fire scenerio, including:

(1) Horizontal Grid Distribution.
(2) 3-dimensional temperature profile at a time of one minute.
(3) 3-dimensional temperature profile at a time of 10 minutes.
(4) Horizontal temperature profile at a time of one minute.
(5) Horizontal temperature profile at a time of 10 minutes.
(6) Temperature vs. index profile at a time of one minute.
(7) Temperature vs. index profile at a time of 10 minutes.
(8) Temperature vs. time plot for monitor point 1.
(9) Temperature vs. time plot for monitor point 2.
(10) Temperature vs. time plot for monitor point 3.

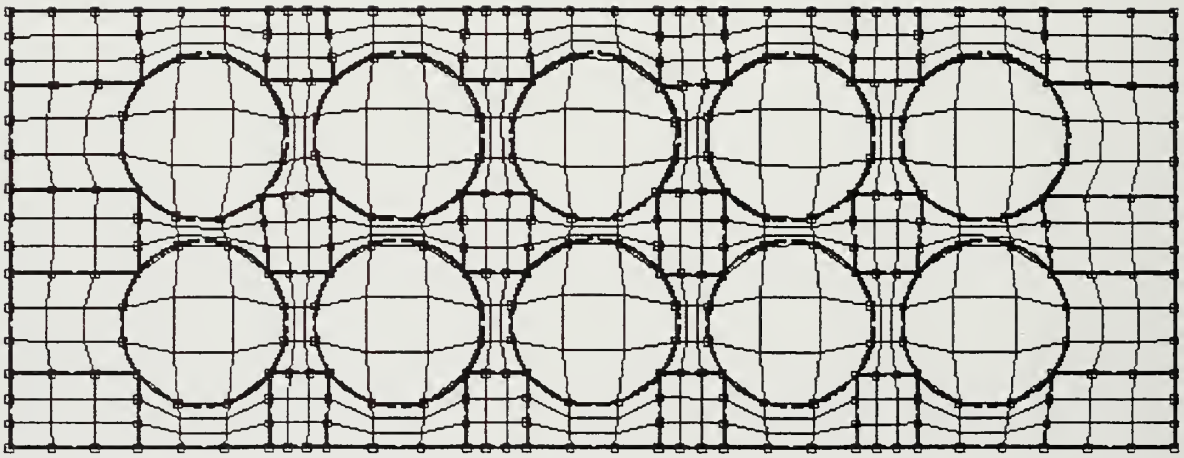

Figure 123. Horizontal Grid Distribution for Close Wall.

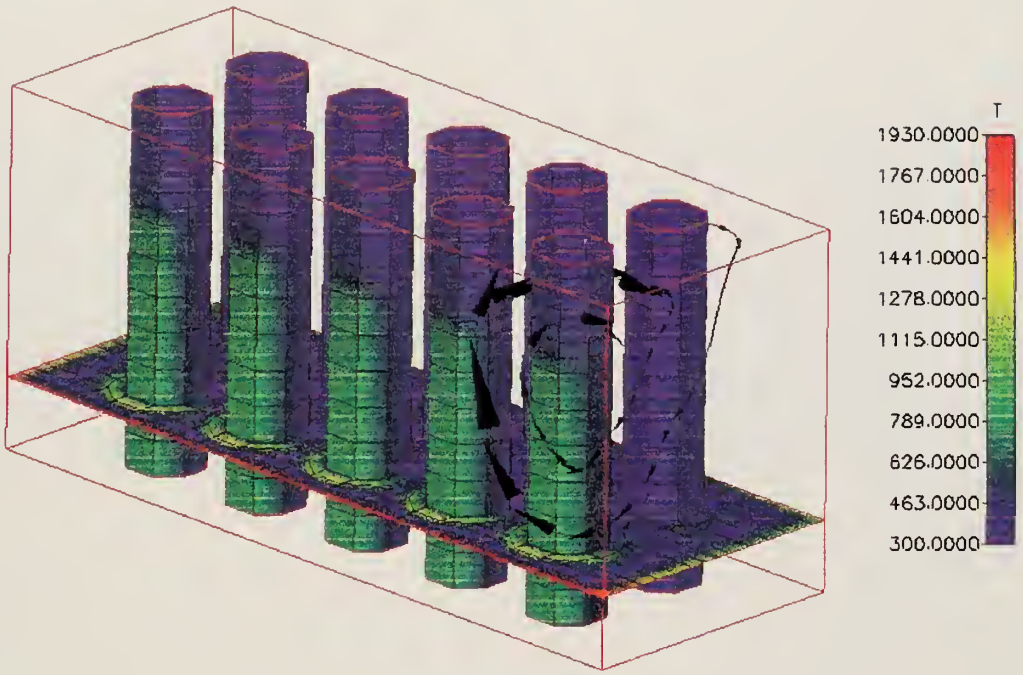

Figure 124. Exocet Fire - Close Wall. 3-Dimensional Temperature Profile at a Time of 1 Minute.

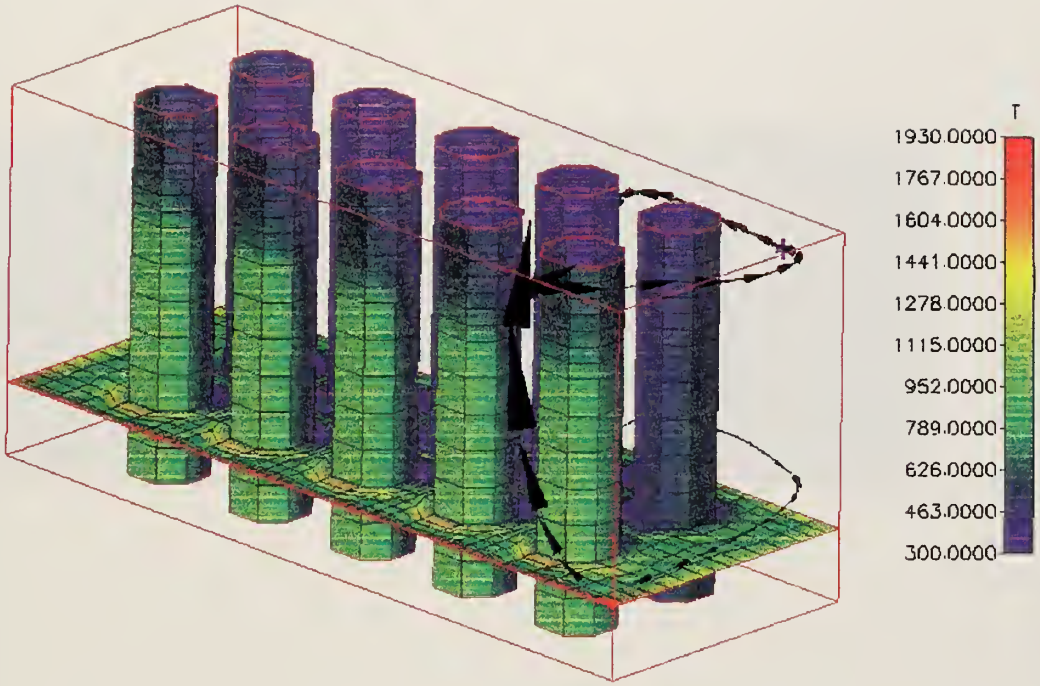

Figure 125. Exocet Fire - Close Wall. 3-Dimensional Temperature Profile at a Time of 10 Minutes.

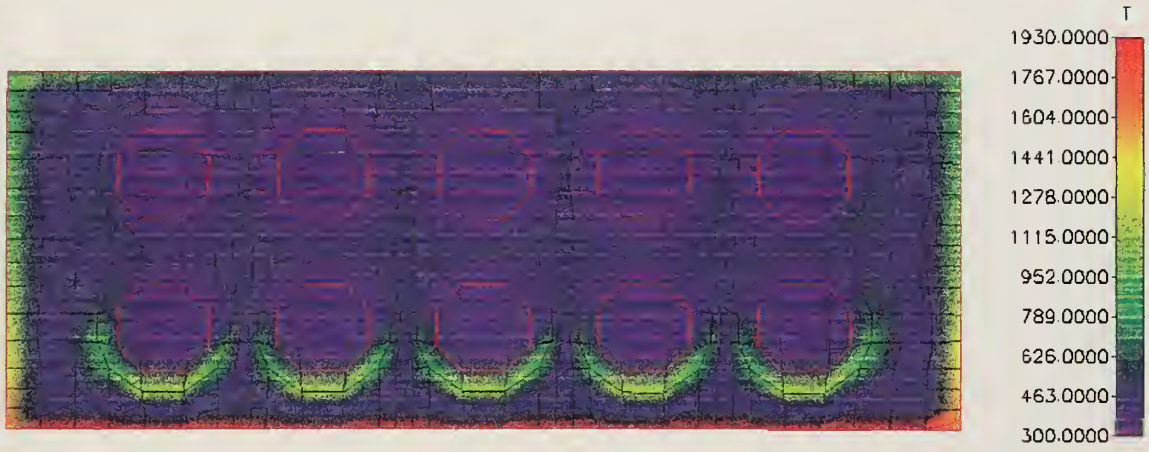

Figure 126. Exocet Fire - Close Wall. Horizontal Temperature Profile at a Time of 1 Minute.

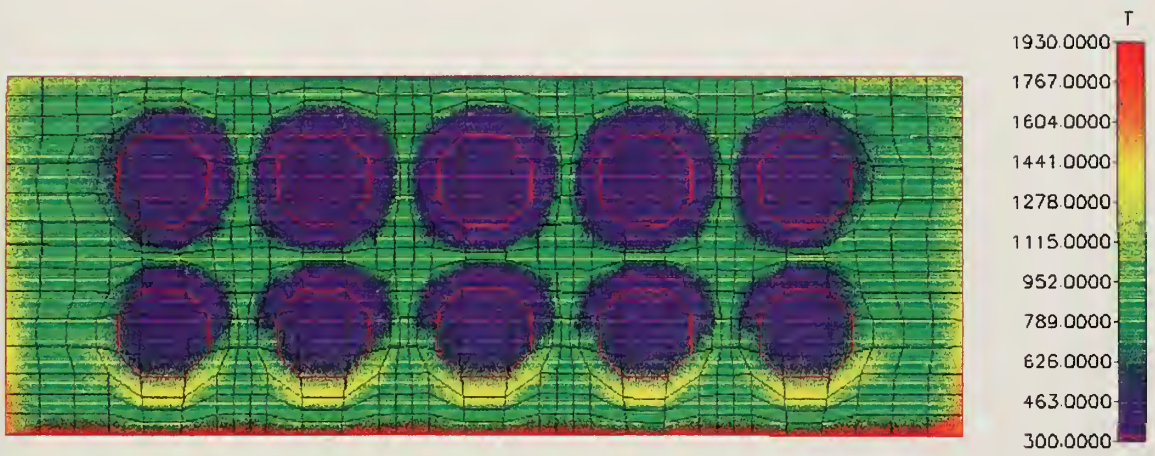

Figure 127. Exocet Fire - Close Wall. Horizontal Temperature Profile at a Time of 10 Minutes.

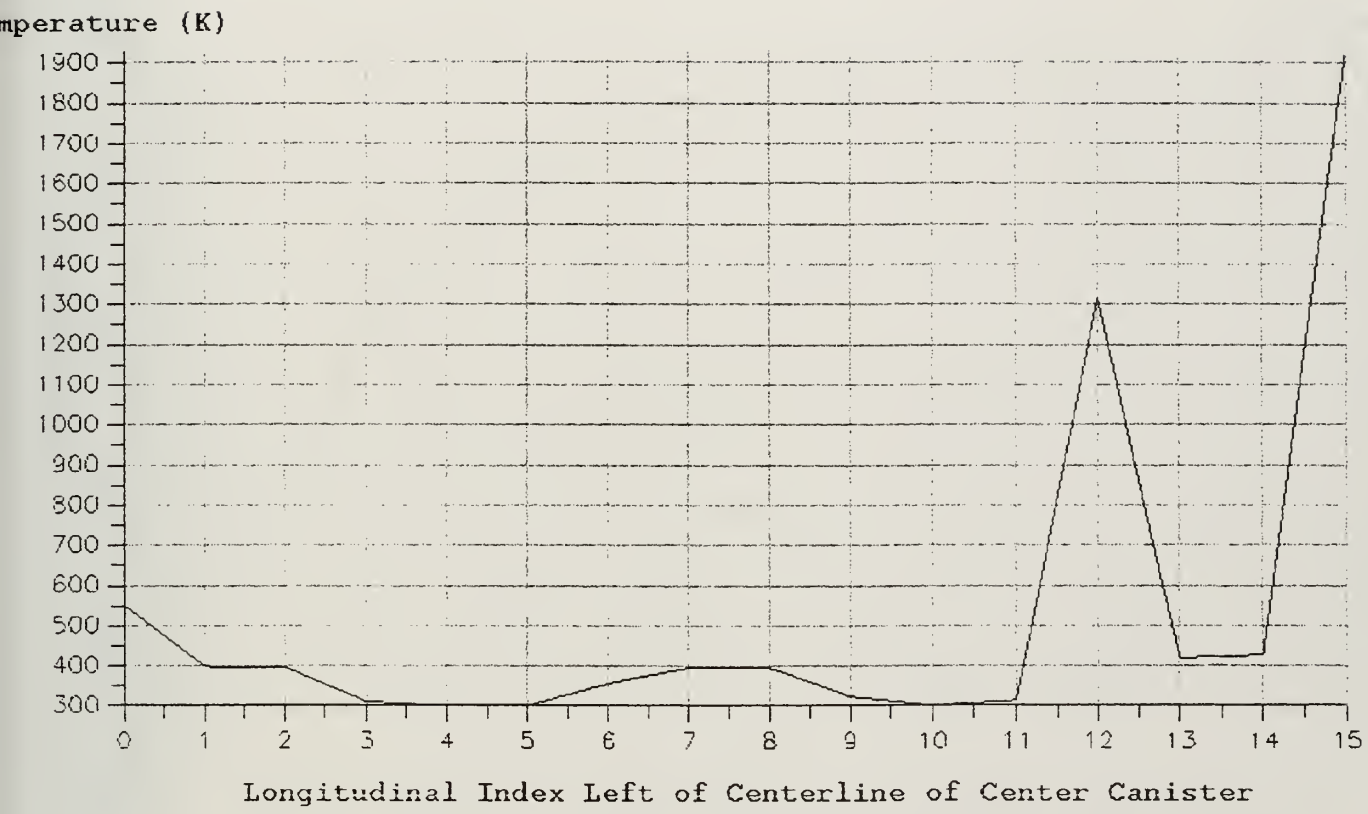

Figure 128. Exocet Fire - Close Wall. Temperature vs. Index Profile at a Time of 1 Minute.

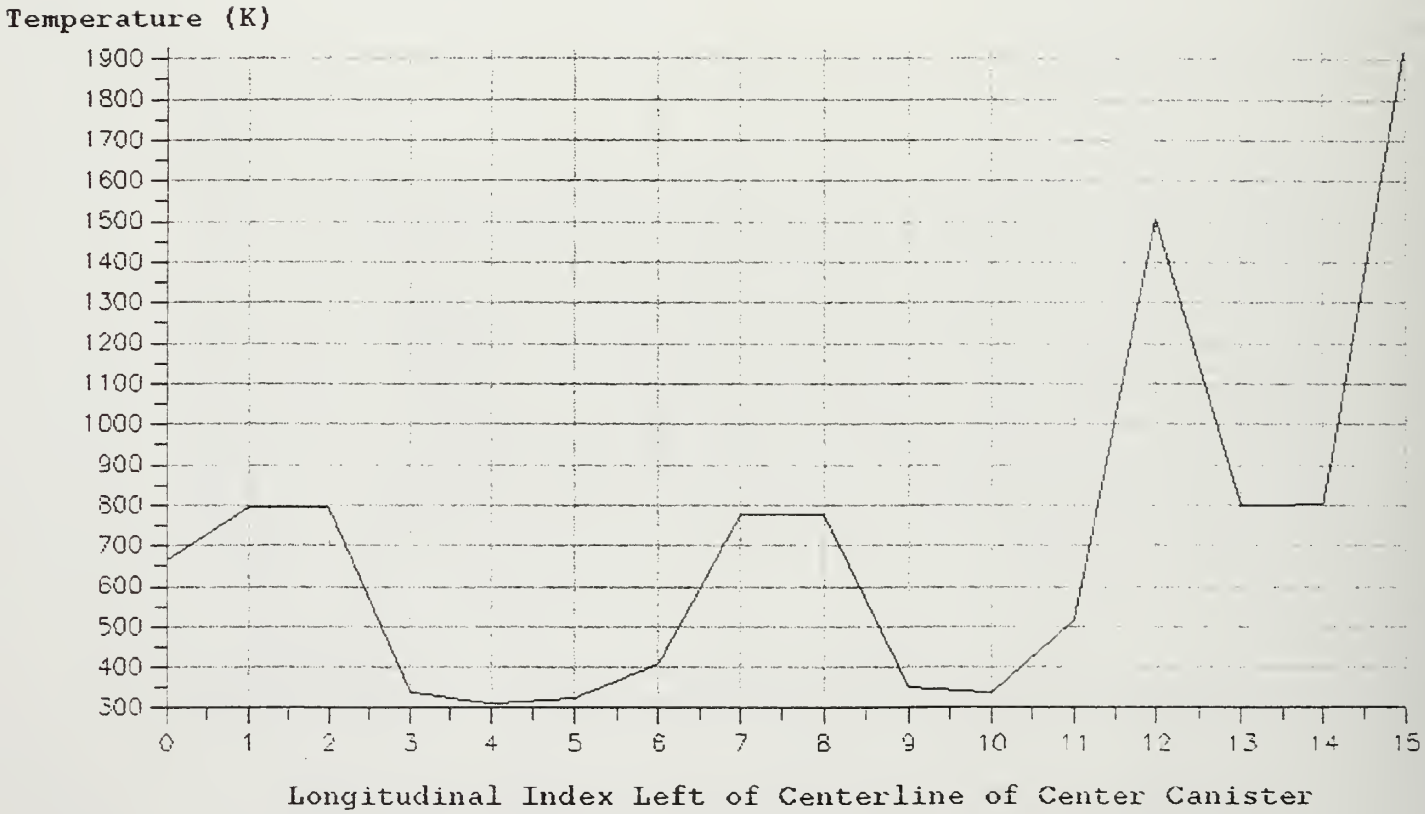

Figure 129. Exocet Fire - Close Wall. Temperature vs. Index Profile at a Time of 10 Minutes.

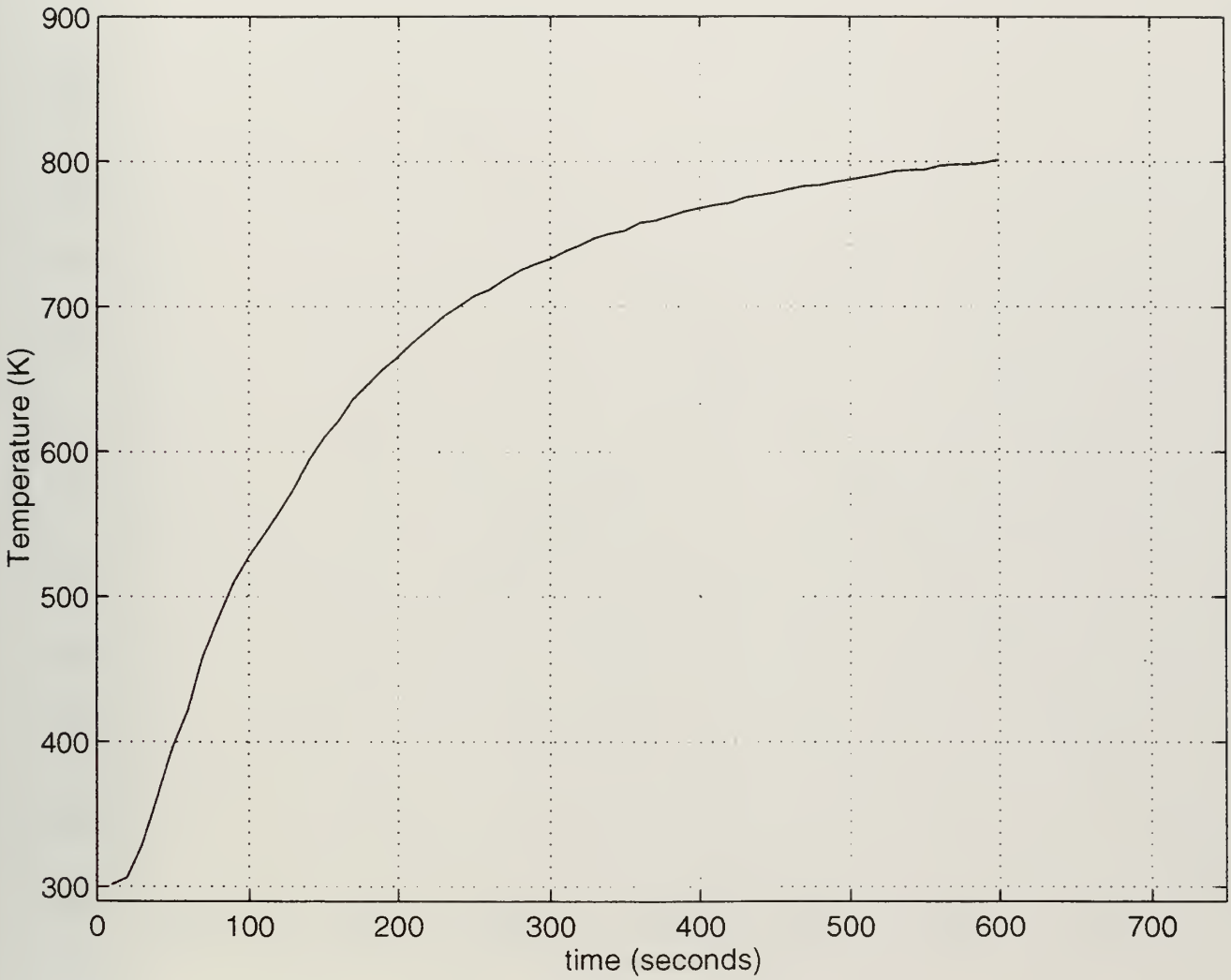

Figure 130. Exocet Fire - Close Wall. Temperature vs. Time Plot for Monitor Point 1.

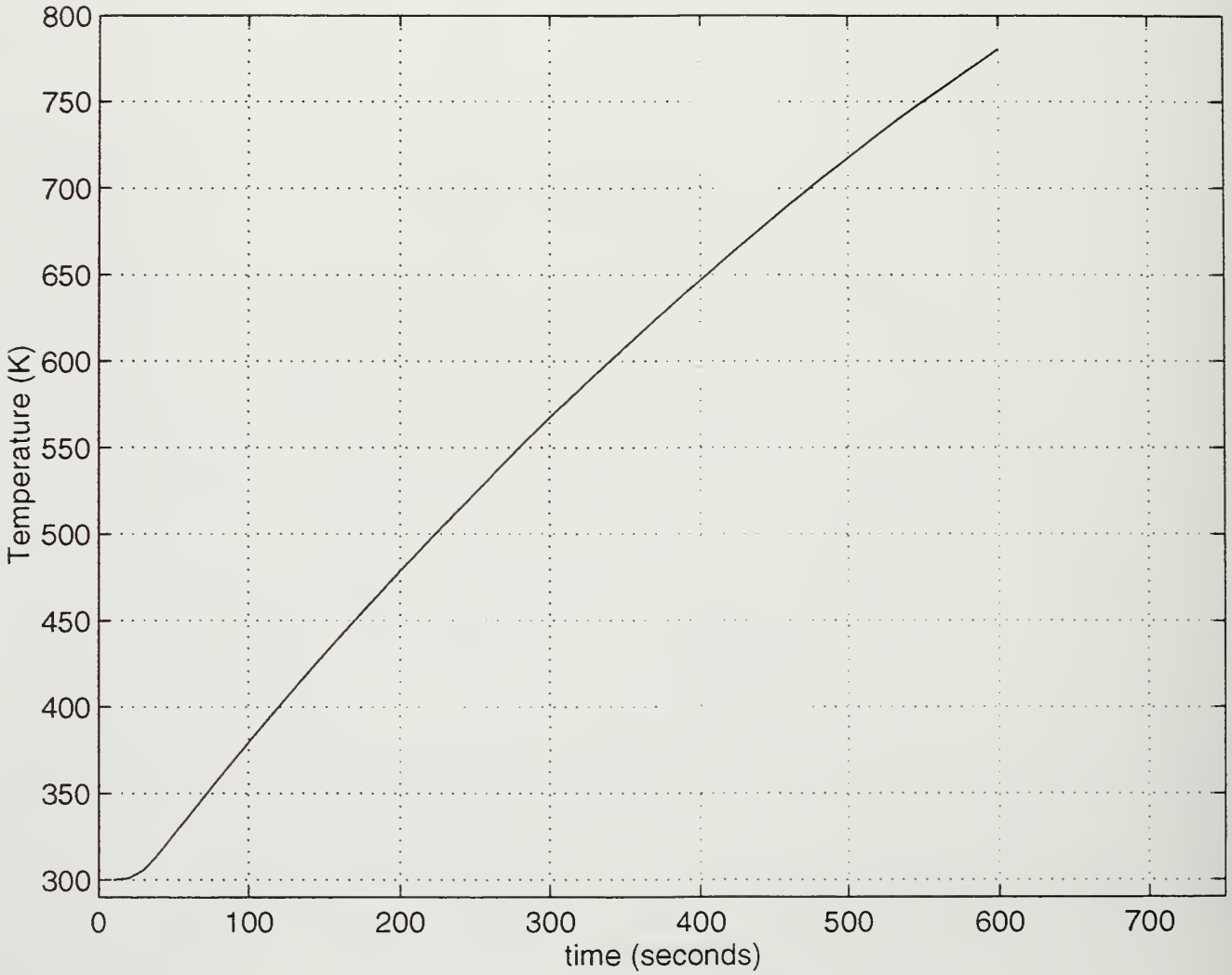

Figure 131. Exocet Fire - Close Wall. Temperature vs. Time Plot for Monitor Point 2.

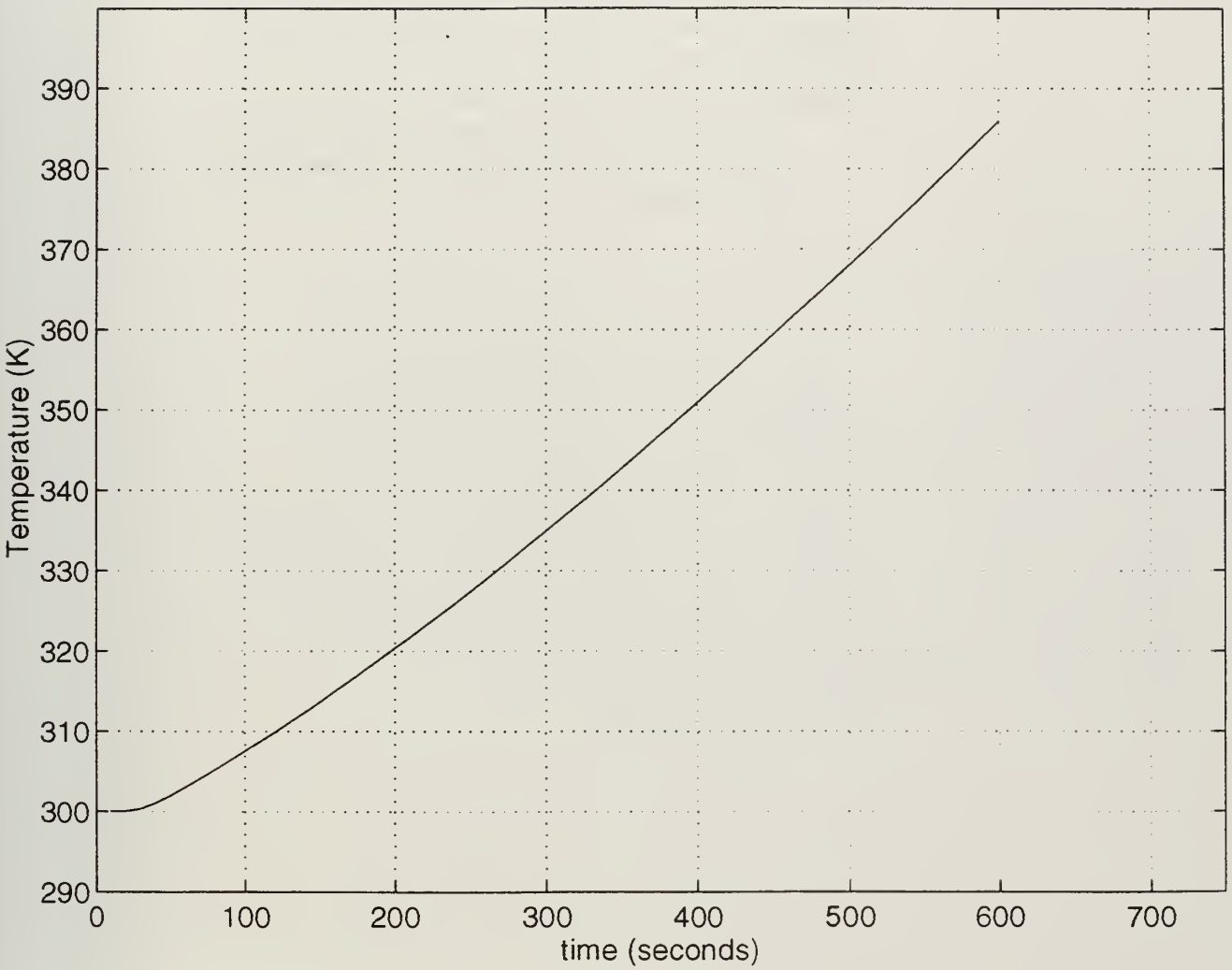

Figure 132. Exocet Fire - Close Wall. Temperature vs. Time Plot for Monitor Point 3.

APPENDIX P. F-76 FIRE - CLOSE WALL

The following data corresponds to a close wall simulation of the F-76 fire scenerio, including:

(1) Horizontal Grid Distribution.
(2) 3-dimensional temperature profile at a time of one minute.
(3) 3-dimensional temperature profile at a time of 10 minutes.
(4) Horizontal temperature profile at a time of one minute.
(5) Horizontal temperature profile at a time of 10 minutes.
(6) Temperature vs. index profile at a time of one minute.
(7) Temperature vs. index profile at a time of 10 minutes.
(8) Temperature vs. time plot for monitor point 1.
(9) Temperature vs. time plot for monitor point 2.
(10) Temperature vs. time plot for monitor point 3.

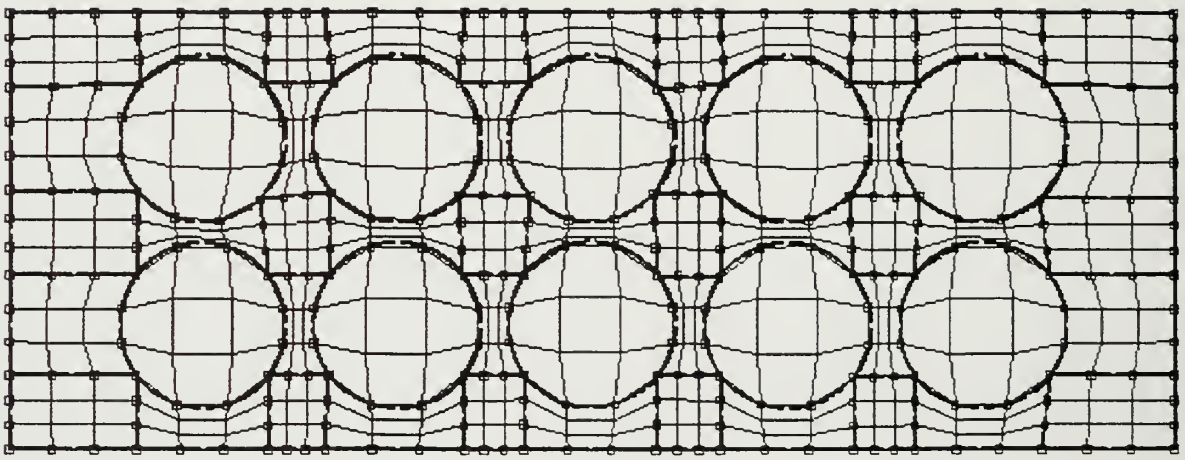

Figure 133. Horizontal Grid Distribution for Close Wall.

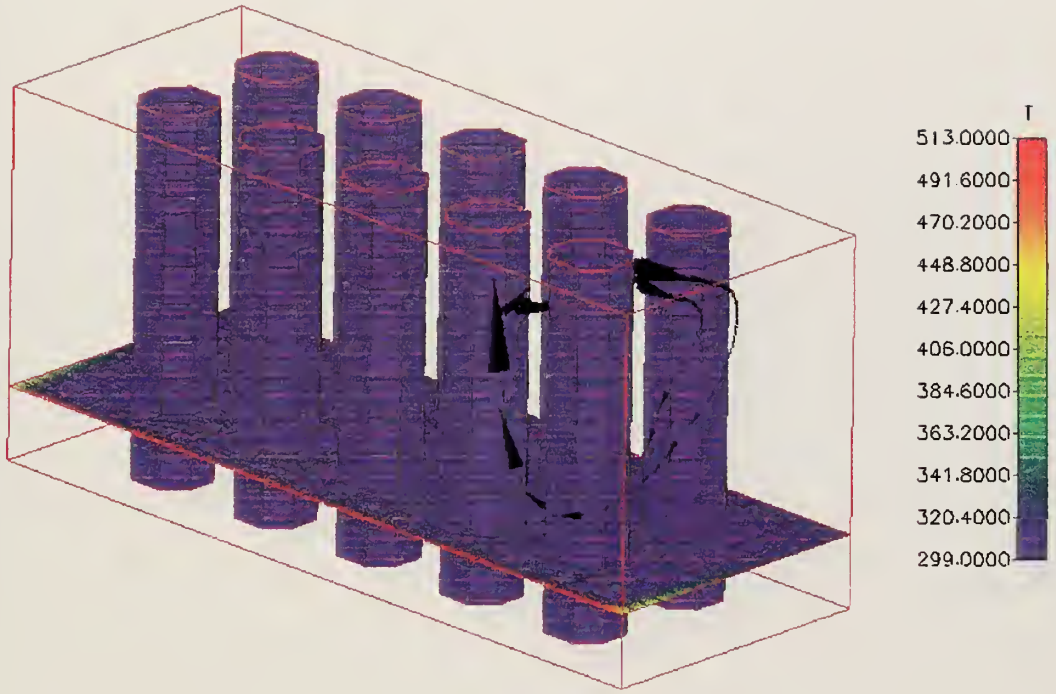

Figure 134. F-76 Fire - Close Wall. 3-Dimensional Temperature Profile at a Time of 1 Minute.

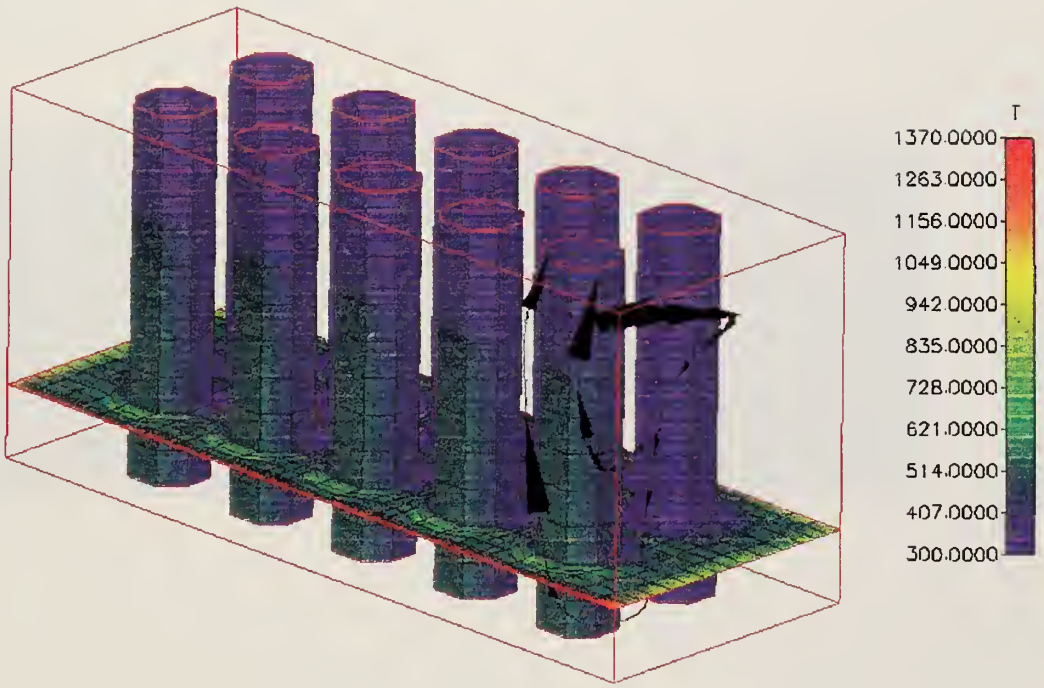

Figure 135. F-76 Fire - Close Wall. 3-Dimensional Temperature Profile at a Time of 10 Minutes.

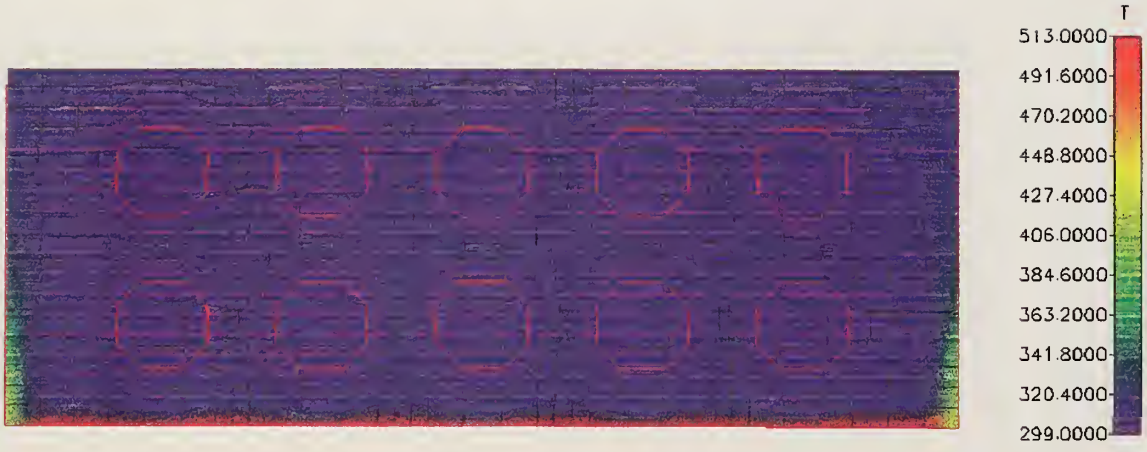

Figure 136. F-76 Fire - Close Wall. Horizontal Temperature Profile at a Time of 1 Minute.

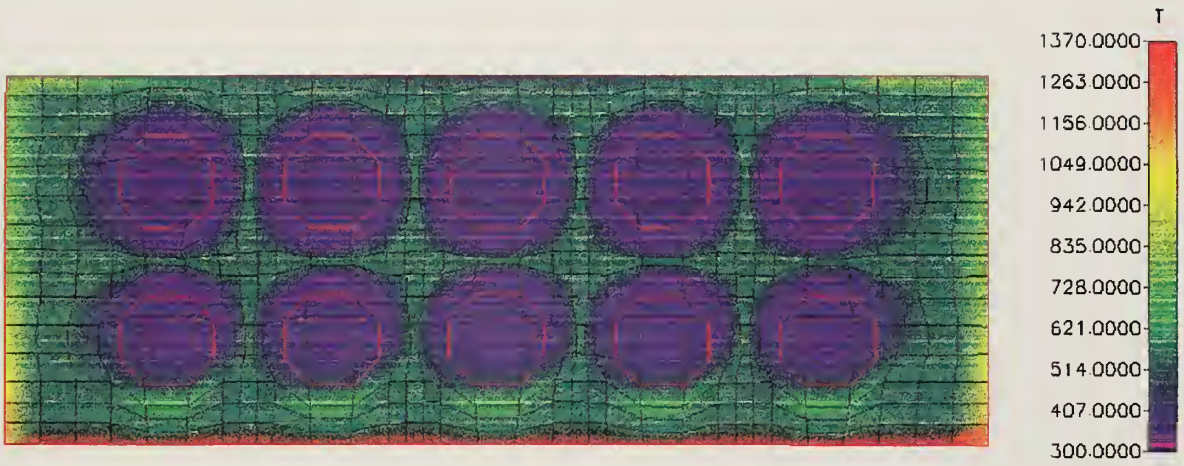

Figure 137. F-76 Fire - Close Wall. Horizontal Temperature Profile at a Time of 10 Minutes.

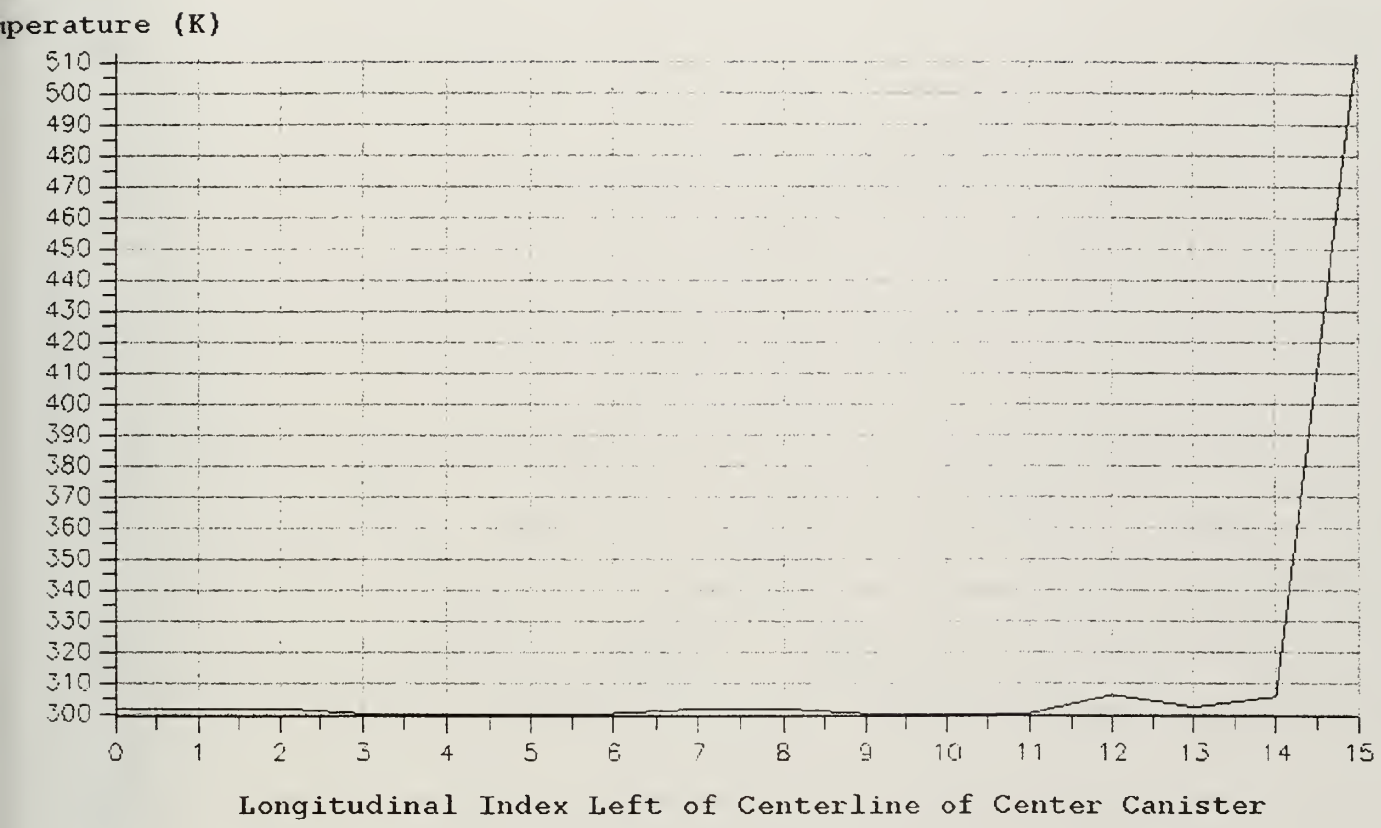

Figure 138. F-76 Fire - Close Wall. Temperature vs. Index Profile at a Time of 1 Minute.

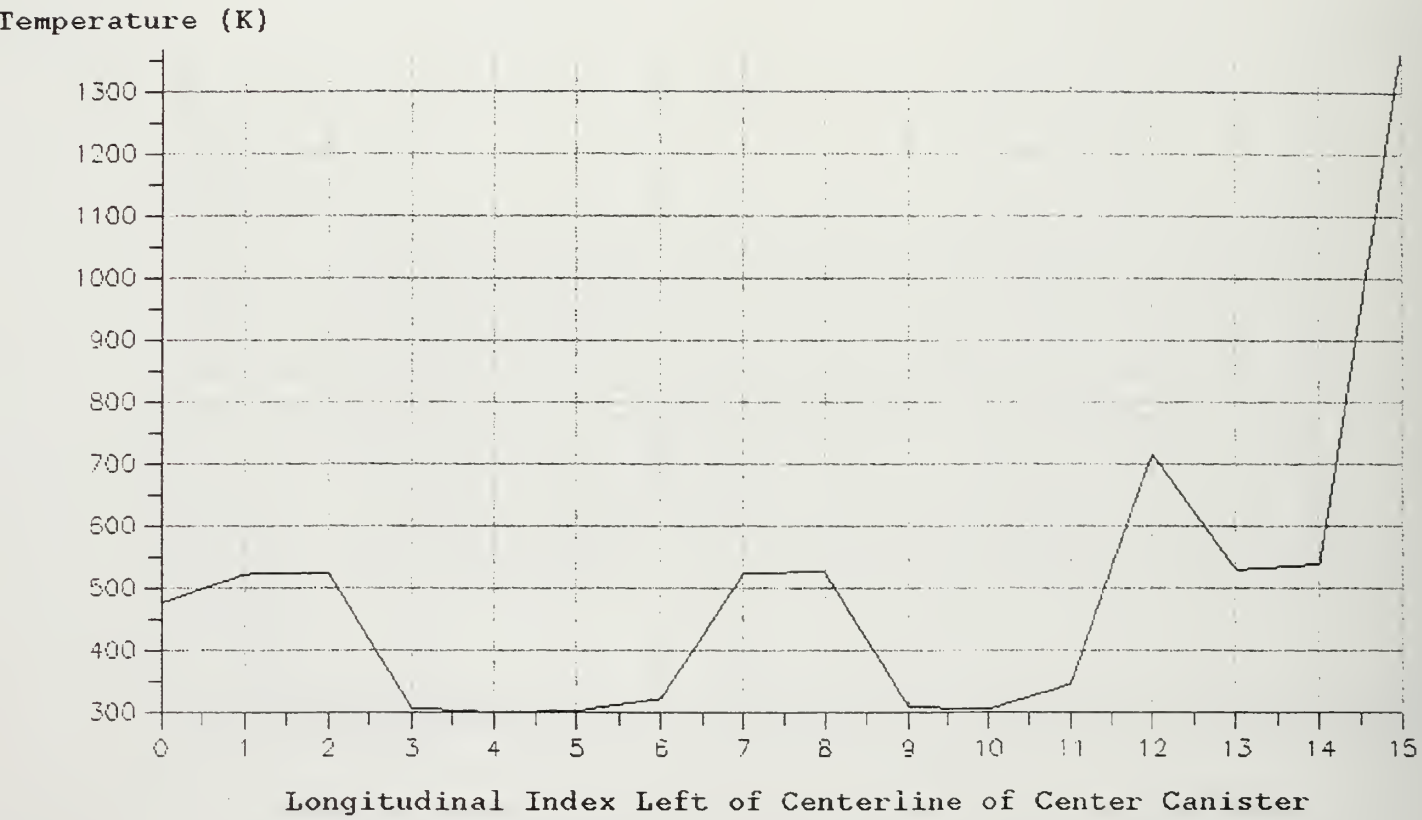

Figure 139. F-76 Fire - Close Wall. Temperature vs. Index Profile at a Time of 10 Minutes.

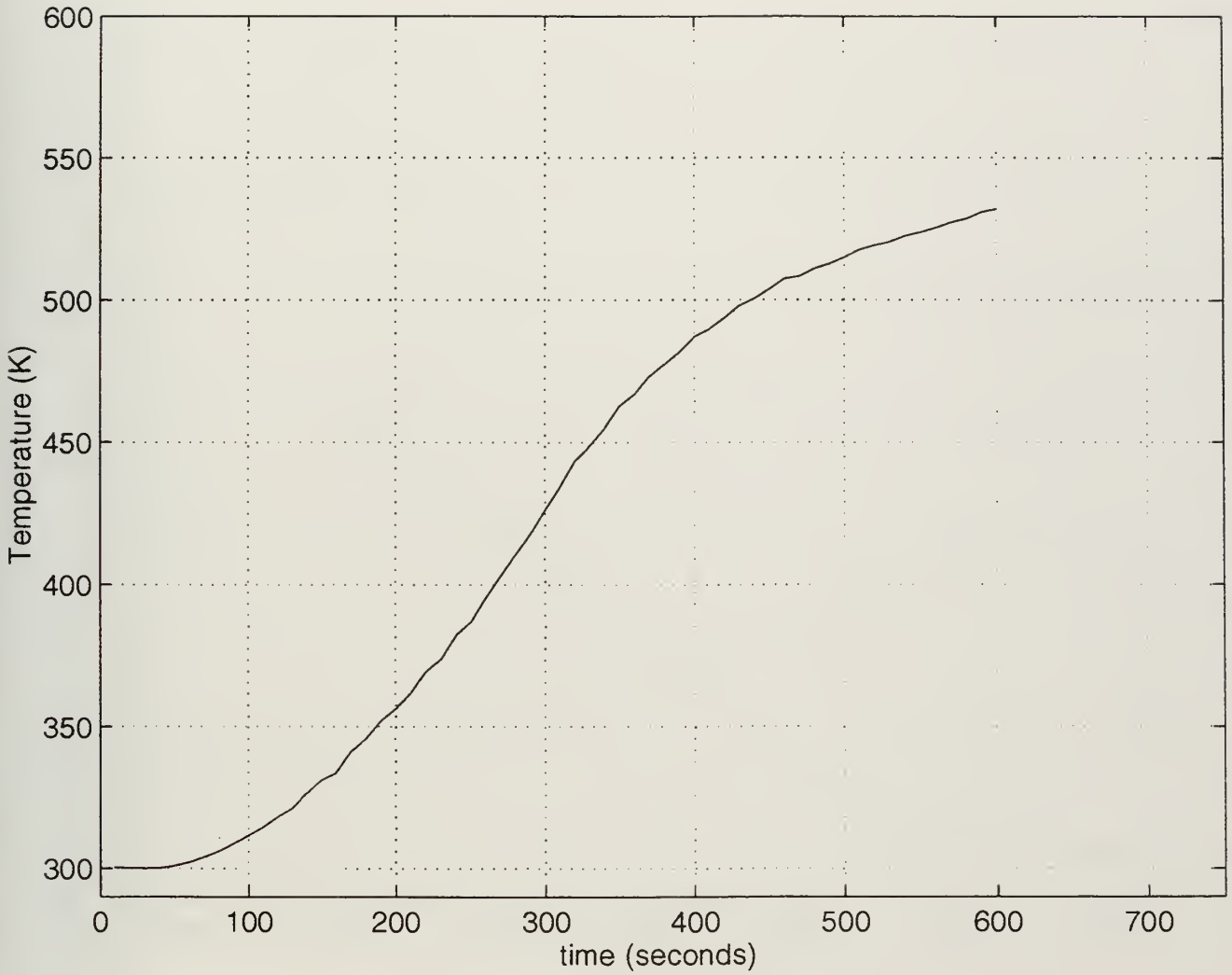

Figure 140. F-76 Fire - Close Wall. Temperature vs. Time Plot for Monitor Point 1.

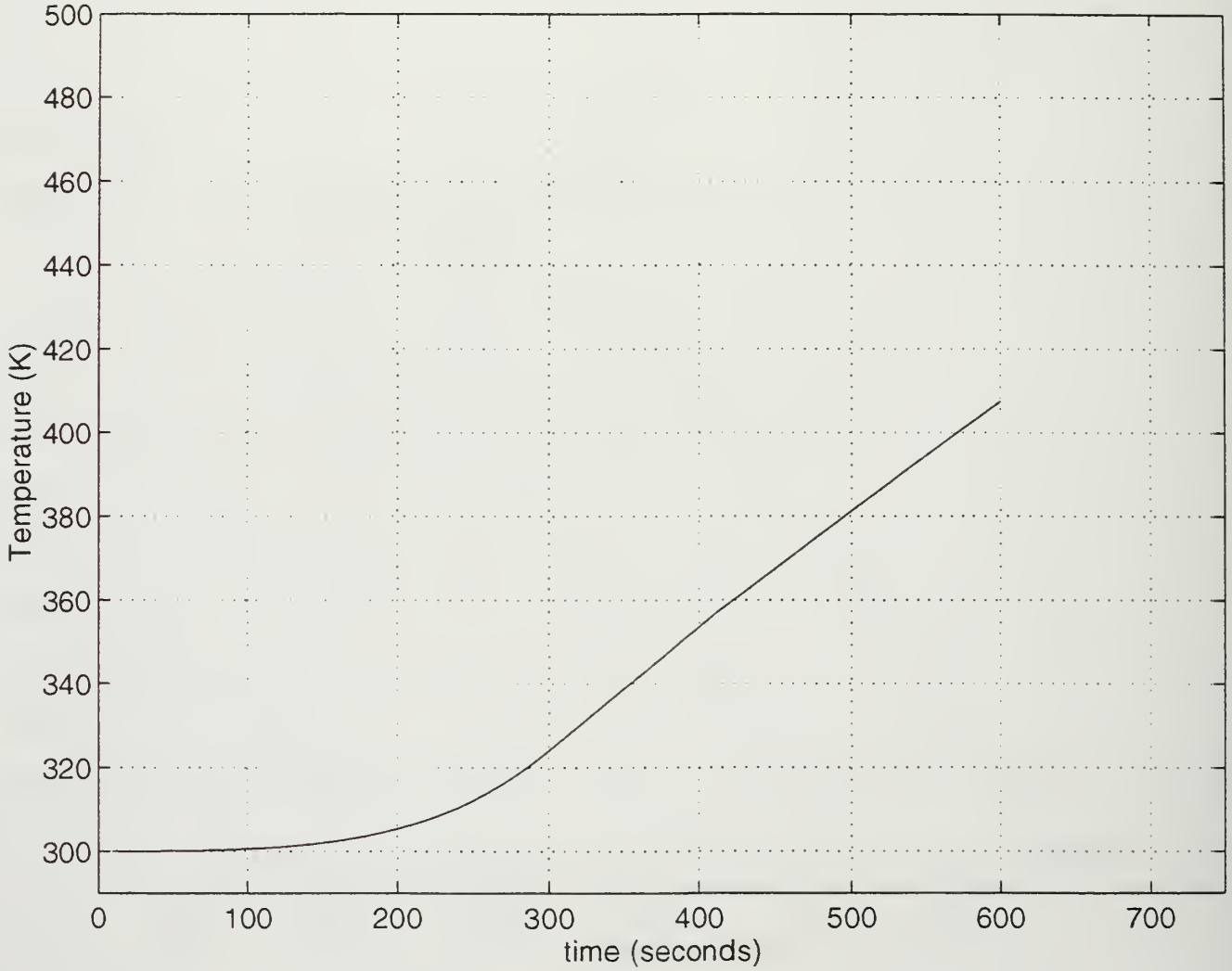

Figure 141. F-76 Fire - Close Wall. Temperature vs. Time Plot for Monitor Point 2.

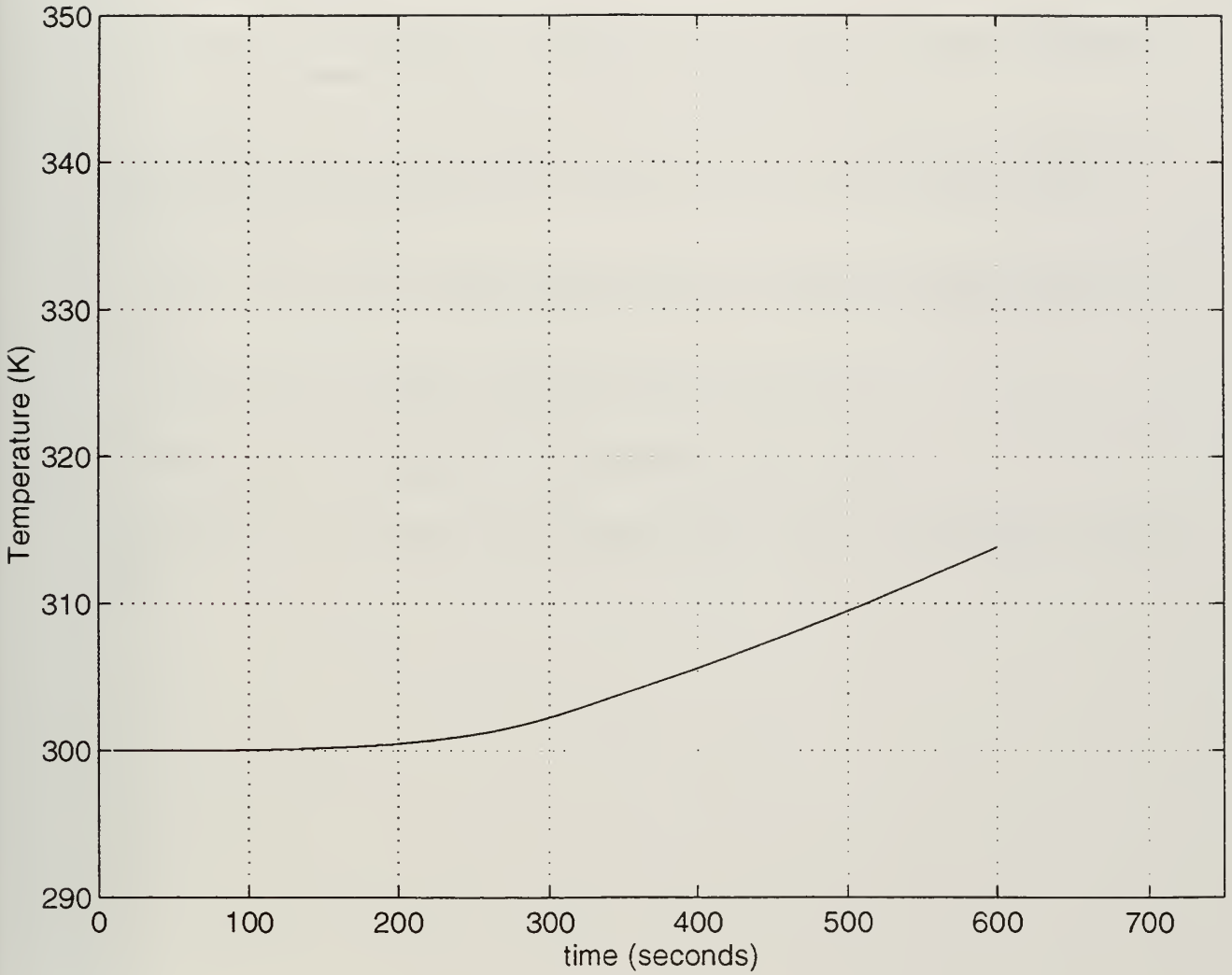

Figure 142. F-76 Fire - Close Wall. Temperature vs. Time Plot for Monitor Point 3.

LIST OF REFERENCES

1. Barker, T., Maillie, F., Burton, T., Rudnicki, R., and Frick, J., *Concentric Canister Launcher Concept Evaluation Report*, Dahlgren Division, Naval Surface Warfare Center, Oct 94.

2. Yagla, J., *Vertical Launch Capability* Presentation, Dahlgren Division, Naval Surface Warfare Center, Jul 96.

3. Callaham, T. and Kelleher, M., *Fire Modeling for Cook-off in Ordnance Magazines*, Mechanical Engineering Department, Naval Postgraduate School, Dec 96.

4. Bowman, H. and Lee, M., *Magazine Fire Protection: An Assessment of Magazine Vulnerability to Fire*, Research and Technology Division, Naval Air Warfare Center Weapons Division, Mar 95.

5. Kelly, E., *USS STARK (FFG-31) Battle Damage Assessment* Presentation, SEA 91T, Jun 87.

6. CFD Research Corporation, *CFD-ACE Theory Manual*, Jul 96.

7. CFD Research Corporation, *CFD-ACE Course Binder*, Sep 96.

8. Incropera, F. and DeWitt, D., *Introduction to Heat Transfer*, John Wiley & Sons, Inc., 1990.

INITIAL DISTRIBUTION LIST

1. Defense Technical Information Center 2
   8725 John J. Kingman Road, Ste 0944
   Ft. Belvoir, Virginia 22060-6218

2. Dudley Knox Library 2
   Naval Postgraduate School
   411 Dyer Road
   Monterey, California 93943-5101

3. Naval/Mechanical Engineering Curricular Officer, Code 34 1
   Naval Postgraduate School
   Monterey, California 93943-5101

4. Professor Matthew D. Kelleher 2
   Mechanical Engineering Department, Code ME/KK
   Naval Postgraduate School
   Monterey, California 93943-5101

5. LT Gary L. Null, USN 1
   317 Willamont Road
   Toledo, Ohio 43612

6. CFD Research Corporation 1
   Cummings Research Park
   215 Wynn Drive
   Huntsville, Alabama 35805

7. Commander, NSWCDD 1
   Attn: J. Yagla, G70
   Dahlgren, Virginia 22448

8. NAWC-Weapons Division 1
   Fire Research Office Code: 4B3100D
   Attn: L. Bowman
   China Lake, California 93555-6100

9. NAWC-Weapons Division 1
Fire Research Office Code: 4B3100D
Attn: J. Hoover
China Lake, California 93555-6100

10. Naval Sea Systems Command 1
Attn: Brian Smale
NAVSEA 03R12
2531 Jefferson Davis Highway
Arlington, Virginia 22242-5160

11. Naval Sea Systems Command 1
Attn: Bob Darwin
NAVSEA 03G2
2531 Jefferson Davis Highway
Arlington, Virginia 22242-5160

12. Naval Sea Systems Command 1
Attn: Roger Nutting
NAVSEA 03P4
2531 Jefferson Davis Highway
Arlington, Virginia 22242-5160

3 483NPG
TH 2545
10/99 22527-200

DUDLEY KNOX LIBRARY
3 2768 00366812 0